Advances in Clinical and Experimental Medicine

MONTHLY ISSN 1899-5276 (PRINT) ISSN 2451-2680 (ONLINE) advances.umw.edu.pl

2024, Vol. 33, No. 1 (January)

Impact Factor (IF) – 2.1
Ministry of Science and Higher Education – 70 pts
Index Copernicus (ICV) – 161.11 pts

Wroclaw Medical University

Advances
in Clinical and Experimental
Medicine

Advances
in Clinical and Experimental Medicine

ISSN 1899-5276 (PRINT) ISSN 2451-2680 (ONLINE) advances.umw.edu.pl

MONTHLY 2024
Vol. 33, No. 1
(January)

Advances in Clinical and Experimental Medicine (*Adv Clin Exp Med*) publishes high-quality original articles, research-in-progress, research letters and systematic reviews and meta-analyses of recognized scientists that deal with all clinical and experimental medicine.

Editorial Office
ul. Marcinkowskiego 2–6
50-368 Wrocław, Poland
Tel.: +48 71 784 12 05
E-mail: redakcja@umw.edu.pl

Publisher
Wroclaw Medical University
Wybrzeże L. Pasteura 1
50-367 Wrocław, Poland

Online edition is the original version of the journal

Editorial Policy

Advances in Clinical and Experimental Medicine (Adv Clin Exp Med) is an independent multidisciplinary forum for exchange of scientific and clinical information, publishing original research and news encompassing all aspects of medicine, including molecular biology, biochemistry, genetics, biotechnology and other areas. During the review process, the Editorial Board conforms to the "Uniform Requirements for Manuscripts Submitted to Biomedical Journals: Writing and Editing for Biomedical Publication" approved by the International Committee of Medical Journal Editors (www.ICMJE.org). The journal publishes (in English only) original papers and reviews. Short works considered original, novel and significant are given priority. Experimental studies must include a statement that the experimental protocol and informed consent procedure were in compliance with the Helsinki Convention and were approved by an ethics committee.

For all subscription-related queries please contact our Editorial Office: redakcja@umw.edu.pl
For more information visit the journal's website: advances.umw.edu.pl

Pursuant to the ordinance of the Rector of Wroclaw Medical University No. 12/XVI R/2023, from February 1, 2023, authors are required to pay a fee for each manuscript accepted for publication in the journal Advances in Clinical and Experimental Medicine. The fee amounts to 990 EUR for original papers and meta-analyses, 700 EUR for reviews, and 350 EUR for research-in-progress (RIP) papers and research letters.

Advances in Clinical and Experimental Medicine has received financial support from the resources of Ministry of Science and Higher Education within the "Social Responsibility of Science – Support for Academic Publishing" project based on agreement No. RCN/SP/0584/2021.

Ministry of Education and Science
Republic of Poland

Czasopismo Advances in Clinical and Experimental Medicine korzysta ze wsparcia finansowego ze środków Ministerstwa Edukacji i Nauki w ramach programu „Społeczna Odpowiedzialność Nauki – Rozwój Czasopism Naukowych" na podstawie umowy nr RCN/SP/0584/2021.

Ministerstwo
Edukacji i Nauki

Indexed in: MEDLINE, Science Citation Index Expanded, Journal Citation Reports/Science Edition, Scopus, EMBASE/Excerpta Medica, Ulrich's™ International Periodicals Directory, Index Copernicus

Typographic design: Piotr Gil, Monika Kolęda
DTP: Wydawnictwo UMW
Cover: Monika Kolęda
Printing and binding: PRINT PROFIT Sp. z o.o., Koźmin 27, 59-900 Zgorzelec

Advances
in Clinical and Experimental Medicine

MONTHLY 2024, Vol. 33, No. 1 (January)

ISSN 1899-5276 (PRINT)
ISSN 2451-2680 (ONLINE)
advances.umw.edu.pl

Contents

The role of neridronate in the management of osteoporosis: A meta-analysis

Qiaojie Chen[1,A,D–F], Pingping Shen[2,B,C,F], Bo Zhang[1,B,C,F], Yang Chen[1,B,C,F], Chunli Zhen[3,B,C,F]

[1] Department of Orthopedics, Ningbo No. 2 Hospital, China
[2] Department of Gastroenterology, Yinzhou Ningbo No. 2 Hospital, China
[3] Department of Traditional Chinese Medicine Rehabilitation, Ningbo No. 2 Hospital, China

A – research concept and design; B – collection and/or assembly of data; C – data analysis and interpretation; D – writing the article; E – critical revision of the article; F – final approval of the article

Advances in Clinical and Experimental Medicine, ISSN 1899–5276 (print), ISSN 2451–2680 (online) *Adv Clin Exp Med*. 2024;33(1):5–12

Address for correspondence
Qiaojie Chen
E-mail: qiaoj_chen@yeah.net

Funding sources
This research has been supported by Medical Scientific Research Foundation of Zhejiang Province (grant No. 2023KY278).

Conflict of interest
None declared

Received on December 29, 2021
Reviewed on December 30, 2022
Accepted on April 1, 2023

Published online on May 30, 2023

Abstract

Background. It is estimated that 1 in 3 women and 1 in 5 men over the age of 50 worldwide will experience an osteoporosis fracture during their lives. Neridronate is a third-generation bisphosphonate with established efficacy in metabolic bone disease. It can be used in the treatment of osteoporosis.

Objectives. We aimed to conduct a meta-analysis of the effect of neridronate on the treatment of osteoporosis.

Materials and methods. The Preferred Reporting Items for Systematic Reviews and Meta-Analyses (PRISMA) recommendations were used to guide the present study. We searched PubMed and the Cochrane Central Register of Controlled Trials (CENTRAL) for reports published until August 31, 2021, related to neridronate and osteoporosis. The modification of the bone mineral density (BMD, g/cm^2) of the patient is the core indicator for neridronate treatment.

Results. Significant increases in the BMD of the lumbar spine (mean difference (MD) = 5.99, 95% confidence interval (95% CI): 3.96–8.02), femoral neck (MD = 4.51, 95% CI: 2.01–7.01) and total hip (MD = 2.55, 95% CI: 2.10–3.00) were found. Greater improvement in the BMD of the lumbar spine and femoral neck could also be detected in patients with postmenopausal osteoporosis than with other causes of osteoporosis. Moreover, significant decreases in serum C-telopeptide of collagen type I (sCTX, standardized mean difference (SMD) = −0.84, 95% CI: −1.32–−0.37) and bone alkaline phosphatase (ALP, MD = −5.29, 95% CI: −7.31–−3.26) levels were observed.

Conclusions. The pool analysis of the selected clinical trials indicates the great benefit of neridronate in improving the condition of patients with osteoporosis of all causes, particularly patients with postmenopausal osteoporosis, which causes an increase in BMD as well as in sCTX and bone ALP levels.

Key words: osteoporosis, bone mineral density, neridronate, bisphosphonates, meta-analysis

Cite as
Chen Q, Shen P, Zhang B, Chen Y, Zhen C. The role of neridronate in the management of osteoporosis: A meta-analysis. *Adv Clin Exp Med*. 2024;33(1):5–12. doi:10.17219/acem/162921

DOI
10.17219/acem/162921

Introduction

Osteoporosis is a condition distinguished by gradually decreasing bone mass and deteriorating bone structure.[1] It is a serious health problem, which is characterized by an increased susceptibility to fragility fractures, leading to poor quality of life and increased morbidity and mortality. It is estimated that 1 in 3 women and 1 in 5 men over the age of 50 worldwide will experience an osteoporotic fracture during their lives.[2] Osteoporosis puts heavy economic burden on patients and society.[3] Although 1/3 of patients with osteoporosis are postmenopausal women, many risk factors can lead to the disease.[4] Despite the cause of osteoporosis, various medications are available to prevent fractures.

Besides the supplementation of calcium and vitamin D, oral bisphosphonates are the most widely used agents in the treatment of osteoporosis.[5,6] A meta-analysis has shown that bisphosphonates are effective in treating thalassemia-induced osteoporosis.[7] However, the broad use of oral bisphosphonates, their low bioavailability,[8] and the fact that they occasionally cause severe gastrointestinal side effects[9] lead to low adherence and compliance by patients. These limitations resulted in the development of intermittent intravenous infusions of bisphosphonates, including neridronate. Neridronate is an amino-bisphosphonate with a structure similar to alendronate and pamidronate. It inhibits bone resorption without changing the mineralization process.[10] Neridronate has been evaluated in several clinical trials for the treatment of osteogenesis imperfecta[11–17] and Paget's disease[18–21] to prevent bone loss and increase bone mineral density (BMD). It can also be used in the treatment of osteoporosis.

Objectives

In this paper, we screened and selected 6 randomized control trials (RCTs) evaluating the effect of neridronate in the treatment of osteoporosis in postmenopausal women,[22,23] β-thalassemia patients,[24] osteoporotic patients with prostate cancer,[25,26] and patients after transplantation[27] to conduct a meta-analysis on the effect of neridronate in the treatment of osteoporosis.

Materials and methods

Search strategy

The Preferred Reporting Items for Systematic Reviews and Meta-Analyses (PRISMA) recommendations were used to guide the present study. PubMed and the Cochrane Central Register of Controlled Trials (CENTRAL) were searched for clinical trials with "neridronate" and "osteoporosis" as keywords. Studies published until August 31, 2021, were considered. The search was limited to studies on humans, with no language restrictions, and included articles published ahead of print. The search strategy for PubMed was: ("neridronate" [all fields] AND "osteoporosis" [all fields]) AND (randomized clinical trial [filter]). The search strategy for CENTRAL was: (neridronate in title abstract keyword AND osteoporosis in title abstract keyword – in trials (word variations were searched)). The reference lists of the identified publications were reviewed manually for additional relevant studies.

Inclusion and exclusion criteria

The inclusion criteria were RCTs using neridronate to treat osteoporosis of any cause. The exclusion criteria were non-RCTs and trials using neridronate for the treatment of diseases other than osteoporosis.

Assessment of risk of bias

Quality assessment and risk of bias evaluations of the selected studies were rated using the Cochrane Collaboration's tool for assessing risk of bias (The Cochrane Collaboration, London, UK), which includes 6 items for the ranking.[28]

Measures of treatment effect

The changes in BMD (expressed as g/cm^2) from baseline were selected as the core indicator, with 95% confidence intervals (95% CIs), and were calculated using the Review Manager (RevMan) v. 5.3 (The Nordic Cochrane Centre, The Cochrane Collaboration, Copenhagen, Denmark; https://revman.cochrane.org/info). Secondary endpoints, such as changes in serum C-telopeptide of collagen type I (sCTX) and bone alkaline phosphatase (ALP) levels were also collected for analysis, when available.

GRADE

Grading of Recommendations, Assessment, Development, and Evaluations for the studies were performed using the GRADEpro website service (https://www.gradepro.org/).[29]

Statistical analyses

The changes in BMD, calcium homeostasis and bone turnover markers were presented as mean ± standard deviation (M ±SD) from baseline. If the BMD changes were presented as mean (95% CI upper level and lower level), the transformation of the data was calculated to find the SD of the data with the RevMan Calculator (https://training.cochrane.org/resource/revman-calculator).[30] Data analysis and the forest plot chart were performed with RevMan v. 5.3 using the inverse variance statistical method

with the random-effects model. The subgroup analysis was employed to explore the potential sources of heterogeneity. Begg's test was utilized to analyze the risk of publication bias using Stata v. 12 software (StataCorp LLC, College Station, USA).

Results

Literature search

The flow diagram of our literature search is presented in Fig. 1. PubMed and CENTRAL databases were independently searched for clinical trials evaluating neridronate for the treatment of osteoporosis. Of the 42 retrieved reports, there were 28 records that required title/abstract screening. Six clinical trial studies were eligible for further analysis.

Study characteristics

The characteristics of the 6 selected studies are summarized in Table 1. All the studies were performed in Italy. The sample sizes of the studies were relatively small (39–118 patients). The study subjects were young adults with β-thalassemia,[24] middle-aged patients needing organ transplantation,[27] osteoporotic patients with prostate cancer,[25,26] and elderly postmenopausal women.[22,23] One study used a neridronate dosage of 50 mg bimonthly,[22] 3 studies[23,26,27] used a dosage of 25 mg monthly, and 1 study used a dosage of 100 mg every 90 days.[24] Two studies[22,24] lasted 24 months, while the other studies[23,25–27] lasted 12 months. All of the studies were randomized and controlled (dosing with calcium and vitamin D). Giannini et al.[27] and Morabito et al.[25] used a double-blind method.

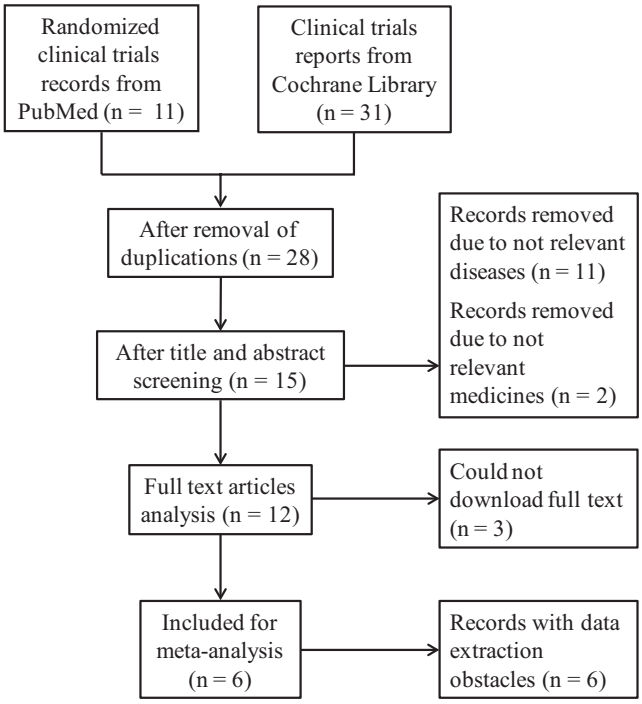

Fig. 1. Flow diagram of the search strategy and study selection process

Assessment of risk of bias

The results of the risk of bias assessments are presented in Fig. 2. Four of the 6 selected studies were open-label studies, which resulted in uncertainty about the blinding methods.

The effect of neridronate on BMD

Our pooled analysis showed that the administration of neridronate significantly increased the BMD compared

Table 1. Summary of analyzed studies with respect to study designs, medication and anthropometric assessment. All studies were conducted in Italy

Study	Disease	Study design	Dose	Duration [months]	Samples (n, neridronate)	Samples (n, control)	Co-intervention	Chelation therapy	Age [years]
Braga et al.[22] 2003	postmenopausal osteoporosis	randomized, open-label, controlled	50 mg i.v. for 2 months	24	39	39	calcium, vitamin D	not mentioned	64.6 ±7.7
Cascella et al.[23] 2005	postmenopausal osteoporosis	randomized, open-label, controlled	25 mg i.m. for 1 month	12	20	20	calcium, vitamin D	not mentioned	72.7 ±5.2
Forni et al.[24] 2012	β-thalassemia patients with osteoporosis	randomized, open-label, controlled	100 mg i.v. for 90 days	24	54	64	calcium, vitamin D	deferirpone	33.1 ±8.8
Morabito et al.[25] 2004	osteoporotic patients with prostate cancer	randomized, double-blind, controlled	25 mg i.m. for 1 month	12	24	24	calcium, vitamin D	not mentioned	74.85 ±4.1
Magno et al.[26] 2005	osteoporotic patients with prostate cancer	randomized, controlled	25 mg i.m. for 1 month	12	30	30	calcium, vitamin D6	not mentioned	73.4 (range: 68–80)
Giannini et al.[27] 2021	transplantation-related osteoporosis	randomized, double-blind, controlled	25 mg i.m. for 1 month	12	22	17	calcium, vitamin D	not mentioned	49.3 ±9.1

i.v. – intravenously; i.m. – intramuscularly.

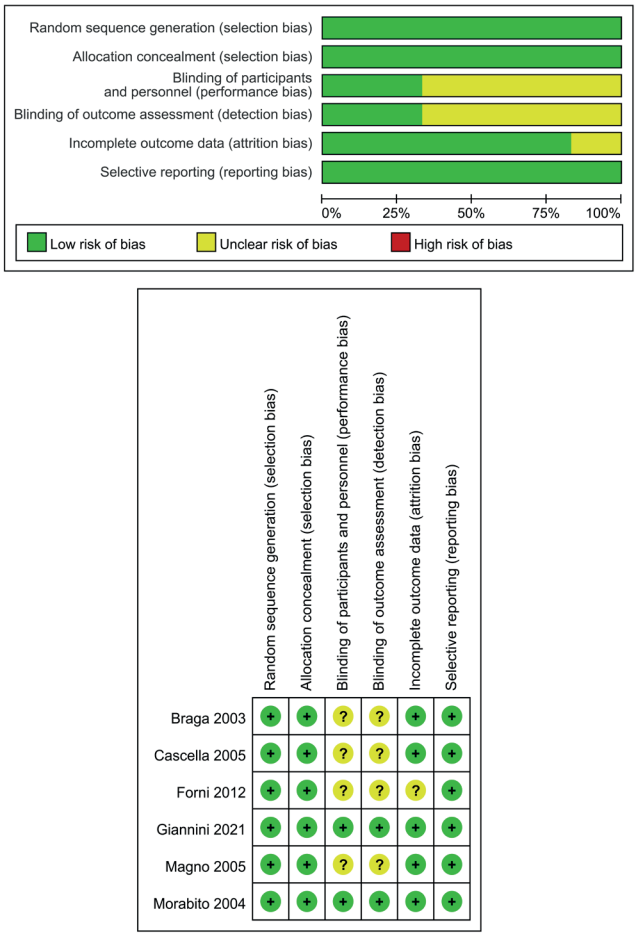

Fig. 2. Risk of bias of the selected studies

to using only calcium and vitamin D, which did not bring about significant improvements in BMD. Six studies[22–27] described an increase in the BMD of the lumbar spine (mean difference (MD) = 5.99, 95% CI: 3.96–8.02; Fig. 3A) and 5[22–25,27] reported BMD changes in the femoral neck (MD = 4.51, 95% CI: 2.01–7.01; Fig. 3B). Four studies[24–27] described changes in the BMD of the total hip (MD = 2.55, 95% CI: 2.10–3.00; Fig. 3C). The results of our pooled analysis suggested that neridronate administration can significantly increase the BMD of the lumbar spine, femoral neck and total hip in patients with osteoporosis, regardless of cause of the disease. The subgroup analysis indicated that greater improvement could be detected in patients with postmenopausal osteoporosis than in those with other causes of osteoporosis when evaluating BMD changes in the lumbar spine and femoral neck (Fig. 3A,B).

The effect of neridronate on sCTX and bone ALP levels

Five of the 6 selected studies recorded a drastic decrease in sCTX and bone ALP level after neridronate administration. Significant decreases in sCTX (standardized mean difference (SMD) = −0.84, 95% CI: −1.32−−0.37; Fig. 4A) and ALP (MD = −5.29, 95% CI −7.31−−3.26, Fig. 4B) levels after neridronate administration were detected at the end of the studies in our pooled analysis. The results suggested that neridronate can significantly reduce sCTX and bone ALP levels.

GRADE

The certainty of evidence for all indicators was graded as high according to GRADE.

Heterogeneity

The analysis of the effect of neridronate on BMD showed significant heterogeneity. A subgroup analysis was based on whether the subgroup approach using postmenopausal osteoporosis significantly reduced this heterogeneity.

Publication bias

Results of Begg's test for each pooled analysis on the effect of neridronate on BMD indicated no evidence of publication bias (for lumbar spine: z = 0.64, p = 0.520; for femoral neck: z = 0.46, p = 0.643; for total hip: z = 0.34, p = 0.734; Fig. 5).

Discussion

Over 200 million people are suffering from osteoporosis worldwide, with aging increasing the incidence rate.[31] It is estimated that 9 million cases of fractures occur due to osteoporosis each year.[2] Bisphosphonates, including alendronate and risedronate, are used as the first line of treatment for osteoporosis.[32] Neridronate is emerging as a potential treatment for several orthopedic diseases, including osteoporosis. This meta-analysis evaluated the efficacy of neridronate on patients with osteoporosis. Six RCTs were included in the analysis. The core indicator of the pharmacological effect were the patient's BMD changes in the lumbar spine, femoral neck and total hip. Secondary indicators were changes in sCTX and bone ALP levels. The GRADE analysis of the studies indicated a high degree of certainty for the evidence.

The main findings of our study are as follows. The administration of neridronate could significantly increase the BMD [g/cm^2] of the lumbar spine (MD = 5.99, 95% CI: 3.96–8.02), femoral neck (MD = 4.51, 95% CI: 2.01–7.01) and total hip (MD = 2.55, 95% CI: 2.10–3.00) in patients with osteoporosis of all causes. The subgroup analysis indicated that a greater improvement could be detected in patients with postmenopausal osteoporosis than in those with the other causes of osteoporosis regarding BMD changes of the lumbar spine (postmenopausal osteoporosis (MD = 8.68, 95% CI: 7.33–10.02) as opposed to other causes (MD = 4.18, 95% CI: 3.27–5.09)) and femoral neck (postmenopausal osteoporosis (MD = 6.77, 95% CI: 5.56–7.99)

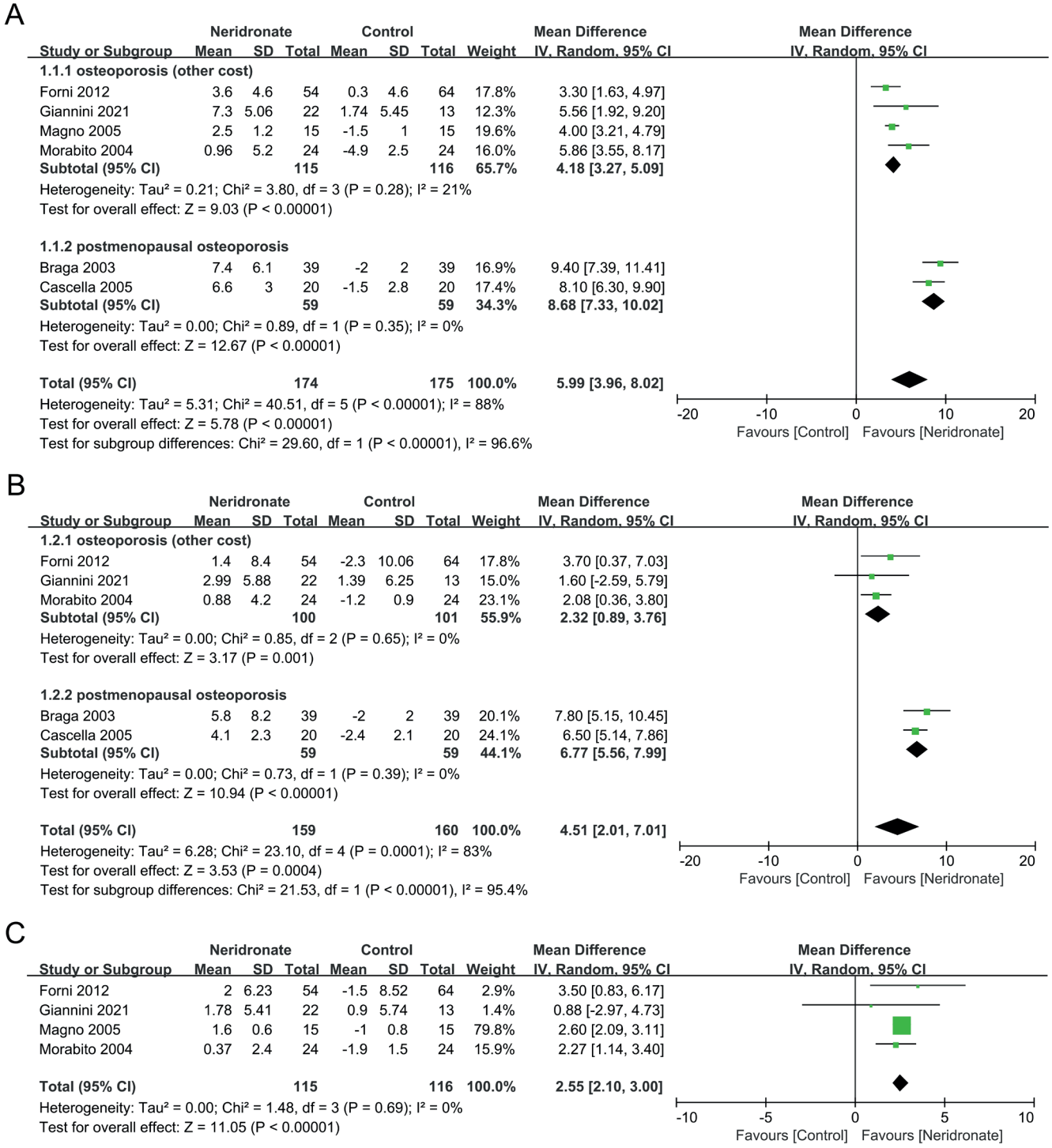

Fig. 3. A. Effect of neridronate on the bone mineral density (BMD) of the lumbar spine expressed as g/cm^2; B. Effect of neridronate on the BMD of the femoral neck expressed as g/cm^2; C. Effect of neridronate on the BMD of the total hip expressed as g/cm^2

SD – standard deviation; 95% CI – 95% confidence interval; df – degrees of freedom.

compared to other causes (MD = 2.32, 95% CI: 0.89–3.76)). This suggests that neridronate brought about better BMD improvements in patients with postmenopausal osteoporosis than in those with osteoporosis resulting from other causes. Different effects of neridronate on the different types of osteoporosis generated high heterogeneity between the 2 subgroups (Fig. 3). However, the subgroup analysis indicated low heterogeneity within the groups. The infusion of neridronate could also significantly reduce sCTX and bone ALP levels.

To our knowledge, this is the first meta-analysis to synthesize the effect of neridronate on BMD and other major indicators in patients with osteoporosis. Neridronate is a bisphosphonate that differs from other oral

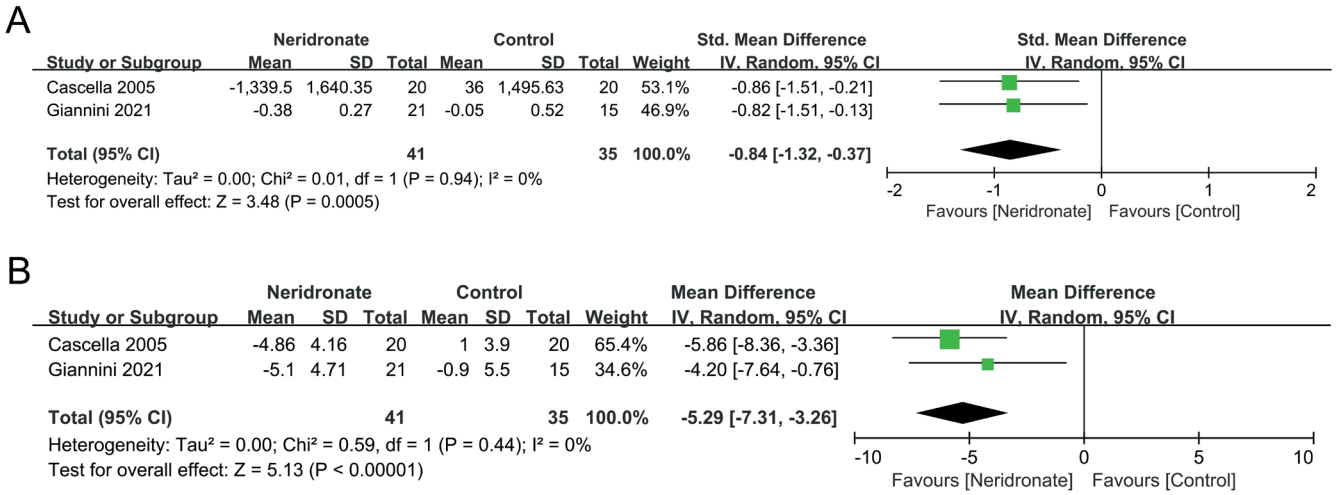

Fig. 4. A. Effect of neridronate on serum C-telopeptide of collagen type I (CTX); B. Effect of neridronate on bone alkaline phosphatase (ALP) concentration

SD – standard deviation; 95% CI – 95% confidence interval; df – degrees of freedom.

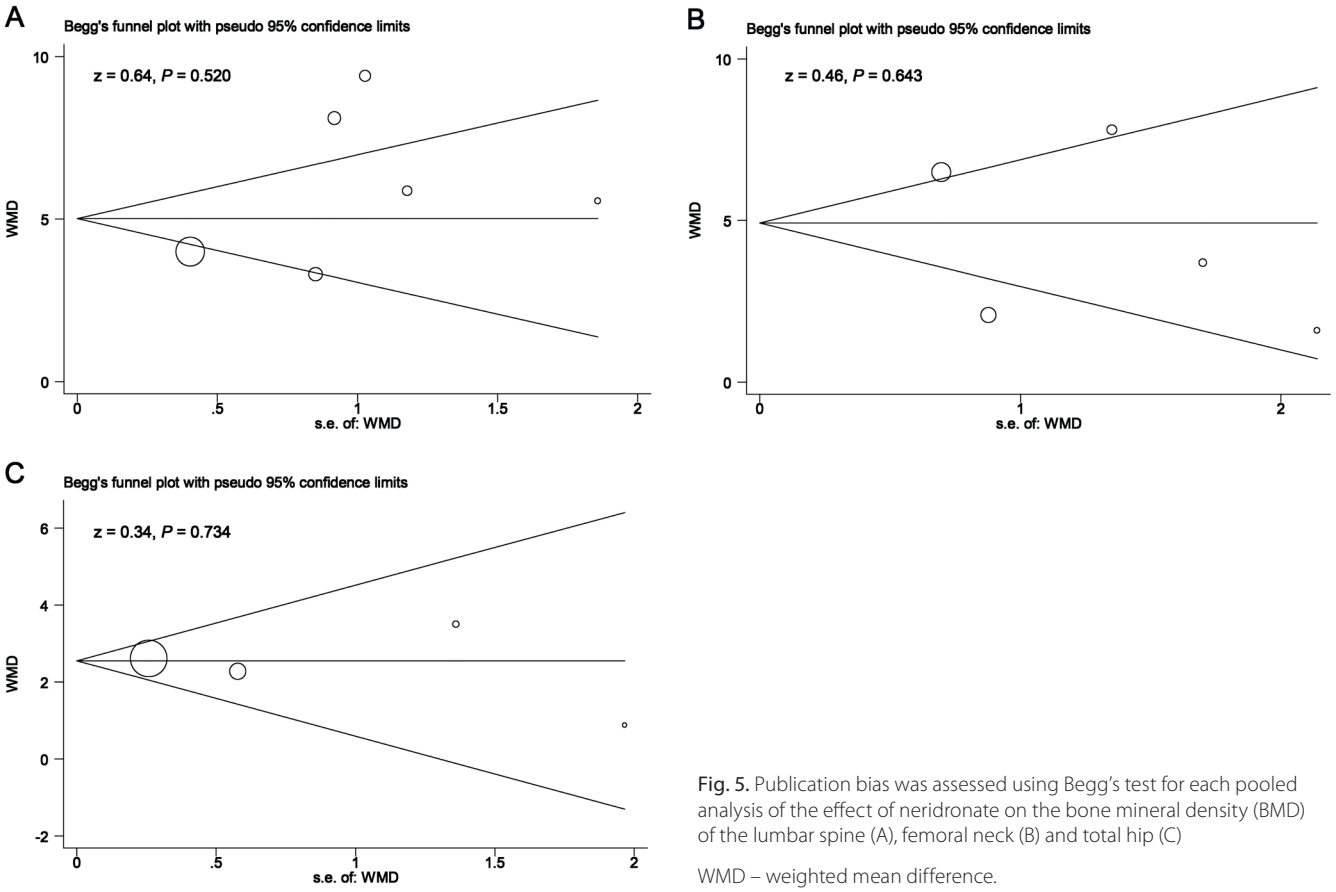

Fig. 5. Publication bias was assessed using Begg's test for each pooled analysis of the effect of neridronate on the bone mineral density (BMD) of the lumbar spine (A), femoral neck (B) and total hip (C)

WMD – weighted mean difference.

bisphosphonates because it is administered by infusion. It has been approved in Italy for the treatment of osteogenesis imperfecta and Paget's disease.

Adami et al. demonstrated that neridronate could significantly increase the BMD of the spine and total hip in a dose-dependent manner during a 12-month course of treatment.[33] Their study also reported a dose-dependent effect on sCTX and ALP levels, which is in accordance with our findings. In our analysis, neridronate brought about significant lumbar spine and femoral neck BMD improvements in patients with postmenopausal osteoporosis. This finding is in line with a 6-year prospective study conducted by Guiducci et al.[34] Another study indicated that neridronate shares the same virtue as the other bisphosphonates of improving postmenopausal osteoporosis.[35] Besides the improvement of postmenopausal osteoporosis, neridronate could also modify the BMD of patients with osteoporosis resulting from other conditions. In our analysis, the BMD of the lumbar spine,

femoral neck and total hip was significantly improved in patients with prostate cancer, β-thalassemia and after transplantation. It is noteworthy that the effect of neridronate in patients with prostate cancer was to prevent bone loss instead of increasing BMD compared to placebo.[25] When applied to patients with β-thalassemia, neridronate led to a significant increase in BMD.[24] Similar findings were reported in a previous meta-analysis by Tsartsalis et al.[7] However, it was also reported that zoledronate had a better effect than neridronate with regard to improving the BMD of the lumbar spine in patients with β-thalassemia.[7,36] Organ transplantation can result in bone loss. Ho et al. analyzed 9 studies and found that using bisphosphonate after a liver transplant improves BMD and reduces fracture rates,[37] which is in line with the clinical trial results reported by Giannini et al.[27] They stated that neridronate improved BMD in patients after heart, lung and liver transplantation. The pooled analysis of this study indicated that neridronate infusion could significantly increase the BMD of the lumbar spine, femoral neck and total hip compared to a placebo in patients with postmenopausal osteoporosis, prostate cancer, β-thalassemia, and after transplantation. Neridronate infusions also provide benefits by significantly reducing bone turnover biomarkers such as sCTX and ALP levels. This is the basis for the BMD improvement of the medication and can be detected across the clinical trials where bisphosphonates were used.[34] Reduction in these biomarkers signifies a beneficial impact of neridronate on inhibiting osteoclast-mediated bone resorption, a key underlying mechanism in osteoporosis.

Limitations

Although all the selected studies were RCTs, the samples were relatively small. Unfortunately, one RCT[33] was not included due to obstacles in data extraction. More studies are needed to verify the effect of neridronate on osteoporosis with causes other than being a postmenopausal woman. Since neridronate use is permitted only in Italy, the effect of the medication on patients of other nationalities could not be assessed. Finally, based on the current findings, more studies should be done to compare the effect of neridronate and other oral bisphosphonates in the treatment of osteoporosis.

Conclusions

In summary, significant evidence has indicated that the long-term administration of neridronate could significantly increase the BMD of the lumbar spine, femoral neck and total hip in patients with postmenopausal osteoporosis and osteoporosis caused by prostate cancer, β-thalassemia and transplantation. It also decreases sCTX and ALP levels. These results are in accordance with previous findings that bisphosphonate medications, including neridronate, can provide significant improvements in the treatment of osteoporosis. Hence, neridronate treatment offers a promising therapeutic intervention for the management of osteoporosis, particularly among patients with postmenopausal osteoporosis, thus providing hope for improved bone health.

Availability of data and materials

The analyzed datasets generated during the study are available from the corresponding author upon reasonable request.

ORCID iDs

Qiaojie Chen https://orcid.org/0000-0003-0716-190X
Pingping Shen https://orcid.org/0000-0002-8842-606X
Bo Zhang https://orcid.org/0000-0002-6741-3286
Yang Chen https://orcid.org/0000-0001-6883-3402
Chunli Zh https://orcid.org/0000-0001-9234-8589

References

1. Dowson C, Lewis R. Osteoporosis. In: *Rheumatology*. Amsterdam, the Netherlands:Elsevier; 2010:289–305. doi:10.1016/B978-0-443-06934-5.00020-6
2. Porter JL, Varacallo M, Castano M. Osteoporosis (nursing). In: *StatPearls*. Treasure Island, USA: StatPearls Publishing; 2023. PMID:33760540.
3. Osteoporosis prevention, diagnosis, and therapy. *NIH Consens Statement*. 2000;17(1):1–45. PMID:11525451.
4. Zhu X, Bai W, Zheng H. Twelve years of GWAS discoveries for osteoporosis and related traits: Advances, challenges and applications. *Bone Res*. 2021;9(1):23. doi:10.1038/s41413-021-00143-3
5. McClung MR, Geusens P, Miller PD, et al. Effect of risedronate on the risk of hip fracture in elderly women. *N Engl J Med*. 2001;344(5):333–340. doi:10.1056/NEJM200102013440503
6. Chesnut CH, Skag A, Christiansen C, et al. Effects of oral ibandronate administered daily or intermittently on fracture risk in postmenopausal osteoporosis. *J Bone Miner Res*. 2004;19(8):1241–1249. doi:10.1359/JBMR.040325
7. Tsartsalis AN, Lambrou GI, Tsartsalis D, et al. The role of biphosphonates in the management of thalassemia-induced osteoporosis: A systematic review and meta-analysis. *Hormones (Athens)*. 2018;17(2):153–166. doi:10.1007/s42000-018-0019-3
8. Fleisch HA. Osteoclasts in the reticule. Molecular mechanisms of bisphosphonates [in German]. *Pharm Unserer Zeit*. 2001;30(6):500–504. doi:10.1002/1615-1003(200111)30:6<500::AID-PAUZ500>3.0.CO;2-G
9. Adami S, Bhalla AK, Dorizzi R, et al. The acute-phase response after bisphosphonate administration. *Calcif Tissue Int*. 1987;41(6):326–331. doi:10.1007/BF02556671
10. Gatti D, Adami S. New bisphosphonates in the treatment of bone diseases. *Drugs Aging*. 1999;15(4):285–296. doi:10.2165/00002512-199915040-00004
11. Adami S, Gatti D, Colapietro F, et al. Intravenous neridronate in adults with osteogenesis imperfecta. *J Bone Miner Res*. 2003;18(1):126–130. doi:10.1359/jbmr.2003.18.1.126
12. Antoniazzi F, Zamboni G, Lauriola S, Donadi L, Adami S, Tatò L. Early bisphosphonate treatment in infants with severe osteogenesis imperfecta. *J Pediatr*. 2006;149(2):174–179. doi:10.1016/j.jpeds.2006.03.013
13. D'Eufemia P, Finocchiaro R, Zambrano A, et al. Serum creatine kinase isoenzymes in children with osteogenesis imperfecta. *Osteoporos Int*. 2017;28(1):339–346. doi:10.1007/s00198-016-3729-x
14. Gatti D, Antoniazzi F, Prizzi R, et al. Intravenous neridronate in children with osteogenesis imperfecta: A randomized controlled study. *J Bone Miner Res*. 2005;20(5):758–763. doi:10.1359/JBMR.041232
15. Gatti D, Rossini M, Viapiana O, et al. Teriparatide treatment in adult patients with osteogenesis imperfecta type I. *Calcif Tissue Int*. 2013;93(5):448–452. doi:10.1007/s00223-013-9770-2

16. Gatti D, Viapiana O, Lippolis I, et al. Intravenous bisphosphonate therapy increases radial width in adults with osteogenesis imperfecta. *J Bone Miner Res*. 2005;20(8):1323–1326. doi:10.1359/JBMR.050312
17. Idolazzi L, Fassio A, Viapiana O, et al. Treatment with neridronate in children and adolescents with osteogenesis imperfecta: Data from open-label, not controlled, three-year Italian study. *Bone*. 2017; 103:144–149. doi:10.1016/j.bone.2017.07.004
18. Adami S, Bevilacqua M, Broggini M, et al. Short-term intravenous therapy with neridronate in Paget's disease. *Clin Exp Rheumatol*. 2002; 20(1):55–58. PMID:11892710.
19. Filipponi P, Cristallini S, Policani G, Casciari C, Gregorio F. Paget's disease of bone: Benefits of neridronate as a first treatment and in cases of relapse after clodronate. *Bone*. 1998;23(6):543–548. doi:10.1016/S8756-3282(98)00133-1
20. Merlotti D, Gennari L, Martini G, et al. Comparison of different intravenous bisphosphonate regimens for Paget's disease of bone. *J Bone Miner Res*. 2007;22(10):1510–1517. doi:10.1359/jbmr.070704
21. Merlotti D, Rendina D, Gennari L, et al. Comparison of intravenous and intramuscular neridronate regimens for the treatment of Paget disease of bone. *J Bone Miner Res*. 2011;26(3):512–518. doi:10.1002/jbmr.237
22. Braga V, Gatti D, Colapietro F, et al. Intravenous intermittent neridronate in the treatment of postmenopausal osteoporosis. *Bone*. 2003;33(3):342–345. doi:10.1016/S8756-3282(03)00084-X
23. Cascella T, Musella T, Orio F, et al. Effects of neridronate treatment in elderly women with osteoporosis. *J Endocrinol Invest*. 2005;28(5): 202–208. doi:10.1007/BF03345373
24. Forni GL, Perrotta S, Giusti A, et al. Neridronate improves bone mineral density and reduces back pain in β-thalassaemia patients with osteoporosis: Results from a phase 2, randomized, parallel-arm, open-label study. *Br J Haematol*. 2012;158(2):274–282. doi:10.1111/j.1365-2141.2012.09152.x
25. Morabito N, Gaudio A, Lasco A, et al. Neridronate prevents bone loss in patients receiving androgen deprivation therapy for prostate cancer. *J Bone Miner Res*. 2004;19(11):1766–1770. doi:10.1359/JBMR.040813
26. Magno C, Anastasi G, Morabito N, et al. Preventing bone loss during androgen deprivation therapy for prostate cancer: Early experience with neridronate. *Eur Urol*. 2005;47(5):575–581. doi:10.1016/j.eururo.2005.01.012
27. Giannini S, Poci C, Fusaro M, et al. Effect of neridronate in osteopenic patients after heart, liver or lung transplant: A multicenter, randomized, double-blind, placebo-controlled study. *Panminerva Med*. 2021;63(2):214–223. doi:10.23736/S0031-0808.21.04401-3
28. Higgins JP, Altman DG, Gøtzsche PC, et al; Cochrane Bias Methods Group; Cochrane Statistical Methods Group. The Cochrane Collaboration's tool for assessing risk of bias in randomised trials. *BMJ*. 2011;343:d5928. doi:10.1136/bmj.d5928
29. McMaster University and Evidence Prime Inc. GRADEpro GDT: GRADEpro Guideline Development Tool. 2021. https://www.gradepro.org/.
30. Drahota A, Bellor E. RevMan Calculator. 2021. https://training.cochrane.org/resource/revman-calculator.
31. Prince RL, Lewis JR, Lim WH, et al. Adding lateral spine imaging for vertebral fractures to densitometric screening: Improving ascertainment of patients at high risk of incident osteoporotic fractures. *J Bone Miner Res*. 2019;34(2):282–289. doi:10.1002/jbmr.3595
32. Hariri L, Rehman A. Estradiol. In: *StatPearls*. Treasure Island, USA: StatPearls Publishing; 2023. PMID:31747204.
33. Adami S, Gatti D, Bertoldo F, et al. Intramuscular neridronate in postmenopausal women with low bone mineral density. *Calcif Tissue Int*. 2008;83(5):301–307. doi:10.1007/s00223-008-9179-5
34. Guiducci L, Vassalle C, Parchi P, Maffei S. Monthly intramuscular neridronate for the treatment of postmenopausal osteoporosis: Results of a 6-year prospective Italian study. *Int J Endocrinol*. 2019;2019: 9802827. doi:10.1155/2019/9802827
35. Fan Q, Wang J. The efficacy and safety of bisphosphonates for osteoporosis in women older than 65 years: A meta-analysis. *Curr Pharm Des*. 2020;26(32):4022–4030. doi:10.2174/1381612826666200423092602
36. Mamtani M, Kulkarni H. Bone recovery after zoledronate therapy in thalassemia-induced osteoporosis: A meta-analysis and systematic review. *Osteoporos Int*. 2010;21(1):183–187. doi:10.1007/s00198-009-0875-4
37. Ho OTW, Ng WCA, Ow ZGW, et al. Bisphosphonate therapy after liver transplant improves bone mineral density and reduces fracture rates: An updated systematic review and meta-analysis. *Transpl Int*. 2021;34(8):1386–1396. doi:10.1111/tri.13887

Face-like pareidolia images are more difficult to detect than real faces in children with autism spectrum disorder

Gülsüm Akdeniz[A–F]

Faculty of Medicine, Ankara Yıldırım Beyazıt University, Turkey

A – research concept and design; B – collection and/or assembly of data; C – data analysis and interpretation;
D – writing the article; E – critical revision of the article; F – final approval of the article

Advances in Clinical and Experimental Medicine, ISSN 1899–5276 (print), ISSN 2451–2680 (online) *Adv Clin Exp Med*. 2024;33(1):13–19

Address for correspondence
Gülsüm Akdeniz
E-mail: gakdeniz@ybu.edu.tr

Funding sources
None declared

Conflict of interest
None declared

Acknowledgements
The author would like to thank Bilal Sahutoglu for helping us with recruiting participants and Nur Efsan Akinci for statistical analysis.

Received on October 19, 2022
Reviewed on February 28, 2023
Accepted on April 1, 2023

Published online on May 11, 2023

Abstract

Background. Research on the diagnosis, treatment and pathophysiology of neurodevelopmental disorders is multifaceted, requiring the use of genetics, imaging, psychology, and artificial intelligence (AI). Autism spectrum disorder (ASD) is a neurodevelopmental disorder characterized by a limited ability to communicate and a limited interest in social environments. Facial recognition is really important in daily life. Seeing faces in unusual objects, e.g., a face in a cloud, is called face pareidolia.

Objectives. Although more evidence points to a greater role of genetic factors in ASD, neuropsychological tests have an important role in diagnosing ASD. The aim of the study was to investigate how face perception is processed in children with autism using a new digital test that consists of faces and pareidolia images.

Materials and methods. Twenty typically developing (TD) children (8 male, 12 female) between 6 and 16 years of age and 21 children with ASD (14 male, 7 female) between 6 and 14 years of age were included in the study. A new neuropsychological test called the digital pareidolia test was administered to the participants. The study consisted of 2 stages: a face condition and a pareidolia condition.

Results. Our results showed that children with autism (n = 21) were less successful in identifying both face and pareidolia images, and were slower to react in both conditions than children from the TD group. Both children with ASD and the TD group reacted faster to face images than pareidolia images.

Conclusions. The findings in this study are in agreement with atypical and different face perceptions in autism which cause social difficulties. We demonstrated that the digital face and pareidolia test has considerable potential for use as a neuropsychological test that can specify the diagnosis and progression of autism in subclinical areas. Pareidolia faces and real faces are processed in a common way.

Key words: autism spectrum disorders, face, face perception, pareidolia, face-like images

Cite as
Akdeniz G. Face-like pareidolia images are more difficult to detect than real faces in children with autism spectrum disorder. *Adv Clin Exp Med*. 2024;33(1):13–19. doi:10.17219/acem/162922

DOI
10.17219/acem/162922

Background

Recent approach to neurological diseases is not unidirectional but requires multidirectional research in areas such as genetics, imaging, diagnostic testing, treatment, and disease course. For example, to cure neurological diseases, norepinephrine transporter inhibitors are used to change neurotransmitter gradients in the brain.[1] Additionally, in 1 study, researchers used a faster protocol for converting circulating monocytes to neuron-like cells which express neuronal marker genes.[2]

Autism spectrum disorder (ASD) is a neurodevelopmental disorder defined as the reduced ability to communicate in social environments, repetitive behaviors and limited interests.[3] Many factors that affect ASD, such as the disruption of mitochondrial DNA functions, have been identified as a cause of metabolic diseases and have been investigated in relation to the pathogenesis of neurodegenerative diseases. Mitochondrial functions become less flexible under constant stress where mitochondrial functions are compromised. Neurological and psychiatric disorders have also been associated with the activation of the tryptophan–kynurenine (Trp–Kyn) pathway, which contributes to the formation of stress and inflammatory pathological conditions.[4] The Trp–Kyn pathway, its correlation with the immune system, tolerogenic shift against low-grade inflammation, and the relation of this pathway with the autism spectrum, one of the major psychiatric diseases, have also been examined.[5]

The effects of statin therapy in patients with ASD, anxiety and many other neurological disorders, as well as the side effects of medicines are often examined for the risks they are related to in patients with autism.[6] A study by Lee et al. indicated that maternal immune activation increases the ASD risk in rat infants.[7] They analyzed microbiota profile, behavior, anxiety-like recurrent behavior, and myelination levels in rat infants. These rat infants had a brain–gut–microbiota axis with hypomyelination, autism-like microbiota profile, behavioral deficits, and exhibited anxiety-like and recurring behavior.[7] In another study, Abuaish et al. found that gastrointestinal problems and gut bacteria dysbiosis, such as *Clostridium* explosion, are related to autism.[8] The researchers examined 2 methods to control the microbiota in an autistic rat and how they affected the rat's behaviors: 1) different fecal *Clostridium* spp. and grades and 2) hippocampal transcript levels. Their results suggest that preclinical intervention and the brain–gut axis are related to the etiology of autism.[8] Not only gut bacteria are related to behaviors; the Pavlovian-instrumental transfer can be used to guide behaviors. Researchers conducted Pavlovian-instrumental transfers in 100 participants and found a link between outcome-specific Pavlovian-instrumental transfer and individual working memory. The most important finding is that working memory is not associated with the balance between congruent and incongruent choices. The obtained results can be interpreted for human behavior.[9]

Faces are really important in communication. Seeing faces where there are none, e.g., likening a house to a face, is called face pareidolia. When we compared the previous evidence with the new results, it became clear that neurological disorder patients adapt to social signals less than healthy people.[10] Therefore, interpersonal space is very important for these patients. Such space is described as the distance people keep between themselves and other people. Candini et al. suggested a connection between neurobehavioral components of interpersonal space and fundamental physiological processes.[11] In a study by Ellena et al., healthy volunteers' skin conductance responses were measured when observing 3D avatar images of joyful, fearful and neutral faces getting closer.[12] It was found that responses to fearful faces were modulated by distance, yet it did not apply to joyful and neutral faces.

Although atypical face perception is not among the diagnostic criteria for ASD, a study has shown that it is common in this population.[13] Since the recognition of a person's face is a critical aspect of everyday social interactions, it has been studied in ASD.[14] For example, children with

Fig. 1. Examples of presented face and pareidolia images

ASD have difficulties in recognizing facial identity, utilizing facial cues and perceiving face motion.[15–17]

A study revealed that children with autism not only have difficulties with face perception but also with the perception of illusory faces and face-like images.[18] It was observed that children and teenagers with ASD responded to face and pareidolia images less than the typically developing (TD) group and had a higher threshold in recognizing faces.[19] Despite these results, studies examining the relationship between autism and pareidolia are limited.

As mentioned earlier, face pareidolia refers to confusing inanimate objects with faces.[20] Apart from visual pareidolia, there is also noise pareidolia, in which people hear human voices in different, nonhuman noises.[21] Williams and Blagrove examined human voice perception from electronic voices and showed relationships between Highly Sensitive Person Scale points and detection of ambiguous stimuli which were electronic voices.[22]

Table 1. Demographics of the participants

Characteristics		TD (n = 20)	ASD (n = 21)
Age, median (Q1, Q3)		12.0 (6.25, 14.75)	10 (8, 11)
Male/female		8/12	14/7
Age at diagnosis	<2 years	–	1
	2–3 years		4
	4–6 years		11
	7–11 years		3
	>12 years		1
Performance IQ, median (Q1, Q3)		96 (80, 103)	93 (80, 101)
Verbal IQ, median (Q1, Q3)		92 (81, 102)	89 (74, 97)
Inattention, median (Q1, Q3)		2 (0, 5)	6 (1, 8)
Hyperactivity/impulsivity, median (Q1, Q3)		2 (0, 4)	5 (2, 7)
Disruptive behavior [%]		20.71	37.42

TD – typically developing; ASD – autism spectrum disorder; Q1 – 1st quartile; Q3 – 3rd quartile.

Objectives

A new review pointed out that not only establishing the diagnostic criteria in psychiatric disorders but also the research on neurodevelopmental disorders benefit from preclinical studies.[23] Neurological disorders such as schizophrenia and autism are connected to the lack of neuronal construction.[2] Although ASD can be detected using point mutations, chromosome anomalies and microaberrations,[24] new neuroimaging and neuropsychological tests should be developed for diagnosis.

We aimed to examine whether children with ASD and TD children differ from each other in terms of responses to faces and pareidolia images.

Materials and methods

Akdeniz showed that face and face pareidolia perception are processed in the early phases of visual perception.[25] Another study infers that pareidolia is a mirroring of the visual system which perceives human faces as well as evocative and cognitive connection.[20] Based on this information, we tested pareidolia in 21 children with ASD and 20 TD children, after obtaining the consent of their parents. Children in the ASD group were diagnosed by an expert clinician using the Diagnostic and Statistical Manual of Mental Disorders (DSM 5) criteria.[1] None of the children had a comorbid disorder or disease. Additionally, results of the physical and neurological examinations of all the children were within the normal ranges and none of the children used any medications. Table 1 shows the demographics of the participants. The average performance IQ of both groups was similar. Moreover, parents completed a test to determine their child's inattention and hyperactivity/impulsivity. Attention deficit was higher in children with autism than in healthy children, and more parents stated that these children exhibited destructive behaviors. This study was carried out with the approval of the ethics committee of the Dr. Sami Ulus Maternity and Children Training and Research Hospital (Ankara, Turkey; approval No. E-21/02-094).

Sixty photographs with equal numbers of faces, face scrambles, pareidolia images, and pareidolia scrambles were used in this study (Fig. 1). Scrambled photos were disordered versions of faces and pareidolia photos, and were prepared using MATLAB software (MathWorks, Natick, USA). Pareidolia and face images were equal in size, tone and intensity of light, and all images presented neutral faces. All photos were transformed into digital form and loaded into Google Forms platform (Google, Mountain View, USA). The study consisted of 2 stages: a face condition and a pareidolia condition. In both conditions, the photos were shown one by one as a sequence of faces and scrambles, and the children were instructed to press the button when they saw a face or face-like photo on the screen. Scrambled images were non-target stimulis; therefore, they were not included in the statical analyses. In addition to the reaction time to face or face-like images, whether the children recognized them or not was recorded as "yes" or "no".

Statistical analyses

All statistical analyses were conducted using IBM SPSS v. 24 software (IBM Corp., Armonk, USA). A value of $p < 0.05$ was considered statistically significant. Since the sample size was small, the Shapiro–Wilk test was used to analyze whether the participants were normally distributed. It was found that the distribution of variables departed significantly from normality. Based on this outcome, the median (1st quartile (Q1), 3rd quartile (Q3)) scores of all the data were analyzed using descriptive statistics

to report response variables and demographic information of the participants. In addition, descriptive statistics were used to detect the number of correct responses and the accuracy rate. The Mann–Whitney U nonparametric test was used to analyze whether the means of the ASD and TD groups differed significantly in face and pareidolia conditions. Differences in reaction time and accuracy rate between the face and pareidolia conditions within the groups were also investigated and compared with each other.

Results

Twenty TD children (8 male, 12 female) whose age ranged between 6 and 16 (median = 12, Q1 = 6.25, Q3 = 14.75) and 21 children with ASD (14 male, 7 female) who were between 6 and 14 years of age (median = 10, Q1 = 8, Q3 = 11) participated in the study (Table 1).

In terms of the face condition, the median (Q1, Q3) score for reaction time was 2.67 s (1.76, 3.45) in children with ASD, while it was 1.14 s (0.96, 1.27) in the TD children. For the pareidolia condition, the median (Q1, Q3) score for reaction time was 2.55 s (2.32, 3.54) in children with ASD, while it was 1.20 s (1.04, 1.57) in the healthy children (Table 2). As the mean scores for reaction time show, both children in the ASD and TD groups reacted faster to face images than to pareidolia images. However, TD children exhibited larger differences in reaction times between face and pareidolia conditions than children with ASD (Fig. 2).

The Mann–Whitney U nonparametric tests were applied to assess whether the ASD and TD groups differed significantly for the 2 conditions. The results showed that children with ASD reacted significantly later to both face images ($Z = -4.36$, $p = 0.001$) and pareidolia images ($Z = -3.47$, $p < 0.001$) than TD children (Table 2).

The accuracy rate was defined as the percentages of correct responses to each face and pareidolia image by TD children and children with ASD. Even though TD children achieved a 100% accuracy rate for each face image, just 7 out of the 15 face images were responded to with an accuracy rate of 100% by children with ASD. However, since the ASD group achieved 95.2% accuracy in other face images, there were no significant differences between the 2 groups.

For the pareidolia paradigm, the mean accuracy was 96% in healthy children, whereas the mean for children with ASD was 83%. Ten out of 15 pareidolia images were responded to by healthy children with a 100% accuracy rate. However, just the 1st pareidolia image had the greatest

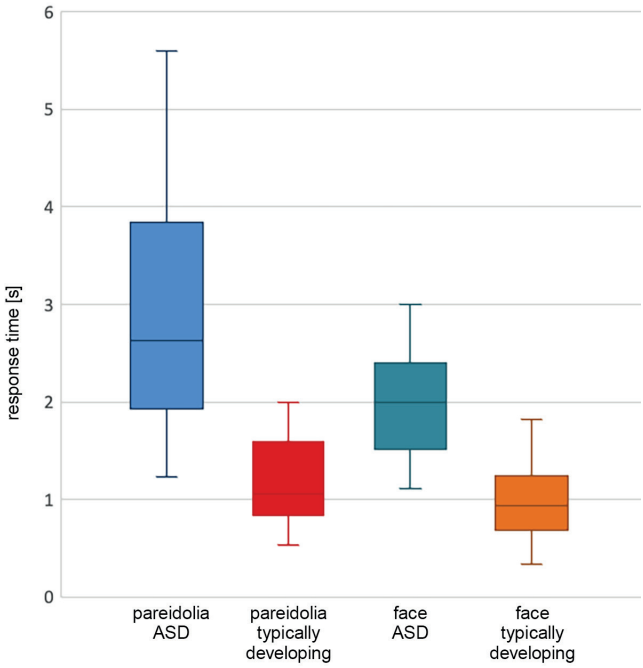

Fig. 2. Comparison of the response time of typically developing (TD) and autism spectrum disorder (ASD) groups to the first images of face and pareidolia images

accuracy rate in children with ASD, which was 90.4%. Moreover, the lowest accuracy rate was 85% in the TD group, while it was 52.3% in the ASD group. The lowest accuracy rates were related to the same pareidolia images, which were the 3rd and 12th images in the 2 groups. Regarding this, the greatest difference in accuracy rates between the TD children and the ASD group again concerned the 3rd and 12th pareidolia images (Fig. 3).

No statistically significant difference was observed when comparing ASD children's disruptive behaviors with the TD group. Responses to stimuli, such as face and pareidolia, affected the participants' performances differently. Also, the age of children with autism did not affect their responses to stimuli.

Discussion

Studies that explore how visual face processing occurs in children with autism are needed. The precise reason for the disordering of face perception in ASD has not yet been fully identified. In this study, we examined whether children with ASD differ from TD children using a new test,

Table 2. Comparison of the groups according to the reaction time for face and pareidolia images

Type of images	RT-TD, median (Q1, Q3)	RT-ASD, median (Q1, Q3)	t; Z	p-value
Pareidolia	1.20 (1.04, 1.57)	2.55 (2.32, 3.54)	–3.47*	0.001
Face	1.14 (0.96, 1.27)	2.67 (1.76, 3.45)	–4.36*	<0.001

RT – reaction time; TD – typically developing; ASD – autism spectrum disorder; Q1 – 1st quartile; Q3 – 3rd quartile; * Mann–Whitney U test (other – Mann–Whitney U nonparametric test).

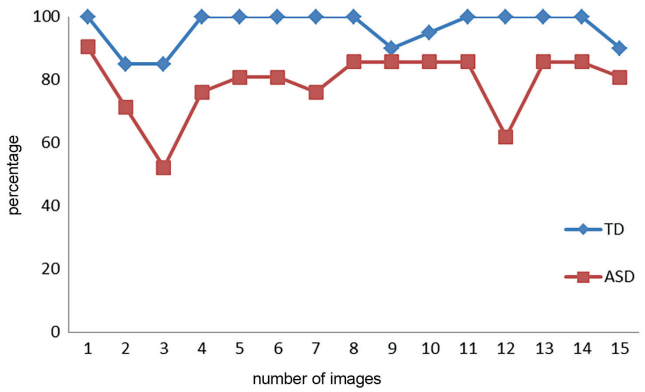

Fig. 3. Percentage of children accurately identifying each of the 15 pareidolia images

TD – typically developing; ASD – autism spectrum disorder.

which utilizes digital face and pareidolia images, to understand how face perception is processed in the brain. Our study had 2 remarkable outcomes. First, the results showed that children with ASD respond to both face and pareidolia images significantly later than TD children. Second, the ASD group had a significantly lower accuracy rate than the controls for pareidolia images, although the 2 groups did not significantly different from each other in terms of the accuracy rate for face images.

Behaviors may be triggered by emotions. Battaglia et al. examined action control capability changes in 60 volunteers via stop-signal task, and used happy, fearful and neutral body postures in an experimental study. They found that both happy and fearful body postures improved the ability to suppress a current action compared to neutral body postures.[26] Emotional expressions are related to gaze cues. From the information obtained as a result of noninvasive brain stimulation, it has been shown that the perception of gaze cues occurs in the amygdala and superior temporal sulcus (STS) regions of the brain.[27] The gaze cue refers to communicating with the gaze direction of others that causes the attention to be directed reflexively and the spatial position of the object to be perceived more quickly.[27]

Emotional expressions are vital for communication and behavior. Quick processing of interpersonal emotional perceptions in the brain is important in social life. Borgomaneri et al. showed happy, neutral and fearful images to healthy volunteers during transcranial magnetic stimulation. Corticospinal excitability increased in the healthy volunteers' right motor cortex when they were looking at fearful and happy images in comparison to neutral images.[28]

In a review of ASD studies, the striatum and cerebellum were associated with changed cognitive, motor and sensory functions.[29] Motor functions are mostly associated with Purkinje cell loss and social dysfunction, which can help with the early diagnosis and valued perspective of the disorder.[29] As we learn more and more about the pathophysiology of the disorder, we can develop more efficient treatments, find ways to avoid the disorder, and more accurately diagnose it. Considering the results of a study that classified the predominant neural endophenotypes of autism, scientists who study different aspects of ASD need to work together to obtain significant data.[30] Due to complexity of these studies neuropsychological tests can be considered a priority and promising area in neuroscience.

Another research on the pathophysiology of neurological disorders is a study of 52 people between 5 and 10 years of age, in which 26 people with autism and 26 healthy controls were examined for brain abnormalities using structural magnetic resonance imaging (sMRI) images from the Autism Brain Imaging Data Exchange (ABIDE) database. The findings showed white matter, gray matter volume and total brain volume increase in the Hammers Atlas of autistic participants. Using sMRI, we can identify the abnormal structural brain regions and their connection with ASD, which can help accurately diagnose autism early. We are even able to improve personal treatment by examining abnormal brain regions and seeing effectiveness of the treatment.[31] However, it is difficult and expensive to apply sMRI in practice. For this reason, even the researchers took the images from the ABIDE database. The digital pareidolia test we recommend is usable, inexpensive and accessible.

Face and face pareidolia perception in neurological disorders is still not precisely elucidated. Poor performance in face perception tests is unlikely to be understood taking into account only divergent general cognitive abilities, but it can be understood in perceptual integration and social cognition.[32] This outcome provides a novel understanding of the origins of face perception in ASD and induces neuropsychological neuroscience research. Face pareidolia is a complex visual illusion where a meaningful object is perceived as a result of seeing random patterns that resemble a face.[33] We found that the ASD group reacted to pareidolia images later and had lower accuracy rates than the TD group. Similarly, a previous study revealed that people with ASD had a significantly higher threshold to recognize face-like images. The ASD patients did not recognize the images that were easily recognized by the TD group and they gave fewer responses to faces.[19] Furthermore, children with ASD could define fewer pareidolia faces than their TD peers, even though the 2 groups did not differ in terms of the number of total defined objects.[18] Our results are consistent with those of the previous studies.

We found that children with autism showed poor performance in terms of face perception. These results are in line with previous studies which showed that children with ASD have different or atypical face processing. For example, Pierce revealed that subject-specific regions (e.g., frontal cortex, primary visual cortex) located opposite to the fusiform face area (FFA) that is active when looking at faces in normal individuals were activated in ASD individuals, meaning that they use different neural pathways to recognize faces.[34] In addition, Hadjikhani et al. observed that the right amygdala, inferior frontal cortex (IFC), STS, and face-related somatosensory and premotor cortex, which are involved in face perception,

showed hypoactivity in ASD adults.[35] Moreover, some researchers claimed that individuals with ASD showed an atypically weak central coherence which is required to unite sensory information in a holistic way; therefore, children with ASD perceived faces in a piecemeal manner.[36,37] However, another recent study revealed that children with autism were able to perceive holistically face-like objects like the TD group after looking at the stimuli, even though the TD group was significantly more likely to exhibit faster response.[38] Our results are consistent with the previous studies.[36,37] We believe these results can be attributed to the slower process of neural mechanisms of facial recognition in children with autism compared to the TD group.

We found that children with ASD showed poor performance in both face and pareidolia conditions. In a study consistent with our results, Rahman and van Boxtel reported that it is harder to perceive non-face stimuli as faces compared to real faces.[39] Findings suggest that face perception in general and in face pareidolia is not related to autism-like traits but to a person's age. Perception ability and inversion effect do not adhere to autism-like traits.[39] It can be explained by the fact that both real and pareidolia face perception require coaction between top-down and bottom-up processing in the FFA, frontal and occipitotemporal areas of the brain.[40] Atypical activation of areas involving face perception in ASD children may also cause the atypical perception of pareidolia faces.[35] On the other hand, the activation of the right prefrontal cortex (PFC) was observed during both real and illusory face processing.[40] Considering the abovementioned findings, we suppose that overgrowth and neural dysfunction in multiple brain regions may cause the early mechanisms of autism. However, some studies which are not consistent with our interpretation suggest that abnormalities in the PFC of children with ASD are mainly seen in the medial and dorsolateral parts of the brain responsible for executive functions, not processing faces.[41–43]

In the future, our new pareidolia test should be used in adults with autism and other psychiatric disorders and the results should be compared. There are more degenerative in cognitive processes in bipolar and schizophrenia diseases.[44] Moreover, further information could be obtained if the parents or siblings of the participating children would also be tested.

Limitations

The present study has some limitations. The fact that the number of male participants was twice the number of female participants in the ASD group may have affected the results, since males have a higher risk of developing ASD than females by a ratio of 4:1.[45] Furthermore, it was suggested that males and females with ASD have different neuroanatomical abnormalities, and males with ASD have greater impairment in recognizing faces.46,47 Technological problems during the application of the digital test were another limitations.

Conclusions

Currently, scientists examine whether there can be spatial attention induced by gaze cues of face-like objects. The findings show that face-like objects are not just an illusion of real faces but also activate the extra face-specific attentional process.[48] Detecting facial expressions shows a positive sequential dependency. We are more likely to perceive face-like expressions on objects as the same as the previously seen expression, and this is the same for real human faces as well.[49] Pareidolia is associated with many mechanisms; for example, dysfunction of the right striatum is connected with pareidolia in patients with Parkinson's disease.[50]

This study indicates that children with ASD displayed poor performance in reacting to face and pareidolia images and recognized those images less correctly when compared to their TD peers. Clinicians need new reliable and accurate noninvasive tests to specify situations during the diagnosis and treatment of autism. The digital face and pareidolia test may be a new promising neuropsychological test of the subclinical areas to be used in children.

The take-home message is understanding that the roles of expression processing and facial features are not inseparable, but pareidolia faces and real faces are perceived by the brain in a similar way.

ORCID iDs

Gülsüm Akdeniz https://orcid.org/0000-0002-9411-3318

References

1. Hu X, Pan L, Li W. Meta-analysis on the efficacy of the norepinephrine reuptake inhibitors reboxetine and atomoxetine for the treatment of schizophrenia and attention deficit hyperactivity disorder [published online as ahead of print on November 30, 2022]. *Adv Clin Exp Med*. 2022. doi:10.17219/acem/155802
2. Bellon A, Hasoglu T, Peterson M, et al. Optimization of neurite tracing and further characterization of human monocyte-derived-neuronal-like cells. *Brain Sci*. 2021;11(11):1372. doi:10.3390/brainsci11111372
3. American Psychiatric Association (APA). *Diagnostic and Statistical Manual of Mental Disorders*. 5th ed. Washington, D.C., USA: American Psychiatric Association (APA); 2013. doi:10.1176/appi.books.9780890425596
4. Tanaka M, Szabó Á, Spekker E, Polyák H, Tóth F, Vécsei L. Mitochondrial impairment: A common motif in neuropsychiatric presentation? The link to the tryptophan–kynurenine metabolic system. *Cells*. 2022;11(16):2607. doi:10.3390/cells11162607
5. Tanaka M, Tóth F, Polyák H, Szabó Á, Mándi Y, Vécsei L. Immune influencers in action: Metabolites and enzymes of the tryptophan-kynurenine metabolic pathway. *Biomedicines*. 2021;9(7):734. doi:10.3390/biomedicines9070734
6. Avan R, Sahebnasagh A, Hashemi J, et al. Update on statin treatment in patients with neuropsychiatric disorders. *Life*. 2021;11(12):1365. doi:10.3390/life11121365
7. Lee GA, Lin YK, Lai JH, et al. Maternal immune activation causes social behavior deficits and hypomyelination in male rat offspring with an autism-like microbiota profile. *Brain Sci*. 2021;11(8):1085. doi:10.3390/brainsci11081085
8. Abuaish S, Al-Otaibi NM, Abujamel TS, et al. Fecal transplant and *Bifidobacterium* treatments modulate gut *Clostridium* bacteria and rescue social impairment and hippocampal BDNF expression in a rodent model of autism. *Brain Sci*. 2021;11(8):1038. doi:10.3390/brainsci11081038

9. Garofalo S, Battaglia S, di Pellegrino G. Individual differences in working memory capacity and cue-guided behavior in humans. *Sci Rep*. 2019;9(1):7327. doi:10.1038/s41598-019-43860-w
10. Romagnano V, Sokolov AN, Steinwand P, Fallgatter AJ, Pavlova MA. Face pareidolia in male schizophrenia. *Schizophrenia*. 2022;8(1):112. doi:10.1038/s41537-022-00315-y
11. Candini M, Battaglia S, Benassi M, di Pellegrino G, Frassinetti F. The physiological correlates of interpersonal space. *Sci Rep*. 2021; 11(1):2611. doi:10.1038/s41598-021-82223-2
12. Ellena G, Battaglia S, Làdavas E. The spatial effect of fearful faces in the autonomic response. *Exp Brain Res*. 2020;238(9):2009–2018. doi:10.1007/s00221-020-05829-4
13. Brewer R, Bird G, Gray KLH, Cook R. Face perception in autism spectrum disorder: Modulation of holistic processing by facial emotion. *Cognition*. 2019;193:104016. doi:10.1016/j.cognition.2019.104016
14. Stantić M, Ichijo E, Catmur C, Bird G. Face memory and face perception in autism. *Autism*. 2022;26(1):276–280. doi:10.1177/1362361321 1027685
15. Weigelt S, Koldewyn K, Kanwisher N. Face identity recognition in autism spectrum disorders: A review of behavioral studies. *Neurosci Biobehav Rev*. 2012;36(3):1060–1084. doi:10.1016/j.neubiorev.2011.12.008
16. Ipser A, Ring M, Murphy J, Gaigg SB, Cook R. Similar exemplar pooling processes underlie the learning of facial identity and handwriting style: Evidence from typical observers and individuals with autism. *Neuropsychologia*. 2016;85:169–176. doi:10.1016/j.neuropsychologia.2016.03.017
17. Shah P, Bird G, Cook R. Face processing in autism: Reduced integration of cross-feature dynamics. *Cortex*. 2016;75:113–119. doi:10.1016/j.cortex.2015.11.019
18. Ryan C, Stafford M, King RJ. Seeing the man in the Moon: Do children with autism perceive pareidolic faces? A pilot study. *J Autism Dev Disord*. 2016;46(12):3838–3843. doi:10.1007/s10803-016-2927-x
19. Pavlova MA, Guerreschi M, Tagliavento L, et al. Social cognition in autism: Face tuning. *Sci Rep*. 2017;7(1):2734. doi:10.1038/s41598-017-02790-1
20. Palmer CJ, Clifford CWG. Face pareidolia recruits mechanisms for detecting human social attention. *Psychol Sci*. 2020;31(8):1001–1012. doi:10.1177/0956797620924814
21. Hashimoto Y, Kano O, Ebihara S. Noise pareidolia test for predicting delirium in hospitalized older patients with cognitive decline. *Geriatrics Gerontology Int*. 2022;22(10):883–888. doi:10.1111/ggi.14477
22. Williams JM, Blagrove M. Paranormal experiences, sensory-processing sensitivity, and the priming of pareidolia. *PLoS One*. 2022;17(9): e0274595. doi:10.1371/journal.pone.0274595
23. Tanaka M, Spekker E, Szabó Á, Polyák H, Vécsei L. Modelling the neurodevelopmental pathogenesis in neuropsychiatric disorders: Bioactive kynurenines and their analogues as neuroprotective agents. In celebration of 80th birthday of Professor Peter Riederer. *J Neural Transm (Vienna)*. 2022;129(5–6):627–642. doi:10.1007/s00702-022-02513-5
24. Łaczmańska I, Stembalska A, Złocińska M, et al. Multiplex ligation-dependent probe amplification as a screening test in children with autism spectrum disorders. *Adv Clin Exp Med*. 2020;29(1):101–106. doi:10.17219/acem/112609
25. Akdeniz G. Brain activity underlying face and face pareidolia processing: An ERP study. *Neurol Sci*. 2020;41(6):1557–1565. doi:10.1007/s10072-019-04232-4
26. Battaglia S, Cardellicchio P, Di Fazio C, Nazzi C, Fracasso A, Borgomaneri S. Stopping in (e)motion: Reactive action inhibition when facing valence-independent emotional stimuli. *Front Behav Neurosci*. 2022;16: 998714. doi:10.3389/fnbeh.2022.998714
27. Battaglia S, Fabius JH, Moravkova K, Fracasso A, Borgomaneri S. The neurobiological correlates of gaze perception in healthy individuals and neurologic patients. *Biomedicines*. 2022;10(3):627. doi:10.3390/biomedicines10030627
28. Borgomaneri S, Vitale F, Battaglia S, Avenanti A. Early right motor cortex response to happy and fearful facial expressions: A TMS motor-evoked potential study. *Brain Sci*. 2021;11(9):1203. doi:10.3390/brainsci11091203
29. Thabault M, Turpin V, Maisterrena A, Jaber M, Egloff M, Galvan L. Cerebellar and striatal implications in autism spectrum disorders: From clinical observations to animal models. *Int J Mol Sci*. 2022;23(4):2294. doi:10.3390/ijms23042294
30. Sultan S. Translating neuroimaging changes to neuro-endophenotypes of autistic spectrum disorder: A narrative review. *Egypt J Neurol Psychiatry Neurosurg*. 2022;58(1):139. doi:10.1186/s41983-022-00578-3
31. Khadem-Reza ZK, Zare H. Evaluation of brain structure abnormalities in children with autism spectrum disorder (ASD) using structural magnetic resonance imaging. *Egypt J Neurol Psychiatry Neurosurg*. 2022;58(1):135. doi:10.1186/s41983-022-00576-5
32. Rolf R, Sokolov AN, Rattay TW, Fallgatter AJ, Pavlova MA. Face pareidolia in schizophrenia. *Schizophr Res*. 2020;218:138–145. doi:10.1016/j.schres.2020.01.019
33. Gümüşyayla Ş, Bektaş H, Akdeniz G, Vural G, Yön Mİ. Evaluation of visual hallucination based on pareidolia testing in patients with Alzheimer's disease. *Med J Islamic World Acad Sci*. 2018;26(3):55–58. doi:10.5505/ias.2018.69926
34. Pierce K. Face processing occurs outside the fusiform 'face area' in autism: Evidence from functional MRI. *Brain*. 2001;124(10):2059–2073. doi:10.1093/brain/124.10.2059
35. Hadjikhani N, Joseph RM, Snyder J, Tager-Flusberg H. Abnormal activation of the social brain during face perception in autism. *Hum Brain Mapp*. 2007;28(5):441–449. doi:10.1002/hbm.20283
36. Shah A, Frith U. Why do autistic individuals show superior performance on the block design task? *J Child Psychol Psychiatry*. 1993;34(8): 1351–1364. doi:10.1111/j.1469-7610.1993.tb02095.x
37. Shalom DB. The medial prefrontal cortex and integration in autism. *Neuroscientist*. 2009;15(6):589–598. doi:10.1177/1073858409336371
38. Guillon Q, Rogé B, Afzali MH, Baduel S, Kruck J, Hadjikhani N. Intact perception but abnormal orientation towards face-like objects in young children with ASD. *Sci Rep*. 2016;6(1):22119. doi:10.1038/srep22119
39. Rahman M, van Boxtel JJA. Seeing faces where there are none: Pareidolia correlates with age but not autism traits. *Vision Res*. 2022;199: 108071. doi:10.1016/j.visres.2022.108071
40. Akdeniz G, Toker S, Atli I. Neural mechanisms underlying visual pareidolia processing: An fMRI study. *Pak J Med Sci*. 2018;34(6):1560–1566. doi:10.12669/pjms.346.16140
41. Dawson G, Meltzoff AN, Osterling J, Rinaldi J. Neuropsychological correlates of early symptoms of autism. *Child Dev*. 1998;69(5): 1276–1285. PMID:9839415.
42. Gilbert SJ, Bird G, Brindley R, Frith CD, Burgess PW. Atypical recruitment of medial prefrontal cortex in autism spectrum disorders: An fMRI study of two executive function tasks. *Neuropsychologia*. 2008;46(9):2281–2291. doi:10.1016/j.neuropsychologia.2008.03.025
43. Griebling J, Minshew NJ, Bodner K, et al. Dorsolateral prefrontal cortex magnetic resonance imaging measurements and cognitive performance in autism. *J Child Neurol*. 2010;25(7):856–863. doi:10.1177/0883073809351313
44. Abo Hamza EG, Kéri S, Csigó K, Bedewy D, Moustafa AA. Pareidolia in schizophrenia and bipolar disorder. *Front Psychiatry*. 2021; 12:746734. doi:10.3389/fpsyt.2021.746734
45. Newschaffer CJ, Croen LA, Daniels J, et al. The epidemiology of autism spectrum disorders. *Annu Rev Public Health*. 2007;28(1): 235–258. doi:10.1146/annurev.publhealth.28.021406.144007
46. Lai MC, Lombardo MV, Suckling J, et al. Biological sex affects the neurobiology of autism. *Brain*. 2013;136(9):2799–2815. doi:10.1093/brain/awt216
47. Halliday DWR, MacDonald SWS, Sherf SK, Tanaka JW. A reciprocal model of face recognition and autistic traits: Evidence from an individual differences perspective. *PLoS One*. 2014;9(5):e94013. doi:10.1371/journal.pone.0094013
48. Takahashi K, Watanabe K. Gaze cueing by pareidolia faces. *Iperception*. 2013;4(8):490–492. doi:10.1068/i0617sas
49. Alais D, Xu Y, Wardle SG, Taubert J. A shared mechanism for facial expression in human faces and face pareidolia. *Proc Biol Sci*. 2021; 288(1954):20210966. doi:10.1098/rspb.2021.0966
50. Murakami H, Shiraishi T, Umehara T, et al. Face pareidolia is associated with right striatal dysfunction in drug-naïve patients with Parkinson's disease. *Neurol Sci*. 2021;42(12):5327–5334. doi:10.1007/s10072-021-05238-7

Assessment of the risk factors determining the prognosis of major and minor limb amputations in patients with diabetic foot ulcers

Kürşat Tuğrul Okur[A,B,D,F], Fırat Ozan[A,D–F], Murat Kahraman[A,C,E], Muhammed Melez[A,B,D], Ömer Can Ünlü[A–C], İbrahim Altun[A,C–E]

Department of Orthopaedics and Traumatology, Kayseri City Hospital, Turkey

A – research concept and design; B – collection and/or assembly of data; C – data analysis and interpretation;
D – writing the article; E – critical revision of the article; F – final approval of the article

Advances in Clinical and Experimental Medicine, ISSN 1899–5276 (print), ISSN 2451–2680 (online) *Adv Clin Exp Med*. 2024;33(1):21–30

Address for correspondence
Kürşat Tuğrul Okur
E-mail: k_tugrul_okur@hotmail.com

Funding sources
None declared

Conflict of interest
None declared

Received on October 26, 2022
Reviewed on February 21, 2023
Accepted on April 13, 2023

Published online on May 22, 2023

Abstract

Background. Diabetes mellitus (DM) is a major global health problem, and its incidence is growing. Depending on this increase, the number of diabetes-related complications will also rise.

Objectives. This study aimed to determine the risk factors associated with major and minor amputations resulting from diabetes.

Materials and methods. Patients diagnosed with diabetic foot complications (n = 371) and hospitalized between January 2019 and March 2020 were retrospectively evaluated using information obtained from the database of Diabetic Foot Wound Clinic. Examination of the data identified 165 patients for inclusion in the study, who were stratified into major amputation (group 1, n = 32), minor amputation (group 2, n = 66) and non-amputation (group 3, n = 67) groups.

Results. Of the 32 patients who underwent major amputations, 84% had a below-knee amputation, 13% had an above-knee amputation and 3% had knee disarticulation. At the same time, 73% of 66 patients who underwent minor amputation had a single-finger amputation, 17% had a multiple-finger amputation, 8% had a transmetatarsal amputation, and 2% had Lisfranc amputation. Laboratory results showed high acute phase protein and low albumin (ALB) levels in patients from group 1 ($p < 0.05$). Although *Staphylococcus aureus* was found to be the most common infectious agent, Gram-negative pathogens were dominant ($p < 0.05$). Also, there was a significant cost difference between the groups ($p < 0.05$). Furthermore, those aged over 65 had a high Wagner score, high Charlson Comorbidity Index (CCI), long diabetic foot ulcer (DFU) duration, and high white blood cell (WBC) count, all of which were risk factors for major amputation ($p < 0.05$).

Conclusions. This study demonstrated an increased Wagner staging and incidence of peripheral neuropathy (PN) and peripheral arterial disease (PAD) in major amputation patients. In addition, the rate of distal vessel involvement was high in major amputation patients, with elevated acute phase proteins and low ALB levels crucial in laboratory findings.

Key words: prognosis, risk factors, cost, amputation, diabetic foot ulcers

Okur KT, Ozan F, Kahraman M, Melez M, Ünlü ÖC, Altun İ. Assessment of risk factors determining the prognosis of major and minor limb amputations in patients with diabetic foot ulcers. *Adv Clin Exp Med*. 2024;33(1):21–30. doi:10.17219/acem/163240

DOI
10.17219/acem/163240

Background

Diabetes mellitus (DM) is a significant global health concern that is increasing in incidence.[1–3] The number of diabetes-related complications is also rising,[2,3] which carries an economic burden.[1–4]

One of the most disabling complications of DM is diabetic foot ulcers (DFUs), which result from various etiological pathways.[1–6] It is estimated that 15–25% of diabetics will be affected by DFUs at some point in their lives,[1,4–7] and their recurrence is also common, with 70% of patients experiencing recurrent lesions within 5 years of treatment.[1] Moreover, the risk of death after 5 years is 2.5 times higher for a patient with a DFU than for diabetes patients without a DFU.[1] However, the most undesirable potential outcome of DFU, other than death, is lower extremity amputation (LEA).[1,3,7,8]

Amputations due to DFUs are the most common cause of non-traumatic amputations.[7–9] After the 1st amputation, the incidence of a 2nd in the contralateral limb approaches 50% within 2 years.[4,10] In addition to these risks, the medical and psychosocial consequences of LEAs are substantial.[1,7] In this regard, DFU and LEA patients have a significantly reduced quality of life and a higher risk of depression, which may be associated with impaired psychosocial functioning.[1,7]

Diabetic foot ulcers are difficult to treat and often long-term, taking weeks or months to heal, and they may not heal at all.[1] Early diagnosis and treatment of DFUs is vital because of the increasing prevalence of diabetic patients and the growing health burden.[2] Therefore, identifying the risk factors for the prognosis of patients with DFU and those at high risk, as well as taking preventative action, can reduce complications that may develop.[11]

Many risk factors have been identified for DFU development.[1–5,8,9,12,13] Those identified in previous studies include diabetic peripheral neuropathy (PN), infection, peripheral arterial disease (PAD), chronic renal failure (CRF), advanced age, male sex, smoking, foot deformities, poor glycemic control, large ulcer size, hypertension, lipid abnormalities, and comorbidities, along with elevated white blood cell (WBC) count, plasma albumin (ALB), glycosylated hemoglobin A1c (HbA1c), erythrocyte sedimentation rate (ESR), and C-reactive protein (CRP).[1–5,8,9,12–17] However, results from studies on these DFU risk factors are inconsistent.[1–4,11,12]

Lower extremity amputations due to DFU are generally defined as major or minor amputations,[3,4,8,9] and there is a strong association between the type of amputation and the future functional capacity of patients.[4,8,9] However, there are few studies comparing risk factors between major amputation, minor amputation and non-amputation patient groups.[4,8,9,13]

Objectives

This study aimed to determine the clinical differences and risk factors between major amputation, minor amputation and non-amputation patient groups to reduce the possible amputation risk, increase treatment efficiency in DFU patients and develop better treatment strategies.

Methods and materials

Patients

The study retrospectively evaluated 371 patients hospitalized with a DFU diagnosis between January 2019 and March 2020. The data were obtained after examining the database of the Kayseri City Hospital Diabetic Foot Wound Clinic (Kayseri, Turkey). From initially assessed patients, 165 (110 males and 55 females; 94 right-sided and 71 left-sided; mean age: 64.87 ±11.82 years; range: 42–92 years) were included in the study.

Exclusion criteria

Patients who had undergone lower extremity (LE) surgery for any reason were considered for the study. However, those with reduced life expectancy or missing data and patients without a DFU diagnosis were excluded. Also, patients who underwent bilateral amputation, repetitive surgery, or chronic treatment with immunosuppressants or steroids were excluded.

Study design

The patients were divided into major amputation (group 1, n = 32), minor amputation (group 2, n = 66) and non-amputation (group 3, n = 67) groups. A minor LEA was defined as any amputation distal to the ankle joint, whereas a major LEA was understood as any amputation through or proximal to the ankle joint.[18]

Data sources/measurement

Analyzed data included patient age, gender, smoking history, DM duration, DFU duration and side, Wagner classification, amputation history, presence of PN and PAD, laboratory results, microbiologic culture results, length of hospitalization, medical comorbidities, and cost of diabetes care.

Patient comorbidity was evaluated using the Charlson Comorbidity Index (CCI) and the modified CCI (MCCI),[19,20] while the Semmes–Weinstein 5.07 monofilament test assessed PN. Diabetic foot ulcers were classified according to the Wagner system: grade 0 – skin lesions absent, hyperkeratosis below or above bony prominences; grade 1 – skin and immediate subcutaneous tissue are

ulcerated; grade 2 – lesions are deeper and may penetrate to tendons, bone or joint capsule; grade 3 – deep tissues are always involved, osteomyelitis may be present; grade 4 – gangrene of some portion of the toes or forefoot; grade 5 – the entire foot is gangrenous.[21]

Laboratory evaluations included WBC count and hemoglobin (Hb), ALB, plasma creatinine, blood urea nitrogen (BUN), HbA1c, ESR, CRP, and procalcitonin (PCT) levels. The presence of neuropathic arthropathy (Charcot joints) and osteomyelitis were assessed using LE radiographs and magnetic resonance imaging (MRI). The LE Doppler ultrasonography (USG) was used to evaluate PAD. Meanwhile, the dorsalis pedis, tibialis anterior, tibialis posterior, popliteal, and femoral arteries were evaluated for triphasic, biphasic, monophasic, or absence of arterial flow.

Ethical approval

The Kayseri City Hospital Clinical Research Ethics Committee approved the study protocol (approval No. 01.10.2020/166), and the study was conducted in accordance with the principles of the Declaration of Helsinki.

Statistical analyses

All data analyses employed IBM Statistical Package for Social Sciences (SPSS) v. 22.0 (IBM Corp., Armonk, USA) software. Percentages and standard deviations (SDs) were determined for categorical data and continuous variables, and the Shapiro–Wilk test, skewness, kurtosis, and histograms were used to evaluate the data distribution. Pearson's χ^2 test compared categorical data between the groups, and analysis of variance (ANOVA) with post hoc tests assessed between-group differences in normally distributed continuous variables. A value of $p < 0.017$ was considered significant in the post hoc analysis. The Kruskal–Wallis test evaluated the relationship between non-normally distributed continuous variables. Multiple linear regression was used for cost analysis after categorizing the factors affecting the cost. The factors affecting the 3 groups were categorized and evaluated with multinomial logistic regression analysis. A value of $p < 0.05$ was considered significant in the multiple linear regression analysis and multinomial logistic regression analysis.

Results

Of the 32 patients who underwent major amputations, 84% (n = 27) underwent below-knee amputation and 13% (n = 4) above-knee amputation, and 3% (n = 1) had knee disarticulation. Meanwhile, 66 patients underwent minor amputation, with 73% (n = 48) undergoing single-finger amputation, 17% (n = 12) multiple-finger amputation, 8% (n = 5) transmetatarsal amputation, and 2% (n = 1) Lisfranc amputation.

Age, ulcer duration, Wagner classification, PN, PAD, CCI, MCCI, and diabetes care cost varied significantly across between the 3 groups ($p < 0.05$). Table 1 summarizes the baseline characteristics of the patients.

Evaluation of laboratory values indicated significantly higher WBC count and CRP and PCT levels, and lower ALB level in group 1 compared to groups 2 and 3. In addition, group 1 had significantly higher ESR and BUN values than group 3 (Table 2). However, there were no significant between-group differences in HbA1c or creatinine values.

Peripheral neuropathy was detected in 69% (n = 114) of patients, with 24 (75%) patients in group 1, 51 (77%) patients in group 2 and 39 (58%) patients in group 3. There was a significant difference between group 1 and group 2 ($p = 0.043$). Doppler USG examination indicated the involvement of at least 1 peripheral artery in 27 (84%) patients in group 1, 33 (50%) patients in group 2 and 26 (38%) patients in group 3 ($p = 0.000$). The involved arteries and the observed flow form are summarized in Fig. 1.

Wound cultures were obtained from 128 patients, with growth detected in 82% (n = 106) of samples. Ten (10%) cultures had polymicrobial growth, and 96 (90%) contained a single microorganism. Microbial growth was detected in 18 of 21 wound cultures in group 1, 47 of 51 in group 2 and 41 of 56 in group 3 cultures. Furthermore, 19 microorganisms were detected in group 1, 52 in group 2 and 45 in group 3.

In the cultures of group 1 patients, 26.3% (n = 5) Gram-positive bacteria and 73.6% (n = 14) Gram-negative bacteria were detected. The most common Gram-positive bacteria isolated were *Staphylococcus* spp. (n = 4), and *Escherichia coli* (n = 4) was the most common Gram-negative bacteria. In group 2, Gram-positive bacterial growth was detected in 34.6% (n = 18) and Gram-negative bacteria growth in 61.5% (n = 32). *Staphylococcus* spp. (n = 9) were the most common Gram-positive bacteria isolated, while *Acinetobacter baumannii* (n = 6) was the most common Gram-negative bacteria. In group 3, Gram-positive bacterial growth was detected in 46.6% (n = 21) and Gram-negative growth in 51.1% (n = 23). The most common Gram-positive bacteria were *Staphylococcus* spp. (n = 12), while *E. coli* (n = 5) was the most common Gram-negative bacteria (Table 3).

Multinomial logistic regression analysis was performed to investigate independent risk factors. The results showed that major amputation was associated with age, WBC count, Wagner classification, DFU duration, and CCI. For minor amputations, male gender, age, Wagner classification, and ESR were crucial risk factors (Table 4).

The mean treatment cost for major amputations was $1023, for minor amputations – $535 and $762 for non-amputations. There was a significant difference between the major amputation and minor amputation groups in terms of mean treatment cost ($p = 0.032$). Age, gender,

Table 1. Demographic characteristics of the patients and clinical outcomes

Patient characteristics		Group 1 (n = 32)	Group 2 (n = 66)	Group 3 (n = 67)	p-value
Age [years], mean (range) ±SD		69.8 (49–92) ±12.1	65.7 (42–86) ±9.4	61.6 (34–87) ±12.8	0.027*[b]
Gender, n (%)	female	10 (31.2)	23 (34.8)	22 (32.8)	0.933†
	male	22 (68.7)	43 (65.1)	45 (67.1)	
Side of involvement, n (%)	right	19 (59.3)	41 (62.1)	34 (50.7)	0.397†
	left	13 (40.6)	25 (37.8)	33 (49.2)	
Duration of DFU [days], median (range)		30 (6–360)	20 (2–340)	15 (3–360)	0.020+[b]
Duration of DM [years], mean ±SD		18.22 ±9.35	14.97 ±7.87	14.90 ±7.47	0.118*
DM treatment, n (%)	insulin	28 (87.5)	56 (84.84)	54 (80.59)	0.829†
	oral antidiabetic drug	4 (12.5)	7 (10.6)	10 (14.92)	
	new diagnosis	0 (0)	3 (4.54)	3 (4.47)	
Mean length of hospitalization [days], median (range)		13 (3–145)	14 (1–69)	12 (1–150)	0.612+
Wagner classification, n (%)	grade 1	0 (0)	1 (1.51)	21 (31.34)	0.000†[ab]
	grade 2	0 (0)	2 (3.03)	39 (58.2)	
	grade 3	5 (15.62)	37 (56.06)	7 (10.44)	
	grade 4	8 (25)	26 (39.39)	0 (0)	
	grade 5	19 (59.37)	0 (0)	0 (0)	
Number of comorbidities, n (%)	0	3 (9.37)	16 (24.24)	14 (20.89)	0.273†
	1	9 (28.12)	23 (34.84)	30 (44.77)	
	2	14 (43.75)	16 (24.24)	16 (23.88)	
	3	3 (9.37)	7 (10.6)	5 (7.46)	
	4	3 (9.37)	4 (6.06)	2 (2.98)	
CCI, median (range)		2 (1–5)	1 (1–4)	1 (1–6)	0.003+[ab]
MCCI, mean ±SD		5.22 ±1.69	4.06 ±1.71	3.6 ±1.75	0.000*[ab]
PN, n (%)	present	24 (75)	51 (77.27)	39 (58.20)	0.043†[a]
	absent	8 (25)	15 (22.72)	28 (41.79)	
PAD, n (%)	present	27 (84.3)	33 (50)	26 (38.8)	0.000†[ab]
	absent	5 (15.6)	33 (50)	41 (61.1)	
Smoking history, n (%)	present	10 (31.25)	14 (21.21)	11 (16.41)	0.240†
	absent	22 (68.75)	52 (78.78)	56 (83.58)	
Hypertension, n (%)	present	18 (56.25)	34 (51.51)	32 (47.76)	0.726†
	absent	14 (43.75)	32 (48.48)	35 (52.23)	
IHD, n (%)	present	10 (31.25)	25 (37.87)	22 (32.83)	0.754†
	absent	22 (68.75)	41 (62.12)	45 (67.16)	
Nephropathy, n (%)	present	10 (31.25)	11 (16.66)	11 (16.41)	0.168†
	absent	22 (68.75)	55 (83.33)	56 (83.58)	
Hemodialysis, n (%)	present	8 (25)	5 (7.57)	7 (10.44)	0.040†[a]
	absent	24 (75)	61 (92.42)	60 (89.55)	
Cost [USD], median (range)		1023 (228–9362)	535 (111–12,852)	762 (56–13,358)	0.032+[a]

SD – standard deviation; DFU – diabetic foot ulcer; DM – diabetes mellitus; CCI – Charlson Comorbidity Index; MCCI – modified CCI; PN – peripheral neuropathy; PAD – peripheral arterial disease; IHD – ischemic heart disease; * analysis of variance (ANOVA) test; † χ^2 test; + Kruskal–Wallis test; [a] difference between group 1 and group 2 was statistically significant; [b] difference between group 1 and group 3 was statistically significant.

length of hospital stay, DFU duration, Wagner stage, CCI, and MCCI were determined as the variables affecting the cost, and the results of multiple linear regression analysis showed that only the length of stay had a significant relationship with cost (p = 0.000) (Table 5).

Discussion

This study examined the epidemiological factors that may be effective in determining the prognosis of DFU patients grouped into major amputation, minor amputation

Table 2. Comparison of laboratory results of groups

Variables	Group 1 (n = 32)	Group 2 (n = 66)	Group 3 (n = 67)	p-value
HbA1c (%), mean ±SD	9.26 ±2.62	9.48 ±2.31	9.25 ±2.28	0.827*
WBC [10^3/μL], median (range)	15.12 (7.48–33.76)	11.54 (5.54–32.29)	8.89 (4.09–32.73)	0.000^{+ab}
ESR [mm/h], mean ±SD	77.03 ±33.04	59.36 ±33.32	46.72 ±30.88	0.000*^{b}
CRP [mg/L], median (range)	177.6 (22.2–393.5)	69.5 (1.4–369)	43.5 (0.3–361)	0.000^{+ab}
PCT [μg/L], median (range)	0.01 (0.001–100)	0.80 (0.001–13)	0.06 (0.02–15)	0.000^{+b}
Creatinine [mg/dL], median (range)	1.23 (0.51–10.3)	1.08 (0.51–11.55)	1.02 (0.42–6.6)	0.380^{+}
BUN [mg/dL], median (range)	25.05 (9.7–100.5)	22.65 (7–108)	22 (5.7–61.4)	0.042^{+b}
ALB [g/L], mean ±SD	28.42 ±6.91	34.28 ±5.72	35.39 ±6.57	0.000*^{ab}

HbA1c – glycated hemoglobin A1c; SD – standard deviation; WBC – white blood cell; ESR – erythrocyte sedimentation rate; CRP – C-reactive protein; PCT – procalcitonin; BUN – blood urea nitrogen; ALB – albumin; * analysis of variance (ANOVA) test; $^{+}$ Kruskal–Wallis test; ^{a} difference between group 1 and group 2 was statistically significant; ^{b} difference between group 1 and group 3 was statistically significant.

Table 3. Isolated microorganisms and their characteristics

Microorganism	Group 1 (n = 19)	Group 2 (n = 52)	Group 3 (n = 45)	Total (n = 116)
Gram-positive bacteria, n	5	18	21	44
Staphylococcus aureus	2	5	100	17
Enterococcus faecalis	0	4	5	9
Coagulase negative staphylococci	2	4	2	8
Streptococcus agalactiae	1	2	2	5
Dermacoccus nishinomiyaensis	0	1	0	1
Diphtheroid bacillus	0	1	0	1
Kocuria rhizophila	0	0	1	1
Streptococcus thoraltensis	0	0	1	1
Enterococcus avium	0	1	0	1
Gram-negative bacteria, n	14	32	23	69
Escherichia coli	4	4	5	13
Pseudomonas aeruginosa	2	5	4	11
Acinetobacter baumannii	1	6	2	9
Proteus mirabilis	1	3	3	7
Enterobacter cloacae	0	5	1	6
Klebsiella pneumoniae	1	2	2	5
Morganella morganii	1	2	2	5
Klebsiella oxytoca	0	2	2	4
Citrobacter freundii	2	0	0	2
Klebsiella aerogenes	0	2	0	2
Stenotrophomonas maltophilia	1	0	0	1
Citrobacter braakii	1	0	0	1
Acinetobacter lwoffii	0	0	1	1
Serratia rubidaea	0	0	1	1
Proteus hauseri	0	1	0	1
Other microorganisms, n	0	2	1	3
Skin flora	0	0	1	1
Fungi	0	2	0	2

Table 4. Evaluation of risk factors for amputation according to multinomial logistic regression analysis

Variables		Regression coefficient	p-value	OR	95% CI
Major amputation group	male sex	7.110	0.345	1223.778	0.000–3.11
	age	2.708	0.016	15.005	1.645–136.847
	Wagner classification	15.359	0.004	46.822	0.147–148.6
	insulin use	–1.221	0.347	0.295	0.023–3.763
	duration of DFU	0.773	0.048	2.167	0.996–4.715
	number of comorbid diseases	0.052	0.923	1.054	0.365–3.045
	CCI	2.015	0.046	7.503	0.930–60.526
	MCCI	–1.867	0.144	0.155	0.013–1.898
	ALB	–0.122	0.213	0.885	0.730–1.073
	HbA1c	–0.145	0.504	0.865	0.566–1.322
	CRP	0.009	0.105	1.009	0.998–1.019
	WBC	0.001	0.010	1.001	1.000–1.001
	ESR	0.012	0.402	1.012	0.984–1.041
Minor amputation group	male sex	–18.648	0.000	7.96	–4.02–0.0
	age	1.070	0.042	2.916	0.981–8.674
	Wagner grade	2.087	0.031	8.064	1.207–53.859
	insulin use	–0.494	0.314	0.610	0.234–1.595
	duration of DFU	–0.011	0.956	0.989	0.661–1.480
	number of comorbid diseases	0.057	0.835	1.059	0.619–1.810
	CCI	–0.598	0.392	0.550	0.140–2.164
	MCCI	–0.332	0.603	0.717	0.205–2.513
	ALB	0.037	0.411	1.038	0.950–1.133
	HbA1c	0.175	0.131	1.191	0.949–1.493
	CRP	–0.004	0.321	0.996	0.990–1.003
	WBC	0.000	0.265	1.000	1.000–1.000
	ESR	0.019	0.022	1.019	1.003–1.036

OR – odds ratio; 95% CI – 95% confidence interval; DFU – diabetic foot ulcer; CCI – Charlson Comorbidity Index; MCCI – modified CCI; ALB – albumin; HbA1c – glycated hemoglobin A1c; CRP – C-reactive protein; WBC – white blood cell; ESR – erythrocyte sedimentation rate.

and non-amputation groups, and compared the costs associated with each group. The results showed that high acute phase protein values and low ALB levels in group 1 patients, as well as the presence of high Wagner grades, PN and PAD were significant. Furthermore, the Doppler USG examinations demonstrated that the rate of distal vessel involvement was high in group 1 patients.

Although *Staphylococcus aureus* was the most common infectious agent, Gram-negative pathogens were dominant in all 3 groups. There was also a significant difference in cost between the groups, with hospital stay length being the main factor affecting the cost. Furthermore, age >65 years, low ALB values, high Wagner grade, high CCI, long DFU duration, and high WBC count were identified as risk factors for major amputation.

Diabetic foot ulcer is associated with high morbidity and mortality, and is one of the potentially preventable complications of diabetes.[7,13] A wide variety of diabetic foot amputation risk factors have been reported in previous studies.[4,13] Such diversity may be due to differences in study subjects and designs, treatment protocols and cultural characteristics.[4,11–13]

Various studies have produced different results on whether there is a significant relationship between age and amputation.[2,4,6,7,9,12,13] As people age, the wound healing process progressively deteriorates due to many factors, such as impaired defense mechanisms and immunity and the development of PAD.[6,13] In this study, advanced age was an important determinant, with the mean age of the patients who underwent major amputation being significantly higher than in the other groups. Moreover, advanced age increased the risk of major amputation 15-fold and the risk of minor amputation approximately 3-fold in DFU patients.

Gender, smoking, age, and DM duration are prognostic factors for amputation. They have been evaluated in the previous studies, though the results are controversial.[1,6,7,9,12,22–24] Although there was no statistically significant relationship in terms of gender between the groups in the current study, the risk analysis indicated that being male increased the risk of minor amputation approximately

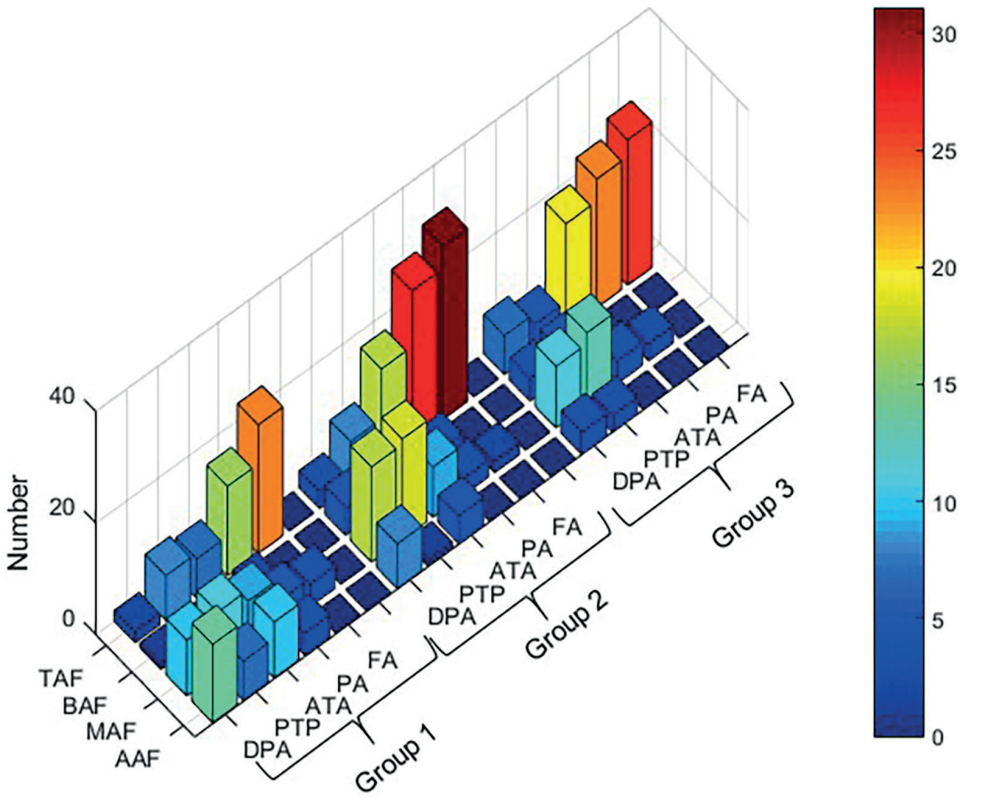

Fig. 1. Distribution of flow phases detected using Doppler ultrasonography in patients with peripheral artery involvement

AAF – absence of arterial flow;
ATA – anterior tibial artery;
BAF – biphasic arterial flow;
DPA – dorsalis pedis artery;
FA – femoral artery;
MAF – monophasic arterial flow;
PA – popliteal artery;
TAF – triphasic arterial flow;
PTP – posterior tibial artery.

8-fold. On the other hand, although the major amputation patients had a longer mean DM duration, there was no significant relationship between the groups. Furthermore, smoking was not identified as a risk factor for LEA in this study.

In the current study, longer DFU duration was significantly associated with major amputation, which increases the risk of wound infections that can result in tissue necrosis. Such infections cause irreversible damage, with deep tissue involvement depending on the processes observed, and increase the risk of complications.[6–9,24,25] In this regard, major amputation risk nearly doubled as the DFU duration increased.

Levels of HbA1c are directly related to the mean glucose concentration over the Hb lifetime,[6,8] and the primary risk factor for developing diabetic complications is poor glycemic control.[2,6,8] According to several studies, the HbA1c level is a predictor of amputation.[2,6,24] However, the current study found no significant difference in HbA1c levels between the groups.

Individuals with DM are more likely to have PAD,[13,25,26] which is a substantial risk factor for LEA.[8,9,12,13,25] Ulcers become complicated due to ischemia, which occurs when PAD causes insufficient blood flow for ulcer healing.[13,25,27] Furthermore, wound granulation and healing require adequate nutritional support to the tissues.[25–27] In the presence of PAD, the concentration of tissue antibiotics decreases, and the risk of multidrug-resistant microbes multiplying in DFUs becomes greater, thereby increasing the possibility of amputation.[25–27] In the current study, there was a significant difference in PAD incidence between the groups, with 84% in the major amputation group, 50% in the minor amputation group and 38% in the non-amputation group. In group 1, group 2 and group 3, the incidence of monophasic flow or absence of flow in the dorsalis pedis artery was 95%, 80% and 60%, respectively. Meanwhile, distal artery involvement was more common in the major amputation group. These findings demonstrate that as PAD incidence and severity increase, so do the rate and level of amputation.

Peripheral arterial disease, DFU depth and presence of infection are the most commonly used parameters for DFU classification.[2,8,13,28,29] It has been shown that the Wagner classification,, the most common classification system used to describe DFU characteristics, is effective for prognosis.[2,8,13,28,29] However, its sensitivity in predicting LEA is 93.6%, and its specificity is 50.8%.[2,8,28] In this study, major amputation patients were classified as Wagner grade 4 or 5, and lower grades were detected in patients with minor amputations and those who did not undergo amputation, with a significant difference between them. Being classified as Wagner grade 4 or 5 increased the risk of major amputation approx. 47 times and the risk of minor amputation 8 times.

Since the CCI includes diabetes severity, PAD status and nearly all independent amputation risk factors, a high score of this index is an amputation indicator and can be used as a clinical tool.[19–21,30,31] There was a significant difference in CCI and MCCI between group 1 and the other 2 groups. In the risk analysis, a CCI ≥ 4 increased the risk

Table 5. Factors determining the cost (with multiple linear regression analysis)

Variables	B	SE	β (95% CI)	t	p-value
		Group 1			
Age	–250.554	4638.022	–0.009	–0.054	0.957
Sex	235.045	4082.116	0.008	0.058	0.955
Length of hospitalization	7597.503	1785.390	0.673	4.255	0.000
Duration of DFU	–552.367	2021.895	–0.048	–0.273	0.787
Wagner grade	900.469	5782.375	0.025	0.156	0.878
CCI	–4094.475	4248.726	–0.176	–0.964	0.345
MCCI	5196.98	5708.88	0.197	0.910	0.372
		Group 2			
Age	–666.167	2873.942	0.028	0.232	0.818
Sex	–4748.349	2604.285	–0.194	–1.823	0.073
Length of hospitalization	5938.442	1141.558	0.543	5.202	0.000
Duration of DFU	–199.733	1309.653	–0.017	–0.153	0.879
Wagner grade	391.490	2621.614	0.016	0.149	0.882
CCI	7127.234	4394.209	0.199	1.622	0.110
MCCI	–4748.349	3272.719	0.023	0.165	0.870
		Group 3			
Age	–4667.808	4569.127	–0.150	–1.022	0.311
Sex	701.266	3855.325	0.021	0.182	0.856
Length of hospitalization	7105.261	1719.424	0.509	4.132	0.000
Duration of DFU	734.218	1519.840	0.057	0.483	0.631
Wagner grade	–1196.057	10618.4	–0.013	–0.113	0.911
CCI	–1489.57	4641.056	–0.042	–0.321	0.749
MCCI	5667.4	5107.638	0.174	1.110	0.272
		Total			
Age	–1566.719	2143.609	–0.58	–0.731	0.466
Sex	–1394.648	1907.803	–0.048	–0.731	0.466
Length of hospitalization	6738.996	836.049	0.543	8.061	0.000
Duration of DFU	241.870	825.283	0.020	0.293	0.770
Wagner grade	–346.083	2006.335	–0.012	–0.172	0.863
CCI	412.549	2347.424	0.013	0.176	0.861
MCCI	4252.942	2426.024	0.154	1.753	0.082

β – standardized coefficients; B – unstandardized coefficients; 95% CI – 95% confidence interval; DFU – diabetic foot ulcer; CCI – Charlson Comorbidity Index; MCCI – modified CCI; SE – standard error.

of major amputation 7.5 times. There was no significant difference in the number of comorbidities between the groups. However, the specific disease, disease stage and the extent of its effect on the tissues in DFUs play a greater role in the prognosis than the number of comorbidities. Therefore, the quality of the accompanying diseases rather than their quantity is a crucial determinant of the level of amputation.

Diabetes mellitus and CRF have important common risk factors that predispose to DFU formation, such as PN, PAD and susceptibility to infection.[2,4,9,32] Moreover, CRF is considered an indicator of future PAD,[2,4,9,32] and a significant association has been established between the deterioration of kidney function and DFU recurrence and amputations.[4,9,22,23] However, a meta-analysis found that nephropathy was not the cause of amputation in patients with a diabetic foot infection, despite its role in the development of DFUs.[2] Furthermore, it has been reported that nephropathy may not be a direct indicator of amputation, as the predictive value of different nephropathy stages may vary.[2,9]

In this study, 19.3% of the patients were diagnosed with CRF, and 62.5% were undergoing hemodialysis. There was no significant relationship between the groups in terms of CRF. However, there was a significant difference between group 1 and group 2 in the proportion of patients undergoing hemodialysis. Therefore, it can be concluded that there may be a possible increase in the number of major amputations in DFU patients as the CRF stage increases.

Peripheral neuropathy is one of the major risk factors for all foot complications.[6,12] In addition to foot deformity caused by PN, neuropathic changes, such as decreased protective sensation and skin cracks due to decreased sweating, lead to the formation of diabetic foot infections.[5,6] Furthermore, the healing of DFUs can occur without complications in patients without PN.[6] Peripheral neuropathy was present in 69% of the patients in this study, and there was a significant difference in PN incidence between group 1 and 2.

Diabetic foot ulcer treatment requires specialist care, orthopedic tools, antimicrobial drugs, various dressing materials, and inpatient care,[1,4,9] which leads to a significant economic burden.[1,4,9,13] The cost of DFU treatment to the healthcare system varies by country,[1] though DFU treatment accounts for approx. 25% of the total hospital costs for a diabetic patient.[1,2,4,13] In the current study, group 1 had the highest mean treatment cost, followed by group 3 and group 2, respectively. The reason for the high cost in group 3 patients is likely due to the extended hospital stay and the dressing equipment used. Meanwhile, the factor that increased the treatment cost of patients who underwent major amputation was hospitalization in the intensive care unit (ICU) after surgery. According to the regression analysis, the length of hospital stay was the only factor affecting the cost, though the costs do not fully represent the total economic burden. Indeed, when associated costs, such as loss of productivity, clinical follow-up, rehabilitation, and home care, are taken into account, higher costs may be encountered.

C-reactive protein and ESR levels and WBC count are the most frequently used parameters for detecting infection in clinical practice,[2,8,9,33] and are useful for showing changes in disease activity.[2,5,9,33] In this study, mean WBC count, CRP level, ESR rate, and PCT values were significantly higher in group 1 than in groups 2 and 3.

Proteins are vital for matrix synthesis and healing at the wound site.[8,34] It has been reported that patients with ALB levels greater than 28–35 g/L recovered without complications.[8,34] In this study, the mean preoperative ALB values were 28.4 g/L (group 1), 34.2 g/L (group 2) and 35.3 g/L (group 3). The comparison of the ALB values between groups showed a significant difference, which is consistent with the supporting literature.[8,34]

Approximately 56% of DFUs are infected, and 20% of them require amputation.[2,5,9,12] Although Gram-positive pathogens, especially *Staphylococcus* spp., are seen more frequently in diabetic foot infections, others have reported detecting Gram-negative pathogens more often.[2,5,9,12] Gram-negative bacteria isolation poses a higher risk of amputation than Gram-positive bacteria isolation,[2,5,9] although *S. aureus* is reported to be a predictor of limb loss.[5,9,12] In this study, Gram-negative microorganisms were most common in all 3 groups. Nonetheless, considering the results of all cultures, *Staphylococcus* spp. were the most common causative microorganisms. Meanwhile, Gram-negative pathogens were predominantly detected in group 1 and 2 patients, and Gram-positive and Gram-negative pathogens were found at an almost equal frequency in group 3.

Early diagnosis and treatment of DFUs are vital due to the increasing prevalence of diabetic patients and the subsequent increased burden on healthcare system and costs. Moreover, improved management of diabetic patients in the initial stages is crucial, as the severity of the condition increases when complications arise. Therefore, identifying risk factors in DFU patients will help to develop effective strategies for diagnosis, management and treatment protocols. We believe that increasing knowledge in the DFU field through the current and similar studies will help define risk assessment models that can be used in clinical practice.

Limitations

This study had several limitations. Although the data were collected prospectively, the study was retrospective in design, meaning that the findings need to be confirmed in prospective studies. Also, the sample size is relatively small, though it is more than sufficient compared to similar studies. Furthermore, stepwise selection methods are widely applied to identify covariates for inclusion in regression models, which leads to biased estimation of the regression coefficients and can cause a significant bias in the estimated regression coefficients. Finally, the study was undertaken in a developing country and may not reflect DFU patients in developed countries.

Conclusions

This study demonstrated high Wagner grades, PN and PAD incidence in major amputation patients. Furthermore, age >65 years, long DFU duration, low ALB values, high Wagner score, increased CCI, and elevated WBC count were risk factors for major amputation. Although *S. aureus* was the most common infectious agent, Gram-negative pathogens dominated. Moreover, major amputation patients had a high rate of distal vessel involvement, higher acute phase protein levels and lower ALB levels. There was also a significant difference in cost between the groups, and the most important factor was the length of hospital stay.

Supplementary data

The Supplementary materials are available at https://doi.org/10.5281/zenodo.7826090. The package contains the following files:

Supplementary linear regression tests file.
Supplementary normality tests file.
Supplementary multinomial logistic regression test results.
Supplementary normality test table.

ORCID iDs

Kürşat Tuğrul Okur https://orcid.org/0000-0003-2749-7945
Fırat Ozan https://orcid.org/0000-0002-2417-8343
Murat Kahraman https://orcid.org/0000-0002-3821-9767
Muhammed Melez https://orcid.org/0000-0002-4592-8844
Ömer Can Ünlü https://orcid.org/0000-0003-0807-7427
İbrahim Altun https://orcid.org/0000-0002-0152-1065

References

1. Hoogeveen RC, Dorresteijn JA, Kriegsman DM, Valk GD. Complex interventions for preventing diabetic foot ulceration. *Cochrane Database Syst Rev*. 2015;2015(8):CD007610. doi:10.1002/14651858.CD007610.pub3
2. Sen P, Demirdal T, Emir B. Meta-analysis of risk factors for amputation in diabetic foot infections. *Diabetes Metab Res Rev*. 2019;35(7):e3165. doi:10.1002/dmrr.3165
3. Jiang Y, Ran X, Jia L, et al. Epidemiology of type 2 diabetic foot problems and predictive factors for amputation in China. *Int J Low Extrem Wounds*. 2015;14(1):19–27. doi:10.1177/1534734614564867
4. Gazzaruso C, Gallotti P, Pujia A, Montalcini T, Giustina A, Coppola A. Predictors of healing, ulcer recurrence and persistence, amputation and mortality in type 2 diabetic patients with diabetic foot: A 10-year retrospective cohort study. *Endocrine*. 2021;71(1):59–68. doi:10.1007/s12020-020-02431-0
5. Barberán J, Granizo JJ, Aguilar L, et al. Predictive model of short-term amputation during hospitalization of patients due to acute diabetic foot infections. *Enferm Infecc Microbiol Clin*. 2010;28(10):680–684. doi:10.1016/j.eimc.2009.12.017
6. Marzoq A, Shiaa N, Zaboon R, Baghlany Q, Alabbood MH. Assessment of the outcome of diabetic foot ulcers in Basrah, southern Iraq: A cohort study. *Int J Diabetes Metab*. 2019;25(1–2):33–38. doi:10.1159/000500911
7. Ugwu E, Adeleye O, Gezawa I, Okpe I, Enamino M, Ezeani I. Predictors of lower extremity amputation in patients with diabetic foot ulcer: Findings from MEDFUN, a multi-center observational study. *J Foot Ankle Res*. 2019;12:34. doi:10.1186/s13047-019-0345-y
8. Sun JH, Tsai JS, Huang CH, et al. Risk factors for lower extremity amputation in diabetic foot disease categorized by Wagner classification. *Diabetes Res Clin Pract*. 2012;95(3):358–363. doi:10.1016/j.diabres.2011.10.034
9. Ozan F, Gürbüz K, Çelïk İ, Beştepe Dursun Z, Uzun E. Evaluation of major and minor lower extremity amputation in diabetic foot patients. *Turk J Med Sci*. 2017;47(4):1109–1116. doi:10.3906/sag-1601-58
10. Oh TS, Lee HS, Hong JP. Diabetic foot reconstruction using free flaps increases 5-year-survival rate. *J Plast Reconstr Aesthet Surg*. 2013;66(2):243–250. doi:10.1016/j.bjps.2012.09.024
11. Lee JH, Yoon JS, Lee HW, et al. Risk factors affecting amputation in diabetic foot. *Yeungnam Univ J Med*. 2020;37(4):314–320. doi:10.12701/yujm.2020.00129
12. Nather A, Bee CS, Huak CY, et al. Epidemiology of diabetic foot problems and predictive factors for limb loss. *J Diabetes Complications*. 2008;22(2):77–82. doi:10.1016/j.jdiacomp.2007.04.004
13. Jeyaraman K, Berhane T, Hamilton M, Chandra AP, Falhammar H. Mortality in patients with diabetic foot ulcer: A retrospective study of 513 cases from a single centre in the Northern Territory of Australia. *BMC Endocr Disord*. 2019;19(1):1. doi:10.1186/s12902-018-0327-2
14. Reisoglu A, Turgut A, Filibelli M, Incesu M, Yalcin E, Parlar O. Analysis of the factors affecting mortality after non-traumatic major lower extremity amputations. *Acta Orthop Traumatol Turc*. 2022;56(6):377–383. doi:10.5152/j.aott.2022.22096
15. Zhang L, Fu G, Deng Y, et al. Risk factors for foot ulcer recurrence in patients with comorbid diabetic foot osteomyelitis and diabetic nephropathy: A 3-year follow-up study. *Int Wound J*. 2023;20(1):173–182. doi:10.1111/iwj.13861
16. Wang L, Li Q, Chen X, Wang Z. Clinical characteristics and risk factors of lower extremity amputation in patients with diabetic foot. *Pak J Med Sci*. 2022;38(8):2253–2258. doi:10.12669/pjms.38.8.5635
17. Monteiro-Soares M, Boyko EJ, Jeffcoate W, et al. Diabetic foot ulcer classifications: A critical review. *Diabetes Metab Res Rev*. 2020;36(Suppl 1):e3272. doi:10.1002/dmrr.3272
18. Unwin N; The LEA Study Group. Comparing the incidence of lower extremity amputations across the world: The Global Lower Extremity Amputation Study. *Diabet Med*. 1995;12(1):14–18. doi:10.1111/j.1464-5491.1995.tb02055.x
19. Charlson ME, Pompei P, Ales KL, MacKenzie CR. A new method of classifying prognostic comorbidity in longitudinal studies: Development and validation. *J Chronic Dis*. 1987;40(5):373–383. doi:10.1016/0021-9681(87)90171-8
20. Turchin A, Matheny ME, Shubina M, Scanlon JV, Greenwood B, Pendergrass ML. Hypoglycemia and clinical outcomes in patients with diabetes hospitalized in the general ward. *Diabetes Care*. 2009;32(7):1153–1157. doi:10.2337/dc08-2127
21. Wagner F. A classification and treatment program for diabetic, neuropathic, and dysvascular foot problems. *Instr Course Lect*. 1979;28:143–165.
22. Gershater MA, Löndahl M, Nyberg P, et al. Complexity of factors related to outcome of neuropathic and neuroischaemic/ischaemic diabetic foot ulcers: A cohort study. *Diabetologia*. 2009;52(3):398–407. doi:10.1007/s00125-008-1226-2
23. Resnick HE, Carter EA, Sosenko JM, et al. Incidence of lower-extremity amputation in American Indians: The Strong Heart Study. *Diabetes Care*. 2004;27(8):1885–1891. doi:10.2337/diacare.27.8.1885
24. Wang DD, Jamjoom RA, Alzahrani AH, Hu FB, Alzahrani HA. Prevalence and correlates of lower-extremity amputation in patients with diabetic foot ulcer in Jeddah, Saudi Arabia. *Int J Low Extrem Wounds*. 2016;15(1):26–33. doi:10.1177/1534734615601542
25. Prompers L, Schaper N, Apelqvist J, et al. Prediction of outcome in individuals with diabetic foot ulcers: Focus on the differences between individuals with and without peripheral arterial disease. The EURODIALE Study. *Diabetologia*. 2008;51(5):747–755. doi:10.1007/s00125-008-0940-0
26. Aysert Yildiz P, ÖzdïL T, DïZbay M, Güzel Tunçcan Ö, Hizel K. Peripheral arterial disease increases the risk of multidrug-resistant bacteria and amputation in diabetic foot infections. *Turk J Med Sci*. 2018;48(4):845–850. doi:10.3906/sag-1803-217
27. Monteiro-Soares M, Boyko EJ, Ribeiro J, Ribeiro I, Dinis-Ribeiro M. Predictive factors for diabetic foot ulceration: A systematic review. *Diabetes Metab Res Rev*. 2012;28(7):574–600. doi:10.1002/dmrr.2319
28. Monteiro-Soares M, Martins-Mendes D, Vaz-Carneiro A, Sampaio S, Dinis-Ribeiro M. Classification systems for lower extremity amputation prediction in subjects with active diabetic foot ulcer: A systematic review and meta-analysis. *Diabetes Metab Res Rev*. 2014;30(7):610–622. doi:10.1002/dmrr.2535
29. Jeon BJ, Choi HJ, Kang JS, Tak MS, Park ES. Comparison of five systems of classification of diabetic foot ulcers and predictive factors for amputation. *Int Wound J*. 2017;14(3):537–545. doi:10.1111/iwj.12642
30. Gurney JK, Stanley J, York S, Rosenbaum D, Sarfati D. Risk of lower limb amputation in a national prevalent cohort of patients with diabetes. *Diabetologia*. 2018;61(3):626–635. doi:10.1007/s00125-017-4488-8
31. Aziz F, Reichardt B, Sourij C, et al. Epidemiology of major lower extremity amputations in individuals with diabetes in Austria, 2014–2017: A retrospective analysis of health insurance database. *Diabetes Res Clin Pract*. 2020;170:108477. doi:10.1016/j.diabres.2020.108477
32. Ndip A, Lavery LA, Boulton AJM. Diabetic foot disease in people with advanced nephropathy and those on renal dialysis. *Curr Diab Rep*. 2010;10(4):283–290. doi:10.1007/s11892-010-0128-0
33. Akinci B, Yener S, Yesil S, Yapar N, Kucukyavas Y, Bayraktar F. Acute phase reactants predict the risk of amputation in diabetic foot infection. *J Am Podiatr Med Assoc*. 2011;101(1):1–6. doi:10.7547/1010001
34. Highlander P, Shinabarger AB. Perioperative laboratory assessment of diabetic foot infections undergoing amputation: A systematic review. *Foot Ankle Spec*. 2013;6(6):465–470. doi:10.1177/1938640013496845

SARS-COV-2 infections in children: The role of fibrinogen in predicting diagnosis and severity: A retrospective cohort study

Gulsen Akkoc[1,A–D], Ayşe Ağbaş[2,A,D], Eralp Göksu[3,B,D], Sevde Beyaz[3,B,D], Funda Yıldız[3,B,C,E], Elvan Bayramoğlu[4,A–C], Canan Yolcu[5,A,B,D], Senem Ayça[6,B,E], Nurcihan Çalışkan Dolu[7,B,C], Kamil Şahin[3,D–F], Macit Koldaş[7,B,C], Murat Elevli[3,D,F]

[1] Department of Pediatric Infectious Diseases, University of Health Sciences, Haseki Training and Research Hospital, Istanbul, Turkey
[2] Department of Pediatric Nephrology, University of Health Sciences, Haseki Training and Research Hospital, Istanbul, Turkey
[3] Department of Pediatrics, University of Health Sciences, Haseki Training and Research Hospital, Istanbul, Turkey
[4] Department of Pediatric Endocrinology, University of Health Sciences, Haseki Training and Research Hospital, Istanbul, Turkey
[5] Department of Pediatric Cardiology, University of Health Sciences, Haseki Training and Research Hospital, Istanbul, Turkey
[6] Department of Pediatric Neurology, University of Health Sciences, Haseki Training and Research Hospital, Istanbul, Turkey
[7] Department of Medical Biochemistry, University of Health Sciences, Haseki Training and Research Hospital, Istanbul, Turkey

A – research concept and design; B – collection and/or assembly of data; C – data analysis and interpretation;
D – writing the article; E – critical revision of the article; F – final approval of the article

Advances in Clinical and Experimental Medicine, ISSN 1899–5276 (print), ISSN 2451–2680 (online) *Adv Clin Exp Med*. 2024;33(1):31–38

Address for correspondence
Gulsen Akkoc
E-mail: agulsenakkoc@gmail.com

Funding sources
None declared

Conflict of interest
None declared

Received on September 3, 2022
Reviewed on November 13, 2022
Accepted on April 18, 2023

Published online on May 16, 2023

Abstract

Background. Evaluating predictors of coronavirus disease 2019 (COVID-19) and severity among children may help clinicians manage the high rate of hospital admissions for suspected cases.

Objectives. This study aimed to evaluate the demographic, clinical and laboratory characteristics of children during the pandemic, and determine the predictors of COVID-19 and moderate-to-severe disease.

Materials and methods. This retrospective cohort study included all consecutive COVID-19 cases in patients aged <18 years who presented to the Pediatric Emergency Department at Haseki Training and Research Hospital (Istanbul, Turkey) between March 15 and May 1, 2020, and underwent severe acute respiratory syndrome coronavirus 2 (SARS-CoV-2) polymerase chain reaction (PCR) analysis of oro-nasopharyngeal swabs (n = 1137).

Results. The frequency of SARS-CoV-2 PCR positivity was 28.6%. The COVID-19 (+) group presented with sore throat, headache and myalgia significantly more frequently than the COVID-19 (–) group. Multivariate logistic regression models showed independent predictors of SARS-CoV-2 positivity as follows: age, contact history, lymphocyte count <1500/mm^3, and neutrophil count <4000/mm^3. In addition, higher age, neutrophil count and fibrinogen levels were independent predictors of severity. The diagnostic cutoff value for fibrinogen (370.5 mg/dL) had a sensitivity of 53.12, specificity of 83.95, positive predictive value (PPV) of 39.53, and negative predictive value (NPV) of 90.07 for predicting severity.

Conclusions. Symptomatology, whether alone or in combination with other approaches, may be an appropriate strategy to guide the diagnosis and management of COVID-19.

Key words: children, fibrinogen, severity, COVID-19, SARS-CoV-2 PCR

Cite as
Akkoc G, Ağbaş A, Göksu E, et al. SARS-COV-2 infections in children: The role of fibrinogen in predicting diagnosis and severity: A retrospective cohort study. *Adv Clin Exp Med*. 2024;33(1):31–38. doi:10.17219/acem/163410

DOI
10.17219/acem/163410

Background

In late 2019, the novel severe acute respiratory syndrome coronavirus 2 (SARS-COV-2) was reported to be spreading globally and causing coronavirus disease 2019 (COVID-19). On February 11, 2020, the World Health Organization (WHO) declared this to be a pandemic.[1]

So far, around 2.5–15% of all reported COVID-19 cases have been in children, and this rate has increased over time.[2,3] The clinical course of COVID-19 in children has ranged from being asymptomatic to requiring intensive-care monitoring; however, a mild disease course has been the most common.[2,3] In children, the most frequent symptoms have been fever and cough, with respective incidence of 46% and 37% in those aged <9 years, and 35% and 41% in those aged ≥10 years.[3] Hospitalization rates have been lower in juveniles than in adult patients, with approx. 20% of pediatric cases requiring hospitalization.[4]

Although most children diagnosed with COVID-19 have been asymptomatic or have had a mild clinical course, the rate of juvenile patients admitted to hospitals has been increasing due to growing concerns about the pandemic. A severe disease course has been seen among juvenile cases, although at a lower incidence than among adults. Therefore, evaluating predictors of COVID-19 and a severe disease course among children may help clinicians to manage the high rate of hospital admissions of suspected cases.

Objectives

The primary objective of this study was to evaluate the demographic, clinical and laboratory characteristics of children with and without COVID-19 who were reported to our pediatric emergency department during the pandemic. The secondary objectives were to determine the predictors of COVID-19 and the predictors of a moderate-to-severe clinical course.

Materials and methods

Patients

The population for this retrospective cohort study included all consecutive pediatric cases aged <18 years who presented to the Pediatric Emergency Department at Haseki Training and Research Hospital (Istanbul, Turkey) between March 15 and May 1, 2020, and underwent SARS-CoV-2 real-time polymerase chain reaction (PCR) analysis of oro- and nasopharyngeal swabs (n = 1137 patients). Children with an indeterminate SARS-CoV-2 PCR result (n = 13) and those with a clinically high suspicion and a negative result (n = 25) were excluded from the study group. In total, 1099 children were enrolled in the study. Asymptomatic cases were excluded, and the remaining patients were divided into 2 groups according to the PCR test results: COVID-19-positive (COVID-19 (+); n = 262) and COVID-19-negative (COVID-19 (–); n = 621). The study population is detailed in Fig. 1.

The SARS-CoV-2 PCR-positive cases, according to clinical findings, were divided into 3 groups as follows: 1) an asymptomatic group, in which patients had undergone a PCR test due to contact history and had no symptoms; 2) a mild group, in which patients had nonspecific symptoms such as cough, fever, malaise, and myalgia; and 3) a moderate-to-severe group, in which patients had pneumonia that was confirmed with physical examination and imaging (chest X-ray and/or computed tomography (CT)), with or without a requirement for oxygen supplementation.

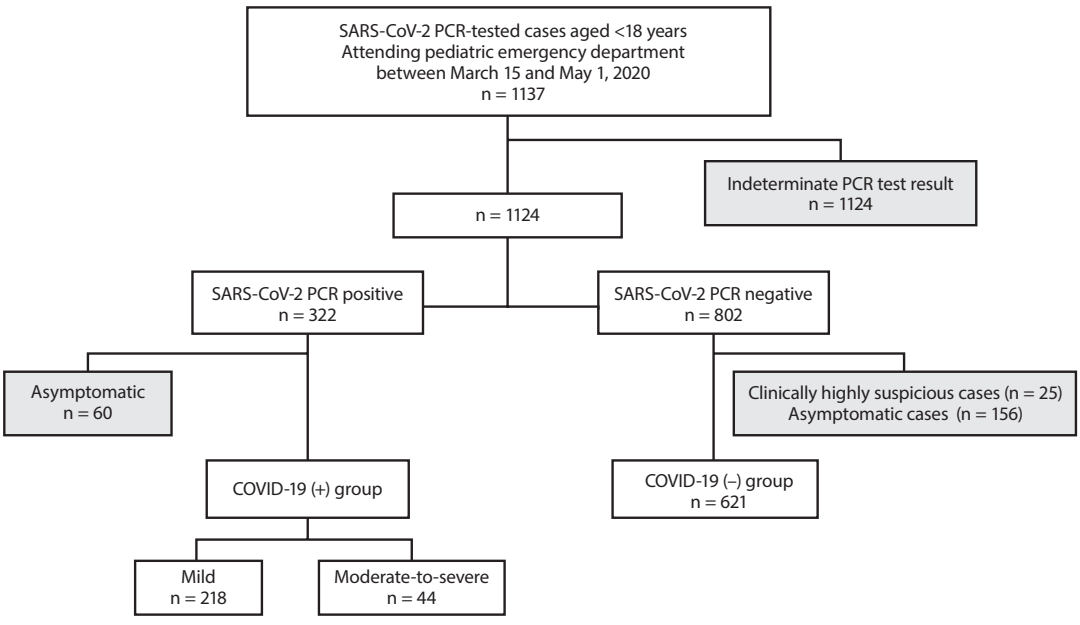

Fig. 1. Diagram showing a summary of the study population

COVID-19 – coronavirus disease 2019; PCR – polymerase chain reaction; SARS-CoV-2 – severe acute respiratory syndrome coronavirus 2.

Data collection

Demographic features, clinical data, and laboratory and imaging (chest X-ray and thorax CT) findings on admission were recorded retrospectively. Potential COVID-19 cases were routinely tested to determine complete blood count, erythrocyte sedimentation rate (ESR) and levels of C-reactive protein (CRP), procalcitonin, biochemical coagulation parameters, fibrinogen, and D-dimers. The SARS-CoV-2 presence was investigated using a reverse-transcription quantitative PCR (RT-qPCR) detection kit with oro-nasopharyngeal swabs (Bioksen ArGe Teknik Co. Ltd, Istanbul, Turkey; Biospeedy®).

The study protocol was in accordance with the Declaration of Helsinki. The protocol was approved by the Ethics Committee of the Haseki Training and Research Hospital (approval No. 2020-80).

Statistical analyses

Statistical analyses were performed using IBM SPSS v. 22.0 software (IBM Corp, Armonk, USA). The Shapiro–Wilk test was used to determine whether the variables were normally distributed. Numbers and percentages were used to express categorical variables. The mean ± standard deviation (M ±SD) or the median with the 25th and 75th percentiles were used to express continuous variables depending on whether they showed a parametric or nonparametric distribution. For the multivariate analysis, all variables were subject to a logistic regression analysis to determine independent predictors of COVID-19. All variables in the sample group without collinearity were included in a logistic regression model to determine the independent predictors of the latter. The Hosmer–Lemeshow test was used to assess the goodness-of-fit of the model. A 5% type-I error level was used to infer statistical significance. Akaike's information criterion (AIC) and Schwarz's Bayesian information criterion (BIC) values for logistic regression analysis models were measured using Jamovi statistical software v. 2.3.18 (https://www.jamovi.org/). A variance influence factor (VIF) of 3 was set as the cutoff value. The VIF values less than 3 indicated a low correlation among the variables included in the model. Since the number of observations totaled 726, the minimum sample size requirement was also met. The Box–Tidwell test was used to test the linearity between the predictors and the logit. Log-transformed interaction terms between the continuous independent variables and their natural logs were added to the model. Then, we re-ran the logistic model with the interaction terms. There were no statistically significant results in interaction terms ($p > 0.05$). Continuous independent variables were linearly related to the logit of the outcome variable, implying that the assumption was met. The capacity of fibrinogen levels in predicting moderate-to-severe clinical courses was analyzed using receiver operating characteristics (ROC) curve analysis. For fibrinogen, sensitivity, specificity, positive predictive value (PPV), negative predictive value (NPV), positive likelihood ratio (LR (+)), negative LR (LR (–)), accuracy, and area under the ROC curve (AUC) were calculated as diagnostic tools for predicting a moderate-to-severe clinical course. When evaluating the AUC, a 5% type-I error level was used to define a statistically significant predictive value for the test variables.

Results

The study population is summarized in Fig. 1. The frequency of SARS-CoV-2 PCR positivity was 28.6% (n = 322/1124) during the study period.

The clinical and laboratory findings of the COVID (+) and COVID (–) groups

The demographic and clinical characteristics of the COVID-19 (+) (n = 262) and COVID-19 (–) (n = 621) groups are shown in Table 1. The ratio of hospitalization was significantly different between the COVID-19 (+) and COVID-19 (–) groups: 38 patients (14.5%) compared to 55 patients (8.9%), respectively ($p = 0.013$). All hospitalized patients were discharged with a good outcome, and none of the hospitalized patients required intensive care.

Among the 883 symptomatic cases, laboratory studies were performed in 726 patients (82.2%) within the first 3 days. The laboratory findings of COVID-19 (+) (n = 228) and COVID-19 (–) (n = 498) groups are shown in Table 2.

Predictors of COVID-19

All variables in the 2 groups were included in the logistic regression analysis. The logistic regression analysis found that age, contact history, lymphocyte count below 1500/mm^3, and neutrophil count below 4000/mm^3 on admission were independent predictors of SARS-CoV-2 PCR positivity (Table 3).

Characteristics of the COVID-19 (+) group

A total of 322 COVID-19 (+) patients were evaluated. The median age was 151 months (81; 192), and 164 (50.9%) were female. According to clinical severity, an asymptomatic course was observed in 18.6% (n = 60), a mild course in 67.7% (n = 218) and a moderate-to-severe course in 13.7% (n = 44) of the patients. Twenty-two cases (7.2%) had underlying comorbidities, the most common of which were asthma, cerebral palsy and familial Mediterranean fever. The most common symptoms were cough, fever and sore throat in the mild subgroup (61.0%, 54.1% and 25.2%, respectively), and cough, fever and shortness of breath in the moderate-to-severe subgroup (84.1%,

Table 1. Comparison of COVID-19 (+) and COVID-19 (–) patient groups and comparison of the mild and the moderate-to-severe COVID-19 (+) subgroups

Variable	COVID-19 (+) (n = 262)			COVID-19 (–) (n = 621)
	Mild (n = 218)	Moderate-to-severe (n = 44)	Total	
Age [months], median (25th; 75th percentile)	152 (70.5; 193)	184 (133; 203)	159 (82; 198)	100 (37; 171)
Male sex, n (%)	103 (47.2)	17 (38.6)	120 (45.8)	339 (54.6)
Contact history, n (%)	199 (91.3)	40 (90.9)	239 (91.2)	332 (53.4)
Fever, n (%)	118 (54.1)	26 (59.1)	144 (55.0)	341 (54.9)
Cough, n (%)	133 (61.0)	37 (84.1)	170 (64.9)	396 (63.8)
Shortness of breath, n (%)	25 (11.5)	14 (31.8)	39 (14.9)	92 (14.8)
Sore throat, n (%)	55 (25.2)	5 (7.1)	60 (22.9)	87 (14.0)
Fatigue, n (%)	41 (18.8)	7 (14.6)	48 (18.3)	86 (13.8)
Headache, n (%)	36 (17.9)	8 (18.2)	47 (17.9)	50 (8.1)
Vomiting, n (%)	11 (5.0)	7 (15.9)	18 (6.9)	57 (9.2)
Diarrhea, n (%)	20 (9.2)	7 (15.9)	27 (10.3)	45 (7.2)
Myalgia, n (%)	24 (11.0)	5 (11.4)	29 (11.1)	42 (6.8)
Abdominal pain, n (%)	11 (5.0)	2 (4.5)	13 (5.0)	37 (6.0)
Fever and cough, n (%)	71 (32.6)	24 (54.5)	95 (36.3)	195 (31.4)
Cough and shortness of breath, n (%)	14 (6.4)	14 (31.8)	28 (10.7)	64 (10.3)
Fever, cough and shortness of breath (at least 2 of the above), n (%)	83 (38.1)	32 (72.7)	115 (43.9)	234 (37.7)

COVID-19 – coronavirus disease 2019.

Table 2. The comparison of inflammation markers between COVID-19 (+) and (–) groups and between COVID-19 (+) subgroups

Variable	Mild COVID-19		Moderate-to-severe COVID-19		Total COVID-19 (+)		COVID-19 (–)	
	n	M ±SD or Me (IQR 25th; 75th)	n	M ±SD or Me (IQR 25th; 75th)	n	M ±SD or Me (IQR 25th; 75th)	n	M ±SD or Me (IQR 25th; 75th)
Leukocytes [cells/mm^3]	182	7544 ±2820	44	5880 ±2073	224	7232 ±2777	491	10.787 ±4457
Neutrophils [cells/mm^3]	182	3555 (2278; 4947)	44	2630 (1860; 3640)	224	3340 (2180; 4690)	491	5070 (3320; 7840)
Neutrophil count <4000/mm^3, n (%)	–	109 (59.9)	–	36 (81.8)	–	145 (64.7)	–	181 (36.9)
Lymphocytes [cells/mm^3]	182	2330 (1605; 3315)	44	1900 (1350; 2480)	224	2280 (1590; 3150)	491	3015 (2137; 4497)
Lymphocyte count <1500/mm^3, n (%)	–	34 (18.9)	–	12 (27.2)	–	46 (20.5)	–	46 (9.4)
Platelets [cells/mm^3]	182	262.846 ±75.892	44	233.750 ±66.542	224	257.152 ±75.095	491	291.081 ±91.313
Platelet count <150,000/mm^3, n (%)	–	5 (2.7)	–	1 (2.3)	–	6 (2.7)	–	13 (2.6)
Neutrophil-to-lymphocyte ratio	182	1.39 (0.83; 2.55)	44	1.25 (0.85; 2.28)	224	1.34 (0.84; 2.41)	491	1.68 (0.88; 3.07)
CRP [mg/dL]	186	1.8 (0,8; 5,9)	44	4.0 (1,2; 13,8)	228	2.1 (0,8; 7.53)	498	3.4 (0,6; 22.95)
CRP level >5 mg/dL, n (%)	–	57 (30.6)	–	21 (47.7)	228	78 (34.2)	498	228 (45.8)
Procalcitonin [µg/dL]	153	0.03 (0.02; 0.07)	40	0.05 (0.02; 0.09)	191	0.03 (0.02; 0.08)	301	0.04 (0.02; 0.12)
Procalcitonin level ≥0.05 µg/dL, n (%)	–	59 (38.6)	–	21 (52.5)	–	80 (41.8)	–	148 (49.2)
D-dimer [mg/L]	145	0.39 (0.29; 0.56)	43	0.47 (0.28; 1.17)	186	0.40 (0.28; 0.62)	311	0.50 (0.30; 0.90)
D-dimer level >0.55 mg/L, n (%)	–	38 (26.2)	–	21 (48.8)	186	59 (31.7)	311	138 (44.4)
Fibrinogen [g/L]	151	2.96 ±0.69	43	3.49 ±0.91	192	3.08 ±0.78	318	3.13 ±1.03
Fibrinogen level >3 g/L, n (%)	–	59 (39.1)	–	32 (74.4)	–	91 (47.4)	–	147 (46.2)
Erythrocyte sedimentation rate [mm/h]	67	8 (4,5; 14,5)	29	15 (7,5; 24)	96	9 (5;17)	122	11 (5.0; 27.0)

COVID-19 – coronavirus disease 2019; M ±SD – mean ± standard deviation; Me – median; IQR – interquartile range; CRP – C-reactive protein.

59.1% and 31.8%, respectively; Table 1). Thoracic CTs were performed in 39.1% (n = 126) of the COVID-19 (+) group, and 27.7% showed abnormal findings (Supplementary Table 1).

Among the 262 symptomatic COVID-19 (+) cases, laboratory studies were performed in 228 (87.0%) within the first 3 days. The laboratory findings of the COVID-19 (+) subgroup are shown in Table 2.

Table 3. Predictors of having COVID-19

Predictors	p-value	OR	95% CI
Age (per year)	**0.024**	1.06	1.01–1.12
Gender	0.580	1.15	0.71–1.89
Fever	0.752	1.14	0.50–2.64
Cough	0.561	1.26	0.58–2.72
Shortness of breath	0.592	1.43	0.38–5.36
Sore throat	0.282	1.42	0.75–2.69
Headache	0.212	1.61	0.76–3.41
Myalgia	0.862	1.09	0.42–2.81
Fatigue	0.997	1.00	0.48–2.08
Diarrhea	0.888	1.06	0.45–2.52
Vomiting	0.755	1.15	0.46–2.92
Abdominal pain	0.554	1.54	0.37–6.47
Fever and cough	0.225	2.41	0.58–10.00
Cough and shortness of breath	0.615	1.44	0.35–6.00
At least 2 of the following: fever, cough or shortness of breath	0.385	0.52	0.12–2.23
Contact history	**<0.001**	11.21	4.92–25.56
Lymphocyte count <1500/mm^3	0.013	3.04	1.27–7.30
Neutrophil count <4000/mm^3	**<0.001**	3.14	1.83–5.39
Platelet count <150,000/mm^3	0.280	2.36	0.50–11.20
CRP >5 mg/dL	0.552	1.25	0.63–2.52
Procalcitonin level ≥0.05 µg/dL	0.144	1.63	0.85–3.15
D-dimer level >0.55 mg/L	**0.021**	0.53	0.31–0.91
Fibrinogen level >3 g/L	0.374	1.29	0.74–2.25

Hosmer–Lemeshow test p= 0.614; model summary Nagelkerke R^2 = 0.332; model fit measures: Akaike's information criterion (AIC) = 470, Bayesian information criterion (BIC) = 566. 95% CI – 95% confidence interval; COVID-19 – coronavirus disease 2019; OR – odds ratio; CRP – C-reactive protein. Values in bold are statistically significant.

Predictors of a moderate-to-severe disease course

All variables in the 2 groups were included in the logistic regression analysis. The logistic regression analysis found higher age, neutrophil count and fibrinogen level to be independent predictors of moderate-to-severe disease (Table 4).

A ROC curve was used to assess the predictive efficacies of fibrinogen levels, which reached AUC values of 0.706 (Fig. 2). Table 5 shows the sensitivity, specificity, PPV, NPV, LR (+) and LR (–) accuracy, and the AUC value for fibrinogen levels in predicting a moderate-to-severe clinical course.

Table 4. Predictors of having moderate-to-severe COVID-19 course

Predictors	p-value	OR	95% CI
Age (per year)	**0.011**	1.17	1.04–1.32
Gender	0.798	1.17	0.36–3.77
Fever	0.304	0.33	0.04–2.71
Cough	0.470	0.54	0.10–2.84
Shortness of breath	0.990	0	0–0
Sore throat	0.928	0.94	0.21–3.99
Diarrhea	0.791	0.79	0.14–4.47
Vomiting	**0.015**	8.92	1.52–58.21
Headache	0.847	0.87	0.21–3.64
Fatigue	0.841	0.87	0.21–3.47
Myalgia	0.804	0.78	0.10–5.75
Abdominal pain	0.781	1.54	0.07–33.08
Fever and cough	0.707	1.90	0.07–53.27
Cough and shortness of breath	0.989	0	0–0
At least 2 of the following: fever, cough or shortness of breath	0.643	2.04	0.10–42.06
Lymphocyte count <1500/mm^3	0.371	1.81	0.49–6.59
Neutrophil count <4000/mm^3	**0.022**	4.36	1.23–15.38
Platelet count <150,000/mm^3	0.627	0.48	0.03–9.11
CRP >5 mg/dL	0.963	1.03	0.29–3.65
Procalcitonin level ≥0.05 µg/dL	0.066	3.62	0.92–14.33
Fibrinogen level >3 g/L	**0.017**	3.75	1.26–11.14
D-dimer level >0.55 mg/L	0.067	3.09	0.93–10.33

Hosmer–Lemeshow test p = 0.906; model summary Nagelkerke R^2 = 0.512; model fit measures: Akaike's information criterion (AIC) = 158, Bayesian information criterion (BIC) = 230. 95% CI – 95% confidence interval; COVID-19 – coronavirus disease 2019; OR – odds ratio, CRP – C-reactive protein. Values in bold are statistically significant.

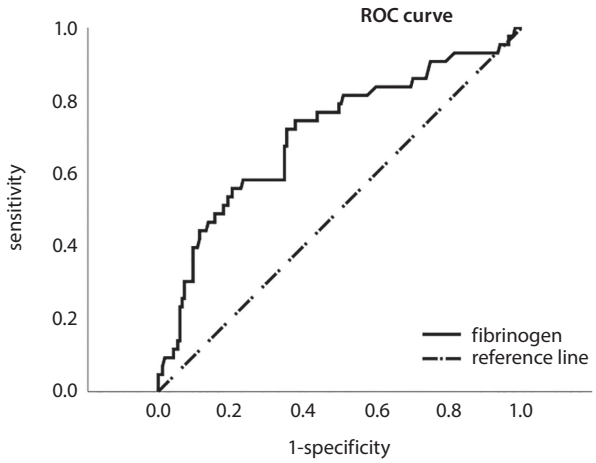

Fig. 2. ROC curve of fibrinogen levels

AUC – area under the ROC curve; ROC – receiver operating characteristics.

Discussion

We comprehensively evaluated the demographic and clinical characteristics and laboratory features of patients who underwent a SARS-CoV-2 infection evaluation. In our study sample, the positive test result rate was 1 in 3 for all groups. The relatively large number of COVID-19 (+) children (n = 322) in this cohort provided an opportunity to report on the descriptive, clinical and laboratory features of COVID-19 in children.

Table 5. Predictive efficacies of fibrinogen for moderate-to-severe COVID-19 course

Parameter	AUC (95% CI)	p-value	Cutoff value	Sensitivity (95% CI)	Specificity (95% CI)	PPV (95% CI)	NPV (95% CI)	LR (+) (95% CI)	LR (–) (95% CI)
Fibrinogen [mg/dL]	0.695 (0.599–0.792)	<0.001	333.5	40.32 (28.05–53.55)	86.36 (79.31–91.71)	58.14 (45.09–70.14)	75.50 (71.29–79.26)	2.96 (1.75–5.00)	0.69 (0.56–0.86)
–	–	–	370.5	53.12 (34.74–70.91)	83.95 (77.37–89.24)	39.53 (28.81–51.37)	90.07 (86.17–92.95)	3.31 (2.05–5.35)	0.56 (0.38–0.81)

AUC – area under curve; COVID-19 – coronavirus disease 2019; LR (+) – positive like hood ratio; LR (–) – negative like hood ratio; NPV – negative predictive value; PPV – positive predictive value; 95% CI – 95% confidence interval.

The frequency of SARS-CoV-2 PCR positivity in this study group was 28.6%, while a 38% rate was reported in adults during the early stages of the pandemic in China.[5] Despite the fact that SARS-CoV-2 infections were observed in children and juveniles of various age, 61.5% of our cases were under the age of 10 compared to previously reported rates of 46.1% to 56.8% among COVID-19 cases in children.[6,7] Asymptomatic cases were found in 18.6% of children in our study, while this rate was 10–35% in other reports concerning COVID-19 in children.[7–11] The ratio of asymptomatic cases did not reflect the true prevalence of asymptomatic disease as we performed PCR tests on children due to contact history, and this was not a screening study for a population.

According to the literature, a mild disease course with upper respiratory tract illness has been the most common presentation of COVID-19 in children, and the incidence rate has ranged between 33% and 79% across studies.[6,8,10,12,13] In the current study, the incidence of mild disease was 67.7%, and the most frequent symptoms were cough, fever and sore throat. The rates of fever and cough were 42–52% and 44–48%, respectively, in mild cases.[8,14,15] The possible reasons for children having a relatively mild disease course have not been validated but are thought to include less intense immune and inflammatory responses, differences in airway epithelial and angiotensin-converting enzyme-2 (ACE2) receptor expression and upregulation, pre-existing immunity to common coronaviruses, better control of viral replication, and fewer preexisting comorbidities.[16–22]

In the current study, a moderate-to-severe disease course was seen in 13.7% of the COVID-19 (+) cases. Although a mild COVID-19 disease course has so far been the most common among children, a moderate-to-severe disease course has been reported in between 9.1% and 33.3% of cases.[13,23] These were mostly comprised of hospitalized patients, which account for 2.3–18.2% of all confirmed pediatric COVID-19 cases.[4,7,24] Therefore, correctly identifying patients with a moderate-to-severe COVID-19 course is essential for healthcare professionals to perform appropriate management and treatment. In the current study, we found that higher age was an independent risk factor for moderate-to-severe COVID-19. Consistent with our results, differences in ACE2 expression during puberty and other age-related factors have been reported to have an important effect on the severity of COVID-19.[16–22]

Moreover, the current study revealed that high fibrinogen levels were an independent predictor of moderate-to-severe COVID-19 course. Fibrinogen concentrations can increase in a setting of injury, inflammation and infection.[25] High fibrinogen levels have been associated with a moderate-to-severe disease course in children.[26] In a meta-analysis by Nugroho et al., a high fibrinogen level on admission was found in patients with a severe disease course.[27] Patients who had high fibrinogen levels (>4 g/L) were more commonly treated in an intensive care unit (ICU) than in a general ward compared to adult COVID-19 cases.[28] Moreover, Bi et al. found that fibrinogen levels were higher in individuals with severe illness.[29] In children, fibrinogen level may be a useful tool to predict severity. However, the cutoff point for this parameter has not been well-defined in children.[23]

The correct identification of patients with a high suspicion of infection by SARS-CoV-2 will be an important tool for physicians in determining which patients should be prioritized for further testing. Some researchers have developed predictive models for the diagnosis of COVID-19 to be used in settings where diagnostic tests may not be available to first-contact physicians.[30–32] In the current study, there was a strong association between higher age and the rate of positive test results in the model. Murillo-Zamora et al. found that age of 13–15 years was associated with a twofold increase in the odds of testing positive for SARS-CoV-2.[33] These results support the finding that younger children (<10 years) are protected (to some extent) from SARS-CoV-2 infection by the possible reason of changes in ACE2 expression and activity in puberty.[16,34] Among the significant symptoms, there was an association between headache and having at least 2 episodes of fever, cough or shortness of breath and COVID-19 infection. Mutiawati et al. revealed that headache was approximately twice more common in COVID-19 patients than in non-COVID-19 patients (with other viral infections).[35] We found that contact history was the major predictor and accounted for the highest increase in the rate of COVID-19 diagnosis, in line with several other studies.[36–38] Moreover, in the current study, experiencing at least 2 episodes of fever, cough and shortness of breath

was significantly associated with SARS-CoV-2 positivity, similarly to previous reports.[39,40]

Abnormal laboratory findings such as lymphopenia, leukopenia, thrombocytopenia, and elevated inflammatory markers (CRP and procalcitonin) were found in this cohort of pediatric COVID-19 patients, which was consistent with the literature.[9,41,42] It was found that a lymphocyte count below 1500/mm^3 and a neutrophil count below 4000/mm^3 were independent predictors of SARS-CoV-2 PCR positivity. Lower leukocyte, neutrophil, lymphocyte, and platelet counts were seen in cases of COVID-19 pneumonia compared to cases of non-COVID-19 pneumonia.[43] In addition, some studies showed that low lymphocyte counts were independent predictors of SARS-CoV-2 infections.[44,45] The SARS-CoV-2 RT-qPCR assay is considered the gold standard test for COVID-19.[46] Nonetheless, determining the predictors of COVID-19 infection and correctly identifying patients with a high suspicion of infection by SARS-CoV-2 are essential for emergency service practitioners before RT-qPCR results are available. Finally, including the symptoms and laboratory findings significantly associated with SARS-CoV-2 infection in a predictive model will allow for a faster and more accurate final diagnosis.

Limitations of the study

There were several limitations to this study. We enrolled all consecutive patients who had undergone a test, so the subgroups were not equal in size. Furthermore, this was a single-center study and it retrospectively evaluated children who had been admitted to the hospital.

However, our study group comprised a significant number of symptomatic patients, which means that the findings and inferences are relevant. The relatively large number of COVID-19 (+) patients (n = 322) in our cohort allowed us to report on the descriptive, clinical and laboratory features of COVID-19 among children. The large number of pediatric cases enrolled and the use of RT-qPCR as a gold standard for SARS-CoV-2 diagnosis of clinical specimens are strengths of this study.

Conclusions

Determining the factors associated with diagnosis and clinical severity are important for childhood COVID-19 cases. The current study sheds light on the absence of specificity regarding the severity of disease and symptoms in children with and without COVID-19. Symptomatology, whether alone or in combination with other approaches, may be an appropriate strategy to use in an emergency department setting to guide the diagnosis and management of the disease. While our models do not justify presumptive SARS-CoV-2 diagnosis without an RT-qPCR assay, they can contribute to developing further screening strategies.

Supplementary data

The Supplementary materials are available at https://doi.org/10.5281/zenodo.7827579. The package contains the following files:

Supplementary Table 1. Radiological characteristics of all COVID-19 (+) cases.

ORCID iDs

Gulsen Akkoc https://orcid.org/0000-0002-1444-1187
Ayşe Ağbaş https://orcid.org/0000-0002-3658-8622
Eralp Göksu https://orcid.org/0000-0001-5306-4102
Sevde Beyaz https://orcid.org/0000-0002-5511-5505
Funda Yıldız https://orcid.org/0000-0002-1008-4848
Elvan Bayramoğlu https://orcid.org/0000-0002-6732-8823
Canan Yolcu https://orcid.org/0000-0002-1728-0497
Senem Ayça https://orcid.org/0000-0001-7486-9655
Nurcihan Çalışkan Dolu https://orcid.org/0000-0002-7171-7661
Kamil Şahin https://orcid.org/0000-0002-0443-2148
Macit Koldaş https://orcid.org/0000-0001-8967-2708
Murat Elevli https://orcid.org/0000-0002-0510-965X

References

1. World Health Organization (WHO). WHO Director-General's Remarks at the Media Briefing on 2019-NCoV on 11 February 2020. Geneva, Switzerland: World Health Organization; 2020. https://www.who.int/director-general/speeches/detail/who-director-general-s-remarks-at-the-media-briefing-on-2019-ncov-on-11-february-2020. Accessed November 21, 2021.
2. Stokes EK, Zambrano LD, Anderson KN, et al. Coronavirus disease 2019 case surveillance: United States, January 22–May 30, 2020. *MMWR Morb Mortal Wkly Rep*. 2020;69(24):759–765. doi:10.15585/mmwr.mm6924e2
3. CDC COVID-19 Response Team. Coronavirus disease 2019 in children: United States, February 12–April 2, 2020. *MMWR Morb Mortal Wkly Rep*. 2020;69(14):422–426. doi:10.15585/mmwr.mm6914e4
4. Otto WR, Geoghegan S, Posch LC, et al. The epidemiology of severe acute respiratory syndrome coronavirus 2 in a pediatric healthcare network in the United States. *J Pediatric Infect Dis Soc*. 2020;9(5):523–529. doi:10.1093/jpids/piaa074
5. Liu R, Han H, Liu F, et al. Positive rate of RT-PCR detection of SARS-CoV-2 infection in 4880 cases from one hospital in Wuhan, China, from Jan to Feb 2020. *Clin Chim Acta*. 2020;505:172–175. doi:10.1016/j.cca.2020.03.009
6. Dong Y, Mo X, Hu Y, et al. Epidemiology of COVID-19 among children in China. *Pediatrics*. 2020;145(6):e20200702. doi:10.1542/peds.2020-0702
7. Leidman E, Duca LM, Omura JD, Proia K, Stephens JW, Sauber-Schatz EK. COVID-19 trends among persons aged 0–24 years: United States, March 1–December 12, 2020. *MMWR Morb Mortal Wkly Rep*. 2021;70(3):88–94. doi:10.15585/mmwr.mm7003e1
8. Lu X, Zhang L, Du H, et al. SARS-CoV-2 infection in children. *N Engl J Med*. 2020;382(17):1663–1665. doi:10.1056/NEJMc2005073
9. Cui X, Zhao Z, Zhang T, et al. A systematic review and meta-analysis of children with coronavirus disease 2019 (COVID-19). *J Med Virol*. 2021;93(2):1057–1069. doi:10.1002/jmv.26398
10. Assaker R, Colas AE, Julien-Marsollier F, et al. Presenting symptoms of COVID-19 in children: A meta-analysis of published studies. *Br J Anaesth*. 2020;125(3):e330–e332. doi:10.1016/j.bja.2020.05.026
11. Zimmermann P, Curtis N. COVID-19 in children, pregnancy and neonates: A review of epidemiologic and clinical features. *Pediatr Infect Dis J*. 2020;39(6):469–477. doi:10.1097/INF.0000000000002700
12. Mantovani A, Rinaldi E, Zusi C, Beatrice G, Saccomani MD, Dalbeni A. Coronavirus disease 2019 (COVID-19) in children and/or adolescents: A meta-analysis. *Pediatr Res*. 2021;89(4):733–737. doi:10.1038/s41390-020-1015-2
13. Liguoro I, Pilotto C, Bonanni M, et al. SARS-COV-2 infection in children and newborns: A systematic review. *Eur J Pediatr*. 2020;179(7):1029–1046. doi:10.1007/s00431-020-03684-7

14. Zheng F, Liao C, Fan QH, et al. Clinical characteristics of children with coronavirus disease 2019 in Hubei, China. *Curr Med Sci*. 2020;40(2): 275–280. doi:10.1007/s11596-020-2172-6
15. Meena J, Yadav J, Saini L, Yadav A, Kumar J. Clinical features and outcome of SARS-CoV-2 infection in children: A systematic review and meta-analysis. *Indian Pediatr*. 2020;57(9):820–826. doi:10.1007/s13312-020-1961-0
16. Yonker LM, Neilan AM, Bartsch Y, et al. Pediatric severe acute respiratory syndrome coronavirus 2 (SARS-CoV-2): Clinical presentation, infectivity, and immune responses. *J Pediatr*. 2020;227:45–52.e5. doi:10.1016/j.jpeds.2020.08.037
17. Yonker LM, Shen K, Kinane TB. Lessons unfolding from pediatric cases of COVID-19 disease caused by SARS-CoV-2 infection. *Pediatr Pulmonol*. 2020;55(5):1085–1086. doi:10.1002/ppul.24748
18. Bunyavanich S, Do A, Vicencio A. Nasal gene expression of angiotensin-converting enzyme 2 in children and adults. *JAMA*. 2020;323(23): 2427–2429. doi:10.1001/jama.2020.8707
19. Zimmermann P, Curtis N. Why is COVID-19 less severe in children? A review of the proposed mechanisms underlying the age-related difference in severity of SARS-CoV-2 infections. *Arch Dis Child*. 2021; 106(5):429–439. doi:10.1136/archdischild-2020-320338
20. Cristiani L, Mancino E, Matera L, et al. Will children reveal their secret? The coronavirus dilemma. *Eur Respir J*. 2020;55(4):2000749. doi:10.1183/13993003.00749-2020
21. García-Salido A. Three hypotheses about children COVID19. *Pediatr Infect Dis J*. 2020;39(7):e157. doi:10.1097/INF.0000000000002701
22. Grifoni A, Weiskopf D, Ramirez SI, et al. Targets of T cell responses to SARS-CoV-2 coronavirus in humans with COVID-19 disease and unexposed individuals. *Cell*. 2020;181(7):1489–1501.e15. doi:10.1016/j.cell.2020.05.015
23. Escosa-García L, Aguilera-Alonso D, Calvo C, Mellado MJ, Baquero-Artigao F. Ten key points about COVID-19 in children: The shadows on the wall. *Pediatric Pulmonol*. 2020;55(10):2576–2586. doi:10.1002/ppul.25025
24. Howard LM, Garguilo K, Gillon J, et al. The first 1000 symptomatic pediatric SARS-CoV-2 infections in an integrated health care system: A prospective cohort study. *BMC Pediatr*. 2021;21(1):403. doi:10.1186/s12887-021-02863-1
25. Weisel JW. Fibrinogen and fibrin. *Adv Protein Chem*. 2005;70:247–299. doi:10.1016/S0065-3233(05)70008-5
26. Guner Ozenen G, Sahbudak Bal Z, Umit Z, et al. Demographic, clinical, and laboratory features of COVID-19 in children: The role of mean platelet volume in predicting hospitalization and severity. *J Med Virol*. 2021;93(5):3227–3237. doi:10.1002/jmv.26902
27. Nugroho J, Wardhana A, Mulia EP, et al. Elevated fibrinogen and fibrin degradation product are associated with poor outcome in COVID-19 patients: A meta-analysis. *Clin Hemorheol Microcirc*. 2021;77(2):221–231. doi:10.3233/CH-200978
28. Chen Y, Geng Y, Xu X, et al. The features comparison between patients in the ICU and general wards and between patients with different outcomes: A 2020 COVID-19 study. *Ann Palliat Med*. 2021;10(1): 672–680. doi:10.21037/apm-21-25
29. Bi X, Su Z, Yan H, et al. Prediction of severe illness due to COVID-19 based on an analysis of initial fibrinogen to albumin ratio and platelet count. *Platelets*. 2020;31(5):674–679. doi:10.1080/09537104.2020.1760230
30. Chow EJ, Schwartz NG, Tobolowsky FA, et al. Symptom screening at illness onset of health care personnel with SARS-CoV-2 infection in King County, Washington. *JAMA*. 2020;323(20):2087–2089. doi:10.1001/jama.2020.6637
31. Tostmann A, Bradley J, Bousema T, et al. Strong associations and moderate predictive value of early symptoms for SARS-CoV-2 test positivity among healthcare workers, the Netherlands, March 2020. *Euro Surveill*. 2020;25(16):2000508. doi:10.2807/1560-7917.ES.2020.25.16.2000508
32. Hopman J, Allegranzi B, Mehtar S. Managing COVID-19 in low- and middle-income countries. *JAMA*. 2020;323(16):1549. doi:10.1001/jama.2020.4169
33. Murillo-Zamora E, Aguilar-Sollano F, Delgado-Enciso I, Hernandez-Suarez CM. Predictors of laboratory-positive COVID-19 in children and teenagers. *Public Health*. 2020;189:153–157. doi:10.1016/j.puhe.2020.10.012
34. Liu J, Ji H, Zheng W, et al. Sex differences in renal angiotensin converting enzyme 2 (ACE2) activity are 17β-oestradiol-dependent and sex chromosome-independent. *Biol Sex Differ*. 2010;1(1):6. doi:10.1186/2042-6410-1-6
35. Mutiawati E, Syahrul S, Fahriani M, et al. Global prevalence and pathogenesis of headache in COVID-19: A systematic review and meta-analysis. *F1000Res*. 2020;9:1316. doi:10.12688/f1000research.27334.2
36. Just J, Puth MT, Regenold F, Weckbecker K, Bleckwenn M. Risk factors for a positive SARS-CoV-2 PCR in patients with common cold symptoms in a primary care setting: A retrospective analysis based on a joint documentation standard. *BMC Fam Pract*. 2020;21(1):251. doi:10.1186/s12875-020-01322-7
37. Oshman L, Caplan A, Ali R, et al. Whom should we test for COVID-19? Performance of a symptom and risk factor questionnaire on COVID-19 test results and patient outcomes in an immediate care setting. *J Prim Care Community Health*. 2020;11:215013272098129. doi:10.1177/2150132720981297
38. Maechler F, Gertler M, Hermes J, et al. Epidemiological and clinical characteristics of SARS-CoV-2 infections at a testing site in Berlin, Germany, March and April 2020: A cross-sectional study. *Clin Microbiol Infect*. 2020;26(12):1685.e7–1685.e12. doi:10.1016/j.cmi.2020.08.017
39. Sudre CH, Keshet A, Graham MS, et al. Anosmia, ageusia, and other COVID-19-like symptoms in association with a positive SARS-CoV-2 test, across six national digital surveillance platforms: An observational study. *Lancet Digit Health*. 2021;3(9):e577–e586. doi:10.1016/S2589-7500(21)00115-1
40. Romero-Gameros CA, Colin-Martínez T, Waizel-Haiat S, et al. Diagnostic accuracy of symptoms as a diagnostic tool for SARS-CoV 2 infection: A cross-sectional study in a cohort of 2,173 patients. *BMC Infect Dis*. 2021;21(1):255. doi:10.1186/s12879-021-05930-1
41. Yasuhara J, Kuno T, Takagi H, Sumitomo N. Clinical characteristics of COVID-19 in children: A systematic review. *Pediatric Pulmonol*. 2020;55(10):2565–2575. doi:10.1002/ppul.24991
42. Badal S, Thapa Bajgain K, Badal S, Thapa R, Bajgain BB, Santana MJ. Prevalence, clinical characteristics, and outcomes of pediatric COVID-19: A systematic review and meta-analysis. *J Clin Virol*. 2021;135: 104715. doi:10.1016/j.jcv.2020.104715

The relationship between the clinical course of SARS-CoV-2 infections and *ACE2* and *TMPRSS2* expression and polymorphisms

Esra Tug[1,A,C–E], Isil Fidan[2,A–F], Gulendam Bozdayi[2,A,B,E], Fatma Yildirim[3,B,E], Ozlem Guzel Tunccan[4,A,B,E], Zubeyde Lale[5,B,D,E], Dogan Akdogan[6,A,B]

[1] Department of Medical Genetics, Medical University of Gazi, Turkey
[2] Department of Medical Microbiology, Medical University of Gazi, Turkey
[3] Department of Chest Diseases, Pulmonary Intensive Care Unit, University of Health Sciences, Diskapi Yildirim Beyazit Research and Education Hospital, Turkey
[4] Department of Infectious Diseases, Medical University of Gazi, Turkey
[5] Department of Medical Microbiology, Dışkapı Yıldırım Beyazit Research and Education Hospital, Turkey
[6] Department of Medical Microbiology, Pursaklar State Hospital, Turkey

A – research concept and design; B – collection and/or assembly of data; C – data analysis and interpretation; D – writing the article; E – critical revision of the article; F – final approval of the article

Advances in Clinical and Experimental Medicine, ISSN 1899–5276 (print), ISSN 2451–2680 (online) *Adv Clin Exp Med*. 2024;33(1):39–51

Address for correspondence
Isil Fidan
E-mail: isilfidan@yahoo.com

Funding sources
This study was supported by research grant from Scientific Research Projects Unit of Gazi University (grant No. 01/2020-49). This study was presented as a poster at the 24th Annual Conference of the European Society for Clinical Virology (ESCV) (September 7–10, 2022, Manchester, UK).

Conflict of interest
None declared

Acknowledgements
The authors would like to thank Gazi University Academic Writing Application and Research Center for proofreading the article.

Received on December 14, 2022
Reviewed on April 1, 2023
Accepted on April 18, 2023

Published online on June 16, 2023

Cite as
Tug E, Fidan I, Bozdayi G, et al. The relationship between the clinical course of SARS-CoV-2 infections and *ACE2* and *TMPRSS2* expression and polymorphisms. *Adv Clin Exp Med*. 2024;33(1):39–51. doi:10.17219/acem/163409

DOI
10.17219/acem/163409

Abstract

Background. The viral spike (S) protein and host *ACE2* and *TMPRSS2* genetic variations may act as a barrier to viral infections or determine susceptibility to severe acute respiratory syndrome coronavirus 2 (SARS-CoV-2) infections.

Objectives. We investigated the relationship between the expression patterns and polymorphisms of the *ACE2* and *TMPRSS2* receptor genes associated with coronavirus disease 2019 (COVID-19) and the clinical course of SARS-CoV-2 infections.

Materials and methods. We examined 147 COVID-19 patients (41 asymptomatic, 53 symptomatic and 53 cases treated in the intensive care unit (ICU)) and 33 healthy controls. The *ACE2* and *TMPRSS2* expression was determined using the One-Run RT-qPCR kit. Genotypic distributions of single nucleotide polymorphisms (SNPs) of *ACE2* and *TMPRSS2* were obtained using reverse transcription quantitative polymerase chain reaction (RT-qPCR).

Results. The expressions of *ACE2* and *TMPRSS2* were different between SARS-CoV-2-positive and -negative groups. The *ACE2* rs714205GG genotype and G-allele showed significant differences in the asymptomatic SARS-CoV-2-positive group. A significant correlation was found between the expression of *TMPRSS2* rs8134378GA, rs2070788GA, rs7364083GA, and rs9974589AC genotypes and SARS-CoV-2 positivity. The rs1978124 G-allele and rs8134378 A-allele expressions were significant in the symptomatic SARS-CoV-2-positive group. The *TMPRSS2* rs2070788GA expression was different in all patient groups compared to the control group. There was a difference between SARS-CoV-2-positive and -negative groups regarding the CTTA haplotype formed by *ACE2* variants. The AGCAG and AGAAG haplotypes formed by the *TMPRSS2* variants were more common in the asymptomatic patient group than in other patient groups.

Conclusions. Identifying the relationship between host genetic variants and COVID-19 susceptibility will contribute to further studies, enabling new vaccines and potential therapeutic approaches to be discovered.

Key words: single nucleotide polymorphisms, expressions, COVID-19, *ACE2* gene, *TMPRSS2* gene

Background

The new type of severe acute respiratory syndrome (SARS) caused by coronavirus (CoV)-2 (2019-nCoV/SARS-CoV-2) led to a life-threatening coronavirus disease 2019 (COVID-19) pandemic all over the world, resulting in multiple organ failure, immune reactions and septic shock.[1,2] The effect of variations on susceptibility to SARS-CoV-2 infections and the severity of symptoms in certain populations have recently been one of the most emphasized areas, and it is thought that these variations may be an important factor in determining susceptibility to infections and severity of the disease.[3] The entry of SARS-CoV-2 into target cells takes place through the binding of the S1 unit of the viral spike (S) protein to the angiotensin-converting enzyme 2 (ACE2) surface receptors of the target cell, then cleaving the S1-S2 unit of the S protein through the transmembrane protease serine 2 (TMPRSS2) receptor, and facilitating the entry of the virus into the cell through membrane fusion of the unit containing S2.[3–5] Virus receptor binding is an important first step in viral infection.[5] Therefore, it is thought that variations may affect the expression patterns in host *ACE2* and *TMPRSS2* receptor genes, and the viral S protein may act as a barrier for viral infection and may determine the susceptibility to COVID-19 infections, affecting the course of the disease.[4,6–9]

The *ACE2* gene localized on chromosome Xp22 is expressed in tissues such as the colon and lung, but is more dominant in the heart, kidney and testicles. In addition to the predominance of respiratory system symptoms during infection, the development of complications, mostly in the heart and lungs, is explained by the abundant expression of the gene on type 2 pneumocytes, especially in the lungs.[7,9–11] Clinical studies have shown that *ACE1/ACE2* polymorphisms are associated with a risk for cardiovascular and pulmonary diseases.[8,12] Therefore, the coexistence of hereditary predispositions or common gene polymorphisms affecting the expression of *ACE1/ACE2* genes may cause increased capillary permeability in alveolar cells, coagulation, fibrosis, apoptosis, acceleration of lung damage, and pulmonary failure. Thus, although it is not always a rule, SARS-CoV-2 infections can be experienced much more severely in patients with existing chronic diseases.[13]

The *ACE2* is a polymorphic gene in the human genome with approx. 140 single nucleotide polymorphism (SNP) loci, some of which are associated with COVID-19.[5] In previous studies, special attention was drawn to rs2285666 (G8790A), which is in the 3rd intron of the *ACE2* and affects the expression of the gene with alternative splicing. It has been suggested that rs1978124 at intron 1 and rs714205 SNPs at intron 16 of the gene show a strong linkage disequilibrium with rs2285666. It has been stated that the rs73635825 variant causes significant differences in intermolecular interactions between the receptor and S protein.[5,9,11] Additionally, polymorphisms in the *TMPRSS2* gene localized at 21q22.3 may have greater importance in society in terms of the spread of influenza A and coronavirus infections. In this context, it has been stated that some SNPs in the *TMPRSS2* gene have functional significance by affecting the expression of the gene in genome-wide association studies.[14,15] Single nucleotide polymorphisms affecting proinflammatory and anti-inflammatory cytokine levels in cytokine genes have been indicated in the development of the "cytokine storm" in severe COVID-19 infection.[16,17]

Objectives

The genetic differences observed in ACE2 and TMRPSS2 receptors, which play a role in the attachment of the virus to host cells, are important for the susceptibility of individuals to infection, and some SNPs in the *ACE2* may affect the susceptibility to SARS-CoV-2 infections by creating a predisposition for hypertension and other cardiovascular diseases.[18] Therefore, in our study, we aimed to determine the expression levels of *ACE2* and *TMPRSS2* in Turkish patients with SARS-CoV-2 infection, as well as the relationship between some common SNPs in these genes and the clinical course of the COVID-19 infection.

Materials and methods

Subjects

Individuals presenting to our hospital between December 2020 and May 2021 due to infection or contact with individuals infected with SARS-CoV-2, and who were tested for COVID-19 using the real-time polymerase chain reaction (PCR) method from a nasal-throat swab at the Gazi University (Ankara, Turkey) were included in this study.

Our case-control study followed the principles of the Declaration of Helsinki and was approved by the Gazi University Faculty of Medicine Clinical Research Ethics Committee (approval No. 2020-611).

The power analysis was conducted using G*Power v. 3.1.9.7 software (https://g-power.apponic.com/) to determine the minimum sample size required to test the study hypothesis. Results indicated that the required total sample size (power = 0.80, $\alpha = 0.05$, effect size = 0.25) was 180. The eta squared (η^2) was used to determine the effect size.

The participant flow diagram for the study is shown in Fig. 1. The individuals included in the study were grouped as follows:

Group 1: Asymptomatic patients who were found to be positive for SARS-CoV-2 (n = 41);

Group 2: Symptomatic patients who were found to be positive for SARS-CoV-2 and did not require treatment in the intensive care unit (ICU) (n = 53);

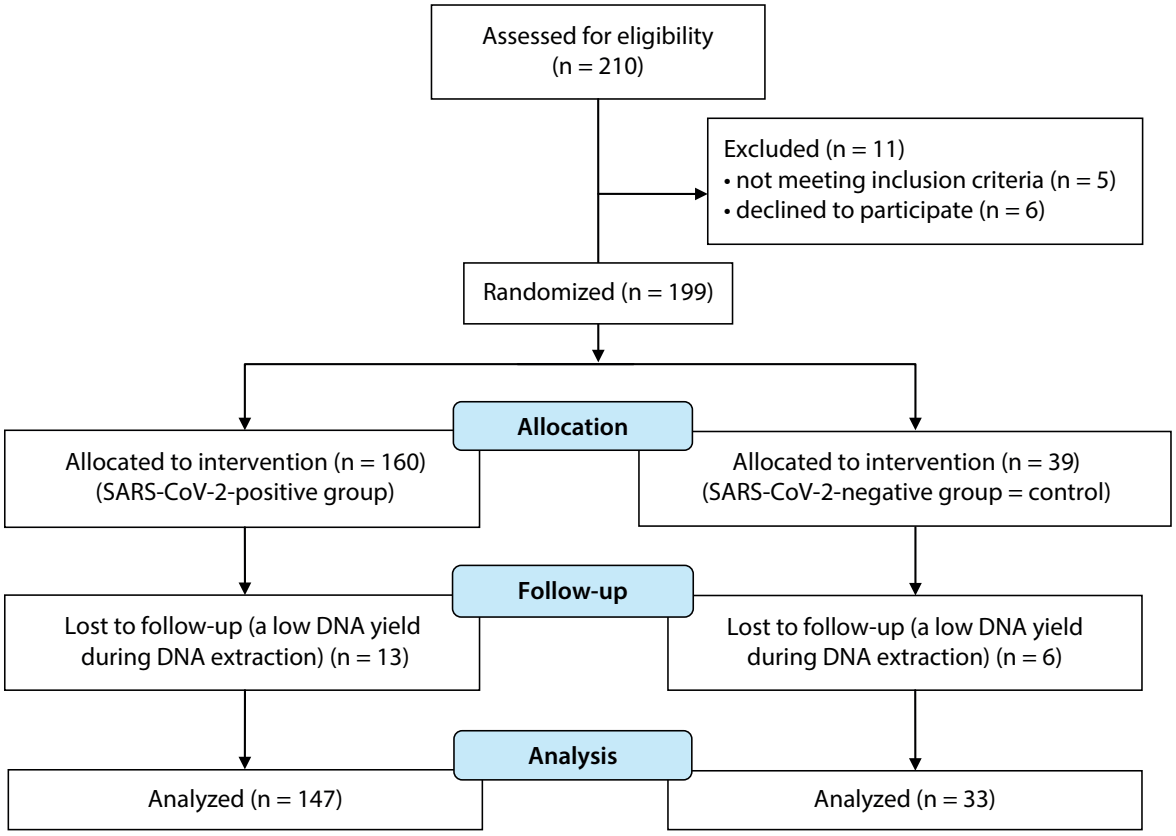

Fig. 1. CONSORT 2010 flow diagram

SARS-CoV-2 – severe acute respiratory syndrome coronavirus 2.

Group 3: Symptomatic patients who were found to be positive for SARS-CoV-2 and treated in the ICU (n = 53);

Group 4: Control group – individuals who had a history of contact with individuals determined to be SARS-CoV-2-positive, who were found to be SARS-CoV-2 negative (n = 33).

Peripheral venous blood samples of each patient who agreed to participate in the study had been stored in 4-milliliter ethylenediaminetetraacetic acid (EDTA) tubes at –80°C until the beginning of the study.

RNA extraction and reverse transcription quantitative PCR (RT-qPCR)

Total RNA was extracted from the peripheral venous blood samples using the NucleoSpin® RNA Blood kit (Macherey-Nagel GmbH & Co. KG, Düren, Germany), following the manufacturer's protocols. The concentration and quality of total RNA were assessed spectrophotometrically at 260 nm absorbance (NanoDrop 1000 Spectrophotometer; Thermo Fisher Scientific, Waltham, USA). We used the NCBI Primer-BLAST designing tool for primer design (https://www.ncbi.nlm.nih.gov/tools/primer-blast/). In primer design, care was taken to ensure that almost all primers had a similar melting temperature, and primers with prominent hairpins, homodimers or heterodimers were excluded.[19] The *ACE2* and *TMPRSS2* expressions were determined using the One-Run RT-qPCR kit (catalog No. 18R-01-100; SNP Biotechnology, Ankara, Turkey), together with the specific primers for *ACE2* and *TMPRSS2* from the total RNA using the CFX96 Thermocycler (Bio-Rad, Hercules, USA). The sequences of oligonucleotides used for the RNA isolations of *ACE2* and *TMPRSS2* genes are given in Table 1. The expressions of *ACE2* and *TMPRSS2* were determined after RT-qPCR consisting of 50 cycles of 8 min at 42°C, 1 s at 96°C and 25 s at 60°C were normalized to the *β-actin* gene as a control. Each real-time PCR reaction was performed in duplicate. The gene expressions were analyzed using the Gene Study software (CFX96; Bio-Rad).

Genomic DNA extraction and determination of SNPs

After obtaining genomic DNA from the 100 µL of peripheral venous blood of the SARS-CoV-2-positive patient groups and control group using the DNA isolation kit (SNP Biotechnology), the genotype and allele distributions of rs714205, rs73635825, rs2285666, and rs1978124 in *ACE2*, and rs8134378, rs2070788, rs7364083, rs13052975, and rs9974589 in *TMPRSS2* were investigated using real-time PCR (CFX96; Bio-Rad), and haplotype analyzes were performed. The RT-qPCR mixture used per sample was prepared with 1.25 µL of primer/probe, 12.5 µL of TaqMan 2x PCR Mix, 9.375 µL of RNAse-free water, and 1.875 µL of template DNA with a total reaction volume of 25 µL, following the manufacturer's recommendations. While PCR amplification was performed,

Table 1. Sequences of oligonucleotides used in the multiplex polymerase chain reaction (PCR) assay for RNA isolation of the *ACE2* and *TMPRSS2* genes

Oligonucleotide name	Sequence
ACTB forward	5′-CCCAGCACAATGAAGATCAAGATC-3′
ACTB reverse	5′-GGGTGTAACGCAACTAAGTCATAGTC-3′
ACTB molecular beacon	5′-FAM-AGATCATTGCTCCTCCTGAGCGCAAG-3′
ACE2 forward	5′-GATCAGAGATCGGAAGAAGAAAAATAAAGC-3′
ACE2 reverse	5′-CTAAAAGGAGGTCTGAACATCATCAGTG-3′
ACE2 molecular beacon	5′-FAM-AGAAAATCCTTATGCCTCCATCGATATTAGC-3′
TMPRSS2 forward	5′-GAATGTGATGGTATTCACGGACTG-3′
TMPRSS2 reverse	5′-CTTGTAAAACGACGTCAAGGACGAAG-3′
TMPRSS2 molecular beacon	5′-TCGACAAATGAGGGCAGACGGCTAATC-3′

ACTB – human B-actin gene; *ACE2* – angiotensin-converting enzyme 2 gene; FAM – fluorescein; *TMPRSS2* – transmembrane protease serine 2 gene.

the genotypes were determined according to the high-resolution melting curve analysis by the glow of the fluorescent dye used (EvaGreen; Metabion, Martinsried, Germany). The genotyping was made according to the melting temperature (Tm) of double-stranded DNA, which was denatured during PCR by increasing the temperature and the presence of DNA binding dye. Homozygous and heterozygous mutations cause the Tm to shift compared to a wild-type sample.[19]

Statistical analyses

The statistical analysis of the data obtained at the end of the study was performed using the IBM SPSS v. 20 software (IBM Corp., Armonk, USA). Parametric variables were expressed as mean and standard deviation (M ±SD). The η^2 was used to determine the effect size. To determine the differences between *ACE2* and *TMPRSS2* expression levels in the SARS-CoV-2-positive and -negative groups, we performed t-tests with Bonferroni correction (Supplementary Table 1). We also compared *ACE2* and *TMPRSS2* expression levels between the subgroups (asymptomatic patients, symptomatic patients, ICU-treated patients, and controls). As a result of the groups not being normally distributed, the Kruskal–Wallis test was used to compare the expression levels between the subgroups (Supplementary Tables 2 and 3). There were statistically significant differences between the subgroups. The homogeneity of variance was examined using Levene's test. Variances were not assumed equal; thus, a post hoc Dunn's test was used to perform pairwise comparisons (Supplementary Table 4). The Hardy–Weinberg balance for the distributions of genotypes was calculated using the χ^2 test. A p-value <0.05 was considered statistically significant. The odds ratio (OR) and corresponding 95% confidence interval (95% CI) values were analyzed using multiple logistic regression tests in order to estimate the association of genotypes, allele frequencies and other variables with the occurrence and severity of COVID-19. Moreover, the correlation between COVID-19 and risk factors such as comorbidities, age, gender, *ACE2*, and *TMPRSS2* expressions was analyzed with a multinomial logistic regression model (Supplementary Table 5).

Results

The demographic data of study groups are shown in Table 2. The multinomial logistic regression results of independent variables affecting COVID-19 severity are presented in Supplementary Table 6.

ACE2 and *TMPRSS2* expression

The *ACE2* expression was determined as 1.34 ±0.14 (M ±SD) in the control group and 21.58 ±4.12 in the SARS-CoV-2-positive group, with a statistical difference between the groups (p = 0.001). The *TMPRSS2* expression was determined as 1.20 ±0.15 and 132 ±41.61 in the SARS-CoV-2-positive and -negative groups, respectively, and

Table 2. Demographic data of the study groups

Demographic and comorbidity data		Controls (n = 33)	Asymptomatic patients (n = 41)	Symptomatic patients (n = 53)	ICU-treated patients (n = 53)
Gender, n (%)	female	16 (48.5)	20 (48.8)	28 (52.8)	26 (49)
	male	17 (51.5)	21 (51.2)	25 (47.2)	27 (51)
Age (M ±SD)		41.72 ±8.16	42.65 ±10.91	42.52 ±9.66	67.15 ±15.35
Comorbid disease*, n (%)		–	3 (7.3)	7 (13.2)	45 (84.9)

* comorbid diseases: hypertension, cardiovascular diseases, diabetes mellitus, chronic lung diseases, kidney diseases, liver diseases, and malignancies; ICU – intensive care unit; M ±SD – mean ± standard deviation.

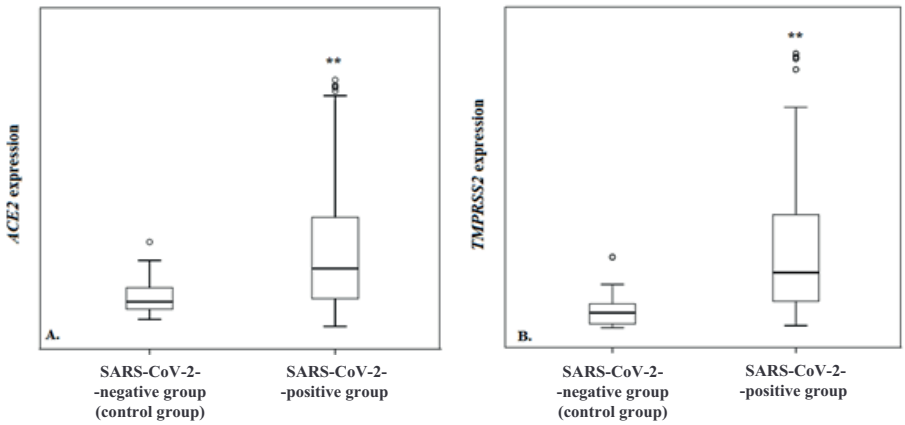

Fig. 2. *ACE2* (A) and *TMPRSS2* (B) expression levels in the severe acute respiratory syndrome coronavirus 2 (SARS-CoV-2)-positive patient group and the control group (**p < 0.05); t-test (t = 4.899 for the *ACE2* and 3.165 for the *TMPRSS2*)

ACE2	Control group	SARS
Maximum	6.26	260.52
Q3	1.69	11.53
Median	0.94	3.05
Q1	0.62	1.07
Minimum	0.31	0.12

TMPRSS2	Control group	SARS
Maximum	7.64	3460.97
Q3	1.19	25.73
Median	0.67	4.24
Q1	0.19	1.18
Minimum	0.07	0.13

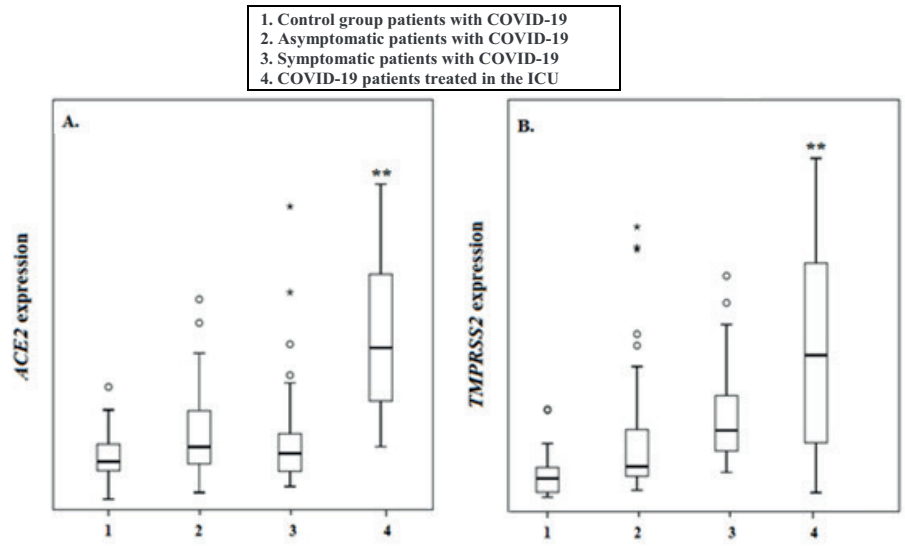

Fig. 3. *ACE2* (A) and *TMPRSS2* (B) expression levels in study groups (**p < 0.05); Kruskal–Wallis test (degrees of freedom (df) = 3 for the *ACE2* and *TMPRSS2*)

ICU – intensive care unit; COVID-19 – coronavirus disease 2019.

ACE2	Group 1	Group 2	Group 3	Group 4
Maximum	6.26	118.59	175.20	260.52
Q3	1.69	5.47	3.06	60.63
Median	0.94	1.39	1.26	11.54
Q1	0.62	0.90	0.77	4.15
Minimum	0.31	0.12	0.25	1.52

TMPRSS2	Group 1	Group 2	Group 3	Group 4
Maximum	7.64	727.90	207.35	3460.97
Q3	1.19	11.40	12.67	141.17
Median	0.67	1.22	4.34	5.65
Q1	0.19	0.77	2.44	0.68
Minimum	0.07	0.13	0.93	0.19

a significant difference was found between the 2 groups (p = 0.002; Fig. 2).

The *ACE2* and *TMPRSS2* expressions were higher in the ICU-treated patient group compared to the control group (p = 0.001). Although *ACE2* and *TMPRSS2* expressions were higher in the asymptomatic and symptomatic patient groups compared to the control group, a significant difference was only observed between the symptomatic patient group and the control group (p = 0.013 and p = 0.041, respectively). The *ACE2* and *TMPRSS2* expressions were also higher in the ICU-treated patient group compared to the other patient groups (p = 0.001 and p = 0.001 for the *ACE2* gene, respectively; p = 0.020 and p = 0.002 for the *TMPRSS2* gene, respectively). There was no difference between the asymptomatic and symptomatic patient groups in terms of *ACE2* and *TMPRSS2* expression (p = 0.456 and p = 0.953, respectively; Fig. 3).

In the study groups, *ACE2* and *TMPRSS2* expressions did not differ according to gender (p > 0.05). There was no significant difference in terms of clinical severity of the disease according to gender among the patient groups (p = 0.956 and p = 0.458 respectively).

The mean age was higher in the SARS-CoV-2-positive patient group who were treated in the ICU compared to the other patient and control groups (p = 0.001). Also, there was a significant difference between the clinical

course of infection and age in the SARS-CoV-2-positive patient groups (p = 0.001). To determine the relationship between patient age and *ACE2* and *TMPRSS2* expressions, the patients were divided into 3 different age groups: 20–40 years, 40–60 years and over 60 years of age. The *ACE2* expression in the over 60 years of age patient group was higher than in the 2 other age groups (p = 0.004 and p = 0.039, respectively). The *TMPRSS2* expression was higher in patients over 60 years of age compared to patients aged 20–40 years (p = 0.049), but not different from patients aged 40–60 years (p = 0.415).

The presence of comorbid diseases was more common in those treated in the ICU than in the other patient groups (p = 0.001). It was determined that *ACE2* and *TMPRSS2* expression levels increased in the presence of comorbid diseases in the SARS-CoV-2-positive patient group (p = 0.001 and p = 0.02, respectively). There was no difference between *ACE2* and *TMPRSS2* expressions and the presence of comorbid diseases in the asymptomatic and symptomatic patient groups (p = 0.795 and p = 0.311 for the *ACE2* gene, respectively; p = 0.469 and p = 0.302 for the *TMPRSS2* gene, respectively). Higher *ACE2* and *TMPRSS2* expression levels were detected in the presence of comorbid diseases in the ICU-treated patient group (p = 0.019 and p = 0.018, respectively).

ACE2 and *TMPRSS2* SNPs

The sum of the genotypes obtained for each of the *ACE2* and *TMPRSS2* SNPs in our study groups was equal to 1, and the genotype and allele distributions were in the Hardy–Weinberg equilibrium. The genotype and allele distributions of *ACE2* SNPs were similar in the SARS-CoV-2-positive and -negative groups (p > 0.05; p-values are given in Table 3). When the genotype and allele distributions of *TMPRSS2* polymorphisms were examined, the expressions of rs2070788GA, rs7364083GA and rs9974589AC genotypes were higher in the SARS-CoV-2-positive group (p-values = 0.001, 0.036 and 0.024, respectively) compared to the control group (Table 3).

Although the rs714205GG genotype was more common in asymptomatic, symptomatic and ICU-treated patients than in the control group, a statistical difference was observed only in the asymptomatic patient group (p = 0.049). Similarly, the expression of rs714205 G-allele was found to be higher in the asymptomatic patient group (p = 0.032). In the symptomatic patient group, the expressions of rs1978124 C-allele, rs8134378GA genotype and A-allele were statistically different compared to the other patient and control groups (p = 0.032, 0.014 and 0.006, respectively). The expression of rs2070788GA genotype was different in all groups compared to the control group (p = 0.039, 0.001 and 0.001, respectively). The expressions of rs7364083GA and rs9974589AC genotypes were statistically different in the symptomatic patient group compared to the other patient and control groups (p = 0.003 and 0.005, respectively; Table 4).

No significant relationship was found between SNPs investigated in our study and *ACE2* and *TMPRSS2* expression levels (p > 0.05).

The multinomial logistic regression results of independent variables affecting genotypic distribution are shown in Supplementary Table 7.

ACE2 and *TMPRSS2* haplotype frequencies

Based on the CCTA haplotype formed by the wild-type alleles of *ACE2* variants, 9 and 8 haplotypes with frequencies above 5% were detected in the patient and control groups, respectively. The CCTA haplotype was the highest in the SARS-CoV-2-positive patient group, and the CCTA and CCCA haplotypes were similar in the control group. While the CTTA haplotype showed a statistical difference between the SARS-CoV-2-positive patient group and the control group (p = 0.02), there was no difference between the SARS-CoV-2-positive patient groups in terms of *ACE2* haplotype frequencies (p > 0.05; p-values are given in Table 5). Thirty haplotypes were identified in the SARS-CoV-2-positive patient groups with *TMPRSS2* variants, 16 haplotypes were identified in the control group, and GGAGG consisting of wild-type alleles was taken as the reference haplotype. There was no statistical difference between the SARS-CoV-2-positive patient and control groups in terms of haplotype distributions (p > 0.05; p-values are given in Table 6).

In the SARS-CoV-2-positive asymptomatic patient group, AGCAG and AGAAG haplotypes had a higher frequency than those in the other patient groups (symptomatic and ICU-treated, p = 0.03 and p = 0.01, respectively).

Discussion

Variations in the nucleotide sequences of the 2 host genes, *ACE2* and *TMPRSS2*, indispensable in the introduction of coronavirus into host cells, may alter the expression and functionality of these proteins.[20] Although recent studies have attempted to associate these variants with susceptibility to SARS-CoV-2 infections,[5,21,22] there is not yet sufficient evidence that rare variants in *ACE2* can modulate susceptibility to SARS-CoV-2 infections. However, *TMPRSS2*, which plays a role in the proteolytic cleavage of the SARS-CoV-2 S proteins and thus facilitates the entry of the virus into the host cell, contains many variants of different frequencies among human populations.[20] Therefore, the relationship between the risk and susceptibility of SARS-CoV-2 infections and different polymorphisms of *ACE2* and *TMPRSS2* and expression levels was investigated in COVID-19 patients and a control group. According to our results, *ACE2* and *TMPRSS2* expressions were significantly increased in the SARS-CoV-2-positive patient group compared to the control group, and the expressions of the genes were higher in the ICU-treated

Table 3. Genotype and allele distribution of *ACE2* and *TMPRSS2* polymorphisms in severe acute respiratory syndrome coronavirus 2 (SARS-CoV-2)-positive and -negative groups

dbSNP ID			SARS-CoV-2-negative* (n = 33)	SARS-CoV-2-positive (n = 147)	OR	95% CI	df	p-value
rs714205	genotype	CC	24	98	1	reference	–	–
		CG	6	18	0.735	0.263–2.050	1	0.556
		GG	3	31	2.531	0.713–8.978	1	0.151
	allele	C	54	214	1	reference	–	–
		G	12	80	1.714	0.872–3.372	1	0.118
rs73635825	genotype	AA	32	146	1	reference	–	–
		AG	1	1	0.219	0.013–3.597	1	0.288
		GG	0	0	–	–	–	–
	allele	A	65	293	1	reference	–	–
		G	1	1	0.221	0.014–3.581	1	0.288
rs2285666	genotype	CC	22	98	1	reference	–	–
		CT	5	17	0.763	0.254–2.291	1	0.630
		TT	6	32	1.197	0.446–3.212	1	0.721
	allele	C	49	213	1	reference	–	–
		T	17	81	1.096	0.597–2.014	1	0.767
rs1978124	genotype	TT	13	74	1	reference	–	–
		CT	8	28	0.615	0.230–1.642	1	0.332
		CC	12	45	0.659	0.277–1.569	1	0.346
	allele	T	34	176	1	reference	–	–
		C	32	118	0.712	0.417–1.218	1	0.215
rs8134378	genotype	GG	29	107	1	reference	–	–
		GA	4	37	2.507	0.826–7.609	1	0.105
		AA	0	3	–	–	–	–
	allele	G	62	251	1	reference	–	–
		A	4	43	2.655	0.919–7.677	1	0.071
rs2070788	genotype	GG	11	32	1	reference	–	–
		GA	4	72	7.535	2.39–23.734	1	**0.001**
		AA	18	43	1.218	0.506–2.932	1	0.660
	allele	G	26	136	1	reference	–	–
		A	40	158	1.324	0.768–2.282	1	0.312
rs7364083	genotype	GG	6	22	1	reference	–	–
		GA	12	83	2.470	0.106–5.750	1	**0.036**
		AA	15	42	1.310	0.446–3.849	1	0.624
	allele	G	24	127	1	reference	–	–
		A	42	167	1.320	0.760–2.294	1	0.324
rs13052975	genotype	GG	23	98	1	reference	–	–
		GA	8	45	1.320	0.548–3.178	1	0.535
		AA	2	4	0.469	0.081–2.720	1	0.399
	allele	G	54	241	1	reference	–	–
		A	12	53	0.990	0.495–1.978	1	0.976
rs9974589	genotype	AA	6	28	1	reference	–	–
		AC	12	81	2.664	1.137–6.242	1	**0.024**
		CC	15	38	1.842	0.635–5.345	–	0.261
	allele	A	24	137	1	reference	–	–
		C	42	157	1.527	0.880–2.650	1	0.132

* individuals who had a history of contact with individuals determined to be SARS-CoV-2-positive, who were found to be SARS-CoV-2-negative using polymerase chain reaction (PCR), and who were not infected with SARS-CoV-2 (control group). OR – odds ratio; 95% CI – 95% confidence interval; df – degrees of freedom; dbSNP – Single Nucleotide Polymorphism Database. Values in bold indicate statistical significance.

Table 4. Genotype and allele distributions of *ACE2* and *TMPRSS2* polymorphisms in the study groups including severe acute respiratory syndrome coronavirus 2 (SARS-CoV-2)-positive patient groups consisting of asymptomatic, symptomatic and ICU-treated individuals, and a SARS-CoV-2-negative group

dbSNP ID			SARS-CoV-2-negative* (n = 33)	SARS-CoV-2-positive asymptomatic patients				SARS-CoV-2-positive symptomatic patients				SARS-CoV-2-positive symptomatic and ICU-treated patients			
				n = 41	OR	95% CI	p-value	n = 53	OR	95% CI	p-value	n = 53	OR	95% CI	p-value
rs714205	genotype	CC	24	25	1	reference	–	40	1	reference	–	33	1	reference	–
		CG	6	4	0.650	1.160–2.553	0.527	6	0.600	0.174–2.073	0.419	8	0.970	0.297–3.162	0.959
		GG	3	12	3.840	0.963–15.319	**0.049**	7	1.400	0.330–5.933	0.648	12	0.209	0.739–11.449	0.127
	allele	C	54	54	1	reference	–	86	1	reference	–	74	1	reference	–
		G	12	28	2.333	1.076–5.061	**0.032**	20	1.098	0.496–2.428	0.818	32	1.946	0.919–4.122	0.082
rs73635825	genotype	AA	32	40	1	reference	–	53	1	reference	–	53	1	reference	–
		AG	1	1	0.800	0.048–13.295	0.876	0	–	–	–	0	–	–	–
		GG	0	0	–	–	–	0	–	–	–	0	–	–	–
	allele	A	65	81	1	reference	–	106	1	reference	–	106	1	reference	–
		G	1	1	0.793	0.049–12.917	0.870	0	–	–	–	0	–	–	–
rs2285666	genotype	CC	22	26	1	reference	–	40	1	reference	–	32	1	reference	–
		CT	5	3	0.508	0.109–2.368	0.388	6	0.660	0.181–2.412	0.530	8	1.100	0.318–3.810	0.880
		TT	6	12	1.692	0.545–5.252	0.363	7	0.642	0.192–2.148	0.472	13	1.490	0.491–4.516	0.481
	allele	C	49	55	1	reference	–	86	1	reference	–	72	1	reference	–
		T	17	27	1.415	0.690–2.903	0.344	20	0.670	0.321–1.399	0.287	34	1.361	0.685–2.703	0.378
rs1978124	genotype	TT	13	19	1	reference	–	30	1	reference	–	25	1	reference	–
		CT	8	7	0.599	0.174–2.060	0.416	12	0.650	0.215–1.965	0.445	9	0.585	0.183–1.875	0.367
		CC	12	15	1.169	0.303–2.411	0.767	11	0.397	0.140–1.130	0.083	19	0.823	0.307–2.206	0.699
	allele	T	34	45	1	reference	–	72	1	reference	–	59	1	reference	–
		C	32	37	1.145	0.598–2.192	0.684	34	0.502	0.267–0.944	**0.032**	47	0.946	0.457–1.568	0.596
rs8134378	genotype	GG	29	35	1	reference	–	32	1	reference	–	41	1	reference	–
		GA	4	6	1.243	0.320–4.830	0.754	19	4.444	1.350–14.624	**0.014**	12	2.122	0.622–7.241	0.230
		AA	0	0	–	–	–	3	–	–	–	0	–	–	–
	allele	G	62	76	1	reference	–	83	1	reference	–	94	1	reference	–
		A	4	6	1.224	0.331–4.530	0.762	25	4.784	1.583–14.459	**0.006**	12	1.979	0.610–6.415	0.255

Table 4. Genotype and allele distributions of *ACE2* and *TMPRSS2* polymorphisms in the study groups including severe acute respiratory syndrome coronavirus 2 (SARS-CoV-2)-positive patient groups consisting of asymptomatic, symptomatic and ICU-treated individuals, and SARS-CoV-2-negative group – cont.

dbSNP ID			SARS-CoV-2-negative* (n = 33)	SARS-CoV-2-positive asymptomatic patients				SARS-CoV-2-positive symptomatic patients				SARS-CoV-2-positive symptomatic and ICU-treated patients			
				n = 41	OR	95% CI	p-value	n = 53	OR	95% CI	p-value	n = 53	OR	95% CI	p-value
rs2070788	genotype	GG	11	11	1	reference	–	9	1	reference	–	12	1	reference	–
		GA	4	14	3.937	1.074–14.438	**0.039**	32	12.000	3.369–42.748	**0.001**	26	7.800	2.221–27.389	**0.001**
		AA	18	16	1.125	0.385–3.291	0.830	12	1.227	0.391–3.854	0.726	15	1.309	0.450–3.806	0.621
	allele	G	26	36	1	reference	–	50	1	reference	–	50	1	reference	–
		A	40	46	1.204	0.623–2.327	0.581	56	1.374	0.736–2.563	0.319	56	1.374	0.736–2.563	0.319
rs7364083	genotype	GG	6	6	1	reference	–	5	1	reference	–	11	1	reference	–
		GA	12	22	2.115	0.761–5.883	0.151	38	4.750	1.695–13.309	**0.003**	23	1.513	0.572–4.001	0.404
		AA	15	13	1.154	0.298–4.467	0.836	10	1.250	0.299–5.230	0.760	19	1.447	0.435–4.821	0.547
	allele	G	24	34	1	reference	–	48	1	reference	–	45	1	reference	–
		A	42	48	1.240	0.636–2.415	0.528	58	1.448	0.760–2.294	0.250	61	1.262	0.670–2.379	0.471
rs13052975	genotype	GG	23	24	1	reference	–	37	1	reference	–	37	1	reference	–
		GA	8	14	1.677	0.593–4.745	0.330	16	1.243	0.459–3.364	0.668	15	1.166	0.427–3.180	0.765
		AA	2	3	1.437	0.220–9.405	0.705	0	–	–	–	1	0.311	0.027–3.624	0.351
	allele	G	54	62	1	reference	–	90	1	reference	–	89	1	reference	–
		A	12	20	1.452	0.650–3.241	0.363	16	0.940	0.517–1.708	0.84	17	0.860	0.381–1.937	0.715
rs9974589	genotype	AA	6	8	1	reference	–	8	1	reference	–	12	1	reference	–
		AC	12	20	1.923	0.686–5.394	0.214	35	4.375	1.555–12.310	**0.005**	26	2.167	0.805–5.831	0.126
		CC	15	13	1.538	0.422–5.606	0.514	10	2.000	0.531–7.539	0.306	15	2.000	0.594–6.730	0.263
	allele	A	24	36	1	reference	–	51	1	reference	–	50	1	reference	–
		C	42	46	1.204	0.623–2.327	0.581	55	1.623	0.864–3.042	0.132	56	1.224	0.832–2.934	0.165

* individuals who had a history of contact with individuals determined to be SARS-CoV-2-positive, who were found to be SARS-CoV-2-negative by polymerase chain reaction (PCR), and who were not infected with SARS-COV-2 (control group); ICU – intensive care unit; OR – odds ratio; 95% CI – 95% confidence interval; dbSNP – Single Nucleotide Polymorphism Database. Values in bold indicate statistical significance.

Table 5. *ACE2* rs714205 (C/G), rs2285666 (C/T), rs1978124 (T/C), and rs73635825 (A/G) haplotype frequencies in the severe acute respiratory syndrome coronavirus 2 (SARS-CoV-2)-positive patient and control groups

Haplotype	SARS-CoV-2-negative (n = 60), n (%)	SARS-CoV-2-positive (n = 225), n (%)	OR	95% CI	df	p-value
CCTA	16 (26.6)	81 (36)	1	reference	–	–
CCCA	16 (26.6)	46 (20.4)	0.568	0.260–1.241	1	0.15
CTTA	**7 (11.6)**	**10 (4.4)**	**0.282**	**0.093–0.852**	1	**0.02**
GTTA	6 (10)	27 (12)	0.889	0.316–2.501	1	0.82
GTCA	5 (8.3)	31 (13.7)	1.225	0.413–3.629	1	0.71
GCTA	4 (6.6)	11 (4.8)	0.543	0.154–1.922	1	0.34
GCCA	3 (5)	9 (4)	0.593	0.144–2.433	1	0.46
CTCA	3 (5)	10 (4.4)	0.658	0.163–2.663	1	0.55
CCTG	0 (0)	1 (0.4)	–	–	–	–

OR – odds ratio; 95% CI – 95% confidence interval; df – degrees of freedom. Haplotypes are given according to the localization of microsatellite markers on the X chromosome. Values in bold indicate statistical significance.

Table 6. *TMPRSS2* rs13052975 (G/A), rs2070788 (G/A), rs9974589 (A/C), rs7364083 (G/A), and rs8134378 (G/A) haplotype frequencies between severe acute respiratory syndrome coronavirus 2 (SARS-CoV-2)-positive patient and control groups

Haplotype	SARS-CoV-2-negative (n = 101), n (%)	SARS-CoV-2-positive (n = 818), n (%)	OR	95% CI	df	p-value
GGAGG	14 (13.9)	95 (11.6)	1	reference	–	–
GACAG	21 (20.8)	106 (13.0)	0.744	0.358–1.545	1	0.42
GGAAG	7 (6.9)	81 (9.2)	1.705	0.657–4.429	1	0.27
GAAGG	7 (6.9)	68 (8.3)	1.432	0.549–3.736	1	0.46
GAAAG	7 (6.9)	74 (9.0)	1.558	0.598–4.056	1	0.36
GACGG	6 (5.9)	71 (8.7)	1.495	0.573–3.896	1	0.41
GGCGG	8 (7.9)	69 (8.4)	1.271	0.505–3.197	1	0.61
GGCAG	7 (6.9)	71 (8.7)	1.495	0.573–3.896	1	0.41
AACAG	6 (5.9)	46 (5.7)	1.130	0.408–3.130	1	0.81
AGAGG	5 (5.0)	24 (3.0)	0.707	0.232–2.157	1	0.54
AGCAG	2 (2.0)	12 (1.5)	0.884	0.179–4.374	1	0.88
AGCGG	3 (3.0)	16 (1.9)	0.786	0.203–3.046	1	0.72
AGAAG	3 (3.0)	13 (1.6)	0.639	0.161–2.526	1	0.52
GGAGA	3 (3.0)	34 (4.2)	1.670	0.452–6.172	1	0.44
GACAA	1 (1.0)	30 (3.7)	4.421	0.558–35.031	1	0.15
AACAA	1 (1.0)	8 (1.0)	1.179	0.137–10.154	1	0.88

OR – odds ratio; 95% CI – 95% confidence interval; df – degrees of freedom. Haplotypes are given according to the localization of microsatellite markers on the chromosome 21.

group compared to the asymptomatic and symptomatic COVID-19 patient groups (Fig. 3). The data obtained from patients with a more severe clinical course of COVID-19 support the claim that *ACE2* and *TMPRSS2* genes may be directly related to the severity of COVID-19. Especially since the ACE2 receptor is the target molecule for the entry of SARS-CoV-2 into cells, and the TMPRSS2 is the main protease facilitating the entry of SARS-CoV-2 into host cells, the increased expression of both genes indicates that these patients have more severe SARS-CoV-2 viremia. In other words, it can be said that there is a cause-effect relationship. This important finding suggests that in the future, inhibition strategies targeting *ACE2* or *TMPRSS2* at the gene or receptor level may be developed and used as an antivirus and/or therapeutic approach to reduce the entry of SARS-CoV-2 into host cells and minimize the mortality rate.

The localization of the *ACE2* gene on the X chromosome leads to the fact that females are potentially heterozygous for the expression of this gene and males are hemizygous.[23] Therefore, it is natural that there are differences in *ACE2* expression between males and females in theory, yet in practice and in our study, no difference was observed between the genders in terms of *ACE2* expression. Although, it is argued that the reactions of females to SARS-CoV-2 viremia may be different due

to the localization of inflammation-related genes, including innate and adaptive immune response-related genes on the X chromosome.[24] The gender difference between females and males and the fact that males were hemizygous in terms of *ACE2* did not have any effect on the more severe course of COVID-19 in our study groups. Similarly, Alimoradi et al. showed that gender was not significantly associated with the severity and incidence of COVID-19.[5] The mean age and the presence of comorbid diseases in COVID-19 patients in the ICU-treated group differed compared to the other groups in our study. The *ACE2* and *TMPRSS2* expression levels were higher in the SARS-CoV-2-positive patients over 60 years old. The *ACE2* and *TMPRSS2* expression levels were different in ICU-treated patients with comorbid diseases compared to those without comorbid diseases.

Of the *ACE2* polymorphisms, only the expression of rs714205GG genotype and G-allele showed a significant difference in the SARS-CoV-2-positive asymptomatic group, suggesting that this variant may be associated with a lighter clinical course. In the SARS-CoV-2-positive symptomatic patient group, the expression of rs1978124 C-allele was statistically different from other groups. According to this result, it can be concluded that the rs1978124 C-allele is effective in the symptomatic course of infection. However, taking into account the patient's immunity and comorbid diseases, such interpretation is appropriate. In addition, other possibilities should be considered, such as gene–RNA interactions and epigenetic factors, where there may be other *ACE2* polymorphisms or interactions of different genes that may affect ACE2 receptor function. Möhlendick et al. reported that carriers of the *ACE2* rs2285666GG genotype or G-allele have a two-fold increased risk for SARS-CoV-2 infections compared to the AA genotype.[9] This conclusion was also supported by Alimoradi et al.[5] In our study, the rs2285666 G- and A-alleles were not found in the patient and control groups, and there was no difference between the groups in terms of the determined C- and T-alleles. However, this result does not reflect the whole population, and allele frequencies may vary between populations. Therefore, the susceptibility of different ethnic groups to SARS-CoV-2 may vary in relation to different genotypes.

According to our results, the expression of *TMPRSS2* rs2070788GA, rs7364083GA and rs9974589AC genotypes showed significant differences in SARS-CoV-2-positive patients. Especially regarding the rs2070788GA genotype, there was a significant difference in all SARS-CoV-2-positive patient groups. Therefore, we believe that the presence of rs2070788GA is associated with SARS-CoV-2 sensitivity rather than the clinical course of COVID-19. The minor allele frequencies (MAFs) of rs7364083 and rs9974589 differed in populations according to the genome aggregation database (gnomAD) (https://gnomad.broadinstitute.org/). In our study groups, the frequency of variant alleles rs7364083 and rs9974589 was found to be higher, which is similar to the literature.[25] Moreover, the rs7364083GA and rs9974589AC genotypes were higher in the SARS-CoV-2-positive groups, and a statistical difference was observed only in the symptomatic patient group. Thus, the rs7364083GA and rs9974589AC genotypes may be associated with SARS-CoV-2 susceptibility and may correlate with the clinical course of COVID-19 infections. The rs8134378 A-allele, which differs significantly in SARS-CoV-2-positive symptomatic patients, may also be associated with infection sensitivity.

Previous studies have suggested that the *ACE2* rs2285666 A-allele is associated with increased *ACE2* expression in healthy individuals as well as in patients with diabetes and cerebral stroke.[9,26] Gómez et al. declared that there was no difference in terms of *ACE2* rs2285666 variants in COVID-19 patients with mild and severe course of the disease, but this variant was associated with hypertension in the elderly population.[12] In patients with multiple sclerosis who have a SARS-CoV-2 infection, *TMPRSS2* rs61735792 and rs61735794 variants are reported to be associated with the severity of the infection.[27] In our study, 13.2% of the SARS-CoV-2-positive symptomatic patients and 84.9% of the ICU-treated patients had at least 1 comorbid disease such as hypertension, cardiovascular disease, diabetes mellitus, chronic lung diseases, kidney diseases, liver diseases, and malignancies. In the SARS-CoV-2-positive patient groups with comorbid diseases, *ACE2* and *TMPRSS2* expressions were higher. In the ICU-treated patient group, *ACE2* and *TMPRSS2* expression levels were higher in the presence of comorbid diseases. There was no relationship between the SNPs examined and *ACE2* and *TMPRSS2* expression levels, but it should not be ignored that there may be other genetic factors, such as other intragenic variations, regulatory genes and epigenetic factors that may affect *ACE2* and *TMPRSS2* expression levels.

Gemmati et al. suggest a strong linkage disequilibrium between *ACE2* rs1978124, rs714205 and rs2285666 variants.[11] According to our results, the CTTA haplotype frequency formed with ACE2 variants in the SARS-CoV-2-positive patient group was lower than in the control group. Therefore, the CTTA haplotype may be more resistant to SARS-CoV-2 infections. In terms of the *TMPRSS2* haplotypes, although there was no difference between the SARS-CoV-2-positive patient groups and the control group, AGCAG and AGAAG haplotypes were identified more frequently in the asymptomatic SARS-CoV-2-positive patient group compared to the other patient groups. Therefore, these haplotypes may have a role in a milder course of COVID-19.

Martínez-Sanz et al. reported that *ACE2* rs2106806 and rs6629110 variants may be responsible for SARS-CoV-2 infection susceptibility in hospital staff not infected with SARS-CoV-2 and in hospitalized COVID-19 patients.[18] Similarly, Hou et al. stated that polymorphisms in *ACE2* and *TMPRSS2* genes may be associated with genetic susceptibility to COVID-19.[4] Irham et al. suggested that

there is an increase in *TMPRRS2* expression associated with rs464397, rs469390, rs2070788, and rs383510 variations in lung tissue, which is the major infection site for SARS-CoV-2, and this increase may affect infection severity as well as SARS-CoV-2 sensitivity.[28] According to our study, the high frequency of the rs2070788GA genotype in the SARS-CoV-2-positive group and the increased *TMPRSS2* expression detected in the ICU-treated group support the view that *TMPRSS2* variants affect the expression of the gene and increase the susceptibility to SARS-CoV-2 infections. Irham et al. showed that there is a higher *TMPRSS2* expression in lung tissues in the rs2070788GG genotype.[28] In our study, although there was no relationship between *ACE2* and *TMPRSS2* expressions and genotypes in the peripheral venous blood of the patient and control groups, it was not possible to evaluate *ACE2* and *TMPRSS2* expressions in target tissues, especially the lungs.

Abdelsattar et al. reported that *ACE2* rs2285666 and *TMPRSS2* rs12329760 variants may be associated with COVID-19 disease severity.[29] However, in our study, no finding reported the relationship between *ACE2* rs2285666 genotype and allele frequency with disease severity. Pandey et al. stated that SARS-CoV-2 host sensitivity in South Asian population is similar to the Western Eurasian population, and this sensitivity is associated with the *TMPRSS2* gene.[30] Thus, there is a significant relationship between rs2070788 G-allele and the COVID-19 mortality rate. In our study, the frequency of the rs2070788GA genotype was also found to be high in the SARS-CoV-2-positive patient groups, especially in the symptomatic and ICU-treated patients, but it was detected at a significantly different frequency from the control group. Therefore, we believe that this variant is associated with COVID-19 disease severity, but it is quite difficult to associate the *TMPRSS2* expression level with this variant alone, and it is more appropriate to conduct multicenter studies from different populations to confirm this finding.

Hussain et al. reported that *ACE2* variants such as rs73635825 and rs143936283 may create a positive prognosis for COVID-19 course in some individuals.[6] The *ACE2* rs73635825 variant, which is quite rare, was found in only 1 patient in our study group, and no difference was observed between the groups.

It is suggested that there is no relationship between *ACE2* expression and variants and severity of COVID-19 and gender in the Italian population. However, *TMPRSS2* expression and variants differed according to gender and may be effective in the prognosis of the disease.[24] According to our results, *ACE2* and *TMPRSS2* expressions, variants and the severity of infection did not differ between the genders in the SARS-CoV-2-positive patient and control groups. However, it would be more appropriate to support these results with similar studies in a larger study population.

Kim and Jeong reported that *ACE2* rs2074192 and *TMPRSS2* rs2298659 showed a higher correlation compared to other *ACE2* and *TMPRSS2* variants, while *IFITM3* rs6598045 was associated with COVID-19-related mortality rates.[31] We found that *ACE2* rs714205 may be effective in the milder clinical manifestation of COVID-19, and even *ACE2* rs1978124 and *TMPRSS2* rs8134378, rs2070788, rs7364083, and rs9974589 may be effective in varying degrees of symptomatic courses of COVID-19. We also demonstrated a correlation between changes in *ACE2* and *TMPRSS2* expression levels and the clinical findings of COVID-19.

Conclusions

In conclusion, our study demonstrated that genetic factors of the host may affect the sensitivity and clinical course of COVID-19. Since SARS-CoV-2 is a new virus on which studies have been conducted for the last 2 years, it is a long process to define the genetic factors affecting infection sensitivity. Conducting studies aimed at determining genetically-based prognostic factors that will enable the early detection of individuals at high risk who require urgent medical treatment for COVID-19 is even more important, especially during epidemic periods. Studies in different populations in which the number of patients, examined genes and polymorphisms are increased will provide more information about the genetic variations at the receptor level and host genetic characteristics that may be effective in the sensitivity and clinical course of COVID-19.

Limitations

The main limitation of our study is that *ACE2* and *TMPRSS2* expression levels can only be studied in peripheral venous blood. We also observed a total of 9 SNPs in these 2 genes. Moreover, the possible role of host genetics on SARS-CoV-2 vaccine efficacy was not evaluated. Future research should address the correlation between host genetic factors and the response to the SARS-CoV-2 vaccine.

Conclusions

The data of our study shed light on the establishment of genetic biomarkers in the predetermination of susceptible populations for COVID-19, the identification of new and effective drug targets for COVID-19 patients, and the development of new vaccines.

Supplementary data

The supplementary materials are available at https://doi.org/10.5281/zenodo.7826506. The package contains the following files:

Supplementary Table 1. T-test (*ACE2* and *TMPRSS2* expression levels in the SARS-CoV-2-positive and negative groups).

Supplementary Table 2. Normal distribution test (*ACE2* and *TMPRSS2* expression levels between the subgroups (asymptomatic patient, symptomatic patient, ICU-treated, and control groups)).

Supplementary Table 3. Kruskal–Wallis test results.

Supplementary Table 4. Post hoc tests results.

Supplementary Table 5. Assumption checking results.

Supplementary Table 6. Multinomial logistic regression results of independent variables affecting COVID-19 disease severity.

Supplementary Table 7. Multinomial logistic regression results of independent variables affecting genotypic distribution.

ORCID iDs

Esra Tug https://orcid.org/0000-0002-2408-5294
Isil Fidan https://orcid.org/0000-0001-6296-5017
Gulendam Bozdayi https://orcid.org/0000-0002-6036-6819
Fatma Yildirim https://orcid.org/0000-0003-3715-3097
Ozlem Guzel Tunccan https://orcid.org/0000-0003-1611-0725
Zubeyde Lale https://orcid.org/0009-0005-8805-1068
Dogan Akdogan https://orcid.org/0000-0002-0970-1597

References

1. World Health Organization (WHO). WHO Coronavirus (COVID-19) Dashboard. https://covid19.who.int/. Geneva, Switzerland: World Health Organization (WHO). Accessed June 30, 2023.
2. Hoffmann M, Kleine-Weber H, Schroeder S, et al. SARS-CoV-2 cell entry depends on *ACE2* and *TMPRSS2* and is blocked by a clinically proven protease inhibitor. *Cell*. 2020;181(2):271–280.e8. doi:10.1016/j.cell.2020.02.052
3. Suh S, Lee S, Gym H, et al. A systematic review on papers that study on single nucleotide polymorphism that affects coronavirus 2019 severity. *BMC Infect Dis*. 2022;22(1):47. doi:10.1186/s12879-022-07034-w
4. Hou Y, Zhao J, Martin W, et al. New insights into genetic susceptibility of COVID-19: An *ACE2* and *TMPRSS2* polymorphism analysis. *BMC Med*. 2020;18(1):216. doi:10.1186/s12916-020-01673-z
5. Alimoradi N, Sharqi M, Firouzabadi D, Sadeghi MM, Moezzi MI, Firouzabadi N. SNPs of *ACE1* (rs4343) and *ACE2* (rs2285666) genes are linked to SARS-CoV-2 infection but not with the severity of disease. *Virol J*. 2022;19(1):48. doi:10.1186/s12985-022-01782-6
6. Hussain M, Jabeen N, Raza F, et al. Structural variations in human ACE2 may influence its binding with SARS-CoV-2 spike protein. *J Med Virol*. 2020;92(9):1580–1586. doi:10.1002/jmv.25832
7. Devaux CA, Rolain JM, Raoult D. ACE2 receptor polymorphism: Susceptibility to SARS-CoV-2, hypertension, multi-organ failure, and COVID-19 disease outcome. *J Microbiol Immunol Infect*. 2020;53(3):425–435. doi:10.1016/j.jmii.2020.04.015
8. Imai Y, Kuba K, Ohto-Nakanishi T, Penninger JM. Angiotensin-converting enzyme 2 (ACE2) in disease pathogenesis. *Circ J*. 2010;74(3):405–410. doi:10.1253/circj.CJ-10-0045
9. Möhlendick B, Schönfelder K, Breuckmann K, et al. *ACE2* polymorphism and susceptibility for SARS-CoV-2 infection and severity of COVID-19. *Pharmacogenet Genomics*. 2021;31(8):165–171. doi:10.1097/FPC.0000000000000436
10. Lukassen S, Chua RL, Trefzer T, et al. SARS-CoV-2 receptor *ACE2* and *TMPRSS2* are primarily expressed in bronchial transient secretory cells. *EMBO J*. 2020;39(10):e105114. doi:10.15252/embj.20105114
11. Gemmati D, Bramanti B, Serino ML, Secchiero P, Zauli G, Tisato V. COVID-19 and individual genetic susceptibility/receptivity: Role of *ACE1/ACE2* genes, immunity, inflammation and coagulation. Might the double X-chromosome in females be protective against SARS-CoV-2 compared to the single X-chromosome in males? *Int J Mol Sci*. 2020;21(10):3474. doi:10.3390/ijms21103474
12. Gómez J, Albaiceta GM, García-Clemente M, et al. Angiotensin-converting enzymes (*ACE*, *ACE2*) gene variants and COVID-19 outcome. *Gene*. 2020;762:145102. doi:10.1016/j.gene.2020.145102
13. Paniri A, Hosseini MM, Akhavan-Niaki H. First comprehensive computational analysis of functional consequences of *TMPRSS2* SNPs in susceptibility to SARS-CoV-2 among different populations. *J Biomol Struct Dyn*. 2021;39(10):3576–3593. doi:10.1080/07391102.2020.1767690
14. Bhattacharyya C, Das C, Ghosh A, et al. Global spread of SARS-CoV-2 subtype with spike protein mutation D614G is shaped by human genomic variations that regulate expression of *TMPRSS2* and *MX1* genes [published as a preprint on May 5, 2020]. doi:10.1101/2020.05.04.075911
15. Xia S, Yan L, Xu W, et al. A pan-coronavirus fusion inhibitor targeting the HR1 domain of human coronavirus spike. *Sci Adv*. 2019;5(4):eaav4580. doi:10.1126/sciadv.aav4580
16. Badawi A. Hypercytokinemia and pathogen–host interaction in COVID-19. *J Inflamm Res*. 2020;13:255–261. doi:10.2147/JIR.S259096
17. Velavan TP, Pallerla SR, Rüter J, et al. Host genetic factors determining COVID-19 susceptibility and severity. *EBioMedicine*. 2021;72:103629. doi:10.1016/j.ebiom.2021.103629
18. Martínez-Sanz J, Jiménez D, Martínez-Campelo L, et al. Role of *ACE2* genetic polymorphisms in susceptibility to SARS-CoV-2 among highly exposed but non infected healthcare workers. *Emerg Microbes Infect*. 2021;10(1):493–496. doi:10.1080/22221751.2021.1902755
19. Erali M, Wittwer CT. High resolution melting analysis for gene scanning. *Methods*. 2010;50(4):250–261. doi:10.1016/j.ymeth.2010.01.013
20. Matsuyama S, Nao N, Shirato K, et al. Enhanced isolation of SARS-CoV-2 by *TMPRSS2*-expressing cells. *Proc Natl Acad Sci U S A*. 2020;117(13):7001–7003. doi:10.1073/pnas.2002589117
21. Benetti E, Tita R, Spiga O, et al. *ACE2* gene variants may underlie interindividual variability and susceptibility to COVID-19 in the Italian population. *Eur J Hum Genet*. 2020;28(11):1602–1614. doi:10.1038/s41431-020-0691-z
22. Suryamohan K, Diwanji D, Stawiski EW, et al. Human *ACE2* receptor polymorphisms and altered susceptibility to SARS-CoV-2. *Commun Biol*. 2021;4(1):475. doi:10.1038/s42003-021-02030-3
23. Pinheiro DS, Santos RS, Jardim PCBV, et al. The combination of ACE I/D and *ACE2* G8790A polymorphisms revels susceptibility to hypertension: A genetic association study in Brazilian patients. *PLoS One*. 2019;14(8):e0221248. doi:10.1371/journal.pone.0221248
24. Klein SL, Flanagan KL. Sex differences in immune responses. *Nat Rev Immunol*. 2016;16(10):626–638. doi:10.1038/nri.2016.90
25. Asselta R, Paraboschi EM, Mantovani A, Duga S. *ACE2* and *TMPRSS2* variants and expression as candidates to sex and country differences in COVID-19 severity in Italy. *Aging (Albany NY)*. 2020;12(11):10087–10098. doi:10.18632/aging.103415
26. Wu YH, Li JY, Wang C, Zhang LM, Qiao H. The *ACE2* G8790A polymorphism: Involvement in type 2 diabetes mellitus combined with cerebral stroke. *J Clin Lab Anal*. 2017;31(2):e22033. doi:10.1002/jcla.22033
27. Torre-Fuentes L, Matías-Guiu J, Hernández-Lorenzo L, et al. *ACE2*, *TMPRSS2*, and Furin variants and SARS-CoV-2 infection in Madrid, Spain. *J Med Virol*. 2021;93(2):863–869. doi:10.1002/jmv.26319
28. Irham LM, Chou WH, Calkins MJ, Adikusuma W, Hsieh SL, Chang WC. Genetic variants that influence SARS-CoV-2 receptor *TMPRSS2* expression among population cohorts from multiple continents. *Biochem Biophys Res Commun*. 2020;529(2):263–269. doi:10.1016/j.bbrc.2020.05.179
29. Abdelsattar S, Kasemy ZA, Ewida SF, et al. *ACE2* and *TMPRSS2* SNPs as determinants of susceptibility to, and severity of, a COVID-19 infection. *Br J Biomed Sci*. 2022;79:10238. doi:10.3389/bjbs.2021.10238
30. Pandey RK, Srivastava A, Singh PP, Chaubey G. Genetic association of *TMPRSS2* rs2070788 polymorphism with COVID-19 case fatality rate among Indian populations. *Infect Genet Evol*. 2022;98:105206. doi:10.1016/j.meegid.2022.105206
31. Kim YC, Jeong BH. Strong correlation between the case fatality rate of COVID-19 and the rs6598045 single nucleotide polymorphism (SNP) of the interferon-induced transmembrane protein 3 (*IFITM3*) gene at the population-level. *Genes (Basel)*. 2020;12(1):42. doi:10.3390/genes12010042

The self-perceived competency of dental students about contagious diseases during the COVID-19 pandemic and its effect on their career plans

Zehra Edebal[1,A–F], Salih Doğan[2,A,B,D–F]

[1] Section of Oral Pathology, Department of Basic Medical Sciences, Faculty of Dentistry, Near East University, North Nikosia, Turkish Republic of Northern Cyprus
[2] Department of Pedodontics, Faculty of Dentistry, Erciyes University, Kayseri, Turkey

A – research concept and design; B – collection and/or assembly of data; C – data analysis and interpretation;
D – writing the article; E – critical revision of the article; F – final approval of the article

Advances in Clinical and Experimental Medicine, ISSN 1899–5276 (print), ISSN 2451–2680 (online) *Adv Clin Exp Med*. 2024;33(1):53–60

Address for correspondence
Zehra Edebal
E-mail: zehradogan81@gmail.com

Funding sources
None declared

Conflict of interest
None declared

Acknowledgements
We want to thank Gözde Bahadır Mercan for English editing.

Received on October 30, 2022
Reviewed on January 27, 2023
Accepted on May 9, 2023

Published online on May 30, 2023

Abstract

Background. Dentistry is reported as a very-high-risk profession for COVID-19 contagion. A lack of face-to-face education and poor information during the COVID-19 pandemic may have impacted dental students.

Objectives. We aimed to evaluate the effects of the COVID-19 pandemic on career plans and self-perception of knowledge levels in undergraduate dental students.

Materials and methods. In this multicenter cross-sectional study, a multiple-choice survey was completed by dental students of Near East University (NEU) in North Nicosia and University of Kyrenia (UoK) in the Turkish Republic of Northern Cyprus (TRNC), and Erciyes University (ERU) in Kayseri, Turkey, in 2020. The χ^2 tests were used to determine statistically significant differences.

Results. Of the 755 students that participated in the study, 66% declared fear of being at risk for contagion. More than half of the students reported not having sufficient knowledge about occupational infections and methods for protection, and the percentages were significantly higher in female and preclinical students. Utilization of credible publications, guidelines (57% compared to 34%, $p < 0.001$) and online education (19% compared to 8%, $p < 0.001$) were significantly higher in students claiming to have adequate knowledge. Eleven percent of the students thought about dropping out of dental education because of the COVID-19 pandemic. These students exhibited a markedly increased fear of being at risk for contagion because of the COVID-19 pandemic (80% compared to 64%, $p = 0.011$). Seventy-six percent of the students were aiming for a dental specialty. Eighteen percent changed their desired specialty, and 25% were in search of a specialty that they believed required fewer close contact procedures.

Conclusions. It is crucial to prepare students for the next possible outbreak using the knowledge gained during this pandemic by modifying the dental curriculum and providing credible information and psychological support to guide dental students in building a healthy career path.

Key words: coronavirus, dental education, career choice, personal protective equipment, dental specialty

Cite as
Edebal Z, Doğan S. The self-perceived competency of dental students about contagious diseases during the COVID-19 pandemic and its effect on their career plans.
Adv Clin Exp Med. 2024;33(1):53–60.
doi:10.17219/acem/166045

DOI
10.17219/acem/166045

Background

The COVID-19, which was first encountered in China in the last days of 2019 and became a pandemic after spreading worldwide over several months, is caused by a virus that belongs to the coronavirus family. Because the infection is easily transmitted by close contact, many healthcare professionals, such as doctors, dentists, nurses, and paramedics, became a target for the disease. Dentistry is classified as a very high-exposure risk profession for COVID-19 due to the aerosol-generating procedures used in some dental procedures and examinations.[1] At the beginning of the pandemic, the American Dental Association (ADA) suggested postponing treatment of all cases other than those requiring urgent or emergency procedures.[2] As COVID-19 became better understood over time and dental practices resumed, it was reported that the number of infected dentists was extremely low, despite the high contagion risk.[3,4] Nevertheless, this fact was not well known to dental students at the early stages of the pandemic.

After the onset of the pandemic, understanding the disease, defining clinical symptoms and findings, developing diagnostic methods, and providing information about protection required a significant amount of time.[1,2,5] Unproven claims had reached a large number of people before evidence-based information on the properties of the virus was obtained and protection methods were established through scientific studies. While the initial distribution of information through social media seemed convenient, this channel often contained misleading headlines and content.[6,7] During the pandemic, many students were overwhelmed by a fear of the disease and faced significant pressure.[8,9] Therefore, institutions like the World Health Organization (WHO), the Centers for Disease Control and Prevention (CDC), and the ADA regularly published announcements to provide a reliable source of information.[2,5]

Many universities could not continue face-to-face education because of the quarantine measures taken during the pandemic. To ensure the continuity of education and keep students motivated, universities with adequate technological infrastructure switched to online education. Different evaluation and measurement methods have been applied to assess the effectiveness of this delivery method. For dentistry, it did not seem plausible that any distance learning course could replace face-to-face education since direct applications, which should be performed on patients during clinical practice and are an integral part of dental education, could not be performed.[10]

The sudden onset of the pandemic, the cessation of face-to-face education and essential clinical practices, and the initial distribution of unproven information may have especially burdened dental students at the beginning of the pandemic. These effects may have led to a decreased self-perceived competency in dental students with regard to understanding the nature of contagious diseases, the effective utilization of personal protective equipment (PPE), obtaining valid scientific information, and verifying the information gathered under lockdown conditions. These effects, in turn, may have led to increased levels of anxiety, a change of career plans or preferred dental specialties, or even dropping out of dental education.

Objectives

In this study, we aimed to survey dental students about their awareness and knowledge of contagious diseases, protection from infections, working conditions, and occupational hazards, and examine how the pandemic impacted their education. We also intended to investigate whether the pandemic affected the students' choice of dental specialties.

Materials and methods

This multicenter cross-sectional study was conducted with the approval of the Near East University (NEU; North Nicosia, Turkish Republic of Northern Cyprus (TRNC)) Scientific Research Ethics Evaluation Board (approval No. 2020/802-1125). It was carried out in the dental faculties of NEU, the University of Kyrenia (UoK; Kyrenia, TRNC) and Erciyes University (ERU; Kayseri, Turkey). A survey was distributed via Google Forms, and the answers were collected through the same platform. The participants were asked to take part in the survey between July 20 and August 5, 2020. There were 15 multiple-choice questions, 4 of which asked about demographics, including questions on age, class, gender, and the university attended (Table 1).

All Turkish-speaking undergraduate students at the abovementioned dental schools were eligible to take part in the survey. To be included in the study, the questionnaires must not have had missing answers and must have been submitted in the required timeframe. Students in the 4th and 5th years were regarded as the clinical student group, and 1st, 2nd and 3rd-year students constituted the preclinical student group. Responses were evaluated for all of the questions. No identifying data about the participants were collected.

The questions were grouped into 3 main sections. The 1st section aimed to gather data about confidence in their knowledge of the COVID-19 pandemic, fear of contracting a contagious disease, feeling informed about protecting themselves from the disease, and ways of gathering information about this topic. In the 2nd section, students were asked whether they ever wanted to drop out of dental education because of the COVID-19 pandemic. In the 3rd section, students were asked if they were planning to have a postgraduate residency in a dental specialty and whether the COVID-19 pandemic affected their dental specialty choice.

The survey was delivered by e-mail to every dental student at the institutions listed above to avoid sampling bias, and it was kept short to reduce the nonresponse rate. The overall number of included participants was

Table 1. Survey questions

Question No.	Question (answer options)
1	Age [years]
2	Gender (female, male)
3	University
4	Class in 2019–2020 academic year (1, 2, 3, 4, 5)
5	In the process of the COVID-19 pandemic, my awareness about the occupational infections that can be transmitted to me from my patients has increased. (agree, disagree, indecisive)
6	The process of the COVID-19 pandemic has caused in me fear of being at risk for contagion while I am practicing my profession. (agree, disagree, indecisive)
7	I think that I have sufficient knowledge about occupational infections and the methods to protect myself from these diseases. (agree, disagree, indecisive)
8	I know how to protect myself from the COVID-19 infection while I am practicing my profession. (agree, disagree, indecisive)
9	I have sufficient information about PPE that I have to use to prevent the transmission of COVID-19 disease from my patients. (yes, no, indecisive)
10	I use …….. as source of information to gather knowledge about prevention methods against COVID-19 infection and PPE, their properties and usage. (participants could select more than 1 option – see Table 3)
11	I have wanted to or have thought of dropping out of dental education because of fear of COVID-19 contagion. (yes, no)
12	I have planned to pursue further education in a dental specialty. (yes, no)
13	I have adequate information about the degree of close contact procedures applied to the patients in the dental specialty of my preference. (yes, no)
14	I have changed the dental specialty I was aiming for because of the COVID-19 pandemic. (yes, no)
15	I am in search for a dental specialty that requires less close contact procedures while treating patients, such as oral diagnosis and radiology or oral pathology. (yes, no)

PPE – personal protective equipment.

determined by the number of eligible students who responded in the given timeframe and filled out the survey without omitting any answers.

Statistical analyses

The Statistical Package for Social Sciences (SPSS) v. 15 (SPSS Inc., Chicago, USA) was used for all statistical analyses. The internal consistency of the given responses was measured using Cronbach's α, and values over 0.70 were regarded as statistically reliable. The demographic data were analyzed using the median and interquartile range (IQR) values and frequency distribution tables. The results were reported as medians (IQR) or percentages. Participants were grouped for certain analyses according to the responses they gave to prior questions. The nominal data were compared using cross tabulations. The χ^2 tests or Fisher's exact tests were used to determine statistically significant differences between these groups. The p-values less than 0.05 were regarded as statistically significant.

Results

Demographic information and reliability

The online survey link was shared with 1532 students in 3 dental faculties in 2 countries. Overall, 755 dental students participated in the study, corresponding to a 49% response rate. More than half of the participating students were from ERU (n = 394, 52%), while 286 NEU students (38%) and 75 UoK students (10%) responded to the survey. The study population consisted of 338 clinical (45%) and 417 preclinical (55%) students. Females comprised 63% (n = 474) of the sample and men 37% (n = 281). There was no difference in the gender distribution between universities (NEU 63% females, UoK 55% females, ERU 64% females; p = 0.292).

Cronbach's α was used to evaluate the consistency of the responses given to the same group of questions. The α values of questions about contagious diseases and PPE usage and education in dental specialties were found to be 0.71 and 0.79, respectively. Removing any of the questions did not increase the corresponding α values.

Fears

Ninety-two percent of the 755 students who participated in the study stated that their awareness of contagious diseases which can be transmitted in the occupational environment increased throughout the COVID-19 pandemic, and the percentages were significantly higher in female and preclinical students (Table 2). Also, fear of being at risk for contagion because of the COVID-19 pandemic emerged in 2/3 of the students and was markedly more intense in females. More than half of the students reported not having sufficient

Table 2. Students' opinions on their knowledge about COVID-19 pandemic and contagious diseases, and comparison of clinical compared to preclinical students and female compared to male students

Questions	Answers	Total (n = 755)	Clinical students (n = 338)	Preclinical students (n = 417)	χ^2	p-value*	Female students (n = 474)	Male students (n = 281)	χ^2	p-value*
In the process of the COVID-19 pandemic, my awareness about the occupational infections that can be transmitted to me from my patients has increased.	agree	698 (92%)	304 (90%)	394 (95%)	6.409	**0.041**	447 (94%)	251 (89%)	9.309	**0.010**
	disagree	19 (3%)	13 (4%)	6 (1%)			12 (3%)	7 (3%)		
	indecisive	38 (5%)	21 (6%)	17 (4%)			15 (3%)	23 (8%)		
The process of the COVID-19 pandemic has caused in me fear of being at risk for contagion while I am practicing my profession.	agree	499 (66%)	225 (67%)	274 (66%)	1.294	0.524	337 (71%)	162 (58%)	17.667	**<0.001**
	disagree	99 (13%)	48 (14%)	51 (12%)			46 (10%)	53 (19%)		
	indecisive	157 (21%)	65 (19%)	92 (22%)			91 (19%)	66 (23%)		
I think that I have sufficient knowledge about occupational infections and the methods to protect myself from these diseases.	agree	348 (46%)	166 (49%)	182 (44%)	11.288	**0.004**	205 (43%)	143 (51%)	7.165	**0.028**
	disagree	75 (10%)	20 (6%)	55 (13%)			43 (9%)	32 (11%)		
	indecisive	332 (44%)	152 (45%)	180 (43%)			226 (48%)	106 (38%)		
I know how to protect myself from the COVID-19 infection while I am practicing my profession.	agree	480 (64%)	215 (64%)	265 (63%)	0.221	0.896	300 (63%)	180 (64%)	0.060	0.971
	disagree	48 (6%)	20 (6%)	28 (7%)			30 (6%)	18 (6%)		
	indecisive	227 (30%)	103 (31%)	124 (30%)			144 (30%)	83 (30%)		
I have sufficient information about PPE that I have to use to prevent the transmission of COVID-19 disease from my patients.	agree	441 (58%)	214 (63%)	227 (54%)	11.644	**0.003**	267 (56%)	174 (62%)	3.568	0.168
	disagree	17 (2%)	2 (1%)	15 (4%)			9 (2%)	8 (3%)		
	indecisive	297 (39%)	122 (36%)	175 (42%)			198 (42%)	99 (35%)		

PPE – personal protective equipment; *Pearson's χ^2 test, degrees of freedom (df) = 2. Values in bold are statistically significant.

knowledge about occupational infections and methods of protection, and this ratio was significantly higher in females and preclinical students. The percentage of students who knew how to protect themselves from COVID-19 while practicing their profession was 64%, which did not differ between the gender or training stage of the students. The ratio of students who stated that they had sufficient information about PPE to protect themselves from COVID-19 was 58%, which was markedly higher for clinical students but did not differ between genders (Table 2).

Social media were found to be the most common source of information about PPE, their properties and usage (57%), followed by reliable publications and organizational guidelines (47%), friends and social circle (37%), television (37%), and online sources (14%; Table 3). There were no statistically significant differences between female and male students regarding the sources used to obtain information, but clinical students pointed at their friends and social circle and social media more often compared to preclinical students.

To investigate the relationship between gathering adequate information and the sources of knowledge, we separated the students who stated that they have adequate knowledge about using PPE to protect themselves from COVID-19 as the PPE group, and compared them with the rest of the students. In the PPE group, the use of reliable publications and guidelines (57% compared to 34%, $p < 0.001$) and online education (19% compared to 8%, $p < 0.001$) to obtain information was significantly more prevalent, and relying on friends and social circle (32% compared to 44%, $p = 0.001$) was significantly rarer. The percentage of students using television or social media as an information source did not differ significantly between the PPE group and the rest of the students ($p = 0.067$ and $p = 0.180$, respectively; Table 4).

Thoughts about dropping out of dental education

The students were asked whether they ever thought of dropping out of dental education because of the COVID-19 pandemic. The responses to these questions are summarized in Table 5. While 675 of the students never considered dropping out, 80 students (11%) had thoughts about quitting dental education. Students who contemplated dropping out had a significantly increased fear of being at risk for contagion because of the COVID-19 pandemic. Furthermore, the proportion of students who reported knowing about occupational infections and how to protect themselves from them, how to be protected from COVID-19 in the occupational environment, and which PPE should be used to prevent infections, was significantly lower among the students who considered dropping out. The percentage of students who considered dropping out of dental education was considerably higher in clinical students compared to non-clinical students, but there was no statistically significant difference between genders (Table 5).

Table 3. Distribution of the responses of students for the source of information they use to gather knowledge about prevention methods against COVID-19 infection, PPE, their properties and usage

Source of information	Frequency (%)[#]	Clinical students (n = 338)	Preclinical students (n = 417)	χ^2	p-value*	Female students (n = 474)	Male students (n = 281)	χ^2	p-value*
Friends and social circle	281 (37%)	144 (43%)	137 (33%)	7.595	**0.006**	179 (38%)	102 (36%)	0.162	0.687
Television and public service broadcasting	281 (37%)	118 (35%)	163 (39%)	1.394	0.238	177 (37%)	104 (37%)	0.008	0.928
Social media	433 (57%)	213 (63%)	220 (53%)	8.034	**0.005**	282 (60%)	151 (53%)	2.390	0.122
Online lectures of my faculty	109 (14%)	48 (14%)	61 (15%)	0.028	0.868	62 (13%)	47 (17%)	1.898	0.168
Credible publications and guidelines issued by organizations (WHO, ADA, Ministry of Health, etc.)	356 (47%)	171 (51%)	185 (44%)	2.905	0.088	234 (49%)	122 (43%)	2.507	0.113
I don't have a specific interest in gathering information and PPE	17 (2%)	12 (4%)	5 (1%)	3.682	0.055	11 (2%)	6 (2%)	0.028	0.868
Other (research papers, family members, lecture notes, etc.)	16 (2%)	6 (2%)	10 (2%)	0.349	0.555	9 (2%)	7 (3%)	0.298	0.585

[#]Participants were allowed to choose more than 1 option. WHO – World Health Organization; ADA – American Dental Association; PPE – personal protective equipment. *Pearson's χ^2 test, degrees of freedom (df) = 1. Values in bold are statistically significant.

Table 4. Difference in the source of information for the students who have knowledge about PPE for protecting themselves from COVID-19 while treating their patients

Source of information	Question: "I have sufficient information about PPE that I have to use to prevent the transmission of COVID-19 disease from my patients."		χ^2	p-value*
	Students who responded "yes" (PPE group, n = 441)	Students who responded "no/ indecisive" (n = 314)		
Friends and social circle	142 (32%)	139 (44%)	11.431	**0.001**
Television and public service broadcasting	152 (35%)	129 (41%)	3.435	0.067
Social media	262 (59%)	171 (55%)	1.839	0.180
Online lectures of my faculty	84 (19%)	25 (8%)	18.247	**<0.001**
Reliable publications and guidelines issued by organizations (WHO, ADA, Ministry of Health, etc.)	249 (57%)	107 (34%)	36.885	**<0.001**
I don't have a specific interest in gathering information and PPE	3 (1%)	14 (5%)	11.896	**0.001**
Other (research papers, family members, lecture notes, etc.)	13 (3%)	3 (1%)	3.510	0.074

*Pearson's χ^2 test, degrees of freedom (df) = 1. PPE – personal protective equipment; WHO – World Health Organization; ADA – American Dental Association. Values in bold are statistically significant.

Career plans

The percentage of students who were aiming for a dental specialty was 76% (n = 574), which was higher in women (82% compared to 69%, p = 0.004) and lower in clinical students (χ^2 test, df = 1, 67% compared to 83%; p < 0.001). Of these 574 students, 18% stated that the COVID-19 pandemic caused a change in the specialty they were aiming for, and 25% of these students stated that they were in search of a dental specialty requiring less close contact while treating patients. Both of these percentages were higher in female students compared to male students (22% compared to 14% and 29% compared to 20%; p = 0.006 and p = 0.006, respectively). In the students who wanted to change their desired dental specialty because of the COVID-19 pandemic, fear of facing contagious diseases while practicing their profession was significantly higher (78% compared to 64%; p = 0.004). The students who wanted to change their desired dental specialty also reported having less knowledge about occupational infections and protection methods (32% compared to 48%; p = 0.007), and the PPE used for protection from COVID-19 (47% compared to 63%; p = 0.002). The students who were aiming for a dental specialty and did not have adequate information about the close contact procedures applied to the patients in their preferred specialty showed a higher tendency to change their choice of dental specialty (29% compared to 15%; p = 0.001), and they were more eager to look for a dental specialty with less close contact with the patients (42% compared to 18%; p < 0.001).

The clinical students aiming for a dental specialty had a higher rate of looking for a specialty requiring less close contact with patients compared to the preclinical students (28% compared to 19%; p = 0.008). The clinical students

Table 5. Students' thoughts on dropping out of dental education

Training stage/gender of the students	Question: "I have wanted to or have thought of dropping out of dental education because of fear of COVID-19 contagion."			
	Yes, I have considered dropping out (n = 80)	No, I have never thought of it (n = 675)	χ^2	p-value*
Cross tabulation with clinical students				
Clinical students	52 (15%)	286 (85%)	14.813	**<0.001**
Preclinical students	28 (7%)	389 (93%)		
Cross tabulation with gender of the students				
Female students (n = 474)	58 (12%)	416 (88%)	3.617	0.057
Male students (n = 281)	22 (8%)	259 (92%)		
Cross-tabulated questions, responded "yes/agree"				
The process of the COVID-19 pandemic has caused fear that I am at risk for contagion while I'm practicing my profession.	64 (80%)	435 (64%)	9.098	**0.011**
I think that I have sufficient knowledge about occupational infections and the methods to protect myself from these diseases.	20 (25%)	328 (49%)	16.674	**<0.001**
I know how to protect myself from the COVID-19 infection while I am practicing my profession.	37 (46%)	443 (66%)	26.564	**<0.001**
I am aware of the PPE that I have to use to prevent the transmission of COVID-19 disease from my patients.	34 (43%)	407 (60%)	17.411	**<0.001**

*Pearson's χ^2 test, degree of freedom (df) = 1. PPE – personal protective equipment. Values in bold are statistically significant.

had also a higher tendency to choose specialties like oral diagnosis and radiology or oral pathology (33% compared to 21%; $p < 0.001$). Only 38% of clinical students stated they would not change their choice of dental specialty due to the COVID-19 pandemic, compared to 53% of the preclinical students ($p < 0.001$).

Discussion

The COVID-19 pandemic has not only affected the health status of individuals but has also had significant impact on social interactions and careers. COVID-19 cases among dentists have been extremely rare thanks to PPE and infection prevention measures.[3,4] However, dentistry was declared a very-high-risk profession for COVID-19 early in the pandemic because of the close physical interactions with patients and the use of aerosol-producing procedures.[1,11] Dental students were also mentally affected during this early period. These students experienced a sudden onset of distance education, were not able to attend laboratory classes, had to cease clinical practice, and suffered from fear of COVID-19 contagion caused by the pandemic.[12] In our study, female students presented an increased fear of being at risk for contagion, which may be attributed to the higher anxiety levels in women reported in other studies.[13,14]

The COVID-19 pandemic has drawn attention to infectious diseases in the general population, and college students are no exception.[15–17] The fear due to COVID-19 has been reported to vary from moderate to high in undergraduate dental students,[15] dentists[16,18] and other college students.[17] This variation may be attributed to differences in social distancing measures and quarantine implementation across governing bodies, together with individual psychological diversity. All of the dental faculties in the TRNC and Turkey suspended face-to-face education and clinical practice due to lockdown measures. As institutions swiftly shifted to online education, students lost opportunities for practical education, sustained personal interactions and clinical experience, which are integral to dental education.[19] This may be one of the reasons for the lack of confidence in having adequate knowledge about protection from contagious infections in more than half of the students in our study. Similar results for the level of knowledge about the COVID-19 pandemic have also been reported in other undergraduate dental students.[20] In contrast to undergraduate dental students, dentists have been reported to have a much higher level of knowledge about COVID-19 and personal protection methods.[3,4] As awareness is higher in this group,[17] more lectures about infectious diseases and protection methods in the curriculum may be beneficial to students and crucial for preparing them for possible future outbreaks.

Proper utilization of PPE is of the utmost importance to protect individuals from COVID-19 infection during dental treatment procedures.[21,22] For this reason, we wanted to evaluate the sources of information students used to gather information on this subject, and whether they thought they had adequate knowledge about using PPE at the beginning of the pandemic. Social media seemed to be the most common source of information for participants of this study. It has been previously reported that students usually used the internet and social media to gather information about the COVID-19 pandemic, but students who used journal articles and the websites of trustworthy organizations had a significantly higher

level of knowledge.[6] These findings are similar to our results. Obtaining knowledge from online faculty lectures or reliable publications and organizations has a more substantial effect compared to gaining knowledge from social media, circle of friends or television. In the age of distance education, it should be a priority to use credible information sources for dentistry education and to ensure that all students have access to these resources.

Although the majority of the surveyed students did not consider dropping out of dental education, 80 did consider this, and their fear of contagion in clinical practice was higher than in those who had not considered dropping out. Their self-confidence regarding the utilization of PPE to protect themselves from COVID-19 was also lower. These factors, in part, may have contributed to their thinking about dropping out of dental education. Students usually feel increased anxiety during outbreaks and pandemics,[21,23] which is even more intense in clinical students,[8,23] and this may directly impact both their daily lives and career plans. Interestingly, the percentages of female and male students who thought of dropping out of dental education did not differ significantly despite their presumed anxiety levels being different. Among the clinical students who had thoughts of dropping out of dental education, the percentage of those who sought for dental specialty that they believed to involve less close contact procedures with patients was significantly higher than of those who did not. This was also true for female students, which may be attributed to increased levels of anxiety among women. These results are consistent with a study that reported that in 15% of otolaryngology trainees, the COVID-19 pandemic affected decisions that could impact their future careers, and that this was more widespread in senior-level trainees.[24] Although otolaryngology and dentistry do not have the same degree of risk according to the Occupational Safety and Health Administration (OSHA) in the USA,[1] they indeed share some degree of similarity, such as working on the same body region and close contact with the upper respiratory tract. To the best of our knowledge, there are no similar studies in the literature comparing clinical and preclinical dental students in this manner.

One of the main goals of this study was to investigate the impacts of the COVID-19 pandemic on the specialty choices of dental students. We found that 18% of the students thought about changing their desired dental specialty due to COVID-19, and that these students declared more intense fear of contagious diseases and felt inadequate in terms of knowledge and protection. In addition, 22% of these students were looking for a dental specialty that involves less close contact with patients. Moreover, the students who did not have enough knowledge about the degree of close contact procedures applied to the patients in the dental specialty that they had planned to pursue were more likely to change their preferred specialty and aimed to choose specialties that require less close contact with patients. In a recent study, it was reported that fear of COVID-19 and future career anxiety are closely related, which also supports the findings of our study.[25] When these findings are evaluated altogether, it may be presumed that these factors are affecting the career plans of the students. Thus, providing psychological support and guidance to the students, in addition to compensating for their lack of information and knowledge during the COVID-19 pandemic, are of crucial importance.

Limitations of the study

Our study was carried out during the summer break and in lockdown conditions, which prevented us from successfully reaching out to students in different dental faculties. The 49% response rate was also lower than we had expected. The inclusion of more universities would have led to a nationwide study and could have provided more robust results. Also, because there were no similar surveys conducted previously when this study was carried out, we had to design our own questionnaire. Given the urgency to better understand the nature of COVID-19, we did not have the time to perform validity and reliability testing before the study. Furthermore, we did not have a scale to measure the anxiety and fear levels of the students. Designing a Likert scale for the anxiety caused by the COVID-19 pandemic and examining associations between the scores on this scale and the career plans of undergraduate dental students may produce valuable outcomes.

Conclusions

After the onset of the COVID-19 pandemic, understanding the disease, developing diagnostic methods, providing information about protection from the disease, and understanding that (with proper safety measures) the contagion risk is not as high as it was initially believed required a significant amount of time and caused severe anxiety. We found that the lack of information during the early period of the pandemic impacted students' dental education and caused changes in their specialty choices. In an unexpected situation like the COVID-19 pandemic, it is crucial to teach students how to obtain reliable information, not only through face-to-face education, but also through online education materials from faculties and reputable organizations. Lack of trustworthy information has also had important effects on the psychological status of students, which may have impacted their dental education and career choices at the beginning of the pandemic. Therefore, it is crucial to prepare students for the next possible outbreak using the knowledge gained during this pandemic by modifying the dental curriculum and providing credible information and psychological support to guide dental students in building a healthy career path.

ORCID iDs

Zehra Edebal https://orcid.org/0000-0001-6518-5972
Salih Doğan https://orcid.org/0000-0001-6554-295X

References

1. U.S. Department of Labor Occupational Safety and Health Administration. OSHA 3990-03 Guidance on Preparing Workplaces for COVID-19. Washington, D.C., USA 2020. https://www.osha.gov/Publications/OSHA3990.pdf. Accessed August 17, 2020.
2. American Dental Association (ADA). As dental practices resume operations, American Dental Association offers continued guidance. https://www.ada.org/about/press-releases/2020-archives/as-dental-practices-resume-operations-ada-offers-continued-guidance. Chicago, USA: American Dental Association (ADA); 2020. Accessed August 18, 2020.
3. Estrich CG, Mikkelsen M, Morrissey R, et al. Estimating COVID-19 prevalence and infection control practices among US dentists. *J Am Dent Assoc*. 2020;151(11):815–824. doi:10.1016/j.adaj.2020.09.005
4. Karayürek F, Yilmaz Çırakoğlu N, Gülses A, Ayna M. Awareness and knowledge of SARS-CoV-2 infection among dental professionals according to the Turkish National Dental Guidelines. *Int J Environ Res Public Health*. 2021;18(2):442. doi:10.3390/ijerph18020442
5. World Health Organization (WHO). World Health Organization Global Infection Prevention and Control Network. Infection prevention and control during health care when novel coronavirus (nCoV) infection is suspected: Interim Guidance. Geneva, Switzerland: World Health Organization (WHO); 2020. https://www.who.int/publications/i/item/10665-331495. Accessed August 10, 2020.
6. Olum R, Kajjimu J, Kanyike AM, et al. Perspective of medical students on the COVID-19 pandemic: Survey of nine medical schools in Uganda. *JMIR Public Health Surveill*. 2020;6(2):e19847. doi:10.2196/19847
7. Zanatta ET, Wanderley GPDM, Branco IK, Pereira D, Kato LH, Maluf EMCP. Fake news: The impact of the internet on population health. *Rev Assoc Med Bras*. 2021;67(7):926–930. doi:10.1590/1806-9282.20201151
8. Wong JGWS, Cheung EPT, Cheung V, et al. Psychological responses to the SARS outbreak in healthcare students in Hong Kong. *Med Teach*. 2004;26(7):657–659. doi:10.1080/01421590400006572
9. Lestari W, Yazid NH, Azhar ZN, Ismail A, Sukotjo C. Impact of COVID-19 on Malaysian dental students' physical, mental, financial and academic concerns. *BMC Oral Health*. 2022;22(1):46. doi:10.1186/s12903-022-02081-w
10. Iyer P, Aziz K, Ojcius DM. Impact of COVID-19 on dental education in the United States. *J Dent Educ*. 2020;84(6):718–722. doi:10.1002/jdd.12163
11. Spagnuolo G, De Vito D, Rengo S, Tatullo M. COVID-19 outbreak: An overview on dentistry. *Int J Environ Res Public Health*. 2020;17(6):2094. doi:10.3390/ijerph17062094
12. Spanemberg JC, Simões CC, Cardoso JA. The impacts of the COVID-19 pandemic on the teaching of dentistry in Brazil. *J Dent Educ*. 2020;84(11):1185–1187. doi:10.1002/jdd.12364
13. Broche-Pérez Y, Fernández-Fleites Z, Jiménez-Puig E, Fernández-Castillo E, Rodríguez-Martin BC. Gender and fear of COVID-19 in a Cuban population sample. *Int J Ment Health Addiction*. 2022;20(1):83–91. doi:10.1007/s11469-020-00343-8
14. Özdin S, Bayrak Özdin Ş. Levels and predictors of anxiety, depression and health anxiety during COVID-19 pandemic in Turkish society: The importance of gender. *Int J Soc Psychiatry*. 2020;66(5):504–511. doi:10.1177/0020764020927051
15. Ataş O, Talo Yildirim T. Evaluation of knowledge, attitudes, and clinical education of dental students about COVID-19 pandemic. *PeerJ*. 2020;8:e9575. doi:10.7717/peerj.9575
16. De Stefani A, Bruno G, Mutinelli S, Gracco A. COVID-19 outbreak perception in Italian dentists. *Int J Environ Res Public Health*. 2020;17(11):3867. doi:10.3390/ijerph17113867
17. Das D, Shenoy R, Mukherjee M, Unnikrishnan B, Rungta N. Awareness among undergraduate students of Mangalore City regarding novel coronavirus (COVID-19): A questionnaire study. *Disaster Med Public Health Prep*. 2021;15(1):e6–e9. doi:10.1017/dmp.2020.204
18. Ahmed MA, Jouhar R, Ahmed N, et al. Fear and practice modifications among dentists to combat novel coronavirus disease (COVID-19) outbreak. *Int J Environ Res Public Health*. 2020;17(8):2821. doi:10.3390/ijerph17082821
19. Kearney RC, Premaraj S, Smith BM, Olson GW, Williamson AE, Romanos G. Massive open online courses in dental education: Two viewpoints. Viewpoint 1: Massive open online courses offer transformative technology for dental education. Viewpoint 2: Massive open online courses are not ready for primetime. *J Dent Educ*. 2016;80(2):121–127. doi:10.1002/j.0022-0337.2016.80.2.tb06066.x
20. Umeizudike KA, Isiekwe IG, Fadeju AD, Akinboboye BO, Aladenika ET. Nigerian undergraduate dental students' knowledge, perception, and attitude to COVID-19 and infection control practices. *J Dent Educ*. 2021;85(2):187–196. doi:10.1002/jdd.12423
21. Gurgel BCDV, Borges SB, Borges REA, Calderon PDS. COVID-19: Perspectives for the management of dental care and education. *J Appl Oral Sci*. 2020;28:e20200358. doi:10.1590/1678-7757-2020-0358
22. Villani FA, Aiuto R, Paglia L, Re D. COVID-19 and dentistry: Prevention in dental practice. A literature review. *Int J Environ Res Public Health*. 2020;17(12):4609. doi:10.3390/ijerph17124609
23. Løset IH, Lægreid T, Rodakowska E. Dental students' experiences during the COVID-19 pandemic: A cross-sectional study from Norway. *Int J Environ Res Public Health*. 2022;19(5):3102. doi:10.3390/ijerph19053102
24. Guo T, Kiong KL, Yao CMKL, et al. Impact of the otolaryngology trainee education. *Head Neck*. 2020;42(10):2782–2790. doi:10.1002/hed.26368
25. Mahmud MdS, Talukder MU, Rahman SkM. Does 'Fear of COVID-19' trigger future career anxiety? An empirical investigation considering depression from COVID-19 as a mediator. *Int J Soc Psychiatry*. 2021;67(1):35–45. doi:10.1177/0020764020935488

Low-level NLRP1 is associated with increased metastasis and risk of recurrence of non-melanoma skin cancer

Jianxiang Tan[A,D,F], Jinzhou Li[B,C,E], Yunquan Zeng[A,E,F]

Department of Plastic Surgery, Meizhou People's Hospital, China

A – research concept and design; B – collection and/or assembly of data; C – data analysis and interpretation;
D – writing the article; E – critical revision of the article; F – final approval of the article

Advances in Clinical and Experimental Medicine, ISSN 1899–5276 (print), ISSN 2451–2680 (online) *Adv Clin Exp Med*. 2024;33(1):61–68

Address for correspondence
Yunquan Zeng
E-mail: yunquanzeng@163.com

Funding sources
None declared

Conflict of interest
None declared

Received on August 5, 2022
Reviewed on November 11, 2022
Accepted on April 25, 2023

Published online on June 6, 2023

Abstract

Background. Cutaneous squamous cell carcinoma (cSCC) and cutaneous basal cell carcinoma (cBCC) are the most common types of non-melanoma skin cancer (NMSC). The NACHT, LRR and PYD domains-containing protein 1 (NLRP1) protein is considered to be inhibited in NMSC, although clinical evidence is still lacking.

Objectives. To investigate the clinical significance of NLRP1 in cSCC and cBCC patients.

Materials and methods. This prospective observational study enrolled 199 cases of cBCC and cSCC patients who reported to our hospital from January 2018 to January 2019. Additionally, 199 blood samples from healthy individuals were collected as the control. Serum NLRP1 and cancer biomarkers of CEA and CYFRA21-1 were then measured using enzyme-linked immunosorbent assay (ELISA). Clinical characteristics collected from patients included age, sex, BMI, TNM stage, cancer type, lymph node metastasis, and myometrial infiltration conditions. All patients were followed up for 1–3 years.

Results. Of all patients, 23 died during the follow-up period, with a mortality rate of 11.56%. Serum NLRP1 showed markedly lower levels in cancer patients compared with healthy controls. Furthermore, the expression of NLRP1 was significantly higher in cBCC patients compared with cSCC patients. The deceased patients, together with those with lymph node metastasis and myometrial infiltration, also showed significantly lower NLRP1 levels. Moreover, lower NLRP1 levels were associated with higher frequencies of tumor–nodule–metastasis (TNM) III–IV stage, lymph node metastasis and myometrial infiltration, as well as higher mortality and recurrence rates. The curvilinear regression showed the relationship between NLRP1 and CEA/or CYFRA21-1 was most appropriate for the reciprocal. Receiver operating characteristic (ROC) curves showed NLRP1 was a potential biomarker for lymph node metastasis, myometrial infiltration and prognosis in NMSC patients, and the Kaplan–Meier analysis found NLRP1 was associated with 1–3-year mortality and recurrence of NMSC.

Conclusions. Lower NLRP1 level is associated with worse clinical outcomes and poorer prognosis in cSCC and cBCC patients.

Key words: diagnosis, prognosis, NLRP1, cutaneous squamous cell carcinoma, cutaneous basal cell carcinoma

Cite as
Tan J, Li J, Zeng Y. Low-level NLRP1 is associated with increased metastasis and risk of recurrence of non-melanoma skin cancer. *Adv Clin Exp Med*. 2024;33(1):61–68. doi:10.17219/acem/163581

DOI
10.17219/acem/163581

Background

Non-melanoma skin cancer (NMSC) accounts for 6.2% of new cancer cases worldwide, with 1,198,073 cases per year and 63,731 cases of cancer-related deaths in 2020.[1,2] Cutaneous squamous cell carcinoma (cSCC) and cutaneous basal cell carcinoma (cBCC) are the most common NMSC types, being approx. 25% and 70% of NMSC cases, respectively.[3,4] In a recent study that included 12,692 skin cancer cases from Chinese, Malays and Indians in Singapore from 1968–2016, it was found that 65.9% of patients were diagnosed with cBCC, 28.3% had cSCC and 5.80% had melanoma.[5] Generally, cSCC has the characteristics of atypical proliferation of invasive squamous cells, the ability to invade and migrate, as well as a high potential of recurrence.[6,7] Patients with cBCC, although it shows low invasive ability, are considered to have a higher risk of developing other skin cancers, including cSCC and melanoma.[8–10] In recent years, the prevalence of cBCC and cSCC increased between 35% and 133% worldwide.[11]

Generally, early diagnosis is of great significance for cancer patients, including those with skin cancer. Thus, new cancer biomarkers are always needed in clinical research. NACHT, LRR and PYD domains-containing protein 1 (NLRP1) belongs to the NLRP family and plays an important role in many bioprocesses, including inflammation, cell function and cancer proliferation.[12–14] NLRP1 was found to be associated with different cancers through several signaling pathways. It was found that NLRP1 polymorphisms were associated with an increased incidence of mesothelioma, specifically with the NLRP1 rs12150220 allele T.[15] Another study demonstrated that NLRP1 could influence cell pyroptosis in breast cancer cells, which was associated with the regulation of caspase-4.[16] Recently, it was reported that both levels of NLRP1 and NLRP1 inflammasome were inhibited in cSCC.[17] Furthermore, NLRP3, another member of the NLRP family which shows biofunctions similar to NLRP1, was also found to be suppressed in cSCC.[18] These data led us to speculate that the expression of NLRP1 in cSCC patients may also be decreased. However, studies of NLRP1 in NMSC patients are still lacking.

Objectives

We conducted an observational study to investigate the clinical significance of NLRP1 in cSCC and cBCC patients. This study may provide a potential novel biomarker for the diagnosis and prognosis of NMSC.

Materials and methods

Patients

This prospective observational study enrolled 199 cases of cBCC and cSCC patients who reported to our hospital from January 2018 to January 2019. The sample size was calculated by the formula $(Z_{1-\alpha/2\times\sigma}/\delta)^2$ proposed by Shalhout et al.[2] The estimated standard deviation (SD) was 36, and the allowable error was 5 (α = 0.05) thus, n = $((1.96\times36)/0.05)^2$ = 199. The inclusion criteria were as follows: 1) patients with cBCC or cSCC confirmed with histological analysis; 2) patients who were diagnosed for the first time with primary NMSC; 3) patients over the age of 18. The following patients were excluded: 1) patients who underwent anti-cancer treatments before participation; 2) patients with metastatic skin carcinoma but not primary skin cancer; 3) patients with severe infections such as severe pneumonia, or other systematic organ dysfunctions. Additionally, blood samples from 199 healthy individuals who reported for medical examination were enrolled as a control group.

All patients signed the informed consent, and the study protocol conformed to the Declaration of Helsinki. Ethical approval was obtained by the Ethical Committee of Meizhou People's Hospital (approval No. 2018-11).

Measurement of serum NLRP1, CEA and CYFRA21-1

Serum NLRP1, as well as cancer biomarkers carcino embryonic antigen (CEA) and CYFRA21-1 were measured using enzyme-linked immunosorbent assay (ELISA). Briefly, fasting elbow vein peripheral blood (5 mL) was collected within 48 h after admission. After obtaining the serum by centrifugation, the serum levels of NLRP1 (range 18.75–1200 pg/mL, sensitivity 4.67 pg/mL; cat. No. EL015864HU; Cusabio, Houston, USA), CEA (range: 312–20000 pg/mL, sensitivity <10 pg/mL, cat. No. EK0904 BOSTER Bio, Pleasanton, CA) and CYFRA21-1 (range: 31.25–2000 pg/mL, sensitivity 18.75 pg/mL; cat. No. EH0364; Wuhan Fine Biotech, Wuhan, China) were tested using commercially available ELISA kits according to the manufacturer's instruction.

Data collection of clinical outcomes and follow-up

All patients were followed up for 1–3 years. The patients' clinical characteristics collected included age, sex, body mass index (BMI), tumor–nodule–metastasis (TNM) stage, cancer type, lymph node metastasis, and myometrial infiltration conditions. Patients' cancer-related death and recurrence conditions were recorded. For survival analysis, overall survival (OS) or disease-free survival (DFS) duration was calculated from the time of admission to death or recurrence, or the last follow-up.

Statistical analyses

Data were expressed as median (Me) (interquartile range (IQR) and range) for non-normally distributed data (all continuous data are non-normally distributed in this study).

Data distribution was analyzed using the Kolmogorov–Smirnov method. Comparisons between 2 groups were made using the Mann–Whitney U test, and Kruskal–Wallis analysis was used for comparisons between 3 groups for age, BMI and NLRP1 level. The χ^2 test was used for analyzing the rates, and curvilinear regression was used for analyzing the correlation between NLRP1 and CEA/or CYFRA21-1. The receiver operating characteristic (ROC) curve was used for the diagnostic value of NLRP1. The Kaplan–Meier curve was applied to the survival analysis. Logistic regression was used for the analysis of risk factors of mortality, and the Hosmer–Lemeshow test was used to show the goodness-of-fit. We used Box–Tidwell method to test the linearity of independent variables and log odds. The variance inflation factor (VIF) value was used to show multicollinearity, with a value above 1.5 indicating multicollinearity. Finally, the Casewise List (Studentized residual) was used to show the influential outliers. A $p < 0.05$ indicated a significant difference between groups, and all calculations were performed using Statistical Package for Social Sciences (SPSS) v. 18.0 (SPSS Inc., Chicago, USA) and GraphPad Prism v. 6.0 (GraphPad Software, San Diego, USA).

Results

Clinical characteristics of patients and the expression of NLRP1

The clinical characteristics of all patients are listed in Table 1. All patients were followed up for 1–3 years, with a median follow-up time of 24 months. From the entire cohort, 23 patients died during the follow-up period, with a mortality rate of 11.56%. Compared with the surviving patients, the deceased ones showed a higher frequency of TNM stage III–IV, lymph node metastasis, myometrial infiltration, and recurrence (all $p < 0.05$). Furthermore, cSCC patients had a higher mortality rate than cBCC patients. No other significant differences were found between the surviving and deceased patients, including their demographics, with no significant difference found for age, sex and BMI between the surviving and deceased patients and healthy controls.

Then, we analyzed the expression of NLRP1 in different patients. It was found that NLRP1 showed markedly lower levels in serum from both cSCC and cBCC patients compared with healthy controls ($p < 0.001$; Fig. 1A). Moreover, the expression of NLRP1 was significantly higher in cBCC patients compared with cSCC patients ($p = 0.048$). Meanwhile, deceased patients, together with those with TNM III–IV, lymph node metastasis and myometrial infiltration, also showed significantly decreased NLRP1 levels compared with surviving patients, the patients with TNM I–II or those without lymph node metastasis or myometrial infiltration, respectively (all $p < 0.05$) (Fig. 1B–E).

Expression of NLRP1 was correlated with CEA and CYFRA21-1 in NMSC patients

Next, the serum levels of cancer biomarkers CEA and CYFRA21-1 were analyzed. It was found that both CEA and CYFRA21-1 levels were significantly higher in deceased patients, as well as in the patients with TNM stage III–IV, lymph node metastasis or myometrial infiltration, compared with surviving patients, patients with TNM I–II or patients without metastasis or infiltration (Table 2).

Table 1. Clinical characteristics of all non-melanoma skin cancer (NMSC) patients on admission

Variables		All patients (n = 199)	Surviving (n = 176)	Deceased (n = 23)	Healthy controls (n = 199)	p_1*	p_2#
Age [years]		56 (23, 34–75)	56 (23, 34–75)	58 (26, 36–75)	53 (21, 34–75)	0.583	0.568
Female sex, n (%)		106 (53.27)	94 (53.41)	12 (52.17)	106 (53.27)	0.861	0.982
BMI [kg/m^2]		24.90 (7.30, 17.04–31.95)	25.09 (7.20, 17.05–31.92)	23.52 (8.66, 17.04–31.95)	23.91 (8.13, 17.12–31.93)	0.363	0.306
TNM stage, n (%)	I–II	153 (76.88)	151 (85.80)	2 (8.70)	–	<0.001	–
	III–IV	46 (23.12)	25 (14.20)	21 (91.30)	–		
Pathological type, n (%)	cSCC	74 (37.19)	56 (31.82)	18 (78.26)	–	<0.001	–
	cBCC	125 (62.81)	120 (68.18)	5 (21.74)	–		
Lymph node metastasis, n (%)		49 (24.62)	28 (15.91)	21 (91.30)	–	<0.001	–
Myometrial infiltration, n (%)		54 (27.14)	32 (18.18)	22 (95.65)	–	<0.001	–
Follow-up [months]		24 (12, 12–36)	24 (13, 12–36)	20 (12, 12–35)	–	0.299	–
Recurrence, n (%)		30 (15.08)	11 (6.25)	19 (82.61)	–	<0.001	–

*p_1 value was obtained by comparison between surviving and deceased patients, while rates were analyzed using χ^2 test. For #p_2 values, age and BMI were compared using Kruskal–Wallis analysis, while the sex rates were compared with χ^2 test among the 3 groups: surviving patients, deceased patients and healthy controls. Continuous data were expressed as median (IQR, range). BMI – body mass index; TNM – tumor–nodule–metastasis; IQR – interquartile range; cSCC – cutaneous squamous cell carcinoma; cBCC – cutaneous basal cell carcinoma.

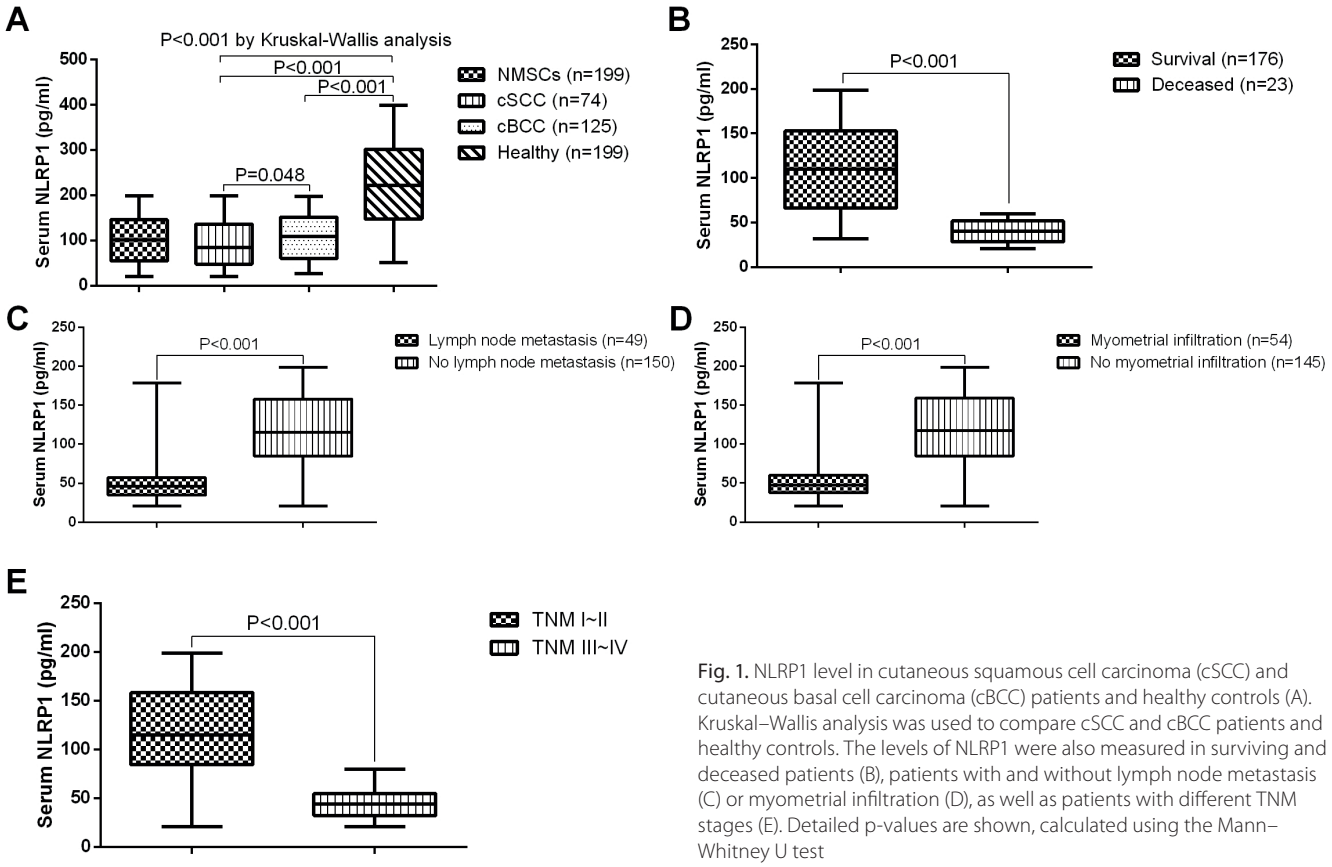

Fig. 1. NLRP1 level in cutaneous squamous cell carcinoma (cSCC) and cutaneous basal cell carcinoma (cBCC) patients and healthy controls (A). Kruskal–Wallis analysis was used to compare cSCC and cBCC patients and healthy controls. The levels of NLRP1 were also measured in surviving and deceased patients (B), patients with and without lymph node metastasis (C) or myometrial infiltration (D), as well as patients with different TNM stages (E). Detailed p-values are shown, calculated using the Mann–Whitney U test

Table 2. Serum expression of CEA and CYFRA21-1 in different groups of patients

Variables	CEA [pg/mL]	CYFRA21-1 [pg/mL]
Surviving (n = 176)	498.41 (198.90, 304.73–941.88)	67.89 (31.73, 31.20–148.99)
Deceased (n = 23)	968.04 (612.37, 548.13–1476.55)	170.69 (67.99, 95.74–241.42)
p[a]	<0.001	<0.001
TNM I–II (n = 153)	488.35 (194.29, 304.73–1313.59)	65.15 (28.58, 31.20–241.42)
TNM III–IV (n = 46)	787.95 (392.61, 405.23–1476.55)	122.24 (70.13, 51.87–222.13)
p[b]	<0.001	<0.001
With lymph node metastasis (n = 49)	783.56 (388.03, 309.54–1476.55)	121.48 (70.89, 51.87–222.13)
Without lymph node metastasis (n = 150)	489.76 (187.83, 304.73–1313.59)	65.37 (28.73, 31.20–241.42)
p[c]	<0.001	<0.001
With myometrial infiltration (n = 54)	704.09 (382.46, 309.54–1476.55)	119.10 (75.19, 36.58–222.13)
Without myometrial infiltration (n = 145)	488.35 (186.91, 304.73–1313.59)	65.15 (28.58, 31.20–241.42)
p[d]	<0.001	<0.001

All p-values were compared using Mann–Whitney U test; [a]p-value was calculated as comparison between surviving and deceased patients; [b]p-value was calculated as comparison between TNM I–II and III–IV patients; [c]p-value was calculated as comparison between patients with and without lymph node metastasis; [d]p-value was calculated as comparison between patients with and without myometrial infiltration. TNM – tumor–nodule–metastasis.

Additionally, the curvilinear regression showed the relationship between NLRP1 and CEA was mostly appropriate for reciprocal (R^2 = 0.282), and similar to the relationship between NLRP1 and CYFRA21-1 (R^2 = 0.392) (Fig. 2). The detailed data for curvilinear regression are shown in the Supplementary data.

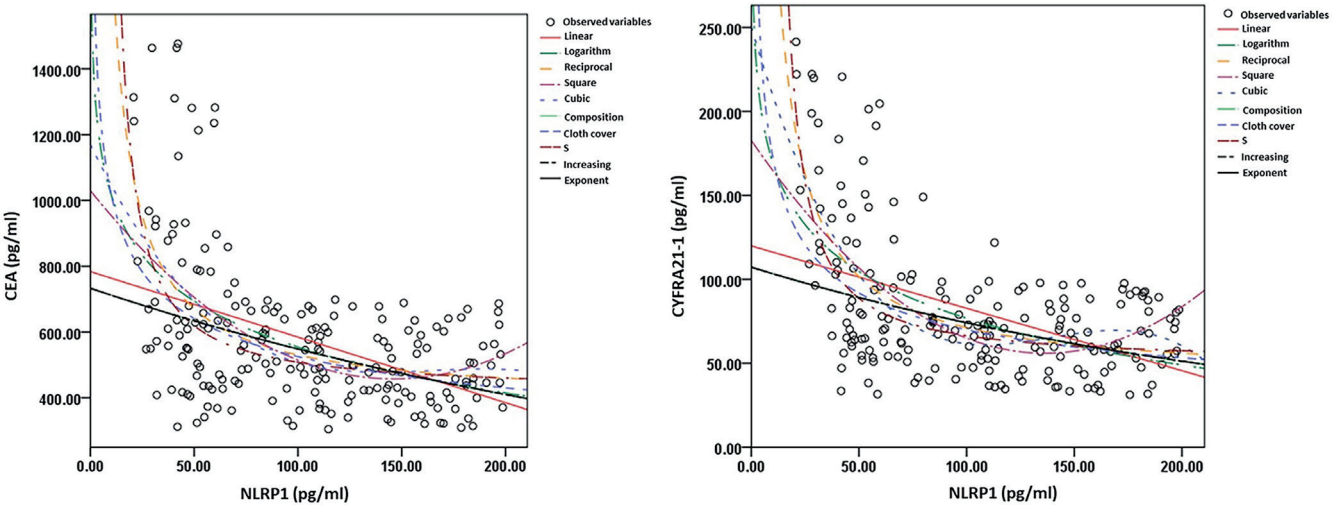

Fig. 2. Curvilinear regression shows the relationship between NLRP1 and CEA levels (A) and between NLRP1 and CYFRA21-1 levels (B)

Low expression of NLRP1 was associated with worse clinical outcomes in NMSC patients

The median value of NLRP1 level (101.65 pg/mL) was used to divide the patients into high (>101.65 pg/mL) or low NLRP1 (≤101.65 pg/mL) level groups (Table 3). Patients with low expression of NLRP1 showed significantly higher incidence of TNM III–IV, lymph node metastasis and myometrial infiltration (all $p < 0.05$). Unexpectedly, BMI in the low NLRP1 group was also markedly lower than in the patients with high NLRP1 level. Moreover, the mortality and recurrence rates were also markedly higher in patients with lower expression of NLRP1. These results suggested that low expression of NLRP1 may be associated with worse clinical outcomes in NMSC patients.

NLRP1 as a potential biomarker for lymph node metastasis, myometrial infiltration and prognosis in skin cancer patients

Next, ROC curves were used to investigate the diagnostic value of NLRP1. It was found that NLRP1 showed good diagnostic value for the diagnosis of lymph node metastasis (area under curve (AUC) 0.913, cutoff <60.94 pg/mL, sensitivity 87.33% (95% confidence interval (95% CI): 80.93–92.20%), specificity 83.67% (95% CI: 70.34–92.68%)), myometrial infiltration (AUC 0.891, cutoff <60.94 pg/mL, sensitivity 87.59% (95% CI: 81.09–92.47%), specificity 77.78% (95% CI: 64.40–87.96%)), recurrence (AUC 0.921, cutoff <52.40 pg/mL, sensitivity 87.57% (95% CI: 81.63–92.14%), specificity 80.00% (95% CI: 61.43–92.29%)), and mortality (AUC 0.933, cutoff <53.65 pg/mL, sensitivity

Table 3. Comparison between patients with high and low NLRP1 expression

Variables		High NLRP1 (n = 99)	Low NLRP1 (n = 100)	p-value
Age [years]		55 (25, 34–75)	57 (20.75, 35–75)	0.948
Female sex, n (%)		54 (54.55)	52 (52.00)	0.718
BMI [kg/m^2]		25.26 (7.52, 17.10–31.92)	24.26 (7.15, 17.04–31.95)	0.018
TNM stage, n (%)	I–II	99 (100.00)	54 (54.00)	<0.001
	III–IV	0 (0.00)	46 (46.00)	
Pathological type, n (%)	cSCC	33 (33.33)	41 (41.00)	–
	cBCC	66 (66.67)	59 (59.00)	
Lymph node metastasis, n (%)		2 (2.02)	47 (47.00)	<0.001
Myometrial infiltration, n (%)		5 (5.05)	49 (49.00)	<0.001
Follow-up [months]		24.00 (12.00, 12–36)	23.50 (12.75, 12–36)	0.569
Mortality, n (%)		0 (0.00)	23 (23.00)	<0.001
Recurrence, n (%)		0 (0.00)	30 (30.00)	<0.001

The p-value was obtained as comparison between surviving and deceased patients using Mann–Whitney U test for continuous data. Rates were analyzed using χ^2 test. Continuous data were expressed as median (IQR, range). BMI – body mass index; TNM – tumor–nodule–metastasis; IQR – interquartile range; cSCC – cutaneous squamous cell carcinoma; cBCC – cutaneous basal cell carcinoma.

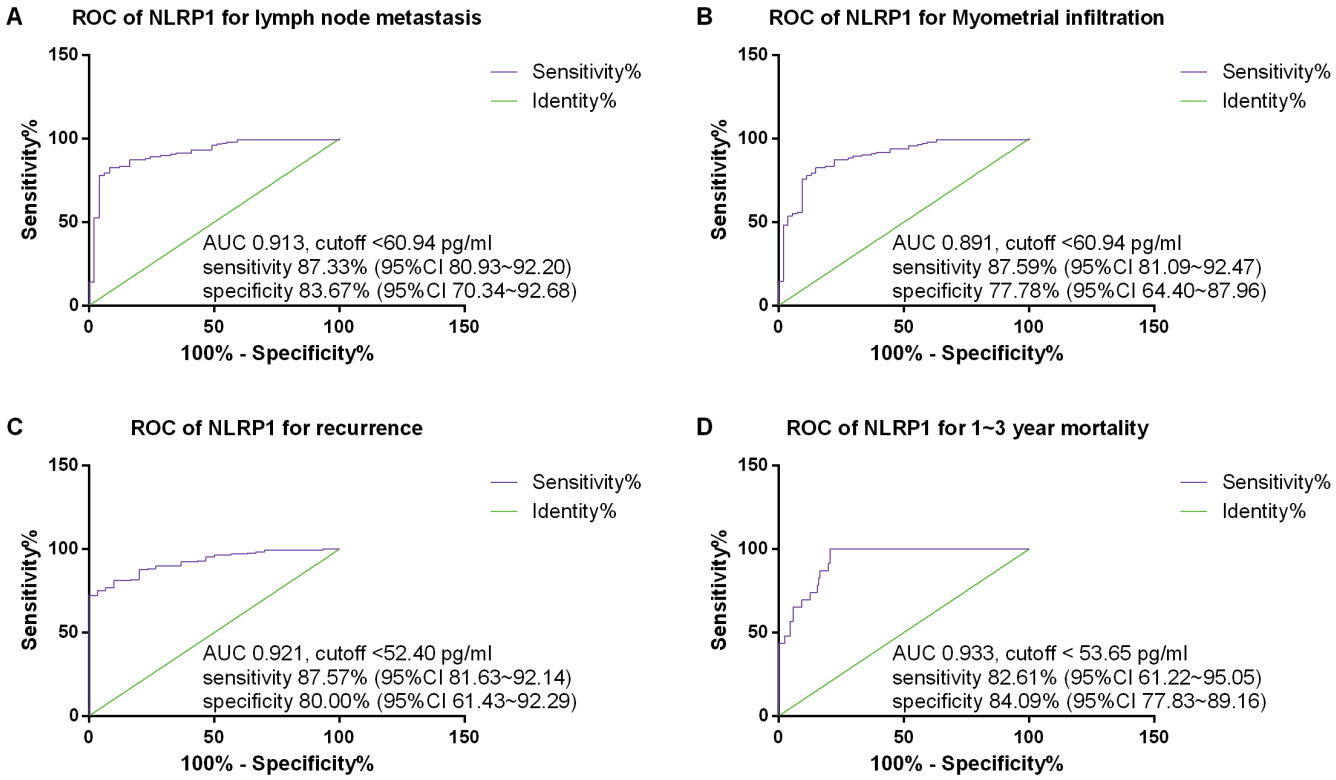

Fig. 3. ROC curves for NLRP1 levels as a tool for the detection of lymph node metastasis (A), myometrial infiltration (B) and recurrence (C) and estimating mortality (D) in non-melanoma skin cancer (NMSC) patients

82.61% (95% CI: 61.22–95.05%), specificity 84.09% (95% CI: 77.83–89.16%)) (Fig. 3).

NLRP1 was associated with 1–3-year mortality and recurrence in NMSC patients

We then used a Kaplan–Meier curve to analyze the effects of NLRP1 on patients' prognoses. It was found that patients with lower expression of NLRP1 showed significantly shorter overall 1–3-year OS and DFS (both $p < 0.001$ using log-rank test; Fig. 4). The logistic regression was performed using 3 models, with model 1 including continuous data (age, BMI, NLRP1, CEA, and CYFRA21-1), model 2 including count data on sex, TNM stage and pathological type, and model 3 including data on lymph node metastasis and myometrial infiltration incidence (Table 4). The p-values of the Hosmer–Lemeshow test were as follows: 0.999, 0.557 and 1.000, while the value of Nagelkerke R^2 were 0.894, 0.598 and 0.499, respectively, indicating the acceptable goodness-of-fit. The detailed original data of our logistic regression and the data on the linearity of independent variables, log odds and multicollinearity, as well as influential outliers are all shown in the Supplementary materials. Interestingly, logistic regression demonstrated that high expression CEA and CYFRA21-1, as well as TNM stage, pathological type and myometrial infiltration, were risk factors for 1–3-year mortality in NMSC.

Discussion

The cSCC and cBCC are the most common types of NMSC, although there is currently a lack of specific cancer biomarkers for both cBCC and cSCC. In recent years, NLRP1 has shown its potential as a novel research target in skin carcinogenesis. However, clinical studies on NLRP1 in NMSC are rare. In the present study, we demonstrated for the first time that lower NLRP1 expression was associated with worse clinical outcomes and poorer prognosis of cSCC and cBCC patients.

The NLRP1 can act as both a cancer promotor or suppressor in different cancer types. In our study, we found NLRP1 had low expression in both cBCC and cSCC, and this was associated with the patient's poor prognosis. It was found that NLRP1 was downregulated in lung adenocarcinoma patients, and decreased NLRP1 expression predicted their poor prognosis, showing its potential as an anti-cancer agent.[19] In colorectal cancer, NLRP1 was also reported to suppress colitis-associated tumorigenesis through activation of the NLRP1 inflammasome.[20] In these studies, NLRP1 was downregulated and acted as a tumor suppressor, which was consistent with our findings in NMSC. However, in breast cancer, NLRP1 was found to be a cancer promotor, its overexpression facilitating tumorigenesis and cell proliferation.[21] The molecular mechanisms of these differences are not fully understood, partly due to the different effects of NLRP1 on cancer-related immunity.

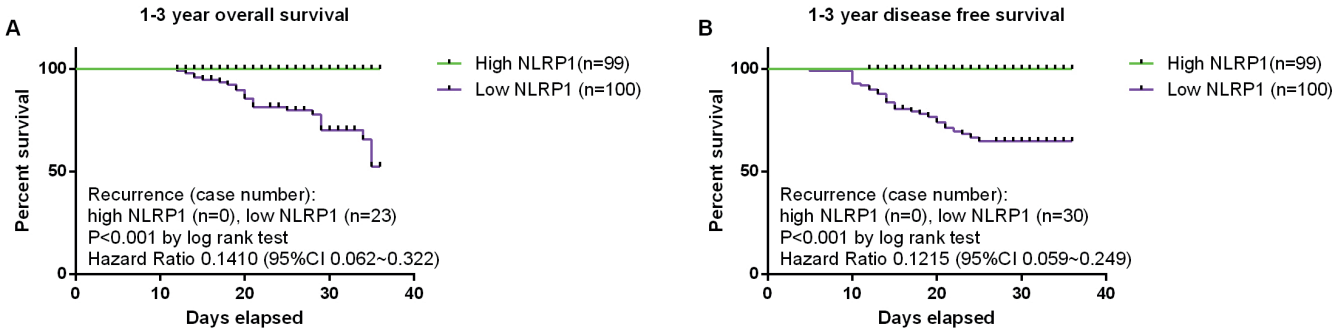

Fig. 4. Kaplan–Meier curve for overall survival (OS) (A) and disease-free survival (DFS) (B)

Table 4. Logistic regression for 1–3-year mortality in non-melanoma skin cancer (NMSC)

Variables	Walds	OR	95% CI	p-value
Age	0.572	1.039	0.941–1.148	0.450
Sex	0.120	0.805	0.236–2.747	0.729
BMI	0.220	0.937	0.714–1.230	0.639
TNM stage	27.916	74.082	15.001–365.841	<0.001
Pathological type	12.238	0.101	0.028–0.365	<0.001
Lymph node metastasis	0.905	3.000	0.312–28.841	0.341
Myometrial infiltration	5.690	36.000	1.895–684.028	0.017
NLRP1	2.315	0.913	0.812–1.027	0.128
CEA	5.206	1.007	1.001–1.013	0.023
CYFRA21-1	6.485	1.082	1.018–1.150	0.011

BMI – body mass index; TNM – tumor–nodule–metastasis; OR – odds ratio; 95% CI – 95% confidence interval.

In skin cancers, NLRP1 also plays different roles in NMSC and melanoma. It was reported that NLRP1 was highly expressed in melanoma, along with activation of the NLRP1 inflammasome, and high NLRP1 expression, in turn, induced resistance to the drug temozolomide.[22] In another study, it was found NLRP1 could facilitate cell proliferation and suppress cell apoptosis through activating the NLRP1 inflammasome in melanoma.[23] In the present research, we mainly focused on the clinical significance of NLRP1 in cBCC and cSCC patients, finding that NLRP1 expression was decreased in both cBCC and cSCC patients, and its low expression was correlated with poorer clinical outcomes and prognosis. However, we failed to show that NLRP1 was an independent risk factor for 1–3-year mortality, indicating more studies should be conducted to confirm our results. Previous research has demonstrated NLRP1 level was decreased in cSCC, along with inhibition of ASC, caspase-1 and IL-1β, the inflammasome-related factors.[17] Furthermore, another study reported that germline NLRP1 mutations were associated with the incidence of multiple self-healing palmoplantar carcinomas (MSPC) and familial chronic lichen keratosis (FKLC), which are risk factors for various types of skin cancers.[24] All these results are consistent with our findings, although up to now, few have reported clinical expression of NLRP1 in NMSC. Interestingly, the expression of another NLRP family member, NLRP3, was also decreased in cSCC,[18] and a study found ultraviolet radiation could activate the expression of NLRP3 in cBCC.[25] Since the pathology and molecular mechanisms between NMSC and melanoma differ a lot, the difference in NLRP1 in these cancers may be caused by other signaling pathways and key genes or other proteins.

Limitations of the study

The study has some limitations. We failed to prove NLRP1 is an independent risk factor for mortality in NMSC. Moreover, we only included a small number of patients.

Conclusions

We found that NLRP1 could be used as a potential biomarker of clinical outcomes and prognosis of NMSC. Lower NLRP1 levels were associated with higher incidence of lymph node metastasis and myometrial infiltration, and higher risk of recurrence and mortality. This study may provide a potential novel biomarker as well as a research target for future NMSC investigations.

Supplementary data

The Supplementary materials are available at https://doi.org/10.5281/zenodo.7871796. The package contains the following files:

Supplementary Table 1. The test of linearity of independent variables and log-odds, multicollinearity and influential outliers. Supplementary Table 2. The original output data of logistic regression from SPSS. Supplementary Table 3. The original output data of curvilinear regression from SPSS.

ORCID iDs

Jianxiang Tan https://orcid.org/0009-0005-7662-6098
Jinzhou Li https://orcid.org/0009-0002-1526-7376
Yunquan Zeng https://orcid.org/0009-0004-1799-3878

References

1. Sung H, Ferlay J, Siegel RL, et al. Global Cancer Statistics 2020: GLOBOCAN estimates of incidence and mortality worldwide for 36 cancers in 185 countries. *CA A Cancer J Clin*. 2021;71(3):209–249. doi:10.3322/caac.21660
2. Shalhout SZ, Emerick KS, Kaufman HL, Miller DM. Immunotherapy for non-melanoma skin cancer. *Curr Oncol Rep*. 2021;23(11):125. doi:10.1007/s11912-021-01120-z
3. Cives M, Mannavola F, Lospalluti L, et al. Non-melanoma skin cancers: Biological and clinical features. *Int J Mol Sci*. 2020;21(15):5394. doi:10.3390/ijms21155394
4. Silva ESD, Tavares R, Paulitsch FDS, Zhang L. Use of sunscreen and risk of melanoma and non-melanoma skin cancer: A systematic review and meta-analysis. *Eur J Dermatol*. 2018;28(2):186–201. doi:10.1684/ejd.2018.3251
5. Oh CC, Jin A, Koh WP. Trends of cutaneous basal cell carcinoma, squamous cell carcinoma, and melanoma among the Chinese, Malays and Indians in Singapore from 1968–2016. *JAAD Int*. 2021;4:39–45. doi:10.1016/j.jdin.2021.05.006
6. Fania L, Didona D, Di Pietro FR, et al. Cutaneous squamous cell carcinoma: From pathophysiology to novel therapeutic approaches. *Biomedicines*. 2021;9(2):171. doi:10.3390/biomedicines9020171
7. Corchado-Cobos R, García-Sancha N, González-Sarmiento R, Pérez-Losada J, Cañueto J. Cutaneous squamous cell carcinoma: From biology to therapy. *Int J Mol Sci*. 2020;21(8):2956. doi:10.3390/ijms21082956
8. Fania L, Didona D, Morese R, et al. Basal cell carcinoma: From pathophysiology to novel therapeutic approaches. *Biomedicines*. 2020;8(11):449. doi:10.3390/biomedicines8110449
9. Kim DP, Kus KJB, Ruiz E. Basal cell carcinoma review. *Hematol Oncol Clin North Am*. 2019;33(1):13–24. doi:10.1016/j.hoc.2018.09.004
10. Marzuka AG, Book SE. Basal cell carcinoma: Pathogenesis, epidemiology, clinical features, diagnosis, histopathology, and management. *Yale J Biol Med*. 2015;88(2):167–179. PMID:26029015. PMCID:PMC4445438.
11. Didona D, Paolino G, Bottoni U, Cantisani C. Non-melanoma skin cancer pathogenesis overview. *Biomedicines*. 2018;6(1):6. doi:10.3390/biomedicines6010006
12. Taabazuing CY, Griswold AR, Bachovchin DA. The NLRP1 and CARD8 inflammasomes. *Immunol Rev*. 2020;297(1):13–25. doi:10.1111/imr.12884
13. Fenini G, Karakaya T, Hennig P, Di Filippo M, Beer HD. The NLRP1 inflammasome in human skin and beyond. *Int J Mol Sci*. 2020;21(13):4788. doi:10.3390/ijms21134788
14. Chavarría-Smith J, Vance RE. The NLRP1 inflammasomes. *Immunol Rev*. 2015;265(1):22–34. doi:10.1111/imr.12283
15. Girardelli M, Maestri I, Rinaldi RR, et al. NLRP1 polymorphisms in patients with asbestos-associated mesothelioma. *Infect Agents Cancer*. 2012;7(1):25. doi:10.1186/1750-9378-7-25
16. Jiao Y, Wang L, Lu L, et al. The role of caspase-4 and NLRP1 in MCF7 cell pyroptosis induced by hUCMSC-secreted factors. *Stem Cells Int*. 2020;2020:8867115. doi:10.1155/2020/8867115
17. Sand J, Fenini G, Grossi S, et al. The NLRP1 inflammasome pathway is silenced in cutaneous squamous cell carcinoma. *J Invest Dermatol*. 2019;139(8):1788–1797.e6. doi:10.1016/j.jid.2019.01.025
18. Nie S, Wang X, Wang H. NLRP3 inflammasome mediated interleukin-1β production in cancer-associated fibroblast contributes to ALA-PDT for cutaneous squamous cell carcinoma. *Cancer Manag Res*. 2019;11:10257–10267. doi:10.2147/CMAR.S226356
19. Shen E, Han Y, Cai C, et al. Low expression of NLRP1 is associated with a poor prognosis and immune infiltration in lung adenocarcinoma patients. *Aging*. 2021;13(5):7570–7588. doi:10.18632/aging.202620
20. Williams TM, Leeth RA, Rothschild DE, et al. The NLRP1 inflammasome attenuates colitis and colitis-associated tumorigenesis. *J Immunol*. 2015;194(7):3369–3380. doi:10.4049/jimmunol.1402098
21. Wei Y, Huang H, Qiu Z, et al. NLRP1 overexpression is correlated with the tumorigenesis and proliferation of human breast tumor. *Biomed Res Int*. 2017;2017:4938473. doi:10.1155/2017/4938473
22. Zhai Z, Samson JM, Yamauchi T, et al. Inflammasome sensor NLRP1 confers acquired drug resistance to temozolomide in human melanoma. *Cancers (Basel)*. 2020;12(9):2518. doi:10.3390/cancers12092518
23. Zhai Z, Liu W, Kaur M, et al. NLRP1 promotes tumor growth by enhancing inflammasome activation and suppressing apoptosis in metastatic melanoma. *Oncogene*. 2017;36(27):3820–3830. doi:10.1038/onc.2017.26
24. Zhong FL, Mamaï O, Sborgi L, et al. Germline NLRP1 mutations cause skin inflammatory and cancer susceptibility syndromes via inflammasome activation. *Cell*. 2016;167(1):187–202.e17. doi:10.1016/j.cell.2016.09.001
25. Ahmad I, Muneer KM, Chang ME, et al. Ultraviolet radiation-induced downregulation of SERCA2 mediates activation of NLRP3 inflammasome in basal cell carcinoma. *Photochem Photobiol*. 2017;93(4):1025–1033. doi:10.1111/php.12725

Real-world effectiveness and safety of vedolizumab induction therapy for ulcerative colitis: A prospective nationwide Polish observational study

Edyta Zagórowicz[1,2,A,B,E,F], Halina Cichoż-Lach[3,B,E,F], Maria Kopertowska-Majchrzak[4,B,E,F], Piotr Eder[5,B,E,F], Kamila Stawczyk-Eder[5,B,E,F], Renata Talar-Wojnarowska[6,B,E,F], Hubert Zatorski[6,B,E,F], Anna Solarska-Półchłopek[1,2,B,E,F], Rafał Filip[7,B,E,F], Maria Janiak[8,B,E,F], Krzysztof Skrobot[8,B,E,F], Maria Kłopocka[9,B,E,F], Ariel Liebert[9,B,E,F], Aleksandra Kaczka[10,B,E,F], Krzysztof Wojciechowski[11,A–C,E,F], Szymon Drygała[11,B,C,E,F], Agata Michalak[3,B,E,F]

[1] Department of Oncological Gastroenterology, Maria Skłodowska-Curie National Research Institute of Oncology, Warsaw, Poland
[2] Department of Gastroenterology, Hepatology and Clinical Oncology, Centre of Postgraduate Medical Education, Warsaw, Poland
[3] Department of Gastroenterology, Medical University of Lublin, Poland
[4] Department of Internal Diseases, General Hospital, Międzychód, Poland
[5] Department of Gastroenterology, Dietetics and Internal Diseases, H. Święcicki University Hospital, Poznan University of Medical Sciences, Poland
[6] Department of Digestive Tract Diseases, Medical University of Lodz, Poland
[7] Department of Gastroenterology with Inflammatory Bowel Disease Unit, Clinical Hospital No. 2, Rzeszów, Poland
[8] Department of Gastroenterology and Hepatology, Medical University of Gdańsk, Poland
[9] Department of Gastroenterology and Nutritional Disorders, Collegium Medicum in Bydgoszcz, Nicolaus Copernicus University in Toruń, Poland
[10] Department of Gastroenterology, Military Medical Academy Memorial Teaching Hospital – Central Veterans' Hospital, Łódź, Poland
[11] Medical Affairs, Takeda Pharma sp. z o.o., Warsaw, Poland

A – research concept and design; B – collection and/or assembly of data; C – data analysis and interpretation;
D – writing the article; E – critical revision of the article; F – final approval of the article

Advances in Clinical and Experimental Medicine, ISSN 1899–5276 (print), ISSN 2451–2680 (online) *Adv Clin Exp Med*. 2024;33(1):69–77

Address for correspondence
Szymon Drygała
E-mail: szymon.drygala@takeda.com

Funding sources
The study was funded by Takeda Pharma sp. z o.o. (Warsaw, Poland).

Received on April 22, 2022
Reviewed on July 17, 2022
Accepted on April 3, 2023

Published online on May 11, 2023

Cite as
Zagórowicz E, Cichoż-Lach H, Kopertowska-Majchrzak M, et al. Real-world effectiveness and safety of vedolizumab induction therapy for ulcerative colitis: A prospective nationwide Polish observational study. *Adv Clin Exp Med*. 2024;33(1):69–77. doi:10.17219/acem/162969

DOI
10.17219/acem/162969

Abstract

Background. Vedolizumab is recommended as a first-line biological treatment, along with other biological drugs, in ulcerative colitis (UC) patients in whom conventional therapy failed and as a second-line biological treatment following a failure of a tumor necrosis factor alpha (TNF-α) antagonist.

Objectives. We aimed to assess the real-world effectiveness and safety of vedolizumab induction therapy in UC patients treated in the scope of the National Drug Program (NDP) in Poland.

Materials and methods. The endpoints were the proportions of patients who reached clinical response, clinical remission and mucosal healing at week 14. Partial Mayo scores, Mayo subscores and C-reactive protein (CRP) levels were also evaluated.

Results. Our study population consisted of 100 patients (55 biologic-naïve and 45 biologic-exposed). The median total Mayo score at baseline was 10 (interquartile range (IQR): 9–11), and 52 patients (52%) had extensive colitis. The clinical response at week 14 was achieved in 83 (83%) and clinical remission in 24 (24%) cases. Mucosal healing was observed in 56 (62%) patients at week 14. In patients with prior failure of biologic treatment (n = 25), 17 (68%) responded to vedolizumab treatment. A decrease in the median CRP level (from 3.7 mg/L to 2.6 mg/L) and the median total Mayo score (from 10 to 4) was observed. No new safety concerns were recorded and no patients discontinued the treatment due to adverse events (AEs).

Conclusions. Vedolizumab was effective and safe as induction therapy for UC in a Polish real-world population including patients with severely active UC and a low number of patients with prior biological treatment failures.

Key words: vedolizumab, ulcerative colitis, induction therapy, real-world evidence, National Drug Program

Conflict of interest

Edyta Zagórowicz received lecture fees from Janssen, Sandoz, Ferring, and Pfizer; consultancy fees from Pfizer, Janssen and Takeda; and other compensations from Takeda and Janssen. Piotr Eder received lecture fees and/or travel grants from Takeda, Ferring, Astellas, Pfizer, and Janssen. Kamila Stawczyk-Eder received travel grants and lecture fees from Janssen, Pfizer and Takeda. Aleksandra Kaczka received lecture fee(s)/travel/accommodation/meeting expenses from Takeda, Janssen-Cilag, Biogen, Astellas, and Alfa-Sigma. Ariel Liebert received payment for lectures from Janssen, Takeda, Egis, Abbvie, and Pharmabest, and travel/accommodation/meeting expenses from Janssen, Takeda, Egis, and Abbvie. Maria Kłopocka has received payment for lectures from Janssen, Takeda, Ferring, Alfa-Sigma, and Pharmabest, and travel/accommodation/meeting expenses from Ferring, Janssen, Takeda, Alfa-Sigma, and Pharmabest. Rafał Filip served as a speaker for Gramineer International AB, Egis, Ferring, Janssen, and Takeda; received investigational grants from Gramineer International AB and Egis; and received support for travelling and congress assistance from MSD, Abbvie, Alfa-Sigma, Egis, Takeda, and Ferring. Hubert Zatorski received lecture fees and travel grants from Takeda. Anna Solarska-Półchłopek received lecture fees and travel grants from Janssen. Renata Talar-Wojnarowska received lecture fees and/or travel grants from Abbvie, Alfasigma, Astellas, Ferring, Janssen, Pfizer, and Takeda. Krzysztof Wojciechowski and Szymon Drygała are permanent employees of Takeda Pharma sp. z o.o. Krzysztof Wojciechowski is now an employee of Independent Public Health Care Center in Tarczyn, Poland. The remaining authors disclose no conflicts of interest.

Acknowledgements

The authors would like to thank the following persons for their contribution to data collection and analysis, assistance with statistical analysis, critical review of the article, and medical writing support: National Cancer Institute: Monika Cichaczewska; Święcicki University Hospital: Agnieszka Dobrowolska, MD, PhD, Anna Królewska; Biostat: Edyta Klemba, Marian Płaszczyca, PhD, Barbara Gorzawska; Proper Medical Writing sp. z o.o.: Maria Kołtowska-Häggström, MD, PhD, Anna Woziwodzka, PhD, Ewa Marczuk.

Background

Ulcerative colitis (UC) is an idiopathic, relapsing disorder of the large bowel, usually characterized by abdominal pain, bloody diarrhea and fatigue.[1] Ulcerative colitis, if uncontrolled, leads to functional deterioration and impaired quality of life of affected individuals.[2] Hospitalization and surgical intervention may be required in patients with severe UC; moreover, chronic inflammation of the bowel increases colorectal cancer risk.[3]

Patients with UC usually need lifelong medical therapy, which typically includes aminosalicylates, corticosteroids, thiopurines, and biologics such as tumor necrosis factor alpha (TNF-α) antagonists.[4] Corticosteroids, thiopurines and TNF-α antagonists act as systemic immunosuppressants and are associated with an increased risk of serious infections. Disease management with agents representing a more selective mechanism of action is therefore highly preferable.

The pathogenesis of UC involves the disruption of the cytokine signaling network responsible for the maintenance of homeostasis between epithelial cells of the intestines and immune cells, which leads to the infiltration of lymphocytes from the systemic circulation to the colon.[5] This process is mediated by interactions between α4β7 integrins located on the lymphocyte cell surface and the mucosal addressin cell adhesion molecule-1 (MAdCAM-1) present on intestinal endothelial cells.[6,7] Vedolizumab, a gut-selective, humanized IgG1 monoclonal antibody directed against the human lymphocyte integrin α4β7, has a well-established efficacy and safety profile in adult patients with inflammatory bowel disease based on extensive clinical trials and real-world data.[8] Due to its gut-selective manner, it does not induce systemic immunosuppression.[9]

In 2014, based on the results of the GEMINI-1 phase III study which confirmed the efficacy and safety of vedolizumab in patients with moderate-to-severe active UC,[10] vedolizumab was approved by the U.S. Food and Drug Administration (FDA) and the European Medicines Agency (EMA) for the treatment of moderate-to-severe UC in adults. Vedolizumab is recommended as a first-line biological treatment, along with other biological drugs, in ulcerative colitis (UC) patients in whom conventional therapy failed and as a second-line biological treatment following a failure of a TNF-α antagonist.[11] The effectiveness and safety of vedolizumab for the treatment of UC patients have been confirmed in real-world studies.[12]

In Poland, vedolizumab and infliximab are the only reimbursed biologic treatments for UC within the scope of the National Drug Program (NDP).[13] Thus, the baseline characteristics of patients treated with vedolizumab in Poland depend on the criteria of the NDP. In the population enrolled in this study, 55% of patients treated with vedolizumab were biological-naïve (bio-naïve), and only 25% had previously failed anti-TNF-α therapy.[14] These characteristics are in contrast to cohorts from other real-world studies investigating the effectiveness and safety of vedolizumab for UC, where most patients failed 1 or 2 anti-TNF-α therapies and bio-naïve patients constituted less than 25% of the studied populations.[12] Failure of previous anti-TNF-α therapy possibly impacts the achieved treatment results.

Objectives

This study aimed to evaluate the real-world effectiveness and safety of vedolizumab induction therapy for UC patients treated within the scope of the NDP in Poland.

Materials and methods

Study design, setting and participants

The POLONEZ study is a multicenter, non-interventional, prospective study to evaluate the effectiveness and safety of vedolizumab for the treatment

of moderate-to-severe active UC in Poland. Consecutive patients who qualified for reimbursed treatment with vedolizumab within the scope of the NDP were recruited between February and November 2019 from 12 centers in Poland. The inclusion criteria, defined by the NDP, were: moderate-to-severe active UC (total Mayo score >6),[15] contraindications to treatment with ciclosporin, and inadequate response, intolerance or other contraindication to conventional therapy (including both corticosteroids and immunosuppressive drugs).[13]

The study protocol was approved by the Bioethics Committee of the Maria Sklodowska-Curie National Research Institute of Oncology (approval No. 79/2018). All patients gave written informed consent to participate in the study. The study was registered in the European Network of Centres for Pharmacoepidemiology and Pharmacovigilance (ENCePP) clinical trial database.

Variables

The data regarding patient sex, age, body mass index (BMI), disease duration, smoking status, type of extraintestinal disease manifestations if present, previous and current concomitant medications (including the status of previous biologic treatment), and disease phenotype (according to the Montreal classification)[16] were collected. The total Mayo score[14] (range: 0–12, with higher scores indicating a more active disease) was used to assess disease activity at week 0 and to assess induction effectiveness at week 14. The partial Mayo score (total Mayo score without the endoscopic component, range: 0–9)[17] was used in subsequent follow-up visits. Clinical response was defined as a total Mayo score reduction by ≥3 points. Clinical remission was established as a Mayo score ≤2 and no subscore higher than 1. Mucosal healing was defined as an endoscopic Mayo score ≤1.

Vedolizumab was administered as induction therapy according to its label (300 mg intravenous (i.v.) at weeks 0, 2 and 6). Concomitant medications such as 5-aminosalicylic acid (5-ASA) derivatives (mesalazine or sulfasalazine), steroids (prednisone, methylprednisolone or budesonide) and immunomodulators (azathioprine or mercaptopurine) were recorded.

Patients were evaluated during their visits at baseline and week 14. The primary endpoint of this study was clinical response and clinical remission, as defined above. The secondary endpoint was the drug's safety. There were also the following exploratory endpoints: mucosal healing, changes in the total and partial Mayo scores, Mayo subscale scores, C-reactive protein (CRP) concentrations, corticosteroid usage, and occurrence of extraintestinal symptoms.

Subgroup analyses included bio-naïve, biologic-exposed (bio-exposed) and biologic-failure (bio-failure) patients. Additionally, clinical response was evaluated separately in the following subgroups: I. patients who had mucosal appearance upon endoscopy indicative of severe disease (Mayo score on an endoscopic subscale = 3) at baseline; II. patients who had a high total Mayo score (>9) at baseline; III. patients who were hospitalized up to 12 months before the enrollment into the study.

Safety

The safety population consisted of all patients who received at least 1 dose of vedolizumab. All adverse events (AEs) which occurred between the visit at week 0 and the visit at week 14 were recorded. The results were expressed according to the Medical Dictionary of Regulatory Activities (MedDRA) 23.0 terminology.[18]

Statistical analyses

Continuous variables are shown as median and interquartile ranges (IQRs; 1st quartile–3rd quartile (Q1–Q3)). Boxplots represent median values and IQRs (boxes) while error bars represent the minimum and maximum values. Categorical variables are shown as the number of observations and percentages. To compare groups, the Mann–Whitney U test or paired Wilcoxon test was used for quantitative variables and the χ^2 test (or Fisher's test) for qualitative variables. All statistical analyses were done using R v. 3.5 software (R Foundation for Statistical Computing, Vienna, Austria).

Results

Patient flow and baseline characteristics

A total of 100 patients were recruited for the study and 91 completed the visit at week 14. Patient dispositions are shown in Fig. 1. A median of 3 vedolizumab doses were administered to each patient.

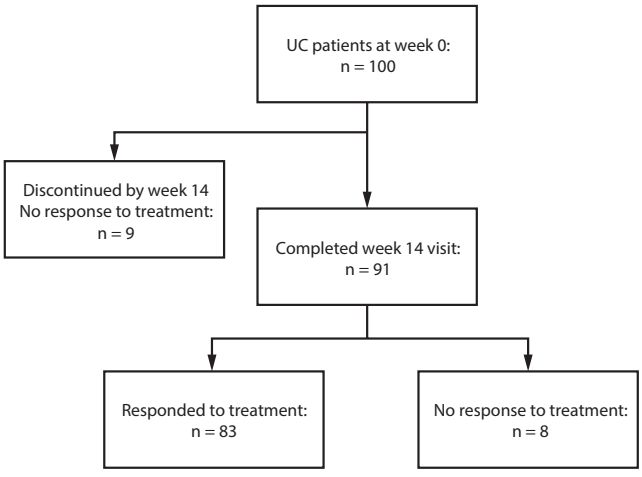

Fig. 1. Patient disposition

UC – ulcerative colitis.

Table 1. Baseline characteristics of the patients (baseline demographic and clinical characteristics of the study population were published elsewhere[14])

Characteristic		Value (n = 100)
Age [years]		35.0 (26.0–43.0)
Male sex, n (%)		51 (51)
BMI [kg/m^2]		23.4 (19.7–26.8)
Smoking status, n (%)	smoker	4 (4)
	ex-smoker	26 (26)
	nonsmoker	70 (70)
Time from diagnosis [years]		6 (3–11)
Total Mayo score		10.0 (9.0–11.0)
Partial Mayo score		7.0 (6.0–8.0)
Disease extent, n (%)	proctitis	6 (6)
	left-sided colitis	42 (42)
	pancolitis	52 (52)
Extraintestinal manifestations at enrollment, n (%)	arthralgia	12 (12)
	primary sclerosing cholangitis	1 (1)
Previous biologic treatment, n (%)	biologic-naïve	55 (55)
	biologic-exposed	45 (45)
	infliximab only	40 (40)
	adalimumab only	2 (2)
	infliximab and adalimumab	2 (2)
	golimumab and vedolizumab within clinical trials	1 (1)
Concomitant immunomodulator, n (%)		45 (45)
Concomitant systemic corticosteroids, n (%)		68 (68)

BMI – body mass index. Values are shown as medians (interquartile range (IQR)) unless stated otherwise.

The baseline characteristics of the patients are given in Table 1. Approximately half of the patients had extensive mucosal involvement (pancolitis). More than half of the patients had not been previously exposed to biological drugs (i.e., they were bio-naïve). Among bio-exposed patients, 44 (98%) received anti-TNF-α treatment (infliximab and/or adalimumab). Failure of anti-TNF-α treatment was reported in 25 individuals (57% of patients treated with anti-TNF-α). At baseline, almost half of the patients received concomitant immunosuppressants, and 2 in 3 received corticosteroids. Detailed baseline demographics and the clinical profile of the study group were described previously.[14]

Effectiveness outcomes

Overall, 83 (83%) patients responded to vedolizumab at week 14. The percentage of responding patients was slightly higher in bio-naïve patients and lower in bio-exposed patients. In patients who had previously failed to respond to anti-TNF-α treatment, approx. 2/3 responded to induction treatment with vedolizumab (Fig. 2A). Twenty-four percent of all patients (27% of bio-naïve patients and 20% of bio-exposed patients) were in clinical remission at week 14 (Fig. 2B). Mucosal healing was achieved in 56 patients (62% of patients reaching week 14, 68% of responders; Fig. 2C, Fig. 3A).

The median total Mayo score decreased from 10 at week 0 to 4 at week 14 (Fig. 2D). The magnitude of change in the total Mayo score was similar across subgroups (Fig. 2D). In the subgroup of responders, the decrease in the median total Mayo score was more pronounced, from 10 at week 0 to 3 at week 14 (Fig. 3B). In the overall study group, a decrease in the median CRP concentration from 3.7 mg/L at baseline to 2.6 mg/L at week 14 was reported (Fig. 2E). The decrease in CRP from baseline to week 14 reached statistical significance only in the bio-naïve patients. In the bio-exposed and bio-failure subgroups, CRP median values increased throughout the study (Fig. 2E). For the subgroup of responders, CRP levels and partial Mayo score at weeks 0 and 14 as well as clinical remission results are presented in Supplementary Fig. 1.

Improvements were reported in all Mayo subscales from baseline to week 14 in the overall study group ($p < 0.001$ for each subscale, Table 2). A quarter of patients had normal stool frequency (compared to 0% at baseline) and almost half of the patients had 1–2 stools more than normal at week 14 (compared to 3.3% at baseline). At week 14, 2/3 of patients reported no rectal bleeding. Approximately 1 in 5 patients had a mucosal appearance graded as normal or corresponding to inactive disease, and had disease activity rated by the physician as normal at week 14. The results for the bio-naïve, bio-exposed and bio-failure subgroups are shown in Supplementary Table 1.

No major change in extraintestinal symptoms throughout the induction therapy with vedolizumab was observed. At baseline, 11 (12%) patients reported extraintestinal symptoms, mostly arthralgia (n = 10, 11%). At week 14, among the 91 evaluated patients, extraintestinal symptoms were present in 12 (13%) individuals and arthralgia in 11 (12%).

Concomitant treatment with corticosteroids

In the overall study group, the percentage of patients treated with corticosteroids dropped by 45% from week 0 to week 14 (Supplementary Fig. 2A). The decrease was most pronounced in the bio-naïve patients (53.1%). In the bio-exposed and bio-failure groups, the number of individuals on corticosteroids decreased by 35.7% and 21.7%, respectively. At week 14, 1 in 8 patients in the bio-naïve subgroup and more than half of the patients in the bio-failure subgroup were on corticosteroids (Supplementary Fig. 2B).

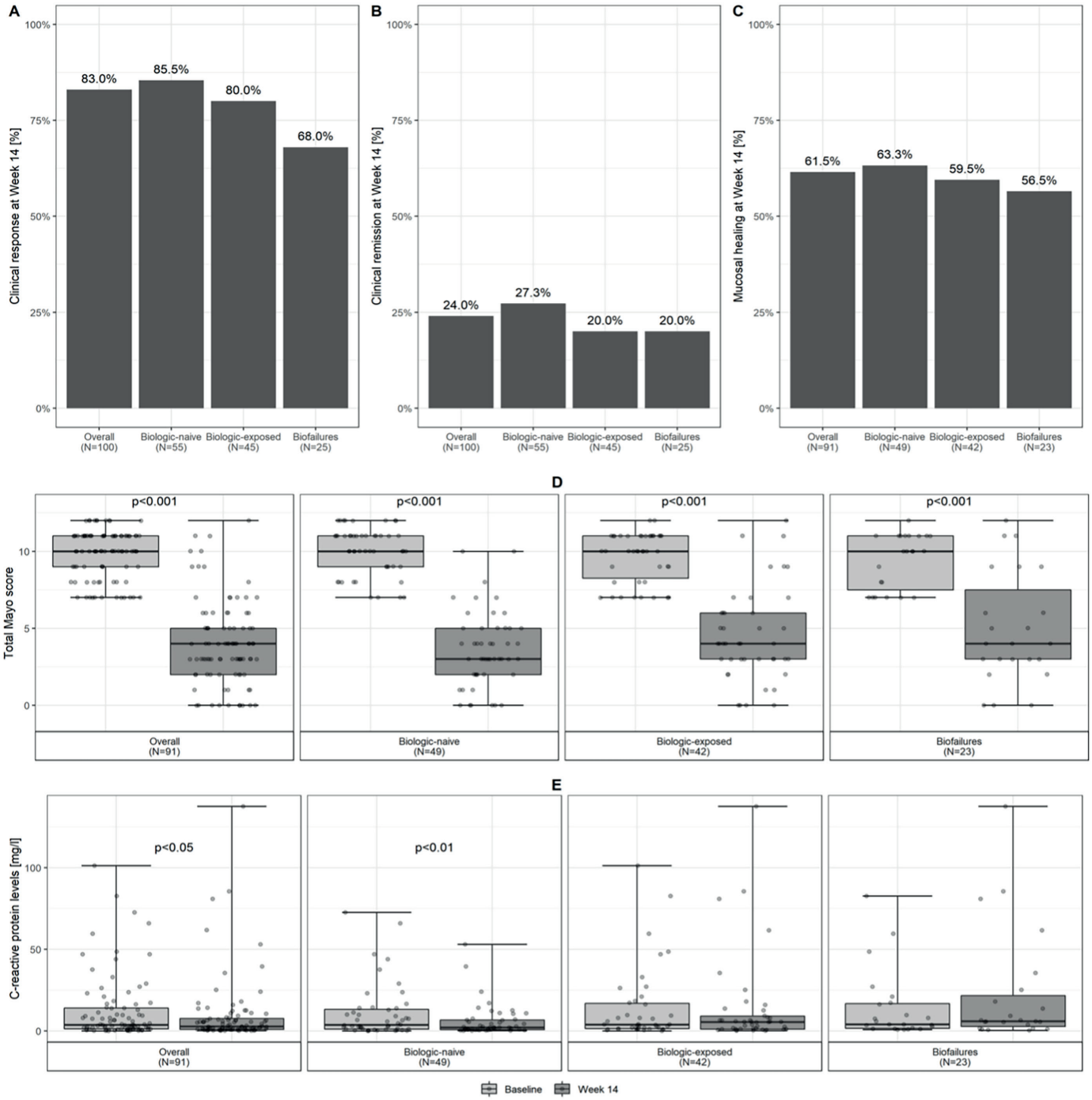

Fig. 2. Clinical effectiveness of vedolizumab in induction therapy for ulcerative colitis in the overall study population. A. Clinical response at week 14; B. Clinical remission at week 14; C. Mucosal healing at week 14; D. Total Mayo score at weeks 0 and 14; E. C-reactive protein (CRP) levels at weeks 0 and 14. Boxes correspond to median values and interquartile ranges (IQRs), and error bars represent minimums and maximums

The median daily dose of prednisolone equivalent decreased in the general study population (from 10 mg at week 0 to 0 mg at week 14) and in each subgroup (Supplementary Fig. 2C), similarly to the subgroup of responders (Supplementary Fig. 2D). Taking into consideration only patients treated with corticosteroids, the median (range) dose of prednisolone equivalent changed from 20 mg (5–60 mg) at week 0 to 15 mg (2.5–40 mg) at week 14 (Supplementary Fig. 2E).

Adverse events

A total of 5 patients experienced AEs during vedolizumab induction therapy (Supplementary Table 3). All recorded AEs were classified as serious AEs (SAEs). In 1 patient, the AE was deemed to be associated with treatment by the treating physician. Two AEs belonged to the MedDRA system organ class (SOC) of infections

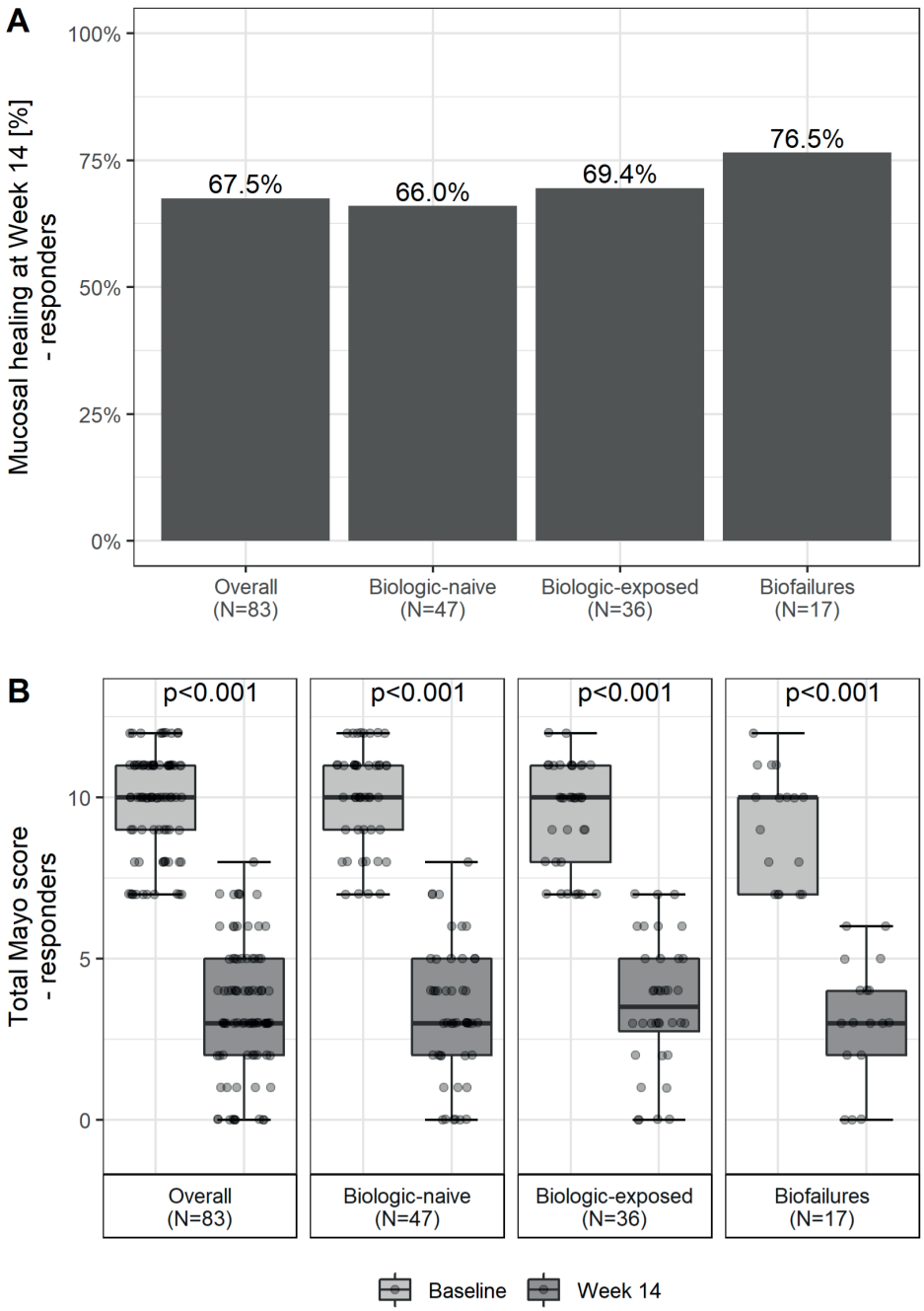

Fig. 3. Clinical effectiveness of vedolizumab in induction therapy for ulcerative colitis in the subgroup of responders. A. Mucosal healing at week 14; B. Total Mayo score at weeks 0 and 14. Boxes correspond to median values and interquartile ranges (IQRs), and error bars represent minimums and maximums

and infestations. None of the patients discontinued vedolizumab treatment due to AEs.

Discussion

In this study, vedolizumab was effective and safe as induction therapy for UC in a Polish real-world study population. Approximately 8 in 10 patients responded to treatment and more than 60% of patients achieved endoscopic remission at week 14. To our knowledge, this is the first report on vedolizumab's real-world effectiveness in UC treatment not only for Poland but also for the Central and Eastern Europe regions.

The clinical response rate observed in our study was higher than in the randomized clinical trials. In a pivotal trial reported by Feagan et al.,[10] 47.1% of patients responded to treatment at week 6, and in a more recent study conducted by Sands et al.,[19] the response rate at week 14 was 67.1%. Across multiple European real-world studies, the clinical response rate at week 14 varied between 43.2% and 67%.[20–24] In our study, a response rate of 68% was reported for patients with a prior failure to biologic treatment. However, our definition of response was generally less stringent than those applied in corresponding studies, as it included only the criterion of a decrease in the Mayo score by at least 3 points. Additionally, our study population included a higher percentage of bio-naïve patients.

Table 2. Changes in Mayo subscales from week 0 to week 14 of induction therapy with vedolizumab (n = 91)

Mayo score on a subscale		Week 0, n (%)	Week 14, n (%)	p-value*
Stool frequency	normal (0)	0 (0.0)	23 (25.3)	<0.001
	1–2 stools/day more than normal (1)	3 (3.3)	43 (47.3)	
	3–4 stools/day more than normal (2)	19 (20.9)	15 (16.5)	
	>4 stools/day more than normal (3)	69 (75.8)	10 (11.0)	
Rectal bleeding	none (0)	3 (3.3)	60 (65.9)	<0.001
	visible blood with stool less than half of the time (1)	19 (20.9)	23 (25.3)	
	visible blood with stool half of the time or more (2)	56 (61.5)	7 (7.7)	
	passing blood alone (3)	13 (14.3)	1 (1.1)	
Mucosal appearance at endoscopy	normal or inactive disease (0)	0 (0.0)	17 (18.7)	<0.001
	mild disease (1)	3 (3.3)	39 (42.9)	
	moderate disease (2)	25 (27.5)	22 (24.2)	
	severe disease (3)	63 (69.2)	13 (14.3)	
Physician rating of disease activity	normal (0)	0 (0.0)	15 (16.5)	<0.001
	mild (1)	0 (0.0)	55 (60.4)	
	moderate (2)	36 (39.6)	17 (18.7)	
	severe (3)	55 (60.4)	4 (4.4)	

* paired Wilcoxon test.

In a study reported by Kopylov et al. on a cohort of bio-naïve patients, the response rate of 79.1% at week 14 was more similar to our findings.[25] Furthermore, a reported mucosal healing rate of 58.5% at week 14 was also similar to the rate reported in our study (61.5%). However, in the aforementioned study, clinical remission was found in almost 40% of patients at week 14, which was a higher percentage than in our patient population (overall: 24%, bio-naïve: 27.3%). Similarly, in a recent observational study including only bio-naïve patients with UC and Crohn's disease, a clinical response after 14 weeks of vedolizumab treatment was reported in 67.9% of UC patients and steroid-free remission – in almost half of them (46.4%).[26]

In line with the observed reduced effectiveness of 2nd and 3rd anti-TNF-α treatments in patients with UC in whom anti-TNF-α therapy failed before,[27,28] vedolizumab was shown to be less effective in anti-TNF-α-experienced individuals. A recent randomized trial by Sands et al. reported that 34.2% of bio-naïve patients achieved clinical remission at week 52, compared with 20.3% of those who were previously treated with anti-TNF-α drugs.[19] These findings were confirmed in real-world populations. In studies reported by Narula et al. and Plevris et al., patients treated with vedolizumab with prior exposure to anti-TNF-α therapy had a reduced probability of achieving clinical remission and mucosal healing than those with no history of anti-TNF-α treatment.[29,30] The greater effectiveness of vedolizumab in bio-naïve patients was also highlighted in a meta-analysis of real-world studies by Schreiber et al.[31] Our study is consistent with these reports – both clinical response and endoscopic remission rates were observed more frequently in bio-naïve compared to bio-failure patients.

Several predictors of response to vedolizumab in UC were described in previous real-world studies. Prior anti-TNF-α exposure is the most recognized negative predictive factor for vedolizumab treatment response and our report seems to confirm those results.[32–35] Also, elevated CRP levels at baseline were associated with a lower chance of achieving response[34,36] or steroid-free remission,[21] which is in line with our findings. Recently, colonic eosinophilia was described as a promising biomarker for response to vedolizumab.[36] Our study, in contrast to other reports,[22,23,32,37] showed no relationship between clinical activity at baseline and treatment outcome.

The number of AEs reported in our study was generally lower than in other real-world studies. In France, SAEs were detected in 8.2% of patients in a 14-week induction trial in inflammatory bowel disease, and in 5.1% of individuals, vedolizumab was discontinued due to the SAEs.[22] Kopylov et al. reported AEs in 14.2% of patients receiving vedolizumab as induction therapy for inflammatory bowel disease in Israel.[23] In a multinational cohort of bio-naïve patients, AEs occurred in 11% of patients during induction therapy with vedolizumab, leading to treatment discontinuation in 3.3% of individuals.[25] However, in a 2018 meta-analysis by Schreiber et al. summarizing safety data from 46 real-world studies on vedolizumab for inflammatory bowel disease, the overall AE rates were reported to range between 0% and 67% (for SAEs, 0–13%).[31] In our study, infections and infestations were the most frequent category of AEs. *Clostridioides difficile* and cytomegalovirus infections were reported in 2.5% of patients from the Israeli cohort,[23] which is in line with our findings. No new safety concerns were identified in our study. Importantly, no patient discontinued the treatment due to AEs.

Limitations

Although the group of 100 consecutive patients with UC represents one of the largest real-world cohorts studied prospectively for vedolizumab,[12,32] the study limitations include a relatively small sample size. For this reason, we could not analyze treatment response in the subgroups of patients co-treated with corticosteroids and/or immunosuppressants. The low number of non-responders to vedolizumab induction therapy impacted the approach to perform statistical analysis for predictors of treatment response and could have also affected the results. Additionally, as this was a multicenter real-world study, certain differences in clinical practice patterns and medical procedures cannot be excluded. Nevertheless, all patients included in our study were treated with vedolizumab in the scope of the NDP, and its requirements allowed for the clinical data to be fully and systematically collected. Furthermore, data for an important therapeutic monitoring biomarker, fecal calprotectin, were not assessed in our study.

Conclusions

In summary, our study showed that vedolizumab is effective as induction therapy for UC, with 8 in 10 patients responding to treatment in a Polish real-world study population characterized by a high severity of UC and a low number of patients with prior anti-TNF-α therapy failure. The observed favorable safety profile of vedolizumab was consistent with the results of randomized clinical trials and other real-world studies.

Supplementary data

The supplementary materials are available at https://doi.org/10.5281/zenodo.7773901. The package contains the following files:

Supplementary Table 1. Changes in Mayo subscales from week 0 to week 14 of induction therapy with vedolizumab in bio-naïve, bio-exposed and bio-failure patients with UC.

Supplementary Table 2. Adverse events in patients with UC treated with vedolizumab using MedDRA 23.0 terminology.

Supplementary Fig. 1. Clinical effectiveness of vedolizumab in induction therapy for UC in the group of responders. A. Clinical remission at week 14; B. Partial Mayo scores at weeks 0 and 14; C. C-reactive protein levels at weeks 0 and 14. Boxes correspond to median values and IQRs, error bars represent minimums and maximums.

Supplementary Fig. 2. Percentage of patients receiving concomitant corticosteroids at weeks 0 and 14 in the overall study population (A) and in the subgroup of responders (B); Doses of prednisolone equivalent (without budesonide) at weeks 0 and 14 in the overall study population (C), in the subgroup of responders (D), and only in patients currently treated with corticosteroids (E). Boxes correspond to median values and IQRs, error bars represent minimums and maximums.

ORCID iDs

Edyta Zagórowicz https://orcid.org/0000-0003-3488-2593
Halina Cichoż-Lach https://orcid.org/0000-0002-7337-835X
Maria Kopertowska-Majchrzak https://orcid.org/0000-0002-7102-2720
Piotr Eder https://orcid.org/0000-0001-9306-5038
Kamila Stawczyk-Eder https://orcid.org/0000-0001-9368-0188
Renata Talar-Wojnarowska https://orcid.org/0000-0003-3887-2712
Hubert Zatorski https://orcid.org/0000-0002-4932-9013
Anna Solarska-Półchłopek https://orcid.org/0000-0003-4245-7984
Rafał Filip https://orcid.org/0000-0002-5954-151X
Maria Janiak https://orcid.org/0000-0003-4949-3128
Krzysztof Skrobot https://orcid.org/0000-0003-2423-1594
Maria Kłopocka https://orcid.org/0000-0003-2149-5826
Ariel Liebert https://orcid.org/0000-0002-1020-4707
Aleksandra Kaczka https://orcid.org/0000-0002-9041-5706
Krzysztof Wojciechowski https://orcid.org/0000-0002-8300-7624
Szymon Drygała https://orcid.org/0000-0002-1355-4737
Agata Michalak https://orcid.org/0000-0003-4426-6321

References

1. Ungaro R, Mehandru S, Allen PB, Peyrin-Biroulet L, Colombel JF. Ulcerative colitis. *Lancet*. 2017;389(10080):1756–1770. doi:10.1016/S0140-6736(16)32126-2
2. Kaplan GG. The global burden of IBD: From 2015 to 2025. *Nat Rev Gastroenterol Hepatol*. 2015;12(12):720–727. doi:10.1038/nrgastro.2015.150
3. Magro F, Gionchetti P, Eliakim R, et al. Third European Evidence-based Consensus on Diagnosis and Management of Ulcerative Colitis. Part 1: Definitions, diagnosis, extra-intestinal manifestations, pregnancy, cancer surveillance, surgery, and ileo-anal pouch disorders. *J Crohn Colitis*. 2017;11(6):649–670. doi:10.1093/ecco-jcc/jjx008
4. Harbord M, Eliakim R, Bettenworth D, et al. Third European Evidence-based Consensus on Diagnosis and Management of Ulcerative Colitis. Part 2: Current management. *J Crohn Colitis*. 2017;11(7):769–784. doi:10.1093/ecco-jcc/jjx009
5. Caviglia GP, Ribaldone DG, Nicolosi A, Pellicano R. Cytokines and biologic therapy in patients with inflammatory bowel diseases. *Gastroenterol Insights*. 2021;12(4):443–445. doi:10.3390/gastroent12040042
6. McLean LP, Shea-Donohue T, Cross RK. Vedolizumab for the treatment of ulcerative colitis and Crohn's disease. *Immunotherapy*. 2012;4(9):883–898. doi:10.2217/imt.12.85
7. Briskin M, Winsor-Hines D, Shyjan A, et al. Human mucosal addressin cell adhesion molecule-1 is preferentially expressed in intestinal tract and associated lymphoid tissue. *Am J Pathol*. 1997;151(1):97–110. PMID:9212736.
8. Battat R, Ma C, Jairath V, Khanna R, Feagan BG. Benefit–risk assessment of vedolizumab in the treatment of Crohn's disease and ulcerative colitis. *Drug Saf*. 2019;42(5):617–632. doi:10.1007/s40264-018-00783-1
9. Rosario M, Dirks NL, Milch C, et al. A review of the clinical pharmacokinetics, pharmacodynamics, and immunogenicity of vedolizumab. *Clin Pharmacokinet*. 2017;56(11):1287–1301. doi:10.1007/s40262-017-0546-0
10. Feagan BG, Rutgeerts P, Sands BE, et al. Vedolizumab as induction and maintenance therapy for ulcerative colitis. *N Engl J Med*. 2013;369(8):699–710. doi:10.1056/NEJMoa1215734
11. Armuzzi A, Gionchetti P, Daperno M, et al. Expert consensus paper on the use of vedolizumab for the management of patients with moderate-to-severe inflammatory bowel disease. *Digest Liver Dis*. 2016;48(4):360–370. doi:10.1016/j.dld.2015.12.016
12. Engel T, Ungar B, Yung DE, Ben-Horin S, Eliakim R, Kopylov U. Vedolizumab in IBD: Lessons from real-world experience. A systematic review and pooled analysis. *J Crohn Colitis*. 2018;12(2):245–257. doi:10.1093/ecco-jcc/jjx143
13. Polish Ministry of Health. Treatment of patients with ulcerative colitis [in Polish]. Warsaw, Poland; 2020. https://www.gov.pl/attachment/93371262-4e40-420d-8e81-9ae3bbf55d9b. Accessed December 21, 2022.

14. Cichoż-Lach H, Michalak A, Kopertowska-Majchrzak M, et al. Characteristics of patients with moderate-to-severe ulcerative colitis treated with vedolizumab: Results from a Polish multicenter, prospective, observational real-life study (the POLONEZ study). *Therap Adv Gastroenterol*. 2021;14:175628482110364. doi:10.1177/17562848211036456
15. D'Haens G, Sandborn WJ, Feagan BG, et al. A review of activity indices and efficacy end points for clinical trials of medical therapy in adults with ulcerative colitis. *Gastroenterology*. 2007;132(2):763–786. doi:10.1053/j.gastro.2006.12.038
16. Silverberg MS, Satsangi J, Ahmad T, et al. Toward an integrated clinical, molecular and serological classification of inflammatory bowel disease: Report of a Working Party of the 2005 Montreal World Congress of Gastroenterology. *Can J Gastroenterol*. 2005;19(Suppl A):5A–36A. doi:10.1155/2005/269076
17. Lewis JD, Chuai S, Nessel L, Lichtenstein GR, Aberra FN, Ellenberg JH. Use of the noninvasive components of the Mayo score to assess clinical response in ulcerative colitis. *Inflamm Bowel Dis*. 2008;14(12):1660–1666. doi:10.1002/ibd.20520
18. MedDRA MSSO. *Introductory Guide MedDRA Version 23.0*. Chantilly, USA: MedDRA Maintenance and Support Services Organization; 2020. https://admin.meddra.org/sites/default/files/guidance/file/intguide_%2023_0_English.pdf.
19. Sands BE, Peyrin-Biroulet L, Loftus EV, et al. Vedolizumab versus adalimumab for moderate-to-severe ulcerative colitis. *N Engl J Med*. 2019;381(13):1215–1226. doi:10.1056/NEJMoa1905725
20. Baumgart DC, Bokemeyer B, Drabik A, Stallmach A, Schreiber S; Vedolizumab Germany Consortium. Vedolizumab induction therapy for inflammatory bowel disease in clinical practice: A nationwide consecutive German cohort study. *Aliment Pharmacol Ther*. 2016;43(10):1090–1102. doi:10.1111/apt.13594
21. Samaan MA, Pavlidis P, Johnston E, et al. Vedolizumab: Early experience and medium-term outcomes from two UK tertiary IBD centres. *Frontline Gastroenterol*. 2017;8(3):196–202. doi:10.1136/flgastro-2016-100720
22. Amiot A, Grimaud JC, Peyrin-Biroulet L, et al. Effectiveness and safety of vedolizumab induction therapy for patients with inflammatory bowel disease. *Clin Gastroenterol Hepatol*. 2016;14(11):1593–1601.e2. doi:10.1016/j.cgh.2016.02.016
23. Kopylov U, Ron Y, Avni-Biron I, et al. Efficacy and safety of vedolizumab for induction of remission in inflammatory bowel disease: The Israeli real-world experience. *Inflamm Bowel Dis*. 2017;23(3):404–408. doi:10.1097/MIB.0000000000001039
24. Chaparro M, Garre A, Ricart E, et al. Short and long-term effectiveness and safety of vedolizumab in inflammatory bowel disease: Results from the ENEIDA registry. *Aliment Pharmacol Ther*. 2018;48(8):839–851. doi:10.1111/apt.14930
25. Kopylov U, Verstockt B, Biedermann L, et al. Effectiveness and safety of vedolizumab in anti-TNF-naïve patients with inflammatory bowel disease: A multicenter retrospective European study. *Inflamm Bowel Dis*. 2018;24(11):2442–2451. doi:10.1093/ibd/izy155
26. Macaluso FS, Fries W, Renna S, et al. Effectiveness and safety of vedolizumab in biologically naïve patients: A real-world multi-centre study. *United European Gastroenterol J*. 2020;8(9):1045–1055. doi:10.1177/2050640620948802
27. Taxonera C, Rodríguez C, Bertoletti F, et al. Clinical outcomes of golimumab as first, second or third anti-TNF agent in patients with moderate-to-severe ulcerative colitis. *Inflamm Bowel Dis*. 2017;23(8):1394–1402. doi:10.1097/MIB.0000000000001144
28. Iborra M, Pérez-Gisbert J, Bosca-Watts MM, et al. Effectiveness of adalimumab for the treatment of ulcerative colitis in clinical practice: Comparison between anti-tumour necrosis factor-naïve and non-naïve patients. *J Gastroenterol*. 2017;52(7):788–799. doi:10.1007/s00535-016-1274-1
29. Narula N, Peerani F, Meserve J, et al. Vedolizumab for ulcerative colitis: Treatment outcomes from the VICTORY Consortium. *Am J Gastroenterol*. 2018;113(9):1345. doi:10.1038/s41395-018-0162-0
30. Plevris N, Chuah CS, Allen RM, et al. Real-world effectiveness and safety of vedolizumab for the treatment of inflammatory bowel disease: The Scottish Vedolizumab Cohort. *J Crohn Colitis*. 2019;13(9):1111–1120. doi:10.1093/ecco-jcc/jjz042
31. Schreiber S, Dignass A, Peyrin-Biroulet L, et al. Systematic review with meta-analysis: Real-world effectiveness and safety of vedolizumab in patients with inflammatory bowel disease. *J Gastroenterol*. 2018;53(9):1048–1064. doi:10.1007/s00535-018-1480-0
32. Barré A, Colombel JF, Ungaro R. Review article: Predictors of response to vedolizumab and ustekinumab in inflammatory bowel disease. *Aliment Pharmacol Ther*. 2018;47(7):896–905. doi:10.1111/apt.14550
33. Stallmach A, Langbein C, Atreya R, et al. Vedolizumab provides clinical benefit over 1 year in patients with active inflammatory bowel disease: A prospective multicenter observational study. *Aliment Pharmacol Ther*. 2016;44(11–12):1199–1212. doi:10.1111/apt.13813
34. Eriksson C, Marsal J, Bergemalm D, et al. Long-term effectiveness of vedolizumab in inflammatory bowel disease: A national study based on the Swedish National Quality Registry for Inflammatory Bowel Disease (SWIBREG). *Scand J Gastroenterol*. 2017;52(6–7):722–729. doi:10.1080/00365521.2017.1304987
35. Kim EM, Randall C, Betancourt R, et al. Mucosal eosinophilia is an independent predictor of vedolizumab efficacy in inflammatory bowel diseases. *Inflamm Bowel Dis*. 2020;26(8):1232–1238. doi:10.1093/ibd/izz251
36. Shelton E, Allegretti JR, Stevens B, et al. Efficacy of vedolizumab as induction therapy in refractory IBD patients: A multicenter cohort. *Inflamm Bowel Dis*. 2015;21(12):2879–2885. doi:10.1097/MIB.0000000000000561
37. Amiot A, Serrero M, Peyrin-Biroulet L, et al. One-year effectiveness and safety of vedolizumab therapy for inflammatory bowel disease: A prospective multicentre cohort study. *Aliment Pharmacol Ther*. 2017;46(3):310–321. doi:10.1111/apt.14167
38. Kurnool S, Nguyen NH, Proudfoot J, et al. High body mass index is associated with increased risk of treatment failure and surgery in biologic-treated patients with ulcerative colitis. *Aliment Pharmacol Ther*. 2018;47(11):1472–1479. doi:10.1111/apt.14665
39. Rosario M, Dirks NL, Gastonguay MR, et al. Population pharmacokinetics-pharmacodynamics of vedolizumab in patients with ulcerative colitis and Crohn's disease. *Aliment Pharmacol Ther*. 2015;42(2):188–202. doi:10.1111/apt.13243

RNA sequencing reveals the transcriptomic landscape and alternative splicing events induced by LGALS1 silencing in non-small cell lung cancer

Hongyang Shi[D], Yonghong Zhang[A], Juan Liu[B], Yu Wang[C], Ping Fang[E,F]

Department of Respiratory and Critical Care Medicine, The Second Affiliated Hospital of Xi'an Jiaotong University, China

A – research concept and design; B – collection and/or assembly of data; C – data analysis and interpretation;
D – writing the article; E – critical revision of the article; F – final approval of the article

Advances in Clinical and Experimental Medicine, ISSN 1899–5276 (print), ISSN 2451–2680 (online) *Adv Clin Exp Med*. 2024;33(1):79–90

Address for correspondence
Hongyang Shi
E-mail: shihy2003@126.com

Funding sources
This research was supported by Natural Science Basic Research Plan of Shanxi Province of China (grant No. 2020JM-410) and hospital fund of the Second Affiliated Hospital of Xi'an Jiaotong University (grant No. RC(GG)201809).

Conflict of interest
None declared

Received on June 17, 2022
Reviewed on February 8, 2023
Accepted on April 21, 2023

Published online on June 21, 2023

Abstract

Background. Non-small cell lung cancer (NSCLC) is a common clinical cancer with high mortality. The lectin galactoside-binding soluble 1 (LGALS1) is an RNA-binding protein (RBP) involved in NSCLC progression. Alternative splicing (AS) is a vital function of RBPs that contributes to tumor progression. It is unknown whether LGALS1 regulates NSCLC progression through AS events.

Objectives. To profile the transcriptomic landscape and LGALS1-regulated AS events in NSCLC.

Materials and methods. The A549 cells either with silenced LGALS1 (siLGALS1 group) or without them (siCtrl group) were subjected to RNA sequencing; differentially expressed genes (DEGs) and AS events were discovered and then the AS ratio was validated using reverse transcription-quantitative polymerase chain reaction (RT-qPCR).

Results. High LGALS1 expression indicates poor overall survival (OS), first progression (FP) and post-progression survival (PPS). A total of 225 DEGs were identified, including 81 downregulated and 144 up-regulated in the siLGALS1 group compared to the siCtrl group. Differentially expressed genes were mainly enriched in interaction-related Gene Ontology (GO) terms and involved in cGMP-protein kinase G (PKG) and calcium signaling pathways. The RT-qPCR validation showed that the expressions of *ELMO1* and *KCNJ2* were upregulated, while *HSPA6* was downregulated after LGALS1 silencing. The expressions of *KCNJ2* and *ELMO1* were upregulated to a peak at 48 h after LGALS1 knockdown, while *HSPA6* expression decreased, after which their expressions returned to baseline. The overexpression of LGALS1 rescued the elevation in *KCNJ2* and *ELMO1* expression, and decrease in *HSPA6* expression induced by siLGALS1. A total of 69,385 LGALS1-related AS events were detected, which produced 433 upregulated and 481 downregulated AS events after LGALS1 silencing. The LGALS1-related AS genes were mainly enriched in the apoptosis and ErbB signaling pathways. The LGALS1 silencing led to a decrease in the AS ratio of BCAP29 and an increase in CSNKIE and MDFIC.

Conclusions. We characterized the transcriptomic landscape and profiled AS events in A549 cells following LGALS1 silencing. Our study provides abundant candidate markers and new insights into NSCLC.

Key words: NSCLC, alternative splicing, RNA binding proteins, LGALS1 silencing, transcriptome landscape

Cite as
Shi H, Zhang Y, Liu J, Wang Y, Fang P. RNA sequencing reveals the transcriptomic landscape and alternative splicing events induced by LGALS1 silencing in non-small cell lung cancer. *Adv Clin Exp Med*. 2024;33(1):79–90. doi:10.17219/acem/163519

DOI
10.17219/acem/163519

Background

Lung cancer is a frequent malignant disease with high mortality,[1] and non-small cell lung cancer (NSCLC) accounts for the majority of lung cancer cases. This disease can be classified as lung adenocarcinoma (LUAD) or lung squamous cell carcinoma (LUSC).[2] Despite considerable progress in early diagnosis, there is still a high recurrence rate after treatment,[3] and the pathogenesis of NSCLC remains largely unknown. Thus, it is urgent to identify new driver genes and elucidate their mechanism to provide clinical advancements.

RNA-binding proteins (RBPs) play an important role in translation and gene regulation,[4,5] driving the development of many diseases and cancers.[6] The RBP lectin galactoside-binding soluble 1 (LGALS1) is a β-galactoside-binding protein that has a carbohydrate recognition domain,[7] and an extensive body of research has revealed that LGALS1 participates in the progression of multiple tumors.[8,9] For example, the upregulated expression of LGALS1 promotes the NSCLC progression by interacting with non-SMC condensin I complex subunit G (NCAPG).[10] Nevertheless, the mechanism and manner by which LGALS1 participates in the NSCLC progression are largely unknown.

Alternative splicing (AS) is a vital function of RBPs. It is reported that more than 90% of genes undergo AS to regulate gene expression, which ultimately results in proteome diversity,[11] but can also increase cancer risk.[12] The LGALS1 participates in pre-mRNA splicing, and it has been reported to regulate gene expression.[13] The LGALS1 was shown to reduce CaV1.2 calcium channel currents resulting in the regulation of vascular constriction via AS.[14] However, whether LGALS1 AS may regulate the NSCLC pathological processes remains unclear.

Objectives

We aimed to evaluate whether LGALS1 exerts its regulatory effects through the regulation of gene expression and AS to discover new prognostic and therapeutic targets for NSCLC. For this purpose, we knocked down LGALS1 in A549 cells and analyzed the differentially expressed genes (DEGs) and LGALS1-regulated AS events associated with NSCLC.

Materials and methods

Public databases

The Kaplan–Meier plotter (http://kmplot.com/analysis/index.php?p=service&cancer=lung) was used to analyze the relationship between LGALS1 expression and survival, including overall survival (OS), first progression (FP) and post-progression survival (PPS), based on the set of NSCLC samples. Data were processed based on the study by Győrffy et al.[15] The Cancer Genome Atlas (TCGA, http://cancergenome.nih.gov) was used to analyze the expression pattern of LGALS1 in NSCLC.

Cell culture and transient transfection

Human A549 (#CL-0016) and H1650 (#CL-0166) cell lines were purchased from China Procell Life Science & Technology (Wuhan, China). Normal human lung epithelial BEAS-2B cells and human H1299 cells were provided by our laboratory. Cells were cultured in a minimum essential medium (OPTI-MEM) supplemented with 10% fetal bovine serum (FBS) and 1% penicillin/streptomycin, and maintained at 37°C with 5% CO_2.

All small interfering RNA (siRNA) duplexes were designed and synthesized in Suzhou Jima Gene Co. Ltd (Suzhou, China). The LGALS1 siRNA sequences (siLGALS1-1) and negative control siRNA sequences (siCtrl) are listed in Supplementary Table 1.

Silencing LGALS1 lentivirus vectors (shLGALS1) were used based on pSLenti-U6-shRNA-CMV-EGFP-2A-Puro, and blank vectors served as the control group (shCtrl).

Transient transfection of siRNA sequences and shRNA vectors was performed using Lipofectamine™ 2000 (Invitrogen, Waltham, USA), according to the manufacturer's instructions. Briefly, 1 day before transfection, A549 cells were seeded in 6-well plates (Corning, Tewksbury, USA) at a density of 5×10^5 cells per well. The siRNA sequences were mixed with OPTI-MEM at a ratio of 5 µL:45 µL. The transfection reagent Lipofectamine™ 2000 (5 µL) was also diluted with 45 µL of OPTI-MEM. Next, 50 µL of diluted siRNA and 50 µL of diluted transfection reagent were mixed and incubated for 15 min at room temperature. After that, the entire mixture was added into the A549 cell sample to incubate for another 24 h until subsequent assays were performed.

Western blot

Radioimmunoprecipitation assay (RIPA) Lysis and Extraction Buffer (#89900; Thermo Fisher Scientific, Waltham, USA) were used to lyse the A549 cells on ice for 15 min; then the product was centrifuged at 12,000 rpm for 10 min at 4°C, and the supernatant was discarded. The concentration of protein precipitate was measured with the bicinchoninic acid (BCA) method and repeated 3 times on each protein extraction. A total of 20 µg of protein was isolated using sodium dodecyl-sulfate polyacrylamide gel electrophoresis (SDS-PAGE) and transferred onto the polyvinylidene fluoride (PVDF) membrane. The transfer efficiency was checked with Ponceau red. The membrane was blocked at 25°C for 3 h with a Tris-HCl buffered salt solution with Tween-20 (TBST) containing 5%

skimmed milk powder. Next, the membrane was incubated with anti-LGALS1 (ab266850, 1:1000; Abcam, Cambridge, UK) or anti-GAPDH (60004-1-Lg, 1:1000; Proteintech, Rosemont, USA) at 4°C overnight. The next day, Goat Anti-Mouse IgG H&L (HRP) (A0216, 1:1000; Beyotime Biotechnology, Shanghai, China) and Goat Anti-Rabbit IgG H&L (HRP) (A0208, 1:1000; Beyotime Biotechnology) were added and incubated for 2 h, washed with Tris-buffered saline containing 0.1% Triton X-100 (TBST) 3 times, and then imaged using ECL chemiluminescence (Thermo Fisher Scientific, Waltham, USA) on the chemiluminescence instrument (ChemiScope series, model 6000EXP, serial No. 610005-7Q; Qinxiang, Shanghai, China).

After imaging, the expression of LGALS1 relative to GAPDH was calculated using ImageJ software (National Institutes of Health, Bethesda, USA).

RNA sequencing and data quality control

The genomic material was removed from A549 cells, and total RNA was separated using the Trizol reagent (Invitrogen) in both the siLGALS1 group (n = 3) and siCtrl group (n = 3). The RNA was purified using an RNA purification kit (Tiangen, Beijing, China) and the concentration and quality of each RNA sample was determined using SmartSpec Plus (BioRad, Hercules, USA) by calculating the absorbance at 260 nm/280 nm (A260/A280). The RNA sequencing (RNA-seq) libraries were prepared with the KAPA Stranded mRNA-seq Kit for Illumina® Platforms (#KK8401; KAPA Biosystems, Boston, USA) according to the manufacturer's instructions. Briefly, 1 μg of intact total RNA was used for library construction. Poly(A) RNA was captured with magnetic oligo-dT beads, which were then resuspended in 1X Fragment, Prime and Elute Buffer to elute the captured RNA. Next, the RNA was fragmented to the desired size by heating in the presence of Mg^{2+}. Then, first-strand cDNA was synthesized with random oligo-dT primers followed by second-strand cDNA synthesis, and double-stranded cDNA was manufactured with RNA while marking the second-strand with dUTP. Next, dAMP was added to the 3'-end of double-strand cDNA fragments to obtain the 3'-dAMP library fragments, followed by 3'-dTMP adapter ligation, and the adapter-ligated library DNA was amplified using polymerase chain reaction (PCR). Finally, library fragment size distribution was confirmed with electrophoresis, and library concentration was determined with quantitative PCR (qPCR). Then, RNA-Seq libraries were sequenced on the Illumina NovaSeq 6000 platform using paired-end 150 nt reads. Raw reads were filtered using the FASTX-Toolkit (v. 0.0.13) (http://hannonlab.cshl.edu/fastx_toolkit/index.html) to discard low-quality reads. The alignment of clean reads was then performed by tophat2[16] mapped to the GRCh38 human reference genome. Uniquely mapped results were used to obtain the read count of a gene as expression and then normalized using the FPKM algorithm.[17]

DEGs analysis

The edgeR package[18] was used to distinguish DEGs between the siLGALS1 group and the siCtrl group employing criteria of the false discovery rate (FDR) less than 0.05 and fold change ≥2 or ≤0.5. To predict functional categories of siLGALS1-related genes, Gene Ontology (GO) and Kyoto Encyclopedia of Genes and Genomes (KEGG) pathway analysis were performed using the KOBAS 2.0 server.[19]

RBP-related AS analysis

The ABLas pipeline was applied for identifying and quantifying the AS events and regulated AS events (RASEs).[20] In short, 10 types of normative AS events were detected in 2 groups based on the splice junction reads, including cassette exons (CE), exon skipping (ES), mutual exclusive exon skipping (MXE), alternative 3' splice site (A3SS), A3SS and ES (A3SS & ES), MXE combined with an alternative polyadenylation site (3pMXE) or an alternative 5' promoter (5pMXE), alternative 5' splice sites (A5SS), A5SS and ES (A5SS & ES), and intron Retained (introR). Next, to determine RBP-related RASEs, the difference in AS events between the siLGALS1 group and the siCtrl group was evaluated using Student's t-test. The difference in AS events with a p-value cutoff corresponding to an FDR cutoff of 5% was considered RBP-related RASE.

RTqPCR verification of DEGs and AS

Primers of DEGs were designed using Primer Premier v. 6.0 (http://www.premierbiosoft.com/primerdesign/) validated with qPCR. For reverse transcription (RT)-qPCR validation (each gene was repeated 9 times), M-MLV Reverse Transcriptase (Vazyme Biotech, Nanjing, China) was used for RNA reverse transcription into cDNA. The SYBR Green PCR Reagents Kit (Yeasen Biotechnology, Shanghai, China) was used for the PCR reaction with 3 repetitions on the StepOne Realtime PCR System. The gene expression level was normalized to GAPDH using the $2^{-\Delta\Delta CT}$ method.[21]

To verify AS events (each gene was repeated 9 times), a boundary-spanning primer was used to detect alternative isoforms for the sequence containing the junction of the alternative exon (according to "model exon" to detect model splicing or "altered exon" to detect altered splicing) and constitutive exon. The sequence containing the constitutive exon was detected with an opposing primer. The primer sequences are listed in Supplementary Table 1.

Statistical analyses

GraphPad Prism v. 9.0 (GraphPad Software, San Diego, USA) was used for statistical analysis. Data were obtained from at least 3 independent samples and indicated

as means ± standard deviation (M ±SD). Considering that the sample size is less than 10, the data are all analyzed using a nonparametric test. The statistical comparison between the siLGALS1 group and the siCtrl group was performed using Mann–Whitney (M–W) test when the total sample >7; otherwise, the t-test was performed (data conformed to the normal distribution and variance homogeneity). The comparison between 3 or 4 groups was determined with Kruskal–Wallis (K–W) test followed by Dunn's multiple comparison test. A p-value <0.05 was considered statistically significant.

Results

High expression of the *LGALS1* gene corresponds to a poor prognosis of NSCLC

To determine whether *LGALS1* expression was associated with NSCLC progression, the Kaplan–Meier plotter was used for drawing OS, FP and PPS curves based on the *LGALS1* mRNA expression, which was stratified into low- and high-expression groups. The results showed that patients in the *LGALS1* high-expression group exhibited a significant decrease in the OS (log-rank p = 6.6e-13), FP (log-rank p = 0.044) and PPS (log-rank p = 0.00026) compared with the *LGALS1* low-expression group (Fig. 1), suggesting that high expression of the *LGALS1* gene correlated with poor prognosis of NSCLC. However, unexpectedly, according to TCGA, *LGALS1* expression was not statistically different in tumor and control tissues (Supplementary Fig. 1).

LGALS1 silencing alters the transcriptomic landscape of A549 cells

First, we performed RT-qPCR to determine LGALS1 expression in 4 NSCLC cell lines and normal cells. The results showed that compared with the BEAS-2B cell, LGALS1 was significantly overexpressed in 3 NSCLC cell lines, with its highest expression observed in A549 cells (K–W test, H = 9.462, p = 0.0067) (Fig. 2A). Therefore, to assess the molecular mechanisms of LGALS1 in NSCLC, we silenced LGALS1 expression in A549 cells using siRNA. The mRNA (M–W test, U = 0, p < 0.0001) and protein (t-test, t = 4.824, degrees of freedom (df) = 4, p = 0.0485) expression of LGALS1 in the siLGALS1 group were significantly lower than in the siCtrl group, suggesting that the knockdown was successful (Fig. 2B,C). Then, A549 cells containing silenced LGALS1 were subjected to transcriptome sequencing. The LGALS1 expression was also significantly reduced in the RNA-seq analysis, supporting the successful LGALS1 knockdown (t-test, p = 7.52e-14) (Fig. 2D). The Q30 and GC content of all 6 samples were larger than 94.9% and 50%, respectively (Supplementary Table 2), indicating that the quality control of transcriptome sequencing was good. Principal component analysis (PCA) showed that samples from the siLGALS1 group and the siCtrl group could be distinguished from each other (Fig. 2E), suggesting that the interference in LGALS1 expression leads to an alteration in transcriptomic profile in A549 cells.

To further investigate the genes regulated by LGALS1, DEGs (|fold change| >2 and FDR < 0.05) induced by LGALS1 silencing were characterized. A total of 225 DEGs were identified, including 144 upregulated and 81 downregulated DEGs in the siLGALS1 group compared to the siCtrl group

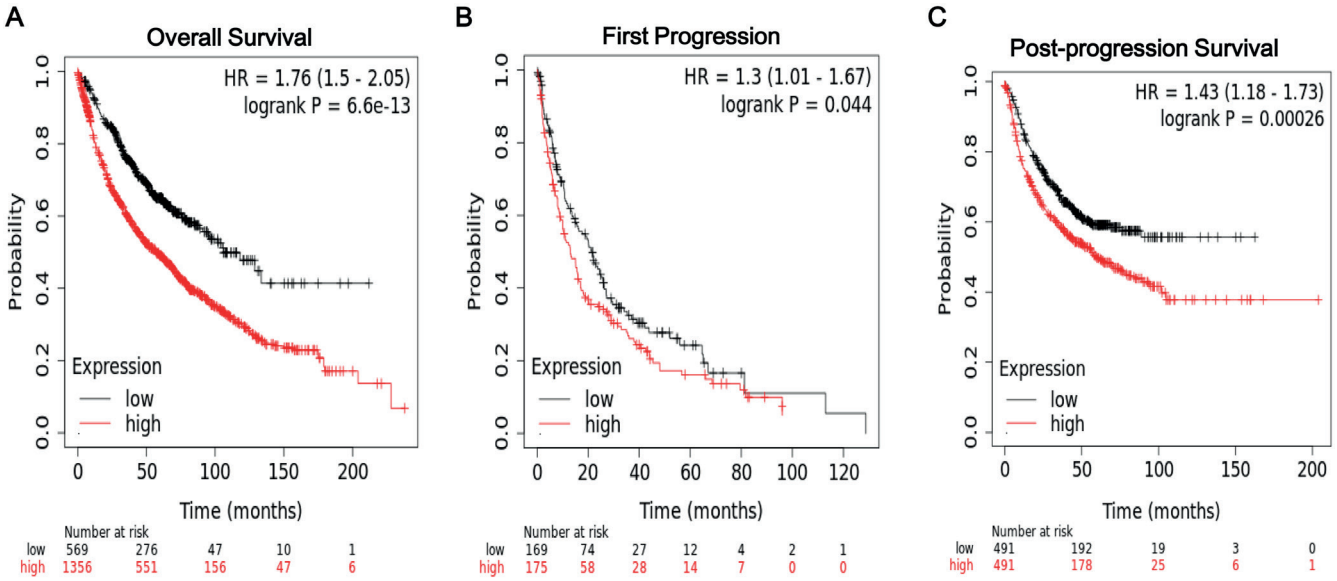

Fig. 1. High expression of lectin galactoside-binding soluble 1 (LGALS1) indicates poor prognosis in non-small cell lung cancer (NSCLC). The pattern of overall survival (OS) (A), first progression (FP) (B) and post-progression survival (PPS) (C) of NSCLC patients with high and low LGALS1 expression levels

HR – hazard ratio.

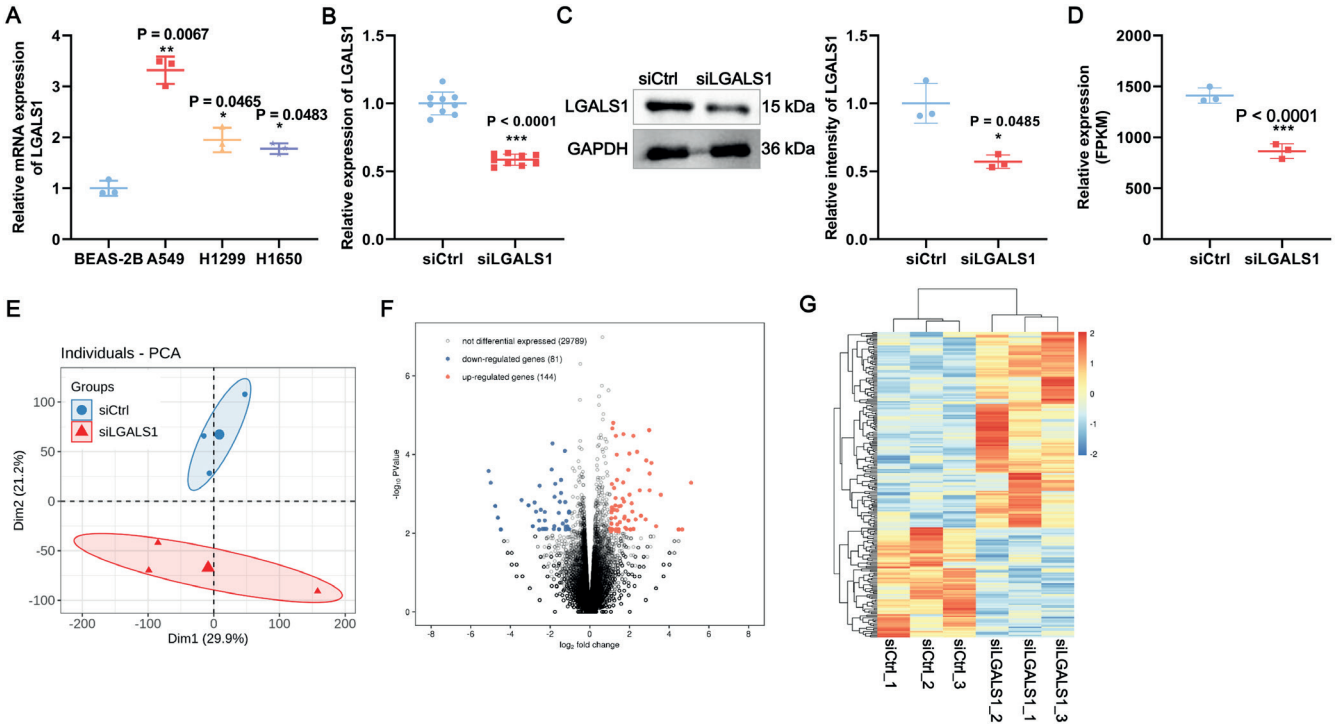

Fig. 2. Lectin galactoside-binding soluble 1 (LGALS1) silencing alters the transcriptomic landscape of A549 cells. A. LGALS1 expression in different cell lines. The silencing efficacy of LGALS1 was quantified using reverse transcription-quantitative polymerase chain reaction (RT-qPCR) (B) and western blot (C) in A549 cells; D. LGALS1 expression in RNA sequencing (RNA-seq) results exhibited by FPKM; E. Principal component analysis (PCA) plot of RNA-seq data for 3 biological replicates in the silenced LGALS1 (siLGALS1) and siCtrl groups; F. Differentially expressed genes (DEGs) when comparing siLGALS1 and siCtrl groups in A549 cells. The upregulated DEGs are marked red, and the downregulated DEGs are marked blue (siLGALS1 compared to siCtrl); G. Heatmap of DEGs

* $p < 0.05$; ** $p < 0.01$; *** $p < 0.001$.

(Fig. 2F). After hierarchical clustering of all the DEGs, a robust distinction was observed between the 2 groups, and a high coincidence among the changes was also observed in the 3 replicates (Fig. 2G). These results suggest that LGALS1 silencing alters the transcriptomic landscape of A549 cells.

Functional clustering analysis of DEGs

Next, we used the KOBAS 2.0 server to predict the molecular functions and metabolic pathways of up- and downregulated DEGs, respectively. The results showed that upregulated DEGs only affected small molecule metabolic processes and DNA transcription, and were mainly involved in cell adhesion molecules and chemical carcinogenesis pathways (Fig. 3A,B). In addition, downregulated DEGs were enriched to interaction-related GO terms such as extracellular matrix, steroid binding, laminin binding, and ankyrin binding (Fig. 3C). The KEGG analysis found that downregulated DEGs were mainly associated with protein digestion and absorption, cGMP-protein kinase G (PKG) signaling pathway, and calcium signaling pathways (Fig. 3D). These results imply that LGALS1 silencing alters numerous physiological processes in A549 cells via DEGs.

RT-qPCR validation of LGALS1-regulated DEGs

To further verify the reliability of RNA-seq results, we selected 5 DEGs which were highly abundant during RT-qPCR validation. Importantly, these 5 genes were reported to be connected to the progression of NSCLC, including *ELMO1*,[22] *KCNJ2*,[23] *IGFBP5*,[24] *HSPA6*,[25] and *TINAGL1*.[26] The RT-qPCR results of 5 DEGs were in concordance with the RNA sequencing results (Fig. 4), with the expression of *KCNJ2* (M–W test, U = 1, p = 0.0002) and *ELMO1* (M–W test, U = 9, p = 0.0289) being upregulated after LGALS1 silencing, whereas *HSPA6* (M–W test, U = 9, p = 0.0465) was downregulated. However, the expression of TINAGL1 (M–W test, U = 33, p = 0.8148) and IGFBP5 (M–W test, U = 8, p = 0.1320) exhibited no significant difference between the siLGALS1 group and siCtrl group with RT-qPCR. These results imply that *KCNJ2*, *HSPA6* and *ELMO1* may be functional genes located downstream from LGALS1 signaling.

Given that gene regulation is time-dependent, we examined the expression of DEGs (*KCNJ2*, *HSPA6* and *ELMO1*) at different timepoints after LGALS1 knockdown to further validate the regulation of DEGs by LGALS1. Gene expression in the shCtrl group did not change with time,

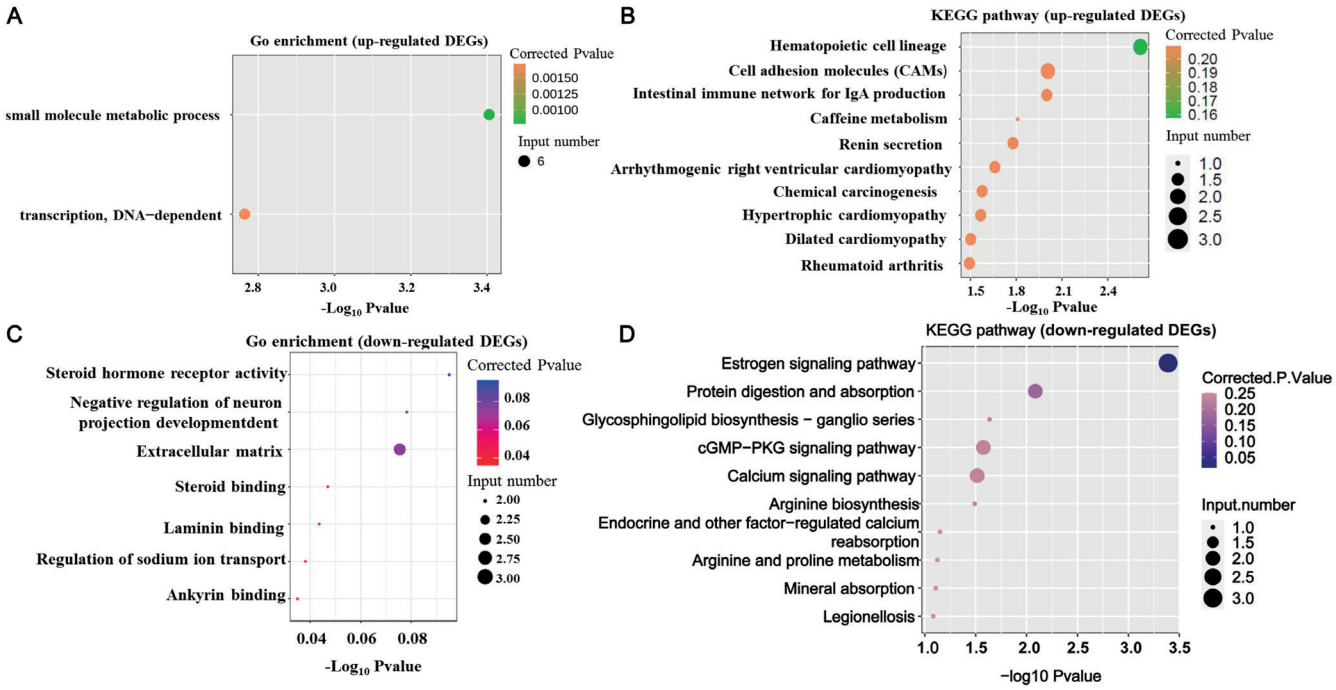

Fig. 3. Functional clustering analysis of differentially expressed genes (DEGs). A. The only 2 Gene Ontology (GO) enrichment terms of upregulated DEGs between silenced lectin galactoside-binding soluble 1 (siLGALS1) and siCtrl group; B. The top 10 enriched Kyoto Encyclopedia of Genes and Genomes (KEGG) pathways for upregulated DEGs between siLGALS1 and siCtrl group. The top 7 GO enrichment terms (C) and top 10 KEGG pathways (D) for downregulated DEGs between siLGALS1 and siCtrl group

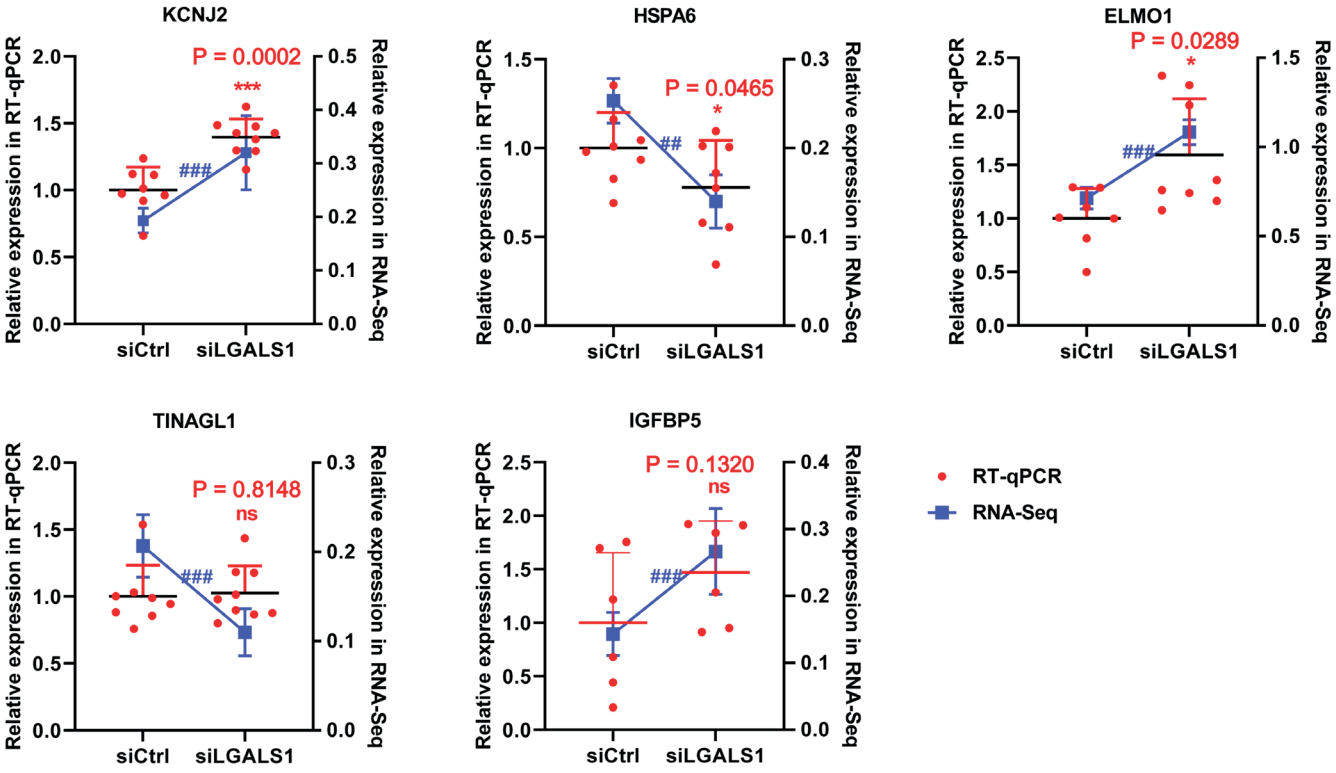

Fig. 4. Reverse transcription-quantitative polymerase chain reaction (RT-qPCR) validation of differentially expressed genes (DEGs). The RNA sequencing (RNA-seq) data are presented as the blue line charts. The RT-qPCR validation results for 5 DEGs are presented in red scatter histogram

$p < 0.001$; ### $p < 0.0001$; ns $p > 0.05$; ** $p < 0.01$; *** $p < 0.001$.

while LGALS1 mRNA expression gradually decreased in the shLGALS1 group compared with the shCtrl group, reaching a minimum at 48 h, after which the transient knockdown effect gradually disappeared (Fig. 5A). As expected, shLGALS1 regulation of DEG expression showed temporal effectiveness for 48 h. The *KCNJ2* and *ELMO1*

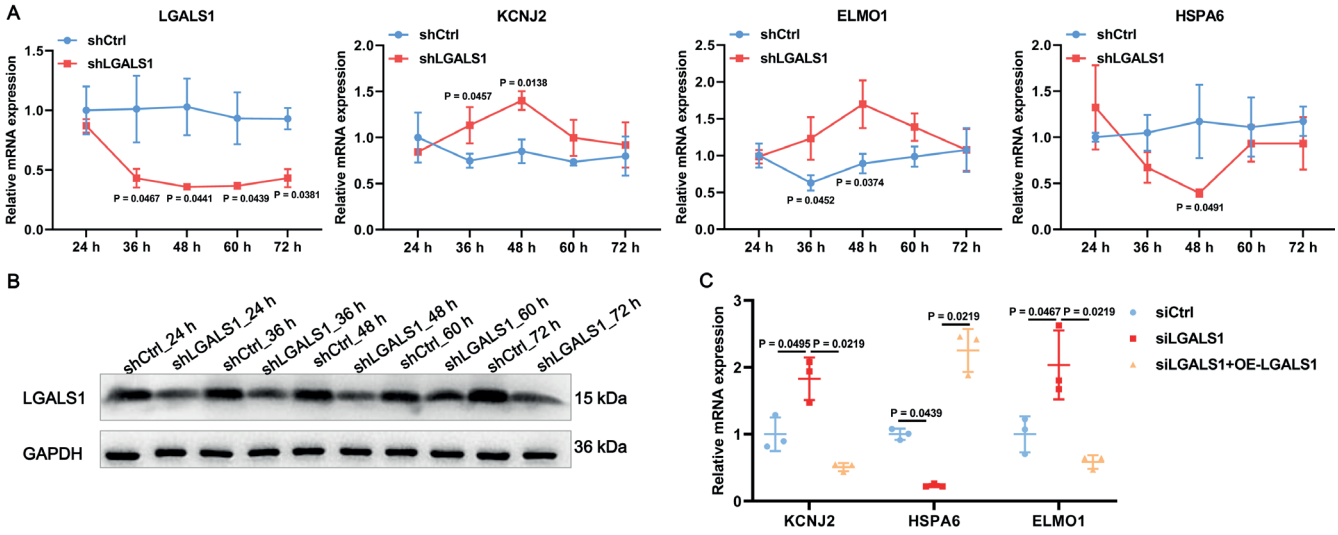

Fig. 5. Differentially expressed genes (DEGs) regulated by lectin galactoside-binding soluble 1 (LGALS1). A. Reverse transcription-quantitative polymerase chain reaction (RT-qPCR) was performed to detect mRNA expression of *LGALS1*, *KCNJ2*, *HSPA6*, and *ELMO1* at different timepoints following LGALS1 knockdown using shRNA; B. Western blot was performed to detect the protein expression of LGALS1 at different timepoints after LGALS1 knockdown using shRNA; C. A rescue experiment was used to verify the regulatory role of LGALS1 on *KCNJ2*, *HSPA6* and *ELMO1* mRNA expression

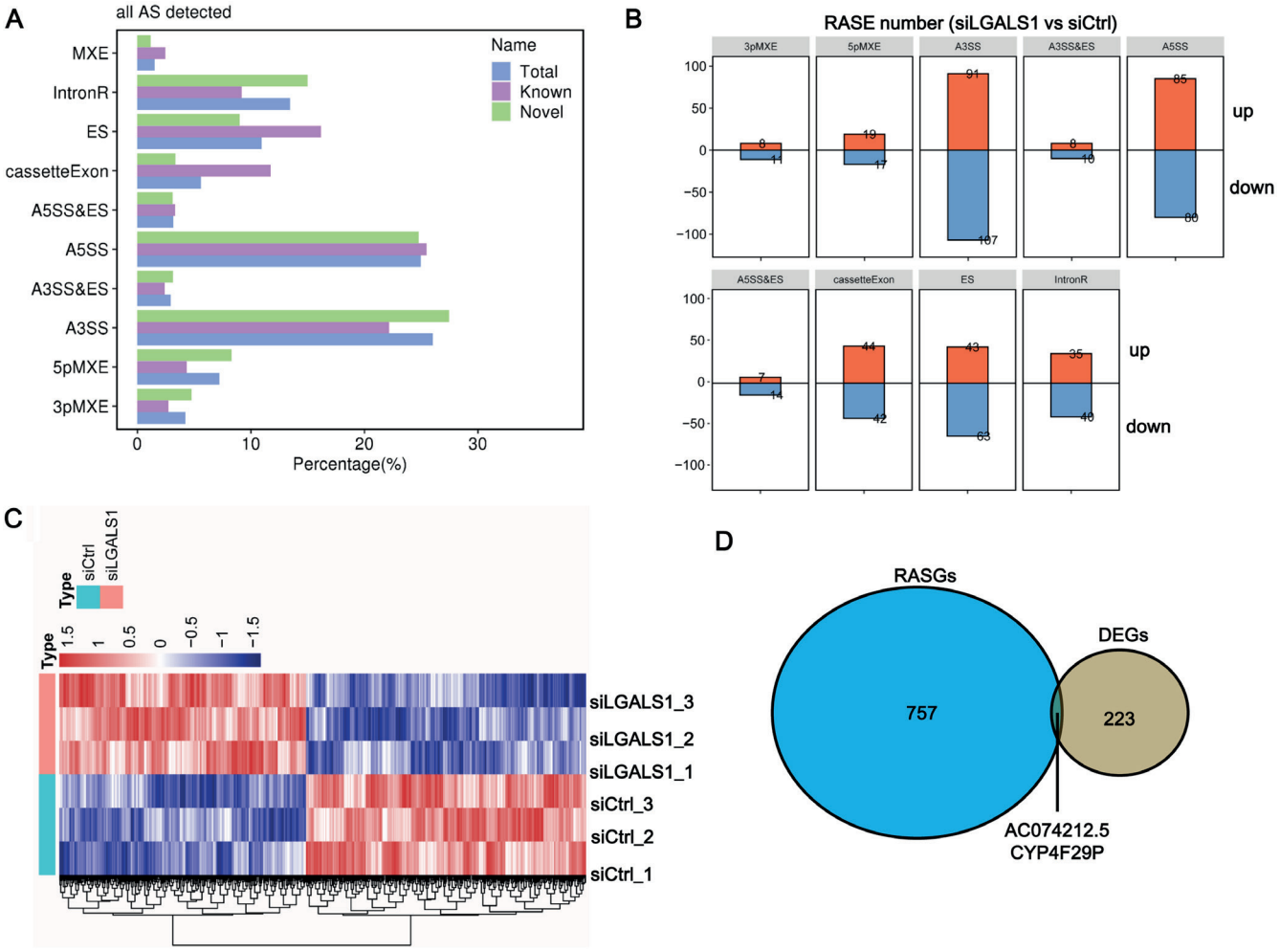

Fig. 6. Identification of lectin galactoside-binding soluble 1 (LGALS1)-mediated alternative splicing (AS) events in A549 cells. A. Classification and proportion of 10 types of AS events detected using RNA sequencing (RNA-seq); B. Classification and numbers of the significant differential regulated AS events (RASEs) between the silenced LGALS1 (siLGALS1) and siCtrl groups; C. Heatmap representation of the pattern of RASEs between the siLGALS1 and siCtrl groups; D. Venn diagram showing the overlap of LGALS1-regulated differentially expressed genes (DEGs) and regulated AS genes (RASGs)

ES – exon skipping; MXE – mutual exclusive exon skipping; A3SS – alternative 3′ splice site; 3pMXE – MXE combined with an alternative polyadenylation site; 5pMXE – alternative 5′ promoter; A5SS – alternative 5′ splice sites; introR – intron Retained.

expressions were upregulated to a peak at 48 h after LGALS1 knockdown, while *HSPA6* expression decreased to a peak, after which their expressions all returned to nondifferential levels from the shCtrl group (Fig. 5A). The shRNA-LGALS1 lentiviral vector also inhibited LGALS1 expression at the protein level (Fig. 5B). In addition, for further validation of the genes regulated by LGALS1, a rescue experiment was conducted. We observed that overexpression of LGALS1 significantly reduced the elevation in *KCNJ2* and *ELMO1* expression and minimized the decrease in *HSPA6* expression induced by siLGALS1 alone (Fig. 5C). Taken together, these results implicate that LGALS1 can regulate the expressions of DEGs, such as *KCNJ2*, *HSPA6* and *ELMO1*.

Identification of LGALS1-mediated AS events in A549 cells

Previous studies have demonstrated that AS is involved in lung cancer development.[27] Thus, we further explored LGALS1-mediated AS events. A total of 69,385 AS events were identified, of which 18,587 were known AS, accounting for 26.79%, and 50,798 were novel AS, accounting for 73.21% (Fig. 6A, Supplementary Table 3). We found that both known and novel AS events contained 10 types (Fig. 6A, Supplementary Tables 4 and 5), of which A3SS and A5SS exhibited the largest share of the total AS events, corresponding to 26.03% and 24.95%, respectively (Fig. 6A, Supplementary Table 6).

Moreover, a total of 914 RASEs mediated by LGALS1 were identified, including 433 upregulated RASEs and 481 downregulated RASEs in the siLGALS1 group compared with the siCtrl group (Fig. 6B). These LGALS1-mediated RASEs were annotated into 9 types of AS events (Fig. 6B). Furthermore, we observed that these RASEs clustered into 2 branches, suggesting that LGALS1 silencing resulted in altered AS in A549 cells (Fig. 6C). Furthermore, LGALS1 silencing led to 914 RASEs residing in 759 genes. We overlapped genes in regulated AS genes (RASGs) and DEGs, finding that only 2 RASGs overlapped with DEG, namely AC074212.5 and CYP4F29P (Fig. 6D).

Functional enrichment analysis of RASGs

To explore the biological function of LGALS1-regulated AS, RASGs were subjected to GO and KEGG enrichment analyses. The GO analysis revealed that RASGs were preferentially enriched in molecular functions related to transcriptional regulation, such as DNA-dependent transcription, regulation of transcription from RNA polymerase, DNA-dependent regulation of transcription, and gene expression (Fig. 7A). In addition, KEGG pathway analysis found that RASGs were mainly enriched in ErbB signaling and apoptosis pathways (Fig. 7B). These results demonstrated that LGALS1 may be involved in the regulation of cell apoptosis through regulating RASGs.

Validation of the LGALS1-mediated RASGs

Given that RASGs may be associated with NSCLC progression, we validated LGALS1-mediated RASGs using qPCR. Out of 9 detected AS events, the results of 3 A3SS AS events validated using RT-qPCR were consistent with the RNA-seq data, namely BCAP29, CSNKIE and MTFP1 (Fig. 8). Among them, the AS ratio of BCAP29 (M–W test, $U = 13$, $p = 0.0142$) and MTFP1 (M–W test, $U = 11$, $p = 0.0078$) were significantly increased in the siLGALS1 group compared to the siCtrl group, whereas CSNKIE (M–W test, $U = 17$, $p = 0.0193$) was found to be opposite. The RT-qPCR validation results of the remaining 6 AS events are shown in Supplementary Fig. 2. These results further confirm the LGALS1-related AS and RASE data.

Discussion

Despite extensive research regarding NSCLC, its mortality rate is still high, and more studies on NSCLC are warranted to understand the mechanism of the disease. In the present study, we have revealed insights into the transcriptomic landscape and AS dataset in NSCLC, driven by LGALS1 through RNA-seq. Many DEGs and RASGs in this study provide new insights and abundant potential candidate markers for NSCLC that could be targeted therapeutically.

As an RBP, LGALS1 is a β-galactoside-binding protein and is alternatively known as galectin-1.[28] Many studies have demonstrated that intervention in the expression of LGALS1 plays a vital role in the progression of numerous human cancers. For instance, a recent study showed that LGALS1 is involved in NSCLC progression by interacting with NCAPG, and the knockdown of LGALS1 significantly suppresses proliferation, migration and invasion of A549 and H1299 cells.[10] In oral cancer, LGALS1 knockdown suppressed cell proliferation by arresting cells at S phase and inhibited wound healing and migration.[29] Furthermore, in certain brain tumors, silencing of LGALS1 downregulated the expression of genes involved in cell cycle progression, resulting in an accumulation of G2/M phase cells and eventually inhibiting tumor progression.[30] There is also an extensive body of literature showing that LGALS1 participates in lung cancer progression. For example, LGALS1 is overexpressed in LUAD cells and induces their growth and invasive ability.[8] The LGALS1 upregulated p38 MAPK, ERK and cyclo-oxygenase-2 expression to promote lung cancer progression.[9] In the current study, we demonstrated that silencing of LGALS1 led to the aberrant expression of 225 genes in A549 cells and involved alterations in transcription and binding-related pathways, suggesting that LGALS1 may function in NSCLC. Therefore, further research is needed on RNA-binding properties and related biological functions of LGALS1.

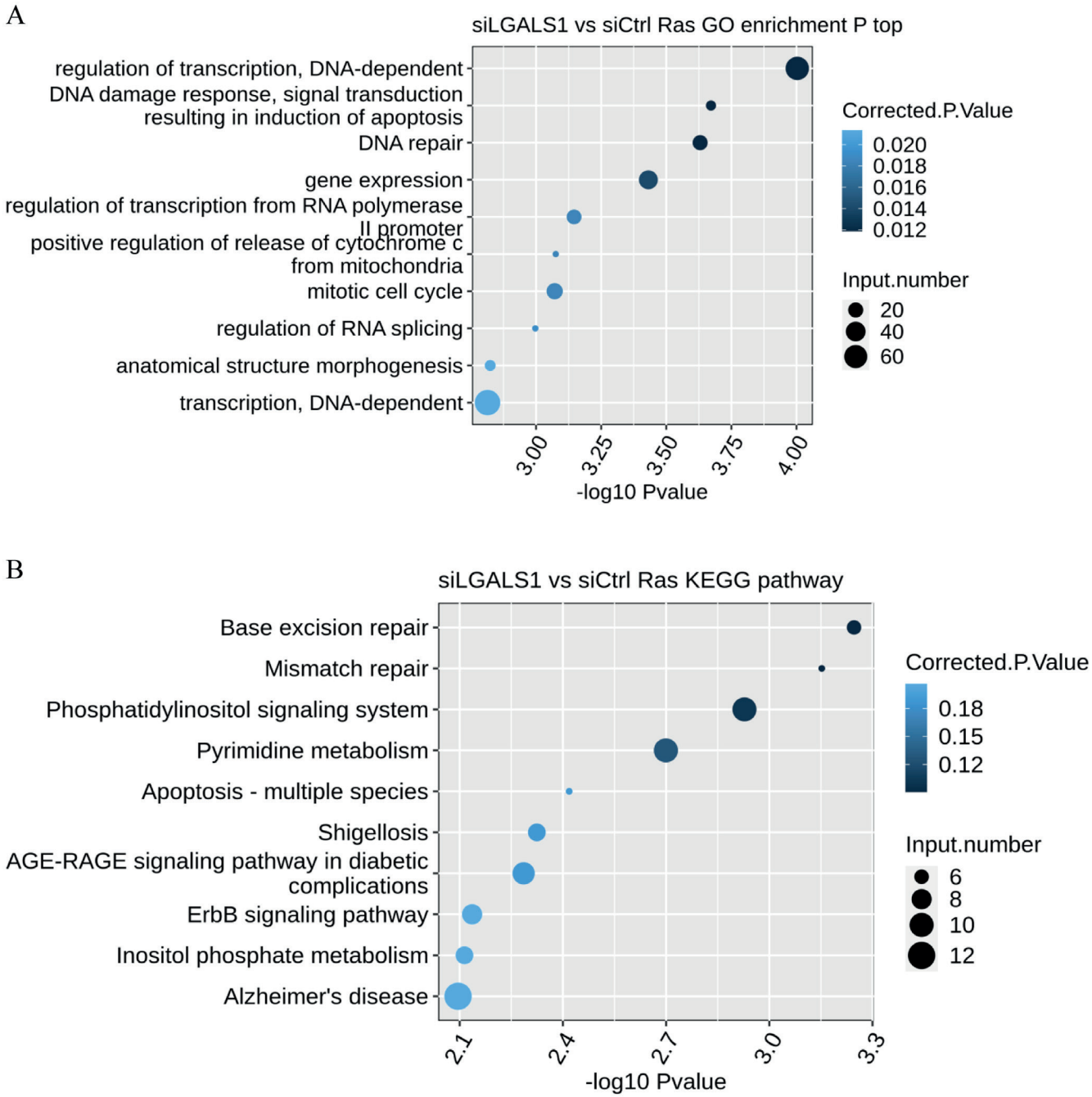

Fig. 7. Functional enrichment analysis of regulated alternative splicing genes (RASGs). A. The top 10 enriched Gene Ontology (GO) terms for RASGs; B. The top 10 enriched Kyoto Encyclopedia of Genes and Genomes (KEGG) pathways for RASGs

Alternative splicing events are closely associated with the function of RBPs and cancer progression,[31] with previous studies showing that AS plays a crucial role in the development of lung cancer. For instance, the AS status of BIN1 with exon 12A inclusion (the BIN1+12A isoform) could recover the activity of tumor cells through the regulation of BIN1 in NSCLC.[32] Furthermore, ESRP1 regulates the chemosensitivity of lung cancer cells through AS by inhibiting TGF-β/Smad signaling in SCLC patients.[33] Moreover, VEGFxxxb family members encoded AS in VEGF-A, and VEGF165b/VEGF165 are positively correlated with lymph node metastasis in NSCLC.[34] The current study showed that a total of 914 AS events were triggered after LGALS1 silencing, and the corresponding RASGs were implicated in ErbB signaling and apoptosis pathways. Encouragingly, some previous results support our observations. Wang et al. demonstrated that LGALS1 modulates vascular constriction by regulating AS of the cav1.2 calcium channel.[14] Therefore, LGALS1-mediated AS events play an important role in NSCLC progression.

In addition, we discovered that LGALS1-related RASGs were significantly enriched in the apoptosis and ErbB signaling pathways. Apoptosis, or programmed cell death,

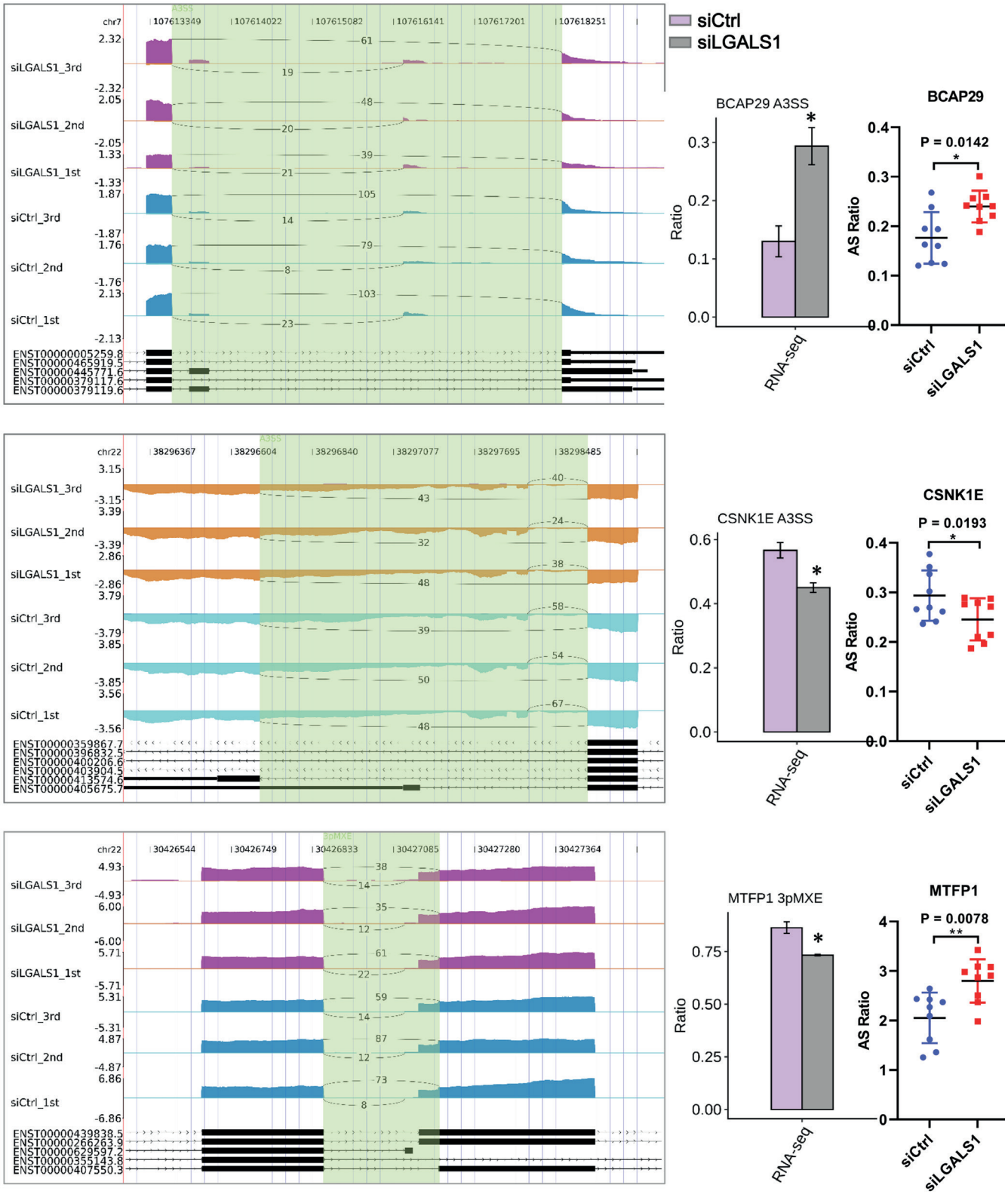

Fig. 8. Validation of the lectin galactoside-binding soluble 1 (LGALS1)-mediated regulated alternative splicing genes (RASGs). RNA-seq results and reverse transcription-quantitative polymerase chain reaction (RT-qPCR) validation results of RASGs are shown in the right panel

* $p < 0.05$; ** $p < 0.01$; *** $p < 0.001$.

plays a critical role in cancer occurrence, progression and drug resistance. Inhibition of LGALS1 in melanoma cells can restore the viability of apoptotic T lymphocytes[35] while targeting LGALS1 by shikonin, and its derivatives were shown to induce apoptosis and autophagy in colorectal carcinoma cells.[36] Moreover, the ErbB signaling pathway is involved in cancer progression, for example, in cervical cancer.[37] Finally, EGFR is a member of the ErbB receptor

family, which regulates epithelial cell growth and survival, and its high expression or abnormal activation is correlated with drug resistance and even tumor progression in multiple cancers, such as breast cancer[38] and NSCLC.[39] Therefore, we suspect that LGALS1 may be involved in the NSCLC progression through the apoptosis and ErbB signaling pathways.

Limitations

There are some limitations of this study, one of which is that our results were not validated in animal models or clinical samples. Second, there are only 3 biological repeats for transcriptomic sequencing. Finally, no molecular experiments were performed to verify the regulatory relationship between LGALS1 on candidate target genes and AS events. Therefore, in the future, we will further explore the mechanism of LGALS1 involvement in NSCLC progression through a series of in vitro and in vivo experiments to address the above limitations.

Conclusions

In the current study, we characterized the transcriptomic landscape of A549 cells following LGALS1 silencing, identifying 225 DEGs that responded significantly to LGALS1 silencing. The expression patterns of *ELMO1*, *KCNJ2* and *HSPA6* were consistent between both RNA-seq and RT-qPCR experiments, and the expression of *ELMO1* and *KCNJ2* was upregulated, whereas *HSPA6* expression was downregulated after LGALS1 silencing. In addition, LGALS1 silencing led to 914 RASEs consisting of 10 types of AS residing in 759 genes. These LGALS1-mediated RASGs were mainly enriched in apoptosis and ErbB signaling pathways. Our results show potential novel molecular mechanisms of RBP LGALS1-mediated AS in NSCLC development.

Supplementary data

The supplementary materials are available at https://doi.org/10.5281/zenodo.8015729. The package contains the following files:

Supplementary Table 1. Primer information used in this study.

Supplementary Table 2. Results of quality control of RNA sequencing.

Supplementary Table 3. Statistics of all AS, known AS, and novel AS and their relative percentages.

Supplementary Table 4. Classification of all the detected known AS events.

Supplementary Table 5. Classification of all the detected novel AS events.

Supplementary Table 6. Distribution of each class of AS events (%).

Supplementary Fig. 1. LGALS1 expression in lung adenocarcinoma and lung squamous cell carcinoma between tumor and normal tissues in the TCGA database.

Supplementary Fig. 2. Validation of the LGALS1-mediated RASGs. RNA sequencing results and RT-qPCR validation results of RASGs were shown (^{ns} $p > 0.05$, * $p < 0.05$, ** $p < 0.01$, *** $p < 0.001$).

ORCID iDs

Hongyang Sh https://orcid.org/0000-0001-5139-970X
Yonghong Zhang https://orcid.org/0000-0003-1677-3537
Juan Liu https://orcid.org/0000-0003-3024-819X
Yu Wang https://orcid.org/0000-0003-1880-072X
Ping Fang https://orcid.org/0000-0002-9016-2323

References

1. Bray F, Ferlay J, Soerjomataram I, Siegel RL, Torre LA, Jemal A. Global cancer statistics 2018: GLOBOCAN estimates of incidence and mortality worldwide for 36 cancers in 185 countries. *CA Cancer J Clin*. 2018;68(6):394–424. doi:10.3322/caac.21492
2. Ferlay J, Colombet M, Soerjomataram I, et al. Estimating the global cancer incidence and mortality in 2018: GLOBOCAN sources and methods. *Int J Cancer*. 2019;144(8):1941–1953. doi:10.1002/ijc.31937
3. Zhou C, Wu YL, Chen G, et al. Final overall survival results from a randomised, phase III study of erlotinib versus chemotherapy as first-line treatment of EGFR mutation-positive advanced non-small-cell lung cancer (OPTIMAL, CTONG-0802). *Ann Oncol*. 2015;26(9):1877–1883. doi:10.1093/annonc/mdv276
4. Masuda K, Kuwano Y. Diverse roles of RNA-binding proteins in cancer traits and their implications in gastrointestinal cancers. *Wiley Interdiscip Rev RNA*. 2019;10(3):e1520. doi:10.1002/wrna.1520
5. Nahalka J. The role of the protein–RNA recognition code in neurodegeneration. *Cell Mol Life Sci*. 2019;76(11):2043–2058. doi:10.1007/s00018-019-03096-3
6. Pereira B, Billaud M, Almeida R. RNA-binding proteins in cancer: Old players and new actors. *Trends Cancer*. 2017;3(7):506–528. doi:10.1016/j.trecan.2017.05.003
7. Fuertes MB, Molinero LL, Toscano MA, et al. Regulated expression of galectin-1 during T-cell activation involves Lck and Fyn kinases and signaling through MEK1/ERK, p38 MAP kinase and $p70^{S6}$ kinase. *Mol Cell Biochem*. 2004;267(1/2):177–185. doi:10.1023/B:MCBI.0000049376.50242.7f
8. Qiu B, Zhang P, Xiong D, et al. CircRNA fibroblast growth factor receptor 3 promotes tumor progression in non-small cell lung cancer by regulating galectin-1-AKT/ERK1/2 signaling. *J Cell Physiol*. 2019;234(7):11256–11264. doi:10.1002/jcp.27783
9. Chung LY, Tang SJ, Sun GH, et al. Galectin-1 promotes lung cancer progression and chemoresistance by upregulating p38 MAPK, ERK, and cyclooxygenase-2. *Clin Cancer Res*. 2012;18(15):4037–4047. doi:10.1158/1078-0432.CCR-11-3348
10. Sun H, Zhang H, Yan Y, et al. NCAPG promotes the oncogenesis and progression of non-small cell lung cancer cells through upregulating LGALS1 expression. *Mol Cancer*. 2022;21(1):55. doi:10.1186/s12943-022-01533-9
11. Wu ZH, Tang Y, Zhou Y. Alternative splicing events implicated in carcinogenesis and prognosis of thyroid gland cancer. *Sci Rep*. 2021;11(1):4841. doi:10.1038/s41598-021-84403-6
12. Fu XD, Ares M. Context-dependent control of alternative splicing by RNA-binding proteins. *Nat Rev Genet*. 2014;15(10):689–701. doi:10.1038/nrg3778
13. Patterson RJ, Wang W, Wang JL. Understanding the biochemical activities of galectin-1 and galectin-3 in the nucleus. *Glycoconj J*. 2002;19(7–9):499–506. doi:10.1023/B:GLYC.0000014079.87862.c7
14. Wang J, Thio SSC, Yang SSH, et al. Splice variant specific modulation of CaV1.2 calcium channel by galectin-1 regulates arterial constriction. *Circ Res*. 2011;109(11):1250–1258. doi:10.1161/CIRCRESAHA.111.248849
15. Győrffy B, Surowiak P, Budczies J, Lánczky A. Online survival analysis software to assess the prognostic value of biomarkers using transcriptomic data in non-small-cell lung cancer. *PLoS One*. 2013;8(12):e82241. doi:10.1371/journal.pone.0082241

16. Kim D, Pertea G, Trapnell C, Pimentel H, Kelley R, Salzberg SL. TopHat2: Accurate alignment of transcriptomes in the presence of insertions, deletions and gene fusions. *Genome Biol*. 2013;14(4):R36. doi:10.1186/gb-2013-14-4-r36
17. Trapnell C, Williams BA, Pertea G, et al. Transcript assembly and quantification by RNA-Seq reveals unannotated transcripts and isoform switching during cell differentiation. *Nat Biotechnol*. 2010;28(5):511–515. doi:10.1038/nbt.1621
18. Robinson MD, McCarthy DJ, Smyth GK. edgeR: A Bioconductor package for differential expression analysis of digital gene expression data. *Bioinformatics*. 2010;26(1):139–140. doi:10.1093/bioinformatics/btp616
19. Xie C, Mao X, Huang J, et al. KOBAS 2.0: A web server for annotation and identification of enriched pathways and diseases. *Nucleic Acids Res*. 2011;39(Suppl 2):W316–W322. doi:10.1093/nar/gkr483
20. Xia H, Chen D, Wu Q, et al. CELF1 preferentially binds to exon-intron boundary and regulates alternative splicing in HeLa cells. *Biochim Biophys Acta Gene Regul Mech*. 2017;1860(9):911–921. doi:10.1016/j.bbagrm.2017.07.004
21. Livak KJ, Schmittgen TD. Analysis of relative gene expression data using real-time quantitative PCR and the $2^{-\Delta\Delta CT}$ method. *Methods*. 2001;25(4):402–408. doi:10.1006/meth.2001.1262
22. Shi L, Zhang B, Sun X, et al. CC chemokine ligand 18(CCL18) promotes migration and invasion of lung cancer cells by binding to Nir1 through Nir1-ELMO1/DOC180 signaling pathway. *Mol Carcinog*. 2016;55(12):2051–2062. doi:10.1002/mc.22450
23. Lee JU, Chang HS, Jung CA, Kim RH, Park CS, Park JS. Upregulation of potassium voltage-gated channel subfamily J member 2 levels in the lungs of patients with idiopathic pulmonary fibrosis. *Can Respir J*. 2020;2020:3406530. doi:10.1155/2020/3406530
24. Li X, Noell G, Tabib T, et al. Single cell RNA sequencing identifies *IGFBP5* and *QKI* as ciliated epithelial cell genes associated with severe COPD. *Respir Res*. 2021;22(1):100. doi:10.1186/s12931-021-01675-2
25. Wang L, Hou J, Wang J, et al. Regulatory roles of HSPA6 in *Actinidia chinensis* Planch. root extract (acRoots)-inhibited lung cancer proliferation. *Clin Transl Med*. 2020;10(2):e46. doi:10.1002/ctm2.46
26. Umeyama H, Iwadate M, Taguchi YH. *TINAGL1* and *B3GALNT1* are potential therapy target genes to suppress metastasis in non-small cell lung cancer. *BMC Genomics*. 2014;15(Suppl 9):S2. doi:10.1186/1471-2164-15-S9-S2
27. Witkiewicz AK, McMillan EA, Balaji U, et al. Whole-exome sequencing of pancreatic cancer defines genetic diversity and therapeutic targets. *Nat Commun*. 2015;6(1):6744. doi:10.1038/ncomms7744
28. Barrientos G, Freitag N, Tirado-González I, et al. Involvement of galectin-1 in reproduction: Past, present and future. *Hum Reprod Update*. 2014;20(2):175–193. doi:10.1093/humupd/dmt040
29. Li JM, Tseng CW, Lin CC, et al. Upregulation of LGALS1 is associated with oral cancer metastasis. *Ther Adv Med Oncol*. 2018;10:175883591879462. doi:10.1177/1758835918794622
30. Sharanek A, Burban A, Hernandez-Corchado A, et al. Transcriptional control of brain tumor stem cells by a carbohydrate binding protein. *Cell Rep*. 2021;36(9):109647. doi:10.1016/j.celrep.2021.109647
31. Oltean S, Bates DO. Hallmarks of alternative splicing in cancer. *Oncogene*. 2014;33(46):5311–5318. doi:10.1038/onc.2013.533
32. Wang J, Liu T, Wang M, et al. SRSF1-dependent alternative splicing attenuates BIN1 expression in non-small cell lung cancer. *J Cell Biochem*. 2020;121(2):946–953. doi:10.1002/jcb.29366
33. Zheng M, Niu Y, Bu J, et al. ESRP1 regulates alternative splicing of CARM1 to sensitize small cell lung cancer cells to chemotherapy by inhibiting TGF-β/Smad signaling. *Aging*. 2021;13(3):3554–3572. doi:10.18632/aging.202295
34. Boudria A, Abou Faycal C, Jia T, et al. VEGF165b, a splice variant of VEGF-A, promotes lung tumor progression and escape from anti-angiogenic therapies through a β1 integrin/VEGFR autocrine loop. *Oncogene*. 2019;38(7):1050–1066. doi:10.1038/s41388-018-0486-7
35. Górniak P, Wasylecka-Juszczyńska M, Ługowska I, et al. BRAF inhibition curtails IFN-gamma-inducible PD-L1 expression and upregulates the immunoregulatory protein galectin-1 in melanoma cells. *Mol Oncol*. 2020;14(8):1817–1832. doi:10.1002/1878-0261.12695
36. Zhang N, Peng F, Wang Y, et al. Shikonin induces colorectal carcinoma cells apoptosis and autophagy by targeting galectin-1/JNK signaling axis. *Int J Biol Sci*. 2020;16(1):147–161. doi:10.7150/ijbs.36955
37. Zhao R, Song J, Jin Y, Liu Y. Long noncoding RNA HOXC-AS3 enhances the progression of cervical cancer via activating ErbB signaling pathway. *J Mol Histol*. 2021;52(5):991–1006. doi:10.1007/s10735-021-10007-z
38. Bolado-Carrancio A, Lee M, Ewing A, et al. ISGylation drives basal breast tumour progression by promoting EGFR recycling and Akt signalling. *Oncogene*. 2021;40(44):6235–6247. doi:10.1038/s41388-021-02017-8
39. Chiu TH, Lin CY, Hsieh MH, Lin SM, Fang YF. Prognostic factors in lung adenocarcinoma with bone metastasis treated with EGFR-TKIs. *Medicina (Kaunas)*. 2021;57(9):967. doi:10.3390/medicina57090967

Degenerative disease of the spine: How to relate clinical symptoms to radiological findings

Marek Sąsiadek[A,B,D–F], Jagoda Jacków-Nowicka[C,D]

Department of General and Interventional Radiology and Neuroradiology, Chair of Radiology, Wroclaw Medical University, Poland

A – research concept and design; B – collection and/or assembly of data; C – data analysis and interpretation;
D – writing the article; E – critical revision of the article; F – final approval of the article

Advances in Clinical and Experimental Medicine, ISSN 1899–5276 (print), ISSN 2451–2680 (online) *Adv Clin Exp Med*. 2024;33(1):91–98

Address for correspondence
Jagoda Jacków-Nowicka
E-mail: jagodajackow@yahoo.pl

Funding sources
None declared

Conflict of interest
None declared

Acknowledgements
The authors would like to thank Prof. Joanna Bladowska and Dr. Barbara Hendrich for providing some of the MR images used in the study.

Received on November 28, 2022
Reviewed on April 5, 2023
Accepted on April 17, 2023

Published online on August 7, 2023

Abstract

Degenerative disease of the spine (DDS) is one of the most common pathological conditions in humans. The clinical presentation of DDS is highly variable, ranging from mild pain to severe neurological symptoms. When more severe clinical symptoms are present, it is necessary to use imaging methods, such as magnetic resonance imaging (MRI), to confirm the diagnosis and establish the extent of the disease in order to determine proper treatment. There are several MRI changes which, based on clinicoradiological studies, are believed to be potential sources of pain and other clinical symptoms in DDS, including compression of the nerve root or spinal cord by disc herniations or osteophytes, recent ("active") disc herniation, Modic type 1 degenerative changes of the vertebral bodies, degenerative changes of the vertebral endplates (erosive intervertebral osteochondrosis), marked degenerative changes of the facet joints and ligamenta flava, degenerative spinal canal stenosis, degenerative spondylolisthesis, and Baastrup's disease. The authors analyzed the relationship of the MRI findings mentioned above with clinical symptoms of DDS, as well as the differentiation between DDS and nondegenerative diseases, which can manifest with similar clinical signs. The role of contrast-enhanced MRI and advanced MR techniques (e.g., high field MRI, functional MRI and MR spectroscopy) was also discussed. To establish an appropriate treatment for DDS, it is important to emphasize in the MRI report specific changes, which might be the cause of the pain and other clinical signs, as well as to rule out nondegenerative lesions, especially neoplasms, infections and rheumatoid disorders.

Key words: degenerative disease of the spine, magnetic resonance imaging, back pain, neurological claudication, myelopathy

Cite as
Sąsiadek M, Jacków-Nowicka J. Degenerative disease of the spine: How to relate clinical symptoms to radiological findings. *Adv Clin Exp Med*. 2024;33(1):91–98. doi:10.17219/acem/163357

DOI
10.17219/acem/163357

Introduction

Degenerative disease of the spine (DDS) is one of the most common pathological conditions in humans. The clinical presentation of DDS is highly variable, ranging from mild pain to severe neurological symptoms.[1,2] In benign cases, the diagnosis of DDS is based on the clinical signs and physical examination. When more severe clinical symptoms are present, it is necessary to use imaging methods to confirm the diagnosis and establish the extent of the disease, which is necessary to determine the proper treatment.[3]

Plain X-rays of the spine are usually used as an initial imaging method in DDS; however, their value is limited to the bone changes (e.g., vertebral body osteophytes) and narrowing of the intervertebral spaces, which are indirect signs of degenerative disc disease (DDD). The imaging modality of choice in patients with more severe DDS is magnetic resonance imaging (MRI).[4] It is believed that MRI can help define the anatomic basis of the pain and autonomic nervous system syndrome in patients with disc herniations.[5] Computed tomography (CT) is a complementary method to better assess bone lesions. The other imaging methods (nuclear medicine modalities, myelography and discography) are rarely used due to their low availability or invasiveness.[6]

The difficulty of interpreting MRI studies in DDS is associated with the multi-level and multistructural patterns seen on MRIs. Degenerative disease of the spine is commonly located at multiple levels, and multiple structures are involved at each level.[7,8] The so-called discosomatic (discovertebral) unit consists of 5 elements: intervertebral disc, vertebral bodies, facet joints, ligamenta flava, and longitudinal ligaments. Each of these structures can be affected by the degenerative process.[9] Moreover, any particular part of the discosomatic unit may show various MRI findings. For instance, DDD can present as a black disc disease (dehydration), disc calcifications, gas in the disc (vacuum phenomenon), disc bulging, and disc herniation.[10–12] Vertebral body degeneration involves Modic type 1, 2 and 3 changes, osteophytes, and erosive osteochondrosis (degeneration of vertebral endplates).[7,8,13,14] There are also specific MRI patterns like degenerative spinal stenosis (changes in all elements of the discosomatic unit), degenerative spondylolisthesis and Baastrup's disease (degeneration of the spinous processes).[3,4,9,15–17]

The most important clinical symptoms of DDS are[6]: 1) persistent back pain; 2) radicular (pain) symptoms; 3) neurological deficits (limb paresis, myelopathy); 4) sensory impairment; and 5) neurogenic claudication. The crucial problem is how to correlate the pain and other clinical symptoms with particular MRI findings, i.e., how to establish which of the multiple MRI changes are responsible for the clinical signs.

MRI findings which may be responsible for the pain and other clinical symptoms in DDS

There are several MRI changes which, based on clinico-radiological studies, are believed to be a potential source of pain and other clinical symptoms in DDS[3,4,7,9,16,17]: 1) compression of the nerve root or spinal cord by disc herniations or osteophytes; 2) recent ("active") disc herniation; 3) Modic type 1 degenerative changes of the vertebral bodies; 4) degenerative changes of the vertebral endplates (erosive intervertebral osteochondrosis); 5) marked degenerative changes of the facet joints and ligamenta flava; 6) degenerative spinal canal stenosis; 7) degenerative spondylolisthesis; and 8) Baastrup's disease.

Compression of the nerve root or spinal cord by disc herniations or osteophytes

This is a very common radiological finding in DDS. The anterior surface of nerve roots and the spinal cord are located very close to the posterior aspect of the intervertebral discs and vertebral bodies. Therefore, even a small disc herniation or osteophyte could compress the adjacent nerve root or spinal cord, especially in patients with degenerative spinal canal stenosis in whom the intraspinal space is already compromised.[7,10,12,18]

On the other hand, many small herniations or osteophytes do not produce clinical symptoms until they compress the epidural space or dural sac. In patients who present clinically with radicular symptoms or myelopathy, one should check MR images for direct compression of the nerve root or spinal cord. The best visualization of nerve root compression is provided by axial T2-weighted images, while spinal cord compression can be appreciated in sagittal and axial planes (Fig. 1).[6,9,19]

Prolonged compression of the spinal cord can lead to secondary changes in the spinal cord, which during earlier phases is compatible with edema and ischemia, while later phases correlate with myelomalacia and gliosis. The longer the compression lasts, the more severe are the myelopathic symptoms. The changes mentioned above can be seen on MR T2-weighted images as hyperintense foci within the spinal cord.[10] However, in many patients with myelopathic symptoms, no changes in the spinal cord are visible on MRI even if it is compressed. The reason for this is the limited spatial resolution of MR images. The sensitivity of MRI in detecting spinal cord lesions can be increased by the use of diffusion tensor imaging (DTI), which provides the quantitative assessment of the spinal cord impairment by calculating fractional anisotropy (FA) and other DTI parameters.[20–22] Another promising technique is functional MRI (fMRI). Some studies demonstrated a positive correlation between functional connectivity and volume of activations in blood-oxygen-level-dependent

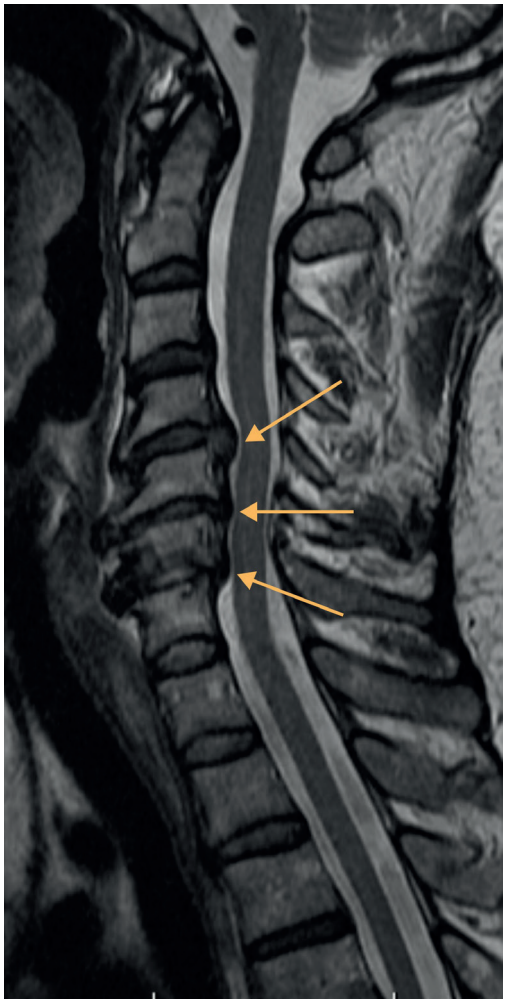

Fig. 1. Sagittal T2-weighted magnetic resonance (MR) image of the cervical spine in a patient with myelopathy shows multi-level disc herniations compressing the anterior surface of the spinal cord (arrows)

(BOLD) signals on fMRI and postsurgical outcomes in patients with degenerative cervical myelopathy.[21] Finally, the use of high-field MRI systems (3 or 7 Tesla units) might improve sensitivity in detecting spinal cord changes in patients with degenerative myelopathy.[23]

A possible cause for the discrepancy between the clinical symptoms of radiculopathy or myelopathy and MRI signs is the supine position of the patient during MRI examination, while in many cases, the compression occurs only in the standing or sitting position. One of the solutions is the use of vertical MRI units, in which the patient stands or sits, and dynamic scanning with flexion or extension is performed.[24] However, such MRI units are rarely available; hence, an alternative known as axial-loaded imaging has been developed. This is based on special devices which provide a calculated compression of the patient's feet and head to imitate natural loading in the standing position.[25] This can help to visualize the compression of the nerve roots or spinal cord, which is not visible on plain MRIs.

Recent ("active") disc herniation

Although disc degeneration is generally associated with low signal intensity on T2-weighted images due to decreased water content (dehydration), foci of high intensity (high intensity zones (HIZ)) can be seen in the posterior parts of bulging or herniated discs.[26] The significance of HIZ is controversial. It is believed by some authors that HIZ in the posterior part of degenerated or bulging discs represents a tear in the annulus fibrosus that can lead to disc herniation.[27] However, it has not been fully confirmed by radiopathological studies. On the other hand, the increased signal in bulging and especially herniated disks means an increased water content that could be caused by edema and inflammation in or around the bulging/herniated disc and, thus, could be the source of pain.[26–28]

This hypothesis can be confirmed by the common occurrence of HIZ in patients with marked back pain and recent disc herniations, even without compression of nerve roots, while in patients with older disc herniations, which usually do not have HIZ, the clinical symptoms are associated with radicular or spinal cord compression (Fig. 2).[10,27,28]

Additional evidence of an inflammatory process in patients with recent disc herniations who present with back pain is the contrast enhancement around the herniations, which can be seen in rare cases when gadolinium contrast medium is used in patients with DDS.[29] As in other places, the inflammatory reaction commonly results in pain.

Injection of gadolinium contrast medium can be useful in patients after herniated disc surgery presenting with failed back surgery syndrome (FBSS) to differentiate between recurrent disc herniation and other causes of persistent pain after surgery.[30,31] The other complementary MRI techniques in FBSS include fMRI and MR neurography.[31]

Further research based on fMRI, T1, T2, and T2* mapping, as well as MR spectroscopy, may provide new information concerning the relationship between pain and degenerative disc changes.[32,33]

Modic type 1 degenerative changes of the vertebral bodies

Modic type 1 degenerative changes are believed to represent inflammatory reactions of the vertebral bodies during the course of DDS. They are located in the direct vicinity of the vertebral endplates, usually on both sides of the degenerated intervertebral disc. Their signal is hyperintense on T2-weighted/Fat-Sat T2-weighted MR images and hypointense on T1-weighted images. This pattern is compatible with the increased water content in Modic type 1 lesions, which are caused by edema and inflammation, and can result in pain.[7,8,11,13] Moreover, if, for any reason, gadolinium contrast medium is used, an enhancement of the Modic type I areas might be

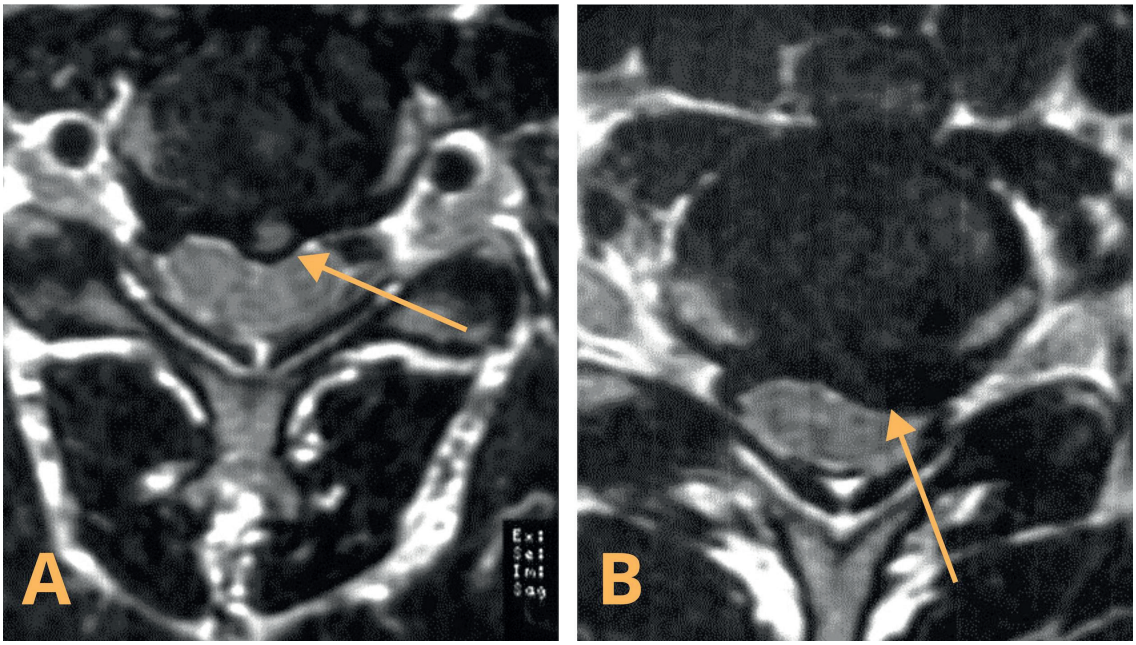

Fig. 2. Cervical disc herniations. Axial T2-weighted magnetic resonance (MR) images of the cervical spine. A. In a patient with cervical spine pain; hyperintense (recent, "active") disc herniation with slight compression of the spinal cord (arrow); B. Another patient presenting with myelopathy and hypointense (chronic) disc herniation; marked compression of the spinal cord can be seen (arrow)

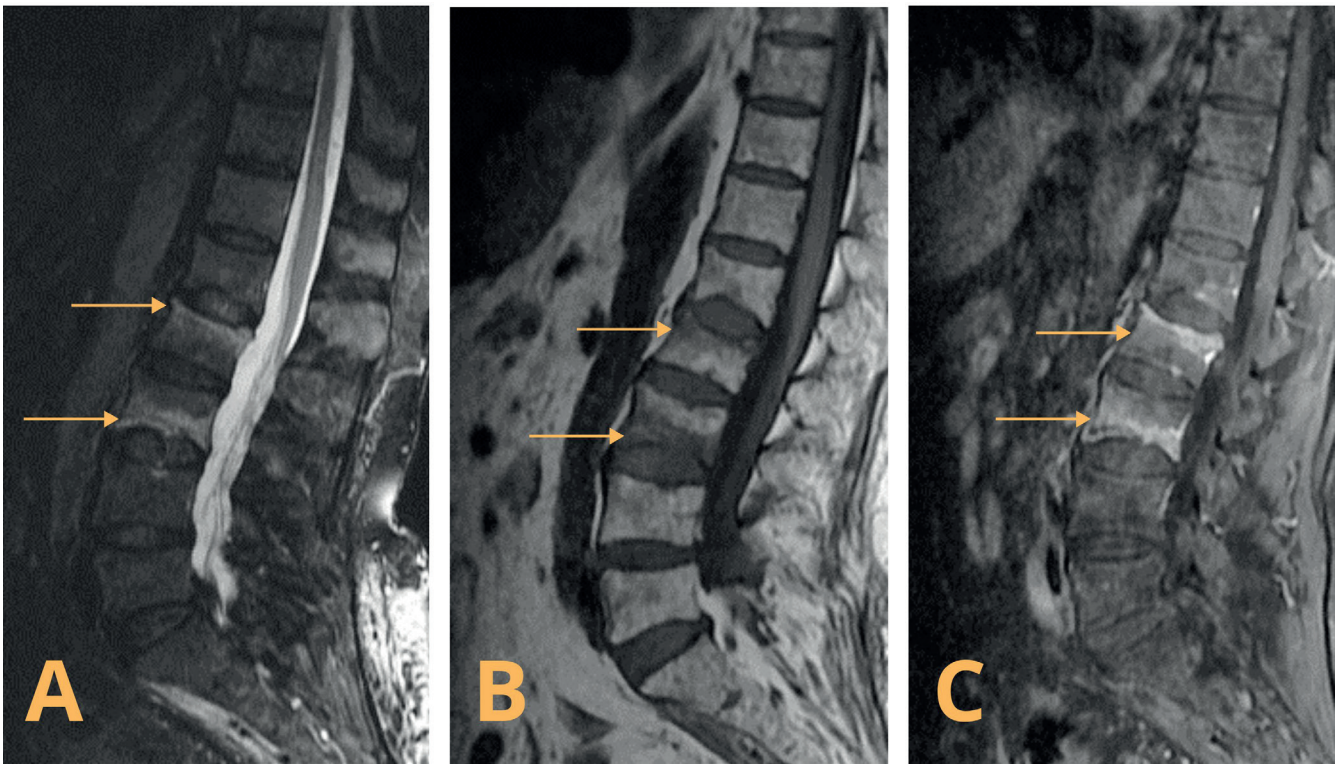

Fig. 3. Sagittal T2-weighted fat-suppressed (A), T1-weighted (B) and T1-weighed fat-suppressed contrast-enhanced (C) magnetic resonance (MR) images of the lumbar spine in a patient with low back pain. In the upper part of the L2 and the lower part of the L3 vertebral bodies, there are areas of hyperintensity on a T2-weighted image and hypointensity on a T1-weighted image, enhancing after contrast administration (arrows), which are compatible with Modic type 1 degenerative changes

observed, which is further evidence of their inflammatory background (Fig. 3).[34]

This inflammatory nature is the reason for the term "aseptic spondylodiscitis", which is sometimes used to describe Modic type 1 changes. Actually, in some cases, Modic type 1 changes must be differentiated from true infectious spondylodiscitis. Apart from clinical and laboratory markers of infection like fever or increased C-reactive protein (CRP) and white blood cell (WBC) levels, the MRI pattern in infectious spondylodiscitis is different. First of all, in Modic type 1 changes, the adjacent intervertebral disk has a low signal on T2-weighted images due to degenerative dehydration, while in infectious spondylodiscitis, the signal of the disc is increased due

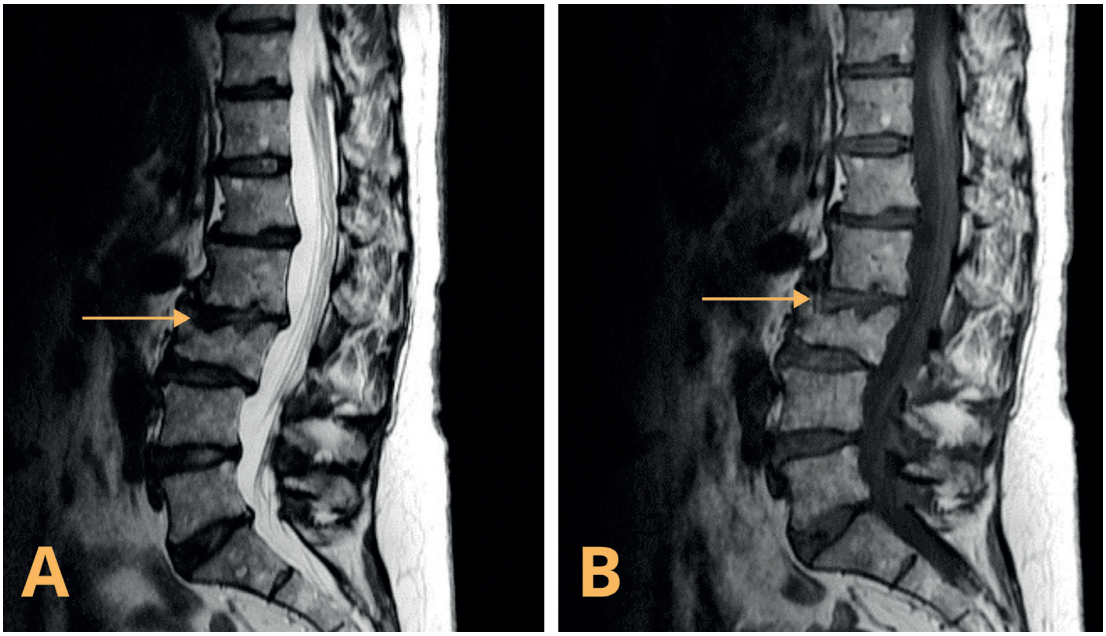

Fig. 4. Sagittal T2-weighted (A) and T1-weighted (B) magnetic resonance (MR) images of the lumbar spine in a patient with low back pain. The adjacent endplates of the L2 and L3 vertebral bodies exhibit markedly irregular outlines with preserved cortical bone and degenerative hypointensity of the L2/L3 intervertebral disc on a T2-weighted image. This appearance is consistent with erosive intervertebral osteochondrosis (degeneration of the vertebral endplates)

to infectious infiltration. Besides, the vertebral endplates in Modic 1 changes are intact, while in infectious spondylodiscitis, they are destroyed. Finally, the infectious infiltration often extends to the paravertebral and extradural spaces, which does not occur in Modic type 1 degenerative changes.[4,35] The pattern of contrast enhancement after administration of gadolinium is a useful clue; in DDS, the enhancement is limited to the regions of the vertebral endplates and facet joints, while in spondylodiscitis, it may also involve extradural and paraspinal areas.[36,37]

Degenerative changes of the vertebral endplates (erosive intervertebral osteochondrosis)

The vertebral endplates consist of cartilage and cortical bone from the vertebral body surfaces adjacent to the intervertebral disc.[38] The endplates are highly vulnerable to the degenerative process as they are, on the one hand, loaded by body weight and, on the other hand, provide the blood supply to the intervertebral disc. Degeneration of the endplates, especially of their cartilaginous component, is considered a source of pain.[9,34,38]

On MR images, the degeneration of the endplates appears as an irregular outline in their cortical bone, which can be seen in all sequences.[6,9] This pattern can also mimic infectious spondylodiscitis. However, in erosive intervertebral osteochondrosis, the black line consistent with the endplate cortical bone is always intact, even if its outline is very irregular (Fig. 4), while in infectious spondylodiscitis, this black line is blurred. The other crucial difference is the signal of the adjacent intervertebral disc, which is low on T2-weighted images in erosive intervertebral osteochondrosis, due to infectious infiltration.[35]

The use of contrast media may also help in the differential diagnosis, as the pattern of enhancement in spondylodiscitis is different from that in vertebral degeneration.[36,37]

Marked degenerative changes of the facet joints and ligamenta flava

Facet joints are commonly affected in DDS. As they bear significant stress and weight, they are highly vulnerable to degeneration.[39] Besides, as the facets are richly innervated, their degeneration can result in back pain or sciatica.[40]

The radiological signs of facet degeneration seen on MRI or CT include deformation and osteophytes of the articular processes as well as narrowing of the joint spaces. (Fig. 5).[6,9,41] In severe degeneration, T2-weighted fat-suppressed MRI sequence could reveal the hyperintense signal of the articular process while post-contrast T1-weighted fat-suppressed sequences can show enhancement.[34,36,37] These findings are compatible with edema and an inflammatory reaction, and thus could be a source of pain. The rare manifestation of a synovial cyst can protrude into the spinal canal.[5,6,9]

Ligamenta flava are located in the posterolateral parts of the spinal canal adjacent to the facet joints. Degeneration of the ligamenta flava causes thickening, which compromises the posterior-lateral parts of the spinal canal and compresses the posterior-lateral aspects of the dural sac.[6] In active degeneration with an inflammatory component, contrast enhancement of the ligamenta flava can be observed.[36,37]

The degeneration of the facet joints and ligamenta flava usually occur together. Apart from pain caused by degenerated facets, they also contribute to spinal stenosis and the clinical symptoms of spinal stenosis (see below).

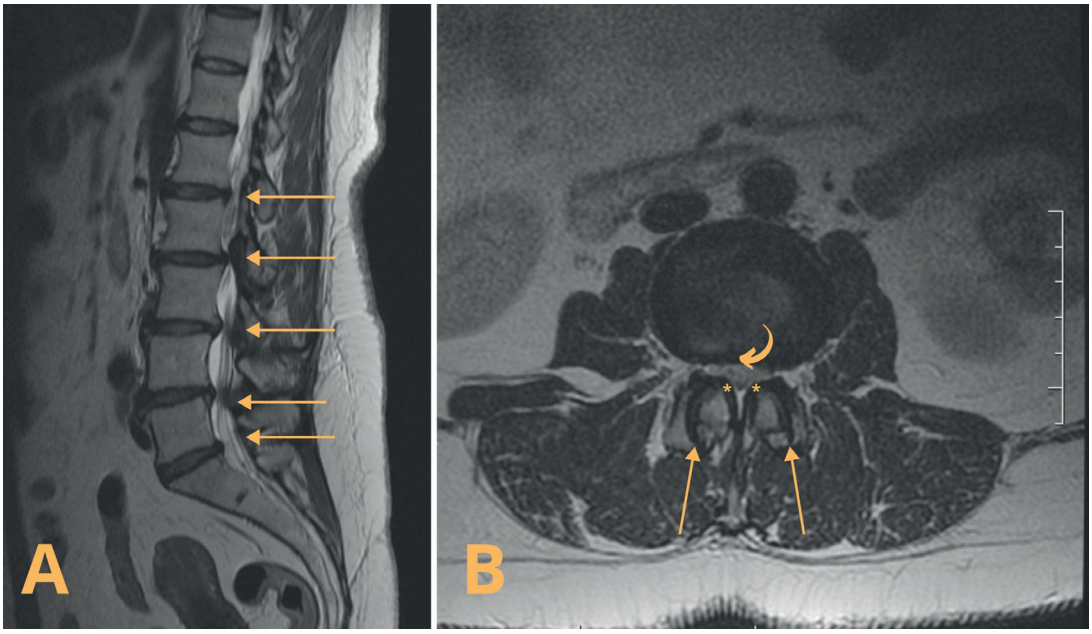

Fig. 5. Sagittal (A) and axial (B) magnetic resonance (MR) images of the lumbar spine in a patient with neurological claudication. Marked multi-level lumbar spinal stenosis. Multi-level narrowing of the spinal canal (arrows) can be seen in the sagittal image (A). The axial image at the level of L4/L5 demonstrates disc bulging (curved arrow), degenerative hypertrophy of the articular processes of the facet joints (straight arrows) and degenerative thickening of the ligamenta flava (asterisks)

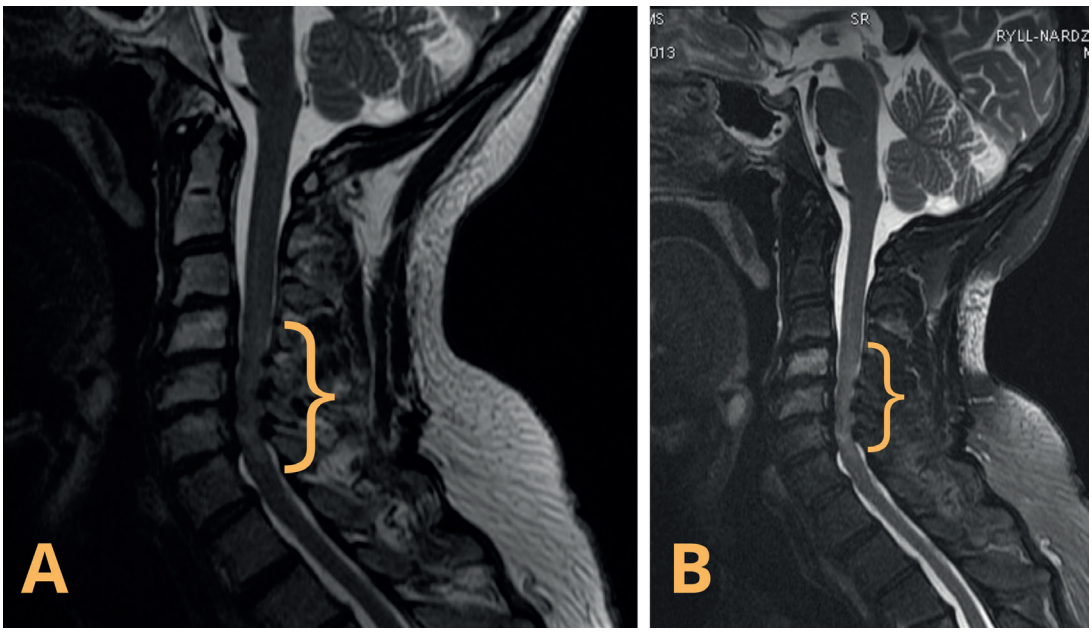

Fig. 6. Sagittal T2-weighted (A) and T2-weighted fat-suppressed (B) magnetic resonance (MR) images of the cervical spine in a patient with myelopathy show marked spinal canal stenosis involving the C4–C7 segment of the spine (brackets) with secondary hyperintense changes in the spinal cord

Degenerative spinal canal stenosis

Narrowing of the spinal canal (stenosis) may be caused by degeneration of any structure of the discosomatic unit, e.g., disk herniation, osteophytes and thickening of the ligamenta flava. However, the term degenerative spinal canal stenosis usually refers to the degeneration of all or most of the structures of the discosomatic unit.[6,9] The typical pattern of spinal canal stenosis consists of: 1) intervertebral disc bulging; 2) osteophytes of the posterior edges of the vertebral bodies; 3) deformation, osteophytes and (rarely) synovial cysts of the facet joints; and 4) thickening of the ligamenta flava.

Stenosis can be increased by degenerative spondylolisthesis (see below). It usually involves multiple levels, most often in the lower lumbar and lower cervical segments of the spine (Fig. 5,6).[4]

Degenerative spinal canal stenosis can be classified as central spinal canal stenosis (narrowing of the central part of the spinal canal) and lateral spinal canal stenosis (narrowing of the lateral recesses of the spinal canal and the neural foramina). The latter could be subdivided into lateral recess stenosis and foraminal stenosis.[5,6,9]

The typical clinical manifestation of central lumbar spinal canal stenosis is neurological claudication, which means pain, tingling or cramping in the lower back, legs, hips, and buttocks that can be accompanied by weakness in the legs. These symptoms are enhanced during standing and walking, and relieved when leaning down and sitting.[42] On the other hand, cervical and

thoracic central spinal canal stenosis causes spinal cord compression and thus presents clinically as myelopathy (pain, numbness and weakness in the neck, back, as well as in upper and/or lower extremities, motor impairment, etc.).[4,10]

Lateral spinal canal stenosis (both lateral recess and foraminal) is associated with compression of the radicles or spinal nerves; therefore, its main clinical manifestation is radicular pain.[9] In fact, most cases of central and lateral stenosis are combined and result in combined clinical symptoms.

Magnetic resonance imaging provides a very good evaluation of degenerative spinal canal stenosis, especially in axial (central and lateral recess stenosis) and lateral sagittal planes (foraminal stenosis). Computed tomography can be used complementarily for better assessment of the boney elements contributing to stenosis. A detailed analysis of the imaging studies can identify the levels or structures responsible for clinical symptoms.[4,6,9,19]

Degenerative spondylolisthesis

Degenerative spondylolisthesis develops due to chronic facet joint and intervertebral degeneration, as well as ligamentous laxity, which finally results in vertebral instability and slipping (subluxation) of the upper vertebral body in relation to the inferior one. Typically, the upper vertebral body moves anteriorly to the adjacent lower vertebral body; however, it can also move posteriorly, which is called retrolisthesis.[16]

The instability caused by spondylolisthesis can cause pain apart from that associated with facet joint degeneration. This can be confirmed by Modic type 1 changes, which are often seen in the vertebral bodies at the level of the spondylolisthesis. Besides, degenerative spondylolisthesis contributes to spinal canal stenosis and can present with clinical symptoms of stenosis.[4,9]

In young patients, degenerative spondylolisthesis needs to be differentiated from spondylolisthesis caused by an interarticular pars defects of the posterior vertebral arch (spondylolysis), which can be detected using CT and MRI (including post-contrast MRI).[36,37,43]

Baastrup's disease

Baastrup's disease (kissing spines syndrome) occurs when the adjacent spinous processes (usually in the lumbar region) are close enough to touch, which results in degenerative changes. It could be a part of generalized DDS or caused by hyperlordosis of the lumbar spine. Patients experience pain in the midline that worsens with extension and is relieved during flexion of the lumbar spine.[17]

In T2 fat-suppressed MRI sequences, the affected spinous processes demonstrate a high signal, which is consistent with edema and an inflammatory reaction, thus explaining the pain. On CT, the space between the involved spinous processes is narrowed, and their adjacent surfaces have irregular outlines and osteosclerotic areas.[4,17]

Differentiation of DDS with nondegenerative diseases

An additional problem with clinicoradiological correlations in DDS is that it is sometimes mimicked by nondegenerative diseases. Although DDS is extremely common, other diseases can present with similar clinical symptoms. One example is infectious spondylodiscitis, which can have similar clinical and MRI appearances to Modic type 1 vertebral body changes and especially erosive osteochondrosis (see above).[35] Back pain can be caused by neoplastic disease, especially metastases. In doubtful cases, MRI and CT can be supplemented with a bone scan or PET/CT. Finally, the source of the pain could be spondyloarthropathies (e.g., ankylosing spondylitis); therefore, it is useful to evaluate the sacroiliac joints which are commonly affected in spondyloarthropathies that could be easily diagnosed on MRIs of the sacroiliac joints.[44]

Conclusions

Magnetic resonance imaging reports in patients with DDS should emphasize all changes which might cause pain and other clinical signs (e.g., compression of the nerve root, Modic 1 changes, degeneration of the endplates, facet joint degeneration, and spinal canal stenosis). It is necessary to rule out nondegenerative lesions, especially neoplasms and infections, as well as possible causes of clinical symptoms from adjacent structures, e.g., sacroiliac joints, and post-contrast imaging is helpful in the differential diagnosis. Advanced MR techniques, such as high-field MRI, fMRI, T1, T2, and T2* mapping, MR spectroscopy, or MR neurography, may contribute to a better understanding of the relationship between clinical symptoms and radiological findings in DDS.

ORCID iDs

Marek Sąsiadek https://orcid.org/0000-0003-3627-118X
Jagoda Jacków-Nowicka https://orcid.org/0000-0002-2449-0310

References

1. Maher C, Underwood M, Buchbinder R. Non-specific low back pain. *Lancet*. 2017;389(10070):736–747. doi:10.1016/S0140-6736(16)30970-9
2. Chou R. Low back pain. *Ann Intern Med*. 2021;174(8):ITC113–ITC128. doi:10.7326/AITC202108170
3. Kushchayev SV, Glushko T, Jarraya M, et al. ABCs of the degenerative spine. *Insights Imaging*. 2018;9(2):253–274. doi:10.1007/s13244-017-0584-z
4. Winegar BA, Kay MD, Taljanovic M. Magnetic resonance imaging of the spine. *Pol J Radiol*. 2020;85:e550–e574. doi:10.5114/pjr.2020.99887
5. Jinkins J, Whittemore A, Bradley W. The anatomic basis of vertebrogenic pain and the autonomic syndrome associated with lumbar disk extrusion. *AJR Am J Roentgenol*. 1989;152(6):1277–1289. doi:10.2214/ajr.152.6.1277

6. Sasiadek MJ, Bladowska J. Imaging of degenerative spine disease: The state of the art. *Adv Clin Exp Med*. 2012;21(2):133–142. PMID:23214277.
7. Takatalo J, Karppinen J, Niinimäki J, et al. Association of Modic changes, Schmorl's nodes, spondylolytic defects, high-intensity zone lesions, disc herniations, and radial tears with low back symptom severity among young Finnish adults. *Spine (Phila Pa 1976)*. 2012;37(14): 1231–1239. doi:10.1097/BRS.0b013e3182443855
8. Lv B, Yuan J, Ding H, et al. Relationship between endplate defects, Modic change, disc degeneration, and facet joint degeneration in patients with low back pain. *Biomed Res Int*. 2019;2019:9369853. doi:10.1155/2019/9369853
9. Popolizio T, Izzo R. Degenerative disorders of the spine: Radiological imaging. In: *Clinical Neuroradiology*. Cham, Switzerland: Springer International Publishing; 2019:1–47. doi:10.1007/978-3-319-61423-6_38-1
10. Karki DB, Gurung G, Adhikary KP, Ghimire RK. Magnetic resonance imaging findings in degenerative disc disease of cervical spine in symptomatic patients. *J Nepal Health Res Counc*. 2015;13(31):196–200. PMID:27005711.
11. Yang X, Karis DSA, Vleggeert-Lankamp CLA. Association between Modic changes, disc degeneration, and neck pain in the cervical spine: A systematic review of literature. *Spine J*. 2020;20(5):754–764. doi:10.1016/j.spinee.2019.11.002
12. Brinjikji W, Diehn FE, Jarvik JG, et al. MRI findings of disc degeneration are more prevalent in adults with low back pain than in asymptomatic controls: A systematic review and meta-analysis. *AJNR Am J Neuroradiol*. 2015;36(12):2394–2399. doi:10.3174/ajnr.A4498
13. Sheng-yun L, Letu S, Jian C, et al. Comparison of Modic changes in the lumbar and cervical spine, in 3167 patients with and without spinal pain. *PLoS One*. 2014;9(12):e114993. doi:10.1371/journal.pone.0114993
14. Yang X, Donk R, Arts MP, Vleggeert-Lankamp CLA. Are Modic vertebral end-plate signal changes associated with degeneration or clinical outcomes in the cervical spine? *World Neurosurg*. 2019;129:e881–e889. doi:10.1016/j.wneu.2019.06.067
15. Hayashi T, Daubs MD, Suzuki A, Phan K, Shiba K, Wang JC. Effect of Modic changes on spinal canal stenosis and segmental motion in cervical spine. *Eur Spine J*. 2014;23(8):1737–1742. doi:10.1007/s00586-014-3406-8
16. Cho IY, Park SY, Park JH, Suh SW, Lee SH. MRI findings of lumbar spine instability in degenerative spondylolisthesis. *J Orthop Surg (Hong Kong)*. 2017;25(2):230949901771890. doi:10.1177/2309499017718907
17. Filippiadis DK, Mazioti A, Argentos S, et al. Baastrup's disease (kissing spines syndrome): A pictorial review. *Insights Imaging*. 2015;6(1):123–128. doi:10.1007/s13244-014-0376-7
18. Splendiani A, Bruno F, Marsecano C, et al. Modic I changes size increase from supine to standing MRI correlates with increase in pain intensity in standing position: Uncovering the "biomechanical stress" and "active discopathy" theories in low back pain. *Eur Spine J*. 2019; 28(5):983–992. doi:10.1007/s00586-019-05974-7
19. Nouri A, Martin AR, Mikulis D, Fehlings MG. Magnetic resonance imaging assessment of degenerative cervical myelopathy: A review of structural changes and measurement techniques. *Neurosurg Focus*. 2016;40(6):E5. doi:10.3171/2016.3.FOCUS1667
20. Banaszek A, Bladowska J, Podgórski P, Sąsiadek MJ. Role of diffusion tensor MR imaging in degenerative cervical spine disease: A review of the literature. *Clin Neuroradiol*. 2016;26(3):265–276. doi:10.1007/s00062-015-0467-y
21. He B, Sheldrick K, Das A, Diwan A. Clinical and research MRI techniques for assessing spinal cord integrity in degenerative cervical myelopathy: A scoping review. *Biomedicines*. 2022;10(10):2621. doi:10.3390/biomedicines10102621
22. Martin AR, Aleksanderek I, Cohen-Adad J, et al. Translating state-of-the-art spinal cord MRI techniques to clinical use: A systematic review of clinical studies utilizing DTI, MT, MWF, MRS, and fMRI. *Neuroimage Clin*. 2015;10:192–238. doi:10.1016/j.nicl.2015.11.019
23. Wright D, Martin S, Pereira EA, Kong Y, Tracey I, Cadoux-Hudson T. High field structural MRI in the management of degenerative cervical myelopathy. *Br J Neurosurg*. 2018;32(6):595–598. doi:10.1080/02688697.2018.1467371
24. Elsig JPJ, Kaech DL. Dynamic imaging of the spine with an open upright MRI: Present results and future perspectives of fMRI. *Eur J Orthop Surg Traumatol*. 2007;17(2):119–124. doi:10.1007/s00590-006-0153-5
25. Lorenc T, Gołębiowski M, Michalski W, Glinkowski W. High-resolution, three-dimensional magnetic resonance imaging axial load dynamic study improves diagnostics of the lumbar spine in clinical practice. *World J Orthop*. 2022;13(1):87–101. doi:10.5312/wjo.v13.i1.87
26. Wang ZX, Hu YG. High-intensity zone (HIZ) of lumbar intervertebral disc on T2-weighted magnetic resonance images: Spatial distribution, and correlation of distribution with low back pain (LBP). *Eur Spine J*. 2012;21(7):1311–1315. doi:10.1007/s00586-012-2240-0
27. Peng B, Hou S, Wu W, Zhang C, Yang Y. The pathogenesis and clinical significance of a high-intensity zone (HIZ) of lumbar intervertebral disc on MR imaging in the patient with discogenic low back pain. *Eur Spine J*. 2006;15(5):583–587. doi:10.1007/s00586-005-0892-8
28. Teraguchi M, Yim R, Cheung JPY, Samartzis D. The association of high-intensity zones on MRI and low back pain: A systematic review. *Scoliosis Spinal Disord*. 2018;13:22. doi:10.1186/s13013-018-0168-9
29. Komori H, Okawa A, Haro H, Muneta T, Yamamoto H, Shinomiya K. Contrast-enhanced magnetic resonance imaging in conservative management of lumbar disc herniation. *Spine (Phila Pa 1976)*. 1998;23(1):67–73. doi:10.1097/00007632-199801010-00015
30. Malhotra A, Kalra VB, Wu X, Grant R, Bronen RA, Abbed KM. Imaging of lumbar spinal surgery complications. *Insights Imaging*. 2015;6(6): 579–590. doi:10.1007/s13244-015-0435-8
31. Witkam RL, Buckens CF, van Goethem JWM, Vissers KCP, Henssen DJHA. The current role and future directions of imaging in failed back surgery syndrome patients: An educational review. *Insights Imaging*. 2022;13(1):117. doi:10.1186/s13244-022-01246-z
32. Mallio CA, Vadalà G, Russo F, et al. Novel magnetic resonance imaging tools for the diagnosis of degenerative disc disease: A narrative review. *Diagnostics (Basel)*. 2022;12(2):420. doi:10.3390/diagnostics12020420
33. Sharma H, Gupta R, Olivero W. fMRI in patients with lumbar disc disease: A paradigm to study patients over time. *J Pain Res*. 2011;4:401–405. doi:10.2147/JPR.S24393
34. D'Aprile P, Nasuto M, Tarantino A, Guglielmi G, Jinkins JR, Cornacchia S. Magnetic resonance imaging in degenerative disease of the lumbar spine: Fat saturation technique and contrast medium. *Acta Biomed*. 2018;89(1-S):208–219. doi:10.23750/abm.v89i1-S.7024
35. Salaffi F, Ceccarelli L, Carotti M, et al. Differentiation between infectious spondylodiscitis versus inflammatory or degenerative spinal changes: How can magnetic resonance imaging help the clinician? *Radiol Med*. 2021;126(6):843–859. doi:10.1007/s11547-021-01347-7
36. D'Aprile P, Tarantino A, Jinkins JR, Brindicci D. The value of fat saturation sequences and contrast medium administration in MRI of degenerative disease of the posterior/perispinal elements of the lumbosacral spine. *Eur Radiol*. 2007;17(2):523–531. doi:10.1007/s00330-006-0324-0
37. D'Aprile P, Tarantino A, Lorusso V, Brindicci D. Fat saturation technique and gadolinium in MRI of lumbar spinal degenerative disease. *Neuroradiol J*. 2006;19(5):654–671. doi:10.1177/197140090601900518
38. Lotz JC, Fields AJ, Liebenberg EC. The role of the vertebral end plate in low back pain. *Global Spine J*. 2013;3(3):153–163. doi:10.1055/s-0033-1347298
39. Jaumard NV, Welch WC, Winkelstein BA. Spinal facet joint biomechanics and mechanotransduction in normal, injury and degenerative conditions. *J Biomech Eng*. 2011;133(7):071010. doi:10.1115/1.4004493
40. Perolat R, Kastler A, Nicot B, et al. Facet joint syndrome: From diagnosis to interventional management. *Insights Imaging*. 2018;9(5): 773–789. doi:10.1007/s13244-018-0638-x
41. Manchikanti L, Manchikanti KN, Cash KA, Singh V, Giordano J. Age-related prevalence of facet-joint involvement in chronic neck and low back pain. *Pain Physician*. 2008;11(1):67–75. PMID:18196171.
42. Deer T, Sayed D, Michels J, Josephson Y, Li S, Calodney AK. A review of lumbar spinal stenosis with intermittent neurogenic claudication: Disease and diagnosis. *Pain Medicine*. 2019;20(Suppl 2):S32–S44. doi:10.1093/pm/pnz161
43. Nakayama T, Ehara S. Spondylolytic spondylolisthesis: Various imaging features and natural courses. *Jpn J Radiol*. 2015;33(1):3–12. doi:10.1007/s11604-014-0371-4
44. Canella C, Schau B, Ribeiro E, Sbaffi B, Marchiori E. MRI in seronegative spondyloarthritis: Imaging features and differential diagnosis in the spine and sacroiliac joints. *AJR Am J Roentgenol*. 2013;200(1): 149–157. doi:10.2214/AJR.12.8858